

2017

# Probabilistic optimal decision making and life-cycle management considering risk, sustainability, and utility: applications to bridges and ships

Samantha Maureen Sabatino  
*Lehigh University*

Follow this and additional works at: <http://preserve.lehigh.edu/etd>



Part of the [Civil and Environmental Engineering Commons](#)

---

## Recommended Citation

Sabatino, Samantha Maureen, "Probabilistic optimal decision making and life-cycle management considering risk, sustainability, and utility: applications to bridges and ships" (2017). *Theses and Dissertations*. 2788.  
<http://preserve.lehigh.edu/etd/2788>

This Dissertation is brought to you for free and open access by Lehigh Preserve. It has been accepted for inclusion in Theses and Dissertations by an authorized administrator of Lehigh Preserve. For more information, please contact [preserve@lehigh.edu](mailto:preserve@lehigh.edu).

Probabilistic optimal decision making and life-cycle management considering risk,  
sustainability, and utility: applications to bridges and ships

by  
Samantha Sabatino

Presented to the Graduate and Research Committee  
of Lehigh University  
in Candidacy for the Degree of  
Doctor of Philosophy  
in  
Structural Engineering

Lehigh University  
May 2017

© Copyright by Samantha Sabatino  
May 2017

Approved and recommended for acceptance as a dissertation in partial fulfillment of the requirements for the degree of Doctor of Philosophy

---

Defense Date

---

Approved Date

---

**Dr. Dan M. Frangopol**

*Dissertation supervisor*

Professor of Structural Engineering

Department of Civil and Environmental Engineering

Lehigh University

Committee Members:

---

**Dr. Spencer Quiel**

*Committee chairman*

Assistant Professor of Structural Engineering

Department of Civil and Environmental Engineering

Lehigh University

---

**Dr. John L. Wilson**

*Committee member*

Professor of Structural Engineering

Department of Civil and Environmental Engineering

Lehigh University

---

**Dr. Sibel Pamukcu**

*Committee member*

Professor of Geotechnical Engineering

Department of Civil and Environmental Engineering

Lehigh University

---

**Dr. Mitsuyoshi Akiyama**

*External committee member*

Professor of Structural Engineering

Department of Civil and Environmental Engineering

Waseda University

## ACKNOWLEDGMENTS

First and foremost, I would like express extreme gratitude to my Ph.D. research advisor, Dr. Dan Frangopol; his patient guidance and unwavering support throughout my graduate studies at Lehigh University is graciously acknowledged. As a result of his continuous support, I had the opportunity to co-author 6 papers for publication in referred scientific journals, in addition to 15 conference and keynote papers. Additionally, I have professionally benefited from being introduced and integrated into Dr. Frangopol's influential network of professional and educational leaders within the fields of structural and life-cycle engineering. Besides my advisor, I must extend gratitude to Dr. John L. Wilson, who serves as Chairperson of my Ph.D. dissertation committee, and committee members Dr. Sibel Pamukcu, Dr. Spencer Quiel, and Dr. Mitsuyoshi Akiyama, for their insightful comments and valuable suggestions regarding my work.

I gratefully acknowledge the support by grants from (a) the National Science Foundation through grant CMS-0639428, (b) the Commonwealth of Pennsylvania, Department of Community and Economic Development, through the Pennsylvania Infrastructure Technology Alliance (PITA), (c) the U.S. Federal Highway Administration Cooperative Agreement Award DTFH61-07-H-00040, and (d) the U.S. Office of Naval Research (contracts N00014-08-1-0188, N00014-12-1-0023, and N00014-16-1-2299, Structural Reliability Program, Director Dr. Paul E. Hess III, ONR, Code 331). Furthermore, as a Ph.D. student, I was awarded the P.C. Rossin Fellowship at Lehigh University in 2014; as a result, I was given the opportunity to

attend a yearlong teacher development course and earned the Teacher Development Certificate for College Teaching (levels I and II). Through this program, I received valuable critiques that motivated self-reflection and constructive changes within my teaching delivery; ultimately, this invaluable experience has helped me prepare for a career as a University professor.

I would also like to thank my former and current colleagues, Dr. Mohamed Soliman and Dr. You Dong for their contributions to parts of this study. Furthermore, the cooperation, constructive comments, inspirational discussions, and helpful suggestions provided by my officemates, Dr. Benjin Zhu, Ph.D., candidates Alysson Mondoro and Liang Liu, and Matthew Horner, are recognized. Additionally, I would like to acknowledge the friendship and warm support provided by Dr. Aman Karamlou, Ph.D., candidate Vasileios Christou, and long-time friend Kelly Sabin throughout my time as a Ph.D. student. I also would like to thank Peter Bryan, the IT Manager of ATLSS, for his consistent, positive support and friendship, in addition to providing technological support and software solutions for the computations performed for this study.

Finally, and most importantly, I would like to express my gratitude for the unconditional love provided by my family members in Basking Ridge, NJ. More specifically, thank you Mom and Dad for providing continuous emotional and financial support; none of this work would have been possible without your consideration, love, and unfaltering support.

# TABLE OF CONTENTS

ACKNOWLEDGMENTS .....	iv
TABLE OF CONTENTS .....	vi
LIST OF TABLES .....	x
LIST OF FIGURES .....	xii
ABSTRACT .....	1
CHAPTER 1 INTRODUCTION.....	3
1.1 Overview.....	3
1.2 Objectives .....	6
1.3 Summary of the proposed approach .....	7
1.4 Contributions .....	10
1.5 Outline .....	11
CHAPTER 2 BACKGROUND.....	15
2.1 Overview.....	15
2.2 Performance evaluation and prediction .....	15
2.2.1 Reliability .....	17
2.2.2 Risk.....	19
2.2.3 Sustainability .....	21
2.2.4 Lifetime functions .....	24
2.2.5 Life-cycle cost .....	25
2.3 Life-cycle assessment, management, and optimization.....	26
2.4 Proposed methodology .....	29
CHAPTER 3 SUSTAINABILITY-INFORMED MAINTENANCE OPTIMIZATION OF HIGHWAY BRIDGES CONSIDERING MULTI-ATTRIBUTE UTILITY AND RISK ATTITUDE .....	43
3.1 Overview.....	43
3.2 Introduction.....	43
3.3 Multi-attribute risk assessment of highway bridges under traffic loading ....	49

3.3.1	Vulnerability analysis .....	49
3.3.2	Effects of maintenance actions .....	51
3.3.3	Evaluation of risk-attributes associated with highway bridges .....	52
3.4	Utility assessment for sustainability evaluation.....	56
3.4.1	Utility function for maintenance cost .....	56
3.4.2	Utility function for risk-attributes .....	57
3.4.3	Multi-attribute utility assessment corresponding to sustainability .....	58
3.5	Optimization of bridge maintenance planning.....	59
3.6	Case study .....	62
3.6.1	Evaluation of risk-attributes .....	63
3.6.2	Utility assessment for maintenance cost and sustainability performance .. .....	65
3.6.3	Optimal maintenance planning.....	66
3.7	Conclusions.....	71
<b>CHAPTER 4 LIFE-CYCLE UTILITY-INFORMED MAINTENANCE PLANNING BASED ON LIFETIME FUNCTIONS: OPTIMUM BALANCING OF COST, FAILURE CONSEQUENCES AND PERFORMANCE BENEFIT .....</b>		<b>97</b>
4.1	Overview.....	97
4.2	Introduction.....	98
4.3	Lifetime functions.....	102
4.3.1	Component analysis.....	103
4.3.2	System analysis .....	106
4.3.3	Effects of essential maintenance .....	106
4.4	Attributes evaluation.....	108
4.4.1	Cost.....	109
4.4.2	Consequences .....	109
4.4.3	Benefit .....	111
4.5	Utility assessment .....	111
4.5.1	Single attribute utility assignment .....	112

4.5.2	Multi-attribute utility .....	113
4.5.3	Utility associated with performance benefit.....	114
4.6	Tri-objective optimization framework for lifetime maintenance planning .	115
4.7	Illustrative example.....	117
4.8	Case Study .....	119
4.9	Conclusions.....	126
<b>CHAPTER 5 DECISION MAKING FRAMEWORK FOR OPTIMAL SHM</b>		
<b>PLANNING OF SHIP STRUCTURES CONSIDERING AVAILABILITY AND</b>		
<b>UTILITY .....</b>		
		161
5.1	Overview.....	161
5.2	Introduction.....	162
5.3	Performance prediction considering SHM data.....	166
5.3.1	SHM data analysis .....	166
5.3.2	Exceedance probability .....	167
5.3.3	Expected average availability.....	168
5.3.4	Monitoring cost .....	171
5.4	Utility assessment .....	172
5.4.1	Risk attitude.....	172
5.4.2	Formulations.....	173
5.5	Optimization framework.....	175
5.6	Case Study .....	177
5.6.1	Uniform time intervals .....	180
5.6.2	Non-uniform time intervals .....	183
5.7	Conclusions.....	185
<b>CHAPTER 6 SUMMARY, CONCLUSIONS, AND FUTURE WORK.....</b>		
		211
6.1	Summary.....	211
6.2	Conclusions.....	214
6.3	Future work.....	216
<b>REFERENCES .....</b>		
		219

APPENDIX A SYSTEM RELIABILITY MODELING OF BRIDGES .....	234
APPENDIX B LIST OF NOTATIONS .....	262
APPENDIX C LIST OF ACRONYMS .....	271
VITA.....	272

## LIST OF TABLES

Table 3.1. Random variables and their corresponding parameters used within the reliability analysis of the E-16-FK highway bridge. ....	74
Table 3.2. Variables and their corresponding parameters used in the evaluation of the risk-attributes associated with the investigated highway bridge. ....	75
Table 3.3. Minimum and maximum values of risk-attributes. ....	76
Table 3.4. Maintenance plans corresponding to the representative risk solutions on the Pareto front shown in Figure 3.8. ....	77
Table 3.5. Minimum annual utility values corresponding to six solutions within the Pareto front in Figure 3.8. ....	78
Table 3.6. Maximum annual utility risk-attribute values corresponding to solutions A and B within the Pareto front in Figure 3.8. ....	79
Table 3.7. Maintenance plans corresponding to solutions C1, C2, and C3 on the Pareto front shown in Figure 3.11. ....	80
Table 3.8. Maintenance plans corresponding to solutions D1, D2, and D3 on the Pareto front shown in Figure 3.13 considering various weighting factors. ....	81
Table 3.9. Maintenance plans and associated utility values corresponding to the representative solutions on the four-dimensional Pareto front contained in Figure 3.14. ....	82
Table 4.1. Minimum and maximum annual values of attributes involved in the risk and benefit assessment of the five four-component systems shown in Figure 4.3. ....	129
Table 4.2. Parameters used in the evaluation of the risk attributes associated with the E-17-HS bridge. ....	130
Table 4.3. Minimum and maximum annual values of attributes involved in the risk and benefit assessment of the E-17-HS bridge ....	131
Table 4.4. Maintenance plans corresponding to the six optimum solutions on the Pareto fronts shown in Figure 4.16a. ....	132
Table 4.5. Optimum utility values corresponding to the six optimum solutions within the Pareto fronts in Figure 4.16a. ....	133

Table 4.6. Attribute values corresponding to the six optimum solutions within the Pareto fronts in Figure 4.16a. ....	134
Table 4.7. Maintenance plans corresponding to the four optimum solutions within the Pareto fronts in Figure 4.16b,c. ....	135
Table 4.8. Maintenance plans corresponding the six optimum solutions within the two Pareto fronts shown in Figure 4.16d. ....	136
Table 4.9. Maintenance plans corresponding to the two optimum solutions within the two Pareto fronts shown in Figure 4.22. ....	137
Table 5.1. Expected average availability corresponding to various combinations of number of exceedances and the residual(s) examined in the prediction process .....	188

## LIST OF FIGURES

Figure 1.1. Informed, utility-based, life-cycle decision making framework.....	14
Figure 2.1. Metrics of sustainability.....	37
Figure 2.2. Multi-attribute utility-based sustainability assessment.....	37
Figure 2.3. Relationship between the PDF of the time-to-failure $f(t)$ , the survivor function $S(t)$ , and the cumulative probability of failure $F(t)$ .....	38
Figure 2.4. Effect of gradual deterioration and essential and preventive maintenance on (a) structural performance and (b) cost. ....	38
Figure 2.5. Integrated life-cycle management framework. ....	39
Figure 2.6. Utility-based decision making procedure. ....	39
Figure 2.7. Computational framework for the life-cycle management of structures. ..	40
Figure 2.8. Qualitative representations of typical exponential utility functions that are monotonically decreasing as the expected value of the risk attribute value increases. ....	40
Figure 2.9. Effect of risk attitude on the optimal solutions for lifetime maintenance considering weighting factors equal to one third .....	41
Figure 2.10. Time-variant profiles of (a) utility associated with sustainability and (b) economic risk for representative solutions A and B in Figure 2.9.....	42
Figure 3.1. Flowchart describing the multi-attribute utility performance assesment..	83
Figure 3.2. Flowchart describing the bi-objective optimization procedure.....	84
Figure 3.3. Transverse cross-section of the superstructure of bridge E-16-FK.....	85
Figure 3.4. System reliability model for the investigated bridge superstructure.....	86
Figure 3.5. Evolution of annual probability of failure over time of the elements of the superstructure and the system, as a whole.....	87
Figure 3.6. Time-variant risk attributes considering no maintenance. ....	88
Figure 3.7. Profiles of annual utility associated with economic, social, and environmental sustainability metrics considering no maintenance and a risk averse attitude ( $\gamma = -1$ ).....	89

Figure 3.8. Pareto optimal solutions for three maintenance actions considering risk accepting and risk averse attitudes. ....	90
Figure 3.9. Profiles of annual utility associated with sustainability corresponding to three (B1, B2, B3) optimal solutions considering a risk averse decision maker as shown in Figure 3.8.....	91
Figure 3.10. Time-variant annual risk associated with CO <sub>2</sub> emissions $R_{EC}$ corresponding to representative optimal solutions considering a risk accepting decision maker as shown in Figure 3.8. ....	92
Figure 3.11. Pareto optimal solutions considering a variable number of essential maintenance actions and a risk averse decision maker. ....	93
Figure 3.12. Annual utility associated with sustainability corresponding to representative solutions on the Pareto front in Figure 3.11.....	94
Figure 3.13. Pareto optimal solutions considering variable multi-attribute utility weighting factors and a risk averse decision maker. ....	95
Figure 3.14: Pareto optimal solutions for the four-objective optimization problem that simultaneously maximizes $u_c$ , $u_{econ}$ , $u_{soc}$ , and $u_{env}$ considering a risk averse attitude ( $\gamma = 1$ ). ....	96
Figure 4.1. Flowchart outlining the computations involved in the decision support tool. ....	138
Figure 4.2. Exponential utility functions that are monotonically (a) decreasing and (b) increasing as the attribute value increase. ....	139
Figure 4.3. Five configurations of a four-component system .....	140
Figure 4.4. Cumulative-time failure probability associated with (a) components and (b) systems in Figure 4.3 considering independence ( $\rho = 0$ ) and full correlation ( $\rho = 1$ ) among components.....	141
Figure 4.5. Hazard associated with (a) components and (b) systems in Figure 4.3 considering independence ( $\rho = 0$ ) and full correlation ( $\rho = 1$ ) among components.....	142
Figure 4.6. Availability associated with (a) components and (b) systems in Figure 4.3 considering independence ( $\rho = 0$ ) and full correlation ( $\rho = 1$ ) among components.....	143

Figure 4.7. Cumulative and annual probability of system failure considering extreme correlation cases among components of (a) System A and (b) System E. .....	144
Figure 4.8. Time-variant profiles of annual direct, indirect, and total risk attributes for systems A and E, considering statistical independence among components ( $\rho = 0$ ). .....	145
Figure 4.9. Time-variant profiles of availability, hazard, risk, and benefit utilities considering system A, independence among components ( $\rho = 0$ ), and (a) risk averse ( $\gamma = 2$ ) or (b) risk taking attitude ( $\gamma = -2$ ). .....	146
Figure 4.10. Time-variant profiles of total risk utilities considering all systems in Figure 4.3, independence among components ( $\rho = 0$ ), and (a) risk averse ( $\gamma = 2$ ) or (b) risk taking attitude ( $\gamma = -2$ ). .....	147
Figure 4.11. Time-variant profiles of benefit utilities considering all systems in Figure 4.3, independence among components ( $\rho = 0$ ), and (a) risk averse ( $\gamma = 2$ ) or (b) risk taking attitude ( $\gamma = -2$ ). .....	148
Figure 4.12. (a) Cumulative-time failure probability, (b) hazard, and (c) availability associated with both the components and the system (i.e., superstructure of the bridge E-17-HS) considering no maintenance and extreme correlation cases. ....	149
Figure 4.13. Cumulative and annual probability of system (i.e. superstructure of bridge E-17-HS) failure considering extreme correlation cases among components.....	150
Figure 4.14. The time-variant profile of each risk attribute considering no maintenance, statistical independence among components ( $\rho = 0$ ), and the annual probability of system failure.....	151
Figure 4.15. The time-variant profile of risk and benefit utilities considering independence among components ( $\rho = 0$ ) and a risk averse attitude ( $\gamma = 2$ ). .....	152
Figure 4.16. Pareto optimum solutions considering the effects of (a) risk attitude $\gamma$ , (b) correlation among components $\rho$ , (c) discount rate of money $r_m$ , and (d) number of maintenance actions $N_{EM}$ . .....	154
Figure 4.17. (a) Risk and (b) benefit utility profiles associated with the six optimum solutions shown in Figure 4.16a.....	155

Figure 4.18. Time-variant (a) risk utilities and (b) economic risk values associated with the optimum solution A2 in Figure 4.16a. ....	156
Figure 4.19. Time-variant (a) utilities associated with benefit, (b) survival probability, (c) availability, and (d) hazard associated with the optimum solution A2 in Figure 4.16a.....	157
Figure 4.20. Pareto optimum solutions associated with benefit utilities $u_{benefit}$ within the range 0.5 – 0.6 associated with Figure 4.16a. ....	158
Figure 4.21. Time-variant (a) risk and (b) benefit utilities corresponding to optimum solutions D1, D2, and D3 in Figure 4.16d. ....	159
Figure 4.22. Pareto optimum solutions associated with both annual failure probability and cumulative-time failure probability considering a risk averse attitude ( $\gamma = 2$ ), independence among components ( $\rho = 0$ ), discount rate of money of 2% ( $r_m = 0.02$ ), and three maintenance actions ( $N_{EM} = 3$ ). ....	160
Figure 5.1. Flowchart describing the performance prediction, expected average availability, and cost of implementing monitoring. ....	189
Figure 5.2. Timeline of monitoring at (a) uniform time and (b) non-uniform time intervals. ....	190
Figure 5.3. Flowchart describing the utility assessment and optimization procedure. ....	191
Figure 5.4. (a) Exponential utility decreasing, (b) exponential utility increasing, and (c) risk attitude as functions of attribute $a$ for different values of $\rho$ and $\gamma_{exp}$ . ....	192
Figure 5.5. (a) Quadratic utility decreasing, (b) quadratic utility increasing, and (c) risk attitude as functions of attribute $a$ for different values of $\alpha$ and $\gamma_{quad}$ . ....	193
Figure 5.6. Logarithmic utility decreasing, (b) logarithmic utility increasing, and (c) risk attitude as functions of attribute $a$ for different values of $\beta$ and $\gamma_{log}$ . ....	194
Figure 5.7. (a) HSV-2 swift and (b) plan view detailing the location of an example sensor, T2-4 on frame 26 (adapted from Soliman <i>et al.</i> 2015). ....	195
Figure 5.8. Pareto optimal solutions considering uniform monitoring time intervals, a risk accepting attitude, and three utility formulations. ....	196

Figure 5.9. Uniform monitoring time interval SHM plans corresponding to four representative solutions on the Pareto front associated with the exponential utility formulation shown in Figure 5.8. ....	197
Figure 5.10. Uniform monitoring time interval SHM plans corresponding to three representative solutions associated with $u_a = 0.4$ on the Pareto fronts in Figure 5.8. ....	198
Figure 5.11. Pareto optimal solutions considering uniform monitoring time intervals, a risk averse attitude, and different number of exceedances (i.e., $ex = 1$ , $ex = 3$ , $ex = 5$ ) for residuals associated with cases (a) L and (b) LS. ....	199
Figure 5.12. Uniform monitoring interval SHM plans corresponding to three representative solutions on the Pareto fronts contained in (a) Figure 5.11a and (b) Figure 5.11b. ....	200
Figure 5.13 Pareto optimal solutions considering uniform monitoring time intervals, a risk averse attitude, and variable number of monitoring cycles. ....	201
Figure 5.14. Uniform interval SHM plans corresponding to five representative solutions on the Pareto front in Figure 5.13. ....	202
Figure 5.15. Effect of the utility formulation on the Pareto optimal solutions considering non-uniform time monitoring intervals and a risk accepting attitude. ....	203
Figure 5.16. Non-uniform interval SHM plans corresponding to four representative solutions on the Pareto front corresponding to the exponential utility formulation shown in Figure 5.15. ....	204
Figure 5.17. Non-uniform interval SHM plans corresponding to three representative solutions associated with $u_a = 0.4$ on the Pareto fronts in Figure 5.15. ....	205
Figure 5.18. Pareto optimal solutions considering non-uniform monitoring intervals, the exponential utility formulation, and two risk attitudes. ....	206
Figure 5.19. Non-uniform interval SHM plans corresponding to four representative solutions on the Pareto front corresponding to a risk accepting attitude shown in Figure 5.18. ....	207
Figure 5.20. Non-uniform interval SHM plans corresponding to four representative solutions on the Pareto front corresponding to a risk averse attitude shown in Figure 5.18. ....	208

Figure 5.21. Effect of the discount rate of money on the Pareto optimal solutions considering non-uniform monitoring intervals, the logarithmic utility formulation, and a risk averse attitude .....	209
Figure 5.22. Non-uniform interval SHM plans corresponding to three representative solutions associated with $u_a = 0.8$ on the Pareto fronts in Figure 5.21...	210
Figure A.1 Component $j$ .....	254
Figure A.2. Eight-component bridge system.....	254
Figure A.3. Sub-systems of a bridge system. ....	255
Figure A.4. Five configurations of a four-component system.....	255
Figure A.5. PDF of the safety margin $f_M(m)$ . ....	256
Figure A.6. Idealized series, parallel, and series-parallel systems. ....	256
Figure A.7. Transverse cross-section and (b) system reliability model of the superstructure of a bridge.....	257
Figure A.8. Force-deformation relationship considering the effect of the post-failure behavior $\delta$ . ....	257
Figure A.9. Correlation coefficient $\rho(X_1, X_2)$ between two random variables $X_1$ and $X_2$ . ....	258
Figure A.10. Simply supported bridge span with two truck loads .....	258
Figure A.11. Simply supported beam with uniform load.....	259
Figure A.12. System reliability model of the beam in Figure A.11 considering bending and shear failure. ....	259
Figure A.13. 10 bar symmetric truss (adopted from Frangopol and Curley 1987) ....	260
Figure A.14. System reliability model for the 10 bar truss in Figure A.13, considering failure of one member and failure of two members including failure of members 3, 4, or 5. ....	260
Figure A.15. System reliability model for investigated steel bridge.....	261
Figure A.16. Refined system reliability model for the investigated bridge. ....	261
Figure A.17. Hypothetical series system model of typical girder (Estes and Frangopol 2001).....	261

## **ABSTRACT**

The condition and performance of infrastructure systems is continuously deteriorating due to various environmental and mechanical stressors. There is a great need to implement optimal mitigation strategies that maintain structural performance within acceptable levels through the life-cycle of deteriorating civil infrastructure. In order to ensure adequate life-cycle performance, cost-efficient interventions must be implemented. This study presents computational frameworks that serve as decision support tools for bridge and ship managers, which ultimately allow them to make cost-, risk-, and sustainability-informed choices in the context of life-cycle engineering. Reliability, risk, sustainability, and utility-based performance indicators are examined and applied to civil and marine infrastructure systems subjected to a variety of hazards in order to determine optimal life-cycle management plans, balancing structural performance, cost of intervention, and available resources. The final product of the proposed decision support tools, optimal life-cycle management plans, describe which performance enhancing measure(s) should be implemented and when to intervene.

Specifically, this study adds to existing probabilistic life-cycle management frameworks by integrating a novel utility-based sustainability metric in the life-cycle maintenance planning of civil and marine infrastructure. The effect of the risk attitude of the decision maker is examined in this study by including utility functions, which in this context, depict the relative desirability of lifetime management plans to the decision maker. Additionally, lifetime functions such as hazard and availability are included as new performance indicators for bridges. Furthermore, the utility-based

decision making framework developed is applied to a ship structure in order to determine optimal structural health monitoring plans under uncertainty. Optimal monitoring plans for the ship are determined by simultaneously maximizing availability and lifetime monitoring costs.

# CHAPTER 1 INTRODUCTION

## 1.1 OVERVIEW

The condition of civil infrastructure systems around the world is degrading due to a variety of deteriorating mechanisms, including aging, environmental stressors, man-made hazards (e.g., blasts and fires) and natural hazards (e.g., earthquakes and hurricanes), among others. Consequently, improving the overall condition and safety of deteriorating infrastructure systems is a key concern worldwide. For example, in 2017, the American Society of Civil Engineers (ASCE) reported, within the Report Card for America's Infrastructure, that the average age of the United States' 614,387 bridges was 43 years. Additionally, nearly a quarter of these highway bridges were classified as either structurally deficient or functionally obsolete (ASCE 2017). These staggering statistics highlight the dire need to implement rational mitigation strategies that maintain structural performance within acceptable levels through the life-cycle of deteriorating civil infrastructure. In order to ensure adequate life-cycle performance, it is crucial to implement rational management strategies that maintain performance of infrastructure systems within acceptable levels through their life-cycle. Life-cycle management is widely recognized as an effective tool for maximizing the cost-effectiveness of implementing intervention actions that improve condition and safety, and extend the service life of deteriorating infrastructure systems.

In order to predict the performance of structural systems during their life-cycle under uncertainty, deterioration mechanisms for the investigated systems (e.g., corrosion and fatigue) must be carefully considered. Aggressive environmental

conditions and natural aging processes facilitate a gradual reduction in the performance (e.g., system reliability) of existing structures. Alternatively, there are extreme events that cause an abrupt reduction of the functionality of structures such as blasts, fires, earthquakes, hurricanes, and terrorist attacks. During their life-cycle, infrastructure systems can be subjected to multiple hazards. Thus, it is necessary to consider the performance of infrastructure systems under multiple hazards in the hazard assessment and mitigation procedure, all in a life-cycle context. Life-cycle assessment of deteriorating infrastructure systems includes aleatory and epistemic uncertainties associated with natural randomness and inaccuracies in the prediction or estimation of reality, respectively (Ang and Tang 2007). Because of these uncertainties, it is imperative for structural engineers to accurately model and assess the structural performance and expected total cost within a probabilistic life-cycle context.

In general, structural performance prediction of deteriorating structural systems is affected by various uncertainties inherent in the load conditions, damage propagation, among others. Although aleatory uncertainties are not reducible, epistemic uncertainties may be reduced by including information collected from inspections and structural health monitoring (SHM) (Peil 2005; Frangopol and Messervey 2009a,b). Utilizing SHM within the performance assessment of deteriorating structural systems is an effective tool to reduce uncertainties in the analysis and derive crucial information on the real-time structural response (Paik and Frieze 2001). Within this dissertation, a decision tool for optimal life-cycle

management of deteriorating infrastructure is developed that determines cost-efficient SHM plans that provide crucial information regarding structural performance.

Furthermore, the effects of maintenance, repair, and rehabilitation on structural life-cycle performance must be well studied. The influence of maintenance and repairs on structural performance can be incorporated in a generalized framework for multi-criteria optimization of the life-cycle management of infrastructure systems. Performance of infrastructure systems may be represented by a variety of indicators. Approaches for the life-cycle management of infrastructure systems involving reliability performance indicators consider uncertainties associated with loads and resistance, but are not able to account for the consequences incurred from bridge failure. Risk-based indicators provide the means to combine the probability of structural failure with the consequences associated with this event. Furthermore, methodologies considering sustainability as a performance indicator are becoming relevant within the field of life-cycle engineering. The incorporation of sustainability in the life-cycle performance assessment and management procedures allows for the effective integration of economic, social, and environmental aspects. A sustainability performance metric may be established considering multi-attribute utility theory, which facilitates the combination of several risks while incorporating the risk attitude of the decision maker.

Utility theory is employed herein to incorporate the influence of the decision maker's risk attitude on the relative desirability of lifetime management plans (Keeney and Raiffa 1993). In general, utility is defined as a measure of desirability to the decision maker. Different formulations of utility functions, always bounded by 0 and

1, are employed to express the relative desirability of lifetime management schedules. Within the context of this work, utility theory is a powerful tool used to conduct rational multi-criteria decision making analyses considering uncertain information.

Overall, life-cycle management concepts for bridge and ship systems under uncertainty and the application of such concepts considering the risk attitude of the decision maker are presented within this study. Risk- and sustainability-informed management of bridges under the effects of deteriorations is investigated. Quantifying the life-cycle performance, risk, and sustainability of bridges at the component and network levels is also addressed. Moreover, bridge and ship management planning, in addition to optimization under a constrictive budget and performance constraints are presented through a probabilistic management framework. The computational frameworks presented can serve as a useful tool in risk mitigation and, in general, decision-making associated with bridges and ships. The approaches presented can provide optimal intervention strategies to the decision maker that will allow for cost- and performance (e.g., risk, sustainability, availability)-informed decisions regarding lifecycle management of highway bridges and ship structures.

## **1.2 OBJECTIVES**

The objectives of this study are:

1. Develop probabilistic a computational framework for optimal decision making for bridge and ship managers that consider multiple objectives and performance constraints under uncertainty.
2. Integrate utility concepts and methods within life-cycle decision support tools.

3. Incorporate the influence of the risk attitude of the decision maker within life-cycle performance assessment.
4. Propose a novel approach to quantify the sustainability performance of infrastructure systems considering hazards that impact the economy, society, and the environment.
5. Utilize lifetime functions in the reliability assessment of structural systems within a life-cycle management framework.
6. Establish a methodology to utilize structural health monitoring (SHM) data to reduce uncertainties associated with structural performance prediction and facilitate cost-efficient, optimal life-cycle SHM planning of ship structures.

### **1.3 SUMMARY OF THE PROPOSED APPROACH**

The overall goal of this study is to develop an integrated life-cycle management and decision making framework for civil and marine infrastructure considering risk attitudes and utility theory. The diagram shown in Figure 1.1 shows the proposed utility-based decision making framework, composed of five interconnected modules that perform specific tasks. This type of decision support tool is applied to bridges and naval vessels, as indicated in Figure 1.1. The first step of the framework involves identifying relevant structural parameters (i.e., module 1) and the stressors that affect the investigated system. Some critical parameters include the structural geometry, material behavior, loading due to multiple hazards, information from SHM, and risk attitude of the decision maker.

Next, the structural performance is assessed and predicted throughout the life-cycle of the investigated system (i.e., module 2). Within this step, time-variant structural performance is evaluated to determine the current and predict the future condition of particular components or the entire structure. The uncertainty inherent within the modeling and due to randomness requires the quantification of loading effects and structural capacity in a probabilistic manner. This study emphasizes the calculation of structural performance in terms of risk, sustainability, and lifetime functions (e.g., availability) (Leemis 1995).

After determining the time-variant structural performance of the system, the utility assessment of each attribute investigated within the decision making problem is conducted (i.e., module 3). Utility theory is utilized in order to depict the relative desirability of maintenance strategies to the decision maker and provides a framework that can measure, combine, and consistently compare these relative values (Ang and Tang 2007). Attributes that are mapped to utility within this study include: risk, cost, benefit, and lifetime functions (e.g., availability, hazard). Multi-attribute utility theory is employed herein in order to effectively capture the sustainability performance of highway bridges and impact of the decision maker's risk attitude (Sabatino *et al.* 2016).

Once all investigated attributes are mapped to utility, the objective functions may be formulated, and a multi-criteria optimization can be carried out (i.e., module 4) with the final goal of determining optimal life-cycle management plans (i.e., when to intervene and which performance measure(s) should be implemented). Life-cycle optimization is an essential task within the life-cycle management (LCM) framework

(Ang and De Leon 2005; Chang and Shinozuka 1996; Estes and Frangopol 1999; Frangopol and Soliman 2015; Okasha and Frangopol 2009; Sabatino *et al.* 2015; Soliman and Frangopol 2014; Soliman *et al.* 2013, Wen and Kang 2001; Yang *et al.* 2006b). In general, in this study, optimal lifetime intervention plans are obtained by carrying out a multi-criteria optimization procedure where the utility associated with total intervention cost and utility corresponding to performance are considered as conflicting objectives. Within this optimization procedure, the utilities associated with total life-cycle cost and performance are simultaneously maximized in order to achieve optimal lifetime management plans. The output of the optimization process, facilitated with genetic algorithms (GAs), is a Pareto optimal set of solutions which provides rational, informed intervention schedule choices to the decision maker that balances both cost and performance (i.e., module 5). Ultimately, based upon the risk attitude, preferences, and budgetary constraints of the decision maker, he/she may choose, amongst a group of trade-off solutions, an optimal intervention schedule for an investigated structural system. Overall, the proposed methodology can be used in assisting decision making regarding intervention actions that improve the performance of structural systems, in a life-cycle context.

In order to build these self-developed, computational decision making frameworks several commercial programs were employed. MATLAB (MathWorks 2013) was used to facilitate probabilistic, optimization calculations and connect other software functions. Additionally, the reliability program RELSYS (Estes and Frangopol 1998) was also used to calculate component and system reliability. The multi-criteria lifetime management problems proposed herein are solved using a

genetic algorithm-based optimization approach (MathWorks 2013) in MATLAB on a Dell Precision R5500 rack workstation equipped with two six cores X5675 Intel Xeon processors with 3.06 GHz clock speed and 24 GB DDR3 memory.

#### **1.4 CONTRIBUTIONS**

This study enhances the capabilities of already established life-cycle techniques, especially with respect to incorporating utility and the influence of the decision maker's risk attitude into making informed choices for lifetime management of civil and marine infrastructure. The main contributions of this study are:

1. Establish a probabilistic methodology to implement risk-informed life-cycle management of deteriorating infrastructure systems (e.g., when to intervene and which performance enhancing measures to implement) taking into account the influence of the risk attitude of the decision maker. This attitude dictates how the decision maker will invest resources in order to mitigate risk.
2. Formulate a decision support framework under uncertainty that incorporates utility theory within the traditional life-cycle structural engineering concepts. In this context, utility theory is utilized in order to depict the relative desirability of lifetime management strategies to the decision maker.
3. Develop a novel sustainability approach at the system level, considering multi-attribute utility theory under uncertainty. In this context, the sustainability performance indicator, mapped to a multi-attribute utility value, is quantified in terms of a combination of utilities associated with economic, social, and environmental risks.

4. Develop a novel approach for optimal structural health monitoring of ship structures considering cost and availability. In order to determine optimal monitoring plans, a bi-objective optimization process is performed that simultaneously maximizes the utilities associated with monitoring cost and availability.
5. Propose a comprehensive life-cycle decision making framework considering the risk attitude of the decision maker, utility theory, cost-benefit analysis, risk, sustainability, and life-cycle cost. This framework was implemented in a computational platform that allows for adjustments in inputs, optimization parameters, and can be applied to a variety of structural applications including bridges and ships.

## **1.5 OUTLINE**

This document is organized as follows:

- **Chapter 1** serves as an introduction to this study.
- **Chapter 2** discusses fundamental topics related to the life-cycle performance assessment and lifetime management of deteriorating infrastructure systems under uncertainty. Risk- and sustainability-informed management of structural under the effects of both gradual and sudden deteriorations is investigated. Methods regarding the quantification of the life-cycle performance, system reliability, risk, and sustainability of infrastructure systems at the component and systems levels are also addressed. Additionally, life-cycle management

planning and optimization under a constrictive budget and performance constraints are presented through a probabilistic management framework.

- **Chapter 3** presents a methodology for determining optimal maintenance strategies for a highway bridge considering sustainability and cost as conflicting objectives. Utility theory is employed to effectively capture the sustainability performance of highway bridges and impact of the decision maker's risk attitude. The main objective of this framework is to reduce the extent of the consequences of structural failure to the economy, society, and the surrounding environment.
- **Chapter 4** emphasizes the use of lifetime functions to quantify structural performance. Lifetime functions are utilized to model, using closed form analytical expressions, the time-variant effect of intervention actions on the performance of civil infrastructure systems. The presented decision-support framework in this chapter has the ability to quantify maintenance cost, failure consequences, and performance benefit in terms of utility. This framework effectively employs tri-objective optimization procedures in order to determine optimum maintenance strategies under uncertainty. It provides optimum lifetime intervention plans allowing for utility-informed decision making regarding maintenance of civil infrastructure systems.
- **Chapter 5** proposes a decision making framework for optimal SHM planning of ship structures considering availability and utility. Uncertainties associated with modeling and performance prediction of structures may be addressed and subsequently reduced by including, within the performance assessment,

information collected from inspections and structural health monitoring. Presented in this chapter is an approach that determines cost-effective SHM plans that consider the probability that the performance prediction model based on monitoring data is suitable throughout the life-cycle of ship structures. This probability is used to compute the expected average availability of monitoring data for prediction during the life-cycle of a system. Utility theory is employed to incorporate the influence of the decision maker's risk attitude on the relative desirability of SHM plans. Optimization techniques are utilized to simultaneously maximize the utilities associated with monitoring cost and expected average availability in order to determine optimal monitoring strategies under uncertainty.

- **Chapter 6** summarizes this study, draws relevant conclusions, and recommends future research.
- **Appendix A** summarizes methodologies for modeling the system reliability of bridge systems. Parts of this appendix were provided to the Federal Highway Administration in 2017 to augment a report on the application of redundancy factors to highway bridge systems.
- **Appendix B** presents a list of notations contained in each chapter.
- **Appendix C** presents a list of acronyms for the entire document.

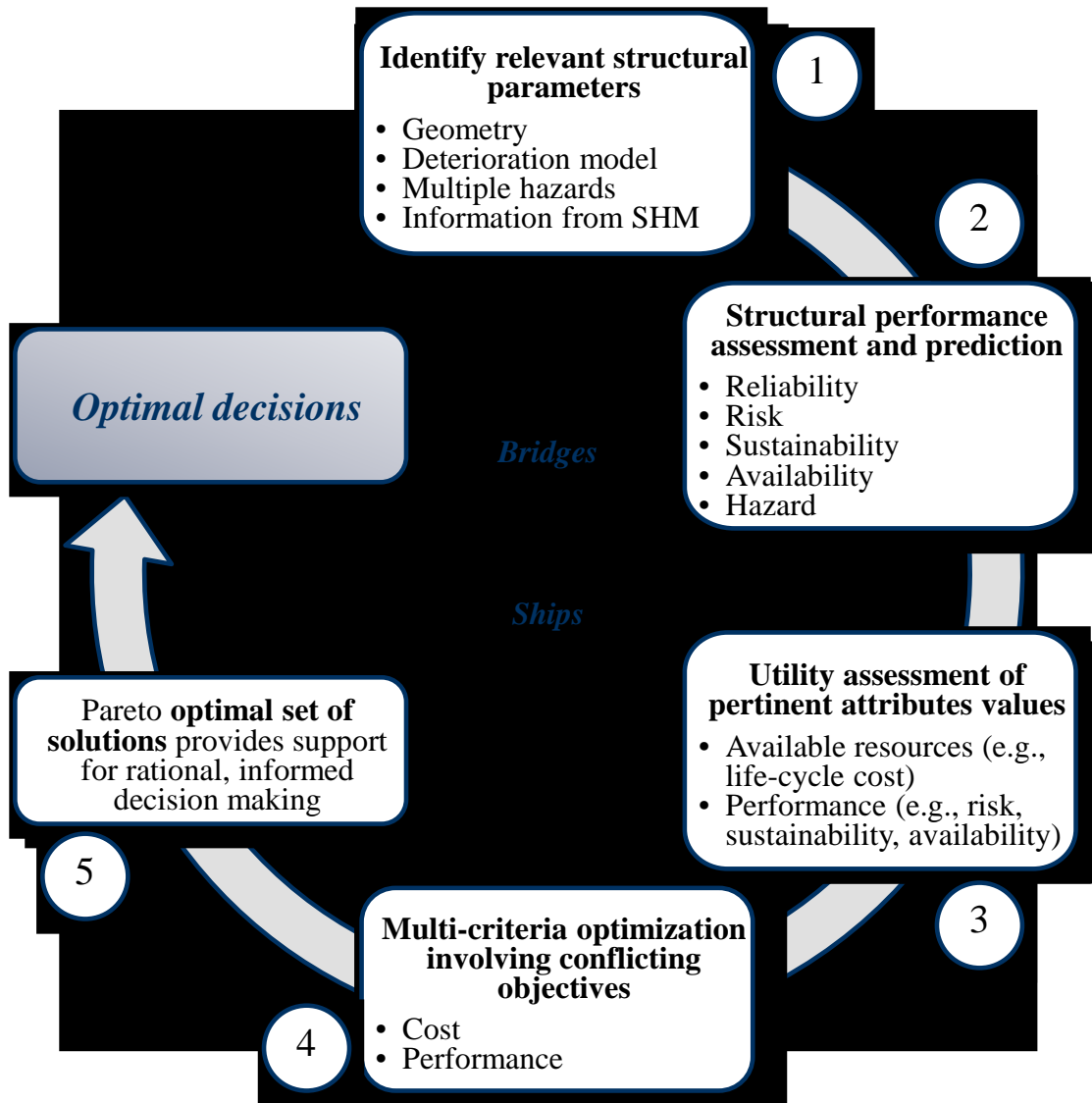


Figure 1.1. Informed, utility-based, life-cycle decision making framework

## **CHAPTER 2 BACKGROUND**

### **2.1 OVERVIEW**

This chapter presents an overview of life-cycle management concepts for infrastructure systems under uncertainty. Risk- and sustainability-informed management of structural under the effects of both gradual and sudden deteriorations is investigated. Quantifying the life-cycle performance, system reliability, risk, and sustainability of infrastructure systems at the component and systems levels is also addressed. Additionally, sustainability assessment considering the risk attitude of the decision maker is discussed. Moreover, life-cycle management planning and optimization under a constrictive budget and performance constraints are presented through a probabilistic management framework. This framework can serve as a useful tool in risk mitigation and, in general, decision-making associated with engineering systems.

### **2.2 PERFORMANCE EVALUATION AND PREDICTION**

Performance of deteriorating infrastructure systems can be quantified at the cross-section, component, overall structural (system), group of structures (network), and networks of network levels. Typically, performance assessment activities associated with the components rely on visual inspections results. For bridges, visual inspection results are usually employed to establish a condition rating index to measure the bridge's remaining load-carrying capacity. The conditions of bridges in the United States are rated using two different methods based on visual inspection. The first method is using National Bridge Inventory (NBI) condition rating system (FHWA

2013). According to the NBI condition rating system, the condition evaluation corresponds to the physical state of the deck, superstructure, and substructure components of a bridge. The second method, Pontis, uses the element-level condition rating method to represent the conditions of bridge components. Generally, bridge management systems characterize the performance of structural elements by discrete condition states which incorporate predefined degrees of damage (Hawk and Small 1998; Thompson *et al.* 1998). Based on the identified condition states, maintenance interventions may be prioritized among all inspected structural components.

Several research efforts have integrated these discrete condition states within the life-cycle management and intervention optimization associated with deteriorating infrastructure systems. Most of these approaches incorporate Markov chain models to depict the structural deterioration process. In a Markov chain model, the current condition states of the investigated system's elements are considered to be dependent only on a finite number of previous states. The main element of a Markov chain model is the transition matrix that specifies the probability that the state of a component changes to another state within a specified period of time. A safety index can also be defined to model the life-cycle performance of deteriorating systems. Note that the condition index is a subjective measure which may not realistically reflect the true load-carrying capacity of structural members (Liu and Frangopol 2006b; Saydam *et al.* 2013b).

Although such an approach may ensure an adequate level of safety of components, it does not provide information about the interaction between the components and overall performance of the whole structure (Saydam and Frangopol

2011). Accordingly, other performance indicators capable of properly modeling the structural performance, while considering various uncertainties associated with resistance and load effects, have been developed and adopted in the life-cycle management of deteriorating infrastructure systems. Structural reliability theory offers a rational framework for quantification of system performance by including the uncertainties both in the resistance, load effects, and relevant correlations. In the following section, probabilistic performance analyses (e.g., reliability analysis) of bridge structures at component level and system level are presented.

### 2.2.1 Reliability

Structural reliability can be defined as the probability that a component or a system will adequately perform its specified purpose for a prescribed period of time under particular conditions (Leemis 1995; Paliou *et al.* 1990). Component, as well as system reliability can be computed for the investigated infrastructure considering that failure of a single component or a combination of individual components may initiate the failure of the system. For instance, if  $R$  and  $S$  represent the resistance and the load effect, respectively, PDFs,  $f_R$  and  $f_S$ , characterizing these respective random variables may be established. The probability that  $S$  will not exceed  $R$ ,  $P(R > S)$ , represents the reliability. As a general case, the time-variant probability of failure  $p_F(t)$  can be expressed in terms of joint probability density function (PDF) of the random variables  $R(t)$  and  $S(t)$ ,  $f_{R,S}(t)$ , as:

$$p_F(t) = \int_0^{\infty} \left( \int_0^S f_{R,S}(t) dr \right) ds \quad (2.1)$$

Furthermore, the reliability index can be expressed as:

$$\beta(t) = \Phi^{-1}(1 - p_F(t)) \quad (2.2)$$

where  $\Phi^{-1}(\cdot)$  is the inverse of the standard normal cumulative distribution function (CDF). In addition to identifying the structural reliability against failure, it is also possible to consider various functionality aspects that affect infrastructure systems such as serviceability limit states.

Overall, system reliability can be evaluated by modeling the bridge system failure as series or parallel or series-parallel combination of component limit states (Hendawi and Frangopol 1994). It is possible to evaluate the reliability of entire structural system by making appropriate assumptions (e.g., series, parallel, or combined system assumptions) (Czarnecki and Nowak 2007; Ditlevsen and Bjerager 1986; Galambos 1989; Rashedi and Moses 1988, Tang and Melchers 1988; Thoft-Christensen and Murotsu 1986; Vu and Stewart 2000) regarding the interaction between individual components. Another approach for reliability assessment of structural systems makes use of finite element (FE) analysis, if the overall non-linear system behavior is of interest. A proper statistical distribution for the output of FE analysis (e.g., stress, displacement, bending moment) can be obtained by repeating the analysis for a large number of samples of the random variables associated with the structure. However, for complex structures, the time required to repeat FE analysis many times may be impractical. In such cases, Response Surface Methods can be used to approximate the relation between the desired output of FE analysis and random variables by performing analyses for only a significantly less number of samples. Response Surface Methods have also been implemented in system reliability of bridge superstructures (Liu *et al.* 2001), substructures (Ghosn and Moses 1998), and bridge

systems (Moses *et al.* 1993; Okasha and Frangopol 2010b,d; Yang *et al.* 2004). Additionally, Enright and Frangopol (1999a,b) used the failure path method to compute the reliability function of a general (i.e., series-parallel) system and developed the computer program RELTSYS for this purpose (Enright and Frangopol 2000). Lifetime functions (Leemis 1995) are adopted for the time-dependent reliability approach, and have been utilized for the life-cycle performance prediction of bridge structures (Sabatino *et al.* 2016; Barone and Frangopol 2013, 2104a,b). Establishing the lifetime function system reliability may be carried out utilizing various methods such as the minimal path and cut sets approaches (Hoyland and Rausand 1994; Leemis 1995).

### 2.2.2 Risk

Risk is quantified by combining the probability of occurrence and the consequences of events generated by hazards. In general, the instantaneous total risk  $R$  of a structural system can be formulated as (CIB 2001)

$$R = \iiint \cdots \int \kappa(x_1, x_2, \dots, x_m) f_{\mathbf{X}}(x_1, x_2, \dots, x_m) \cdot dx_1 \cdot dx_2 \cdots dx_m \quad (2.3)$$

where  $\kappa(\mathbf{x})$  denotes the consequences associated with events resulting from certain hazards  $\mathbf{x}$  and  $f_{\mathbf{X}}(\mathbf{x})$  is the joint PDF describing the probabilistic behavior of the random variables  $\mathbf{X} = \{ X_1, X_2, \dots, X_m \}$ . The  $m$ -fold integral within Eq. (2.3) is difficult to assess and often cannot be solved. Therefore, assumptions are established in order to obtain a simpler expression for total risk. A simplistic approach for calculating instantaneous total risk  $R$  is (Ellingwood 2005)

$$RISK(t) = \sum_{i=1}^n C_m(t) \cdot P_{F|H_i} \cdot P(H_i) \quad (2.4)$$

where  $C_m$  represents the consequences of failure,  $P(H_i)$  describes the probability of occurrence of a hazard,  $P_{F|H_i}(t)$  is the conditional failure probability given the occurrence of a hazard, and  $n$  is the total number of hazards considered within the analysis.

Many research efforts have been conducted involving the risk assessment of bridge structures. Cesare *et al.* (1993) calculated the total risk associated with a bridge using the reliability and consequences of closure of the bridge. Stein *et al.* (1999) used risk concepts for prioritizing scour-vulnerable bridges. Adey *et al.* (2003) focused on the risk assessment of bridges affected by multiple hazards. Lounis (2004) presented a multi-criteria approach regarding bridge structural assessment with emphasis on risk. Similarly, Stein and Sedmera (2006) proposed a risk-based approach for bridges performance evaluation in the absence of foundation information. Ang (2011) focused on life-cycle considerations in risk-informed decision making for the design of civil infrastructure. Decò and Frangopol (2011) developed a rational framework for the quantitative risk assessment of highway bridges under multiple hazards. Saydam *et al.* (2013b) presented an illustrative example for the time-variant expected losses associated with the flexural failure of girders; a risk-based robustness index was calculated for an existing bridge. Furthermore, risk analysis was utilized to assess the performance of networks of infrastructure systems (Bocchini and Frangopol 2013; Dong *et al.* 2014e; Frangopol and Bocchini 2012). For example, the time-dependent expected losses of deteriorated highway bridge networks were investigated within

Saydam *et al.* (2013b). Additionally, Dong *et al.* (2014e,f) and Decò and Frangopol (2011, 2013) proposed a computational framework for the quantitative assessment of life-cycle risk of multiple bridges within a transportation network including the effects of seismic and abnormal traffic hazards. Overall, risk, as a performance indicator, can offer valuable information regarding the performance of individual structures or spatially distributed systems, such as buildings, bridges, and bridge networks.

### **2.2.3 Sustainability**

Within the field of life-cycle engineering, two definitions of sustainability are usually referred to when developing appropriate sustainability metrics. The first representation of sustainability defines it as: “meeting the needs of the present without comprising the ability of future generations to meet their own needs” (Adams 2006). The second definition complements the first one by emphasizing that economic, environmental, and social objectives must be simultaneously satisfied within a sustainable design or plan (Elkington 2004). In general, it is important to measure the performance of bridges and networks of structural systems whose functionality is vital for economic and social purposes. Generally, sustainability should be quantified in terms of economic, social, and environmental metrics as indicated in Figure 2.1.

Recent research efforts have considered a wide variety of risks in order to effectively quantify sustainability. For instance, Dong *et al.* (2013) presented a framework for assessing the time-variant sustainability of bridges associated with multiple hazards considering the effects of structural deterioration. The proposed approach was illustrated on a reinforced concrete bridge and the consequences

considered within the risk assessment were the expected downtime and number of fatalities, expected energy waste and carbon dioxide emissions, and the expected loss. Overall, the inclusions of societal and environmental impacts along with economic consequences effectively encompass the concept of sustainability within the risk analysis framework. Combining the economic, societal, and environmental, risk metrics allows engineers and decision makers to make informed decisions based on sustainability by providing them with a complete picture of system performance (Lundie *et al.* 2004; Marzouk and Hisham 2011; Shinozuka 2008). Generally, a structure is more sustainable if its life-cycle cost (i.e., construction, maintenance, failure, and replacement costs) is relatively low. Similarly, a structure is more sustainable if the energy, carbon dioxide emissions, and user delays arising from its repair are low. In general, the social metrics can include downtime and fatalities.

Utility theory is utilized in order to depict the relative desirability of maintenance strategies to the decision maker. In general, utility is defined as a measure of value to the decision maker. Utility theory provides a framework that can measure, combine, and consistently compare these relative values (Ang and Tang 2007). Multi-attribute utility theory may be used to transfer the utility of each attribute involved in the performance assessment (e.g., economic, social, and environmental risks) into one utility value that effectively combines the effects of all risks investigated as shown in Figure 2.2. In this process, it is usually assumed that there is a single decision maker who possesses a predetermined risk attitude with respect to a specific structural system. Next, all possible solution alternatives are identified and the uncertainties associated with the investigated decision making

problem are accounted for by using a probabilistic approach. Since technical and economic uncertainties are both expected and unavoidable in the life-cycle assessment of civil infrastructure systems, decisions regarding life-cycle management must consider all relevant uncertainties associated with the probability of failure and its corresponding consequences.

Utility theory is employed herein in order to effectively capture the sustainability performance of highway bridges and bridge networks and impact of the decision maker's risk attitude. Once the utility function associated with each attribute of sustainability is appropriately established, a multi-attribute utility that effectively represents all aspects of sustainability can be obtained by combining the utility functions associated with each attribute (Sabatino *et al.* 2016). Within the additive formulation for the multi-attribute utility function, utility values associated with each attribute are multiplied by weighting factors and summed over all attributes involved. The multi-attribute utility associated with a structural system can be computed as (Jiménez *et al.* 2003)

$$u_S = k_{Eco}u_{Eco}(Eco) + k_{Soc}u_{Soc}(Soc) + k_{Env}u_{Env}(Env) \quad (2.5)$$

where  $k_{Eco}$ ,  $k_{Soc}$ , and  $k_{Env}$  are the weighting factors corresponding to each sustainability metric;  $u_{Eco}$ ,  $u_{Soc}$ , and  $u_{Env}$  are the utility functions for the economic, social, and environmental attributes, respectively; and  $Eco$ ,  $Soc$ , and  $Env$  are the values of the three metrics associated with sustainability. Overall, the proposed global strategies may be adopted for a variety of applications, including but not limited to bridges, buildings, and infrastructure networks.

#### 2.2.4 Lifetime functions

This approach for performance quantification involves identifying the PDF of the time-to-failure of a component under investigation. The time-to-failure of a component, treated as a random variable is defined as the time elapsing from the time the component is put into operation until it fails for the first time (Hoyland and Rausand 1994). The exact choice of this PDF is heavily dependent upon the component characteristics and failure pattern. This PDF serves as the basis for calculating a few useful lifetime reliability measures such as the survivor and hazard functions. The survivor function  $S(t)$  represents the probability that a component will not fail before time  $t$  and is calculated as:

$$S(t) = 1 - F(t) = P(T > t) = \int_t^{\infty} f(u) du \quad (2.6)$$

where  $F(t)$  denotes the cumulative probability of failure and  $f(u)$  is the original PDF of time-to-failure. A depiction of the survivor function is shown in Figure 2.3. The survivor function may be used as a basis to calculate other lifetime functions. For example, the availability of a component  $A(t)$ , which is defined as the probability that the component is functioning at a given time instant, coincides with  $S(t)$  when no maintenance is considered (Ang and Tang 1984; Leemis 1995). The availability function has been employed in assessing the effects of implementing intervention strategies to existing civil infrastructure (Biswas *et al.* 2003; Barone and Frangopol 2014a,b).

The hazard function  $h(t)$  is also known as the instantaneous failure rate and can be defined as the conditional probability that given a component has survived until time  $t$  it will fail in the time interval  $t + dt$ . The hazard function is calculated as follows (Leemis 1995).

$$h(t) = \frac{f(t)}{S(t)} \quad (2.7)$$

Barone and Frangopol (2013) highlight the use of the hazard function in reliability analysis of components and systems. The hazard function was used to provide optimal inspection/repair lifetime planning strategies for deteriorating structures via an iterative procedure. The hazard function is also applied to an existing deteriorating bridge deck under corrosion to determine its performance.

### 2.2.5 *Life-cycle cost*

One of the most important measures in the evaluation of bridge performance is life-cycle cost. The proper allocation of resources can be achieved by minimizing the total cost while keeping structural safety at a desired level. The expected total cost during the lifetime of a bridge structure can be expressed as (Frangopol *et al.* 1997)

$$C_{ET} = C_T + C_{PM} + C_{INS} + C_{REP} + C_F \quad (2.8)$$

where  $C_T$  is the initial cost;  $C_{PM}$  is the expected cost of routine maintenance cost;  $C_{INS}$  is the expected cost of inspections;  $C_{REP}$  is the expected cost of repair; and  $C_F$  is expected failure cost. Numerous research efforts have focused on balancing cost and performance to determine optimum planning for life-cycle management of civil infrastructure systems (Ang and De Leon 2005; Chang and Shinozuka 1996; Estes and

Frangopol 2005; Estes *et al.* 2004; Frangopol and Furuta 2001; Frangopol *et al.* 1997, 2001; Gharaibeh and Frangopol 2000; Okasha and Frangopol 2010d).

### **2.3 LIFE-CYCLE ASSESSMENT, MANAGEMENT, AND OPTIMIZATION**

In order to predict performance of structural systems during their life-cycle under uncertainty, deterioration mechanisms for the investigated systems (e.g., corrosion and fatigue) must be carefully considered. Aggressive environmental conditions and natural ageing processes facilitate a gradual reduction in the performance (e.g., system reliability) of existing structures. Alternatively, there are extreme events that cause an abrupt reduction of the functionality of structures such as blasts, fires, earthquakes, hurricanes, and terrorist attacks. Life-cycle assessment of deteriorating highway bridges has uncertainties that are present within modeling the structural resistance (e.g., material properties and element dimensions), the occurrence and magnitude of hazards that may impact the structure (e.g., corrosion, fatigue, earthquakes, floods, and hurricanes), operating conditions, and loading cases (in addition to those associated with the cost of interventions performed during the service life. Due to the uncertainties associated with loads, resistances, and modelling, it is imperative for structural engineers to accurately model and assess the structural performance within a probabilistic life-cycle context. Furthermore, the effects of maintenance, repair, and rehabilitation on structural life-cycle performance must be well understood. The influence of maintenance and repairs on structural performance can be incorporated in a generalized framework for multi-criteria optimization of the life-cycle management of infrastructure systems (Frangopol 2011; Frangopol *et al.* 2015b,2017). Within the

last two decades, several studies introduced techniques which can assist the infrastructure management, including: Biondini *et al.* (2008, 2014), Enright and Frangopol, (1999a,b), Estes and Frangopol (2001), Frangopol and Liu (2007), Frangopol and Okasha, (2009), Frangopol and Soliman (2016), Frangopol *et al.* (2004), Kong and Frangopol (2003, 2005), Kong *et al.* (2002), Morcouc and Lounis (2005), Neves *et al.* (2006), Okasha and Frangopol (2010b), and Stewart and Rosowsky (1998).

In general, the effects of maintenance on the probabilistic performance assessment and cost evaluation are depicted in Figure 2.4. Within this figure, the probabilistic aspect of performance prediction is illustrated by the representations of the probability density functions (PDFs) of the initial performance index, deterioration initiation, rate of deterioration, and service life without maintenance, with preventive maintenance (PM), and with both preventative and essential maintenance (EM). In general, preventive maintenance is applied at a predefined time, in order to delay the deteriorating process of a structural system and to keep the bridge above the required level of structural performance. Preventive maintenance actions for a deteriorating infrastructure system includes replacing small parts, patching concrete, repairing cracks, changing lubricants, and cleaning and painting exposed parts, among others. On the other hand, essential maintenance is typically a performance-based intervention. As depicted in Figure 2.4(a), essential maintenance is applied when the performance level reaches a predefined threshold. Essential maintenance actions can lead to higher levels of performance than preventive maintenance actions, but they typically cost more. Strengthening and replacement of structural components are

examples of essential maintenance actions. Furthermore, the effects of maintenance on the total cost of life-cycle management must be considered; Figure 2.4(b) shows the cumulative maintenance cost as a function of time for preventive and essential maintenance interventions.

Life-cycle optimization is an essential task within the life-cycle management (LCM) framework (Ang and De Leon 2005; Chang and Shinozuka 1996; Estes and Frangopol 1999; Frangopol and Soliman 2015; Frangopol *et al.* 2015b,2016a,2016b,2017; Okasha and Frangopol 2009; Sabatino *et al.* 2015; Soliman and Frangopol 2014; Soliman *et al.* 2013, Wen and Kang 2001; Yang *et al.* 2006b). This process is performed using a probabilistic platform considering various uncertainties associated with LCM as shown in Figure 2.5. A lifetime intervention optimization formulation requires one or more life-cycle performance indicators, such as system reliability (Augusti *et al.* 1998, Estes and Frangopol 1999), system reliability and redundancy (Okasha and Frangopol 2009), lifetime-based reliability (Yang *et al.* 2006b), lifetime-based reliability and redundancy (Deb 2001; Deb *et al.* 2002; Goldberg 1989; Morcous *et al.* 2010; Okasha and Frangopol 2010b), cost and spacing of corrosion rate sensors (Marsh and Frangopol 2007), probabilistic condition and safety indices (Frangopol and Liu 2007; Liu and Frangopol 2006a,b; Neves and Frangopol 2005; Neves *et al.* 2004), damage detection delay (Kim and Frangopol 2011a,c, 2017), probability of damage detection (Soliman *et al.* 2013), and risk and sustainability-informed performance assessment (Dong *et al.* 2014a,b,c,d,e; Frangopol and Sabatino 2016a,b; Sabatino *et al.* 2015, 2016; Zhu and Frangopol 2013c).

For example, planning retrofit actions on bridge networks under tight budget constraints were investigated by Dong *et al.* (2014f). They presented a probabilistic methodology to establish optimum pre-earthquake retrofit plans for bridge networks based on sustainability. A multi-criteria optimization problem was formulated to find the optimum timing of retrofit actions for bridges within a network. The role of optimization is to identify the most effective retrofit strategy in terms of which bridges to be retrofitted and the optimal times for retrofit actions.

Next, utility-informed decision making is investigated. In general, utility-informed decision making may be divided into five separate stages: the pre-analysis, problem set-up, uncertainty quantification, utility assignment, and optimization as shown in Figure 2.6 (Keeney and Raiffa 1993). The application of utility-informed decision making in the optimal lifetime intervention on bridges is a topic of paramount importance and is experiencing growing interest within the field of life-cycle infrastructure engineering. The proposed methodology can be used in assisting decision-making regarding the maintenance/retrofit activities to improve the performance of highway bridge network.

## **2.4 PROPOSED METHODOLOGY**

The formulation of a comprehensive life-cycle framework that has the ability to model a structural system while considering various deterioration models (e.g. corrosion and increase of live loads), multiple hazard effects, and the impact of structural failure on society, the environment, and the economy is crucial for the successful management of the structure. The ultimate goal of this study is to extend the existing life-cycle

management framework to include the effect of multiple hazards and a more comprehensive probabilistic risk assessment with consideration of risk attitudes of decision makers. A depiction of the proposed methodology is presented within Figure 2.7. The novel part of this framework is contained within the blue-shaded, pentagon shapes within Figure 2.7. The contributions of the proposed research fit into the procedures for calculating expected losses of a structural system and for carrying out optimization techniques. The expected losses consider multi-hazard effects as well as the impact of the risk attitude of the structure's decision maker. Novel optimization procedures are implemented that employ utility as objectives to be maximized.

Within a robust risk assessment, it is crucial to consider the economic, social, and environmental impacts of structural failure. Sustainability assessment involves the integration of these various risk values into a convenient index used to measure performance. In general, it is important to measure the performance of infrastructure systems and networks of structural systems whose functionality is vital for economic and social purposes (Saydam *et al.* 2013a). Recent research efforts have considered a wide variety of risks in order to effectively quantify sustainability. For instance, the time-dependent expected losses of deteriorated highway bridge networks were investigated within Saydam *et al.* (2013a). A five-state Markov model was proposed to predict the time-dependent performance of bridges within a network. The probabilistic variation of direct, indirect, and total expected losses in time was computed. The proposed approach was illustrated on an existing highway bridge network in the lower San Francisco Bay Area, California. Additionally, Dong *et al.* (2013) presented a framework for assessing the time-variant sustainability of bridges

associated with multiple hazards considering the effects of structural deterioration. The proposed approach was illustrated on a reinforced concrete bridge and the consequences considered within the risk assessment were the expected downtime and number of fatalities, expected energy waste and carbon dioxide emissions, and the expected loss. Overall, the inclusions of societal and environmental impacts along with economic consequences effectively encompass the concept of sustainability within the risk analysis framework. Combining the economic, societal, and environmental, risk metrics allows engineers and decision makers to make informed decisions based on sustainability by providing them with a complete picture of system performance.

In general, utility-based decision making may be divided into five separate stages: the pre-analysis, problem set-up, uncertainty quantification, utility assignment, and optimization, as shown in Figure 2.6 (Keeney and Raiffa 1993). In this process, it is usually assumed that there is a single decision maker who possesses a predetermined risk attitude with respect to a specific structural system. Next, all possible solution alternatives are identified and the uncertainties associated with the investigated decision making problem are accounted for by using a probabilistic approach. Since technical and economic uncertainties are both expected and unavoidable in the life-cycle assessment of civil infrastructure, decisions regarding life-cycle management must consider all relevant uncertainties associated with the probability of structural failure and its corresponding consequences (Ang 2011). For instance, life-cycle management problems involving deteriorating highway bridges have uncertainties that are present within modeling the structural resistance (e.g.,

material properties and element dimensions), the occurrence and magnitude of hazards that may impact the structure (e.g., corrosion, fatigue, earthquakes, floods, and hurricanes), operating conditions, and loading cases (Stewart 2001), in addition to those associated with the cost of interventions performed during the service life.

After effectively incorporating the appropriate uncertainties, the decision maker may assign utility values to the investigated attributes (e.g. risk attributes) associated with each alternative considering his/her risk attitude. Utility theory is applied in order to normalize each attribute value corresponding to solution alternatives to a number between 0 and 1; this ensures that all attributes are directly comparable to each other. The formulation of the utility function corresponding to each attribute depends on the knowledge, preferential characteristics, and risk attitude of the decision maker. Within the last step of the utility-based decision making framework an optimization procedure is carried out in order to find the alternative that maximizes the utility value.

Once the time-variant risks affecting a deteriorating system are calculated (e.g., using Eq. 2.4), the decision maker may assign utility values to the attributes associated with each alternative considering his/her risk attitude. As an example, the computational procedure for the multi-attribute utility assessment of a highway bridge subjected to a corrosive environment and time-increasing traffic loading is shown in

Figure 2.2, where  $u_i$  and  $k_i$ , respectively, are the utility function and associated weighting factor corresponding to the  $i$ th risk attribute. A multi-attribute utility value is established that effectively represents sustainability performance by consolidating economic, social, and environmental risks.

For the risk attributes analyzed, each of the corresponding utility functions may be formulated as monotonically decreasing functions. Considering an exponential formulation, the utility associated with a single attribute (e.g., economic, social, and environmental risks) can be expressed as (Ang and Tang 1984):

$$u_{RA} = \frac{1}{1 - \exp(-\gamma)} \left[ 1 - \exp\left(-\gamma \frac{RA_{\max} - RA}{RA_{\max} - RA_{\min}}\right) \right] \quad (2.9)$$

where  $RA$  is the mean of the risk attribute value under investigation,  $RA_{\max}$  and  $RA_{\min}$  denote the maximum and minimum value of the risk attribute, respectively, and  $\gamma$  is the risk attitude of the decision maker (i.e.,  $\gamma > 0$  indicates risk-aversion and  $\gamma < 0$  denotes risk-acceptance). A monotonically decreasing function that has bounds of 0 and 1 must be utilized within the utility assignment procedure in order to accurately depict the relative utility of detrimental consequences.

Qualitative plots of the exponential utility function corresponding to a single risk attribute with variable risk attitude, considering the exponential formulation, are provided in Figure 2.8. As indicated by Keeney and Raiffa (1993), for a single risk attribute,  $u_{RA} = 1$  corresponds to the lowest possible loss while  $u_{RA} = 0$  is associated with the largest possible loss. Alternatives associated with high utility values are usually preferred to those associated with small utility values (Howard and Matheson 1989). The concavity of these utility functions is highly dependent on the risk attitude of the decision maker. Risk averse and risk accepting attitudes yield concave and convex utility functions, respectively.

After the utility function associated with each risk attribute is appropriately established, multi-attribute utility theory may be employed to combine them into a

single utility value that effectively represents a sustainability performance metric. Although there are various established types of multi-attribute utility functions, the additive formulation is utilized herein. Within the additive formulation for the multi-attribute utility function, marginal utility values associated with each attribute are multiplied by weighting factors and summed over all attributes investigated, as shown in Eq. 2.5 (Stewart 1996).

Once the appropriate multi-attribute utility-based sustainability metric is established, it may be utilized within a life-cycle optimization to find the best intervention strategies for the investigated structure. In general, the presented generalized decision-support approach may be used to determine optimal repair, rehabilitation, and monitoring interventions. Accordingly, the effect of interventions on the sustainability performance must be examined. Within the generalized decision making methodology presented, two objectives, represented in terms of utility, can be simultaneously maximized: (a) the relative value of investment costs considering the risk attitude of the decision maker  $u_c$ , and (b) the sustainability of each alternative expressed in terms of the utility  $u_s$ . The cost associated with implementing optimal lifetime maintenance actions may be expressed in terms of utility by employing Eq. 6. Given the maximum cost investment that the decision maker can tolerate, a utility function representative of cost considering the attitude of the decision maker may be established. The formulation of the cost utility  $u_c$  effectively captures the decision maker's preference to investing money in the face of risk.

The cost  $u_c$  and sustainability  $u_s$  utilities are used within a multi-criteria optimization process as the objective functions to be maximized. More specifically,

this optimization maximizes the minimum annual utility associated with sustainability while simultaneously maximizing the utility associated with the total maintenance cost. Generally, if the utility values of all the alternatives are available, the solution with the highest utility value is always preferred (Howard and Matheson 1989); thus, the two utility objectives are maximized within the presented optimization procedure. The main output of this bi-objective optimization, often carried out by using genetic algorithms (Davis 1991) in MATLAB (MathWorks 2013), comes in the form of a Pareto-optimal solution set that depicts optimal solutions outlining lifetime maintenance schedules. A solution is Pareto-optimal if there does not exist another solution that improves at least one objective without worsening another one. A plot depicting Pareto fronts for the lifetime maintenance planning of a bridge, considering a varying risk attitude, is shown in Figure 2.9. Within this example, the weighting factors associated with marginal economic, social, and environmental utilities are all assumed to be equal to 1/3; essentially, the decision maker weighs all three risks equally within the sustainability assessment.

Embedded within each Pareto solution contained in Figure 2.9 are the optimum maintenance plans that detail which structural components should be maintained and the optimum maintenance time. In this case, the investigated bridge has a predetermined lifetime of  $T_L$  years and three maintenance actions may be implemented throughout its life-cycle. Representative solutions A and B, denoting typical optimum maintenance plans resulting from a risk averse and risk accepting decision maker, respectively, are shown in Figure 2.9. The time-variant multi-attribute utilities associated with sustainability corresponding to representative solutions A and B are

shown in Figure 2.10a. Similarly, the economic risk profiles associated with solutions A and B are depicted in Figure 2.10b. In general, these plots show that the multi-attribute utility assessment of sustainability is highly dependent upon the risk attitude of the decision maker.

In general, the methods presented herein can be utilized to facilitate informed decision making regarding the lifetime intervention scheduling of deteriorating infrastructure. Although bridge and ship applications are emphasized in this study, the proposed generalized decision making framework can be applied to variety of engineering systems, including, but not limited to, other civil infrastructure (e.g., buildings, tunnels, dams, levees, and roads), aerospace systems (e.g., space structures and airplanes), and construction management applications. If the proposed methodology is applied to a new system, the initial steps (i.e., modules 1 and 2 within Figure 1.1) would be modified accordingly to account for properties of the structure and its loading cases, in addition to integrating relevant performance metrics for the system under investigation.

Overall, multi-attribute utility theory can be used to formulate a utility-based sustainability index which offers a measure of desirability of a given management alternative to the decision maker. An approach that incorporates multi-attribute utility theory provides a framework which can measure, combine, and consistently compare the relative values of different alternatives while taking into account the decision maker's attitude.

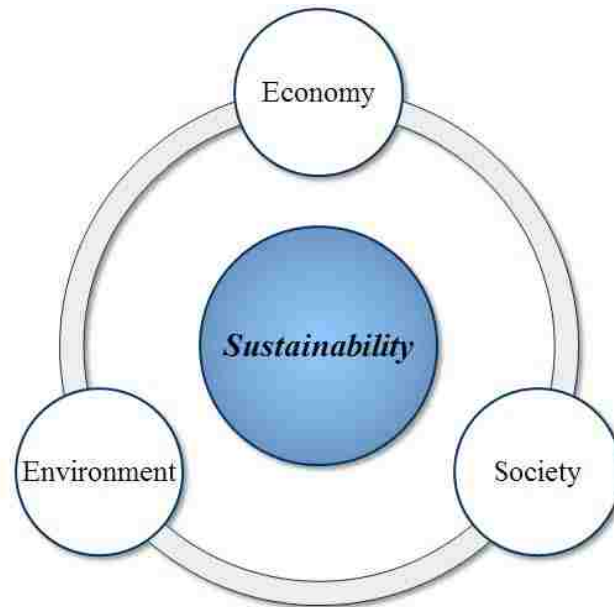


Figure 2.1. Metrics of sustainability.

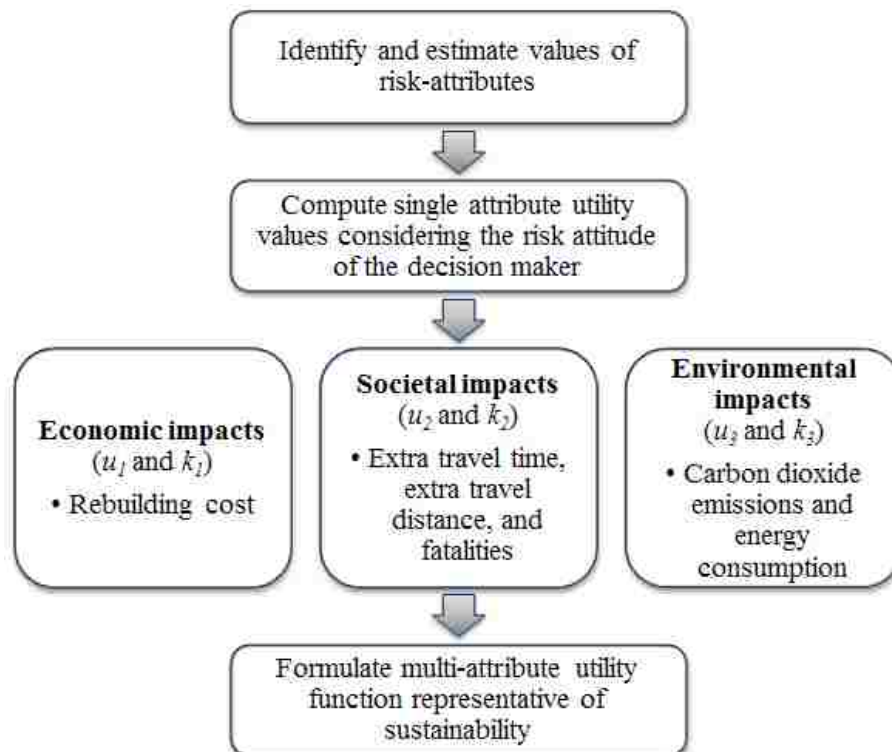


Figure 2.2. Multi-attribute utility-based sustainability assessment.

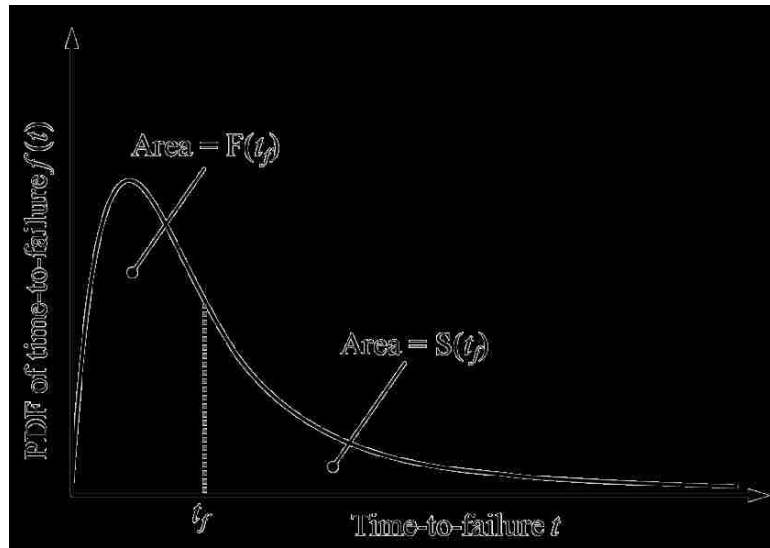


Figure 2.3. Relationship between the PDF of the time-to-failure  $f(t)$ , the survivor function  $S(t)$ , and the cumulative probability of failure  $F(t)$ .

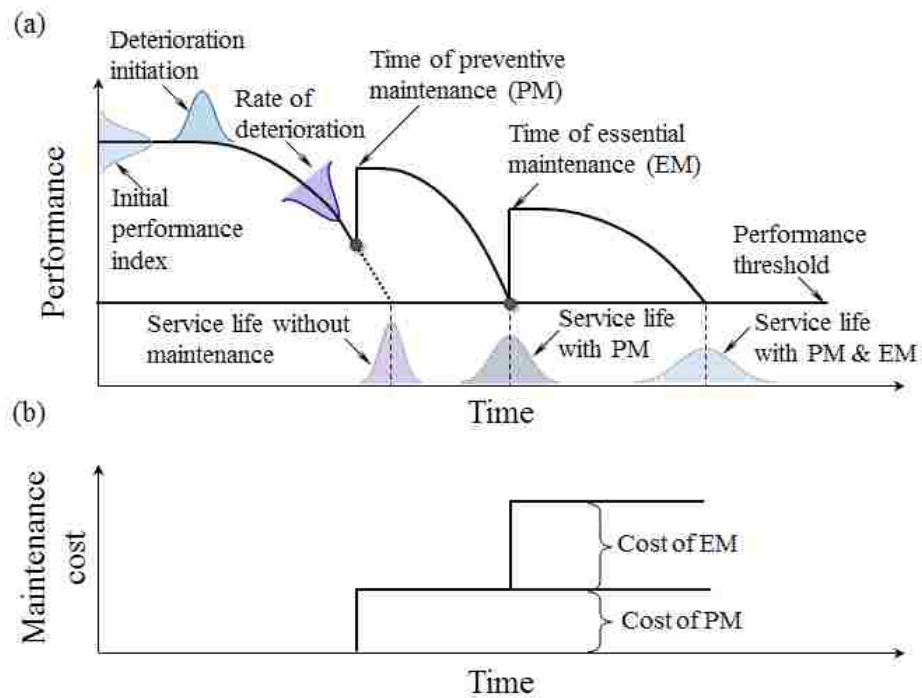


Figure 2.4. Effect of gradual deterioration and essential and preventive maintenance on (a) structural performance and (b) cost.



Figure 2.5. Integrated life-cycle management framework.

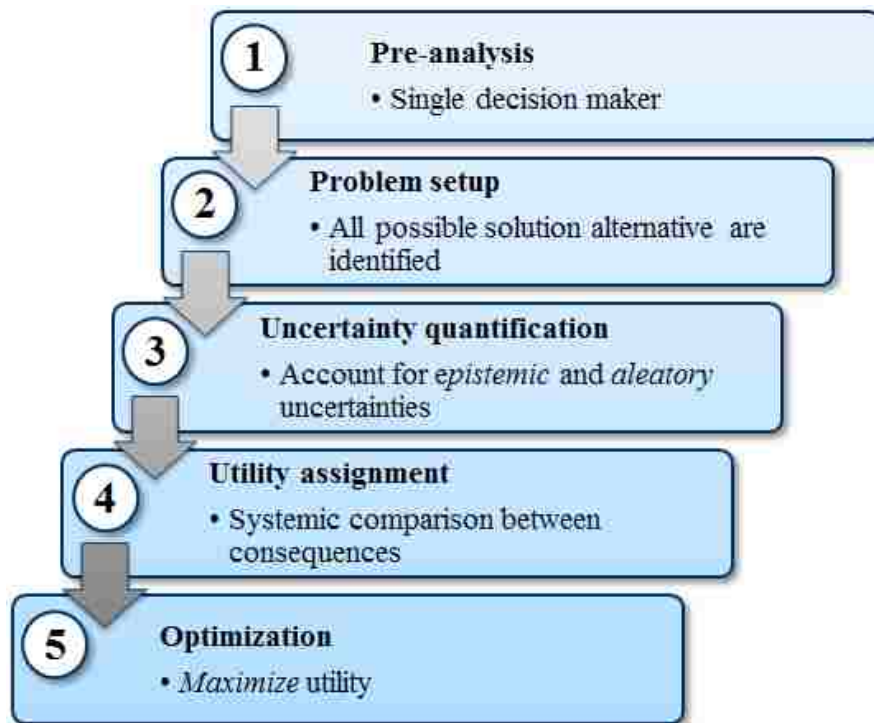


Figure 2.6. Utility-based decision making procedure.

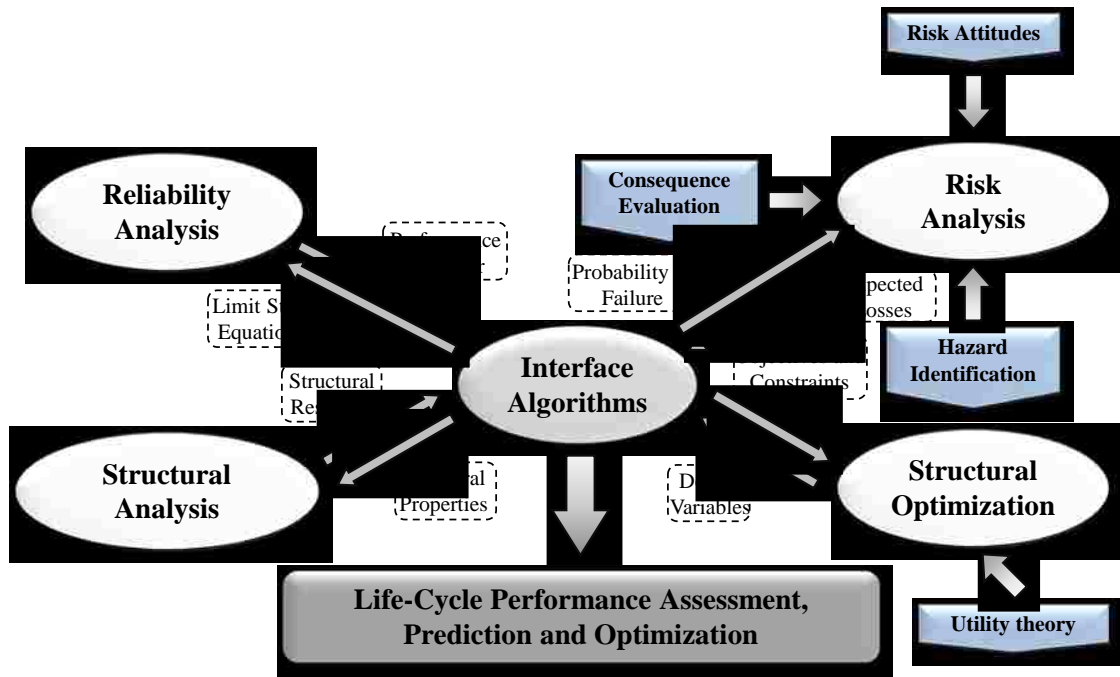


Figure 2.7. Computational framework for the life-cycle management of structures.

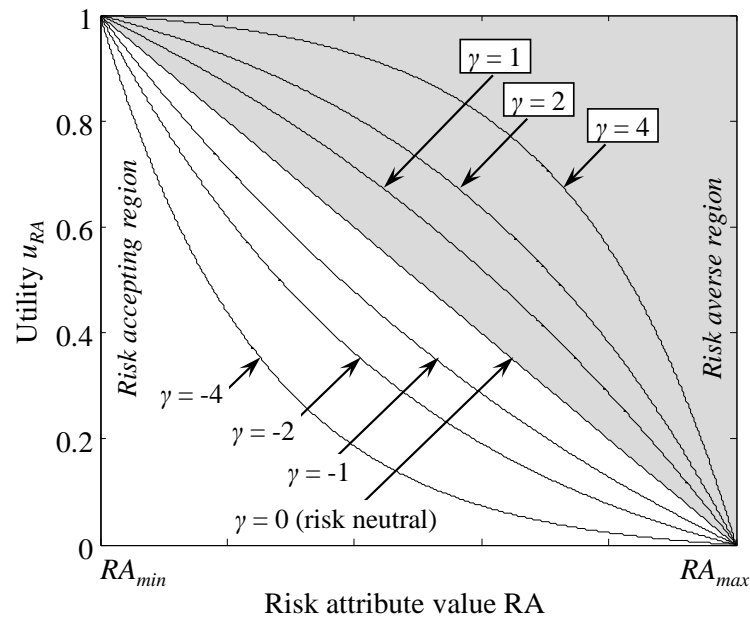


Figure 2.8. Qualitative representations of typical exponential utility functions that are monotonically decreasing as the expected value of the risk attribute value increases.

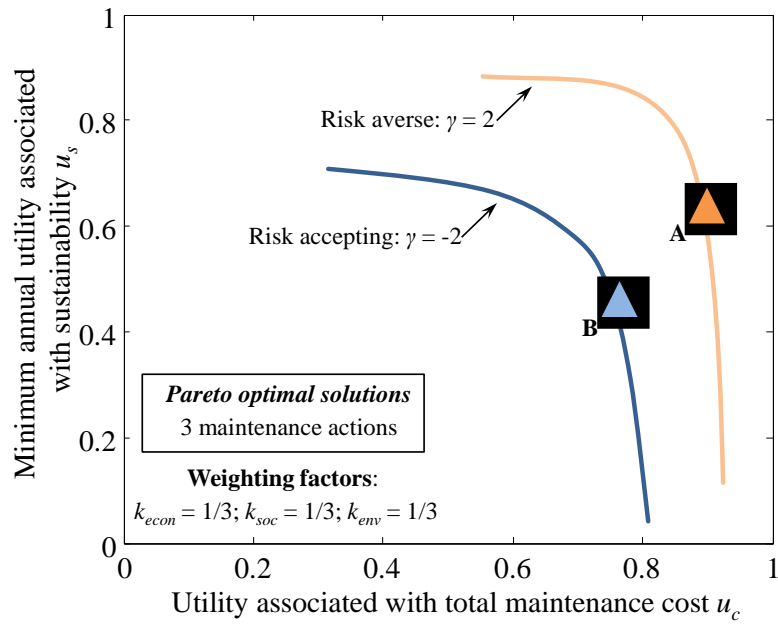


Figure 2.9. Effect of risk attitude on the optimal solutions for lifetime maintenance considering weighting factors equal to one third

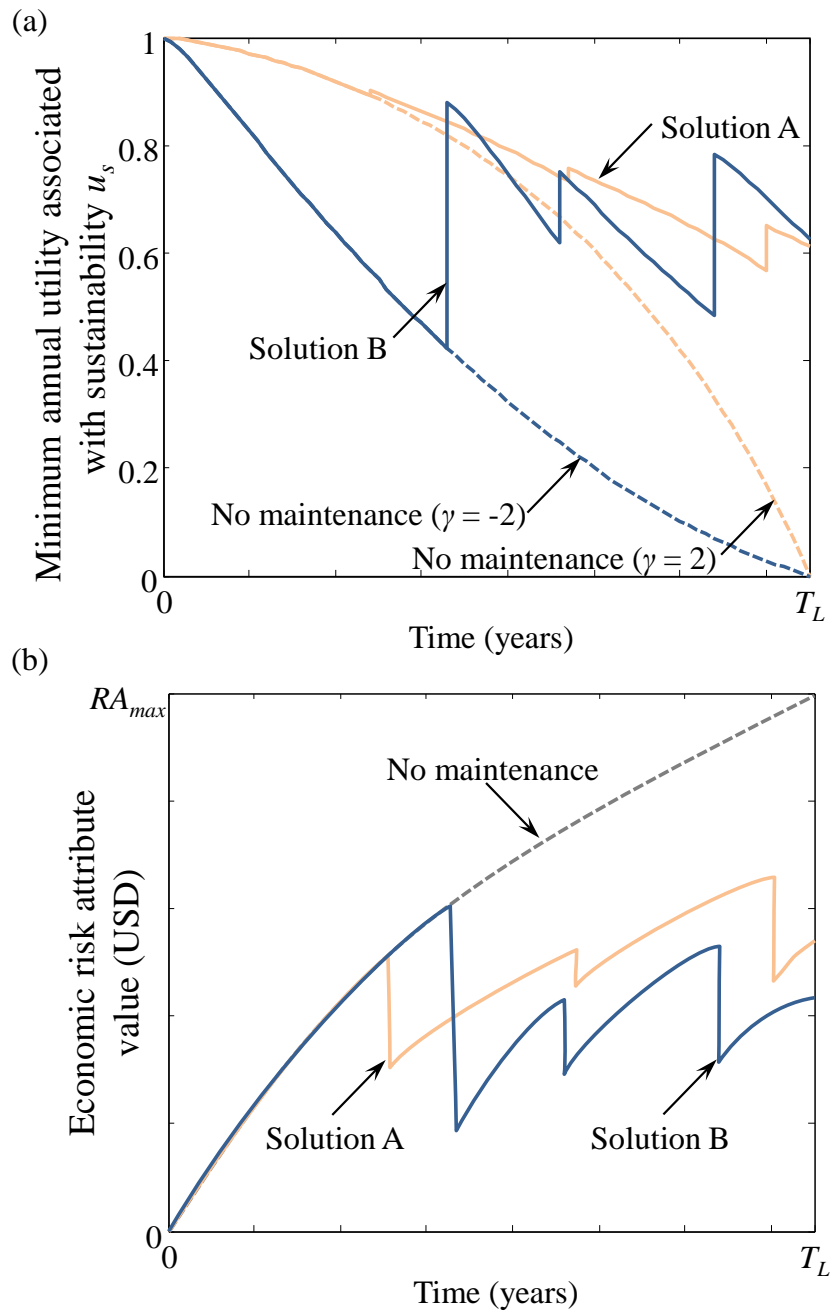


Figure 2.10. Time-variant profiles of (a) utility associated with sustainability and (b) economic risk for representative solutions A and B in Figure 2.9.

# **CHAPTER 3 SUSTAINABILITY-INFORMED MAINTENANCE OPTIMIZATION OF HIGHWAY BRIDGES CONSIDERING MULTI-ATTRIBUTE UTILITY AND RISK ATTITUDE**

## **3.1 OVERVIEW**

Throughout their service life, highway bridges deteriorate due to increasing traffic loads and aggressive environmental conditions. Aging of materials can have significant effects on the structural performance of highway bridges. A comprehensive risk assessment procedure is crucial in evaluating and ultimately mitigating detrimental consequences of structural failure to the economy, society, and the environment. The proposed sustainability-based maintenance optimization decision-support framework provides decision makers with optimal life-cycle maintenance actions that balance conflicting objectives. Utility theory is employed herein in order to effectively capture the sustainability performance of highway bridges and impact of the decision maker's risk attitude. The main objective of this framework is to reduce the extent of the consequences of structural failure to the economy, society, and the surrounding environment. The capabilities of the proposed approach are demonstrated on an existing highway bridge.

This chapter is based on the work published in Sabatino *et al.* (2015); Dong *et al.* (2014a,b,c,d, 2015, 2017); and Frangopol and Sabatino (2016a,b).

## **3.2 INTRODUCTION**

Throughout their service life, highway bridges may be exposed to a multitude of stressors, including aggressive chloride environmental conditions, material aging, and

increasing loads due to traffic. These stressors cause the structural performance of highway bridges to gradually decrease over time leading ultimately to structural failure. The consequences associated with structural failure due to progressive deterioration can be large and widespread. In order to mitigate the detrimental impacts of structural failure, risk and sustainability indicators are utilized within an efficient life-cycle maintenance optimization procedure to find maintenance strategies that balance both cost and performance. The results from this optimization may be employed within a risk-informed decision making process.

The decision-making paradigm associated with the optimal maintenance of civil structures is a fundamental concept studied within the field of life-cycle structural engineering. Generally, five separate stages of decision making may be considered: the pre-analysis, problem set-up, uncertainty quantification, utility assignment, and optimization (Keeney and Raiffa 1993). First, it is assumed that there is a single decision maker who possesses a predetermined risk attitude with respect to a specific structural system. Next, typically, all possible solution alternatives are identified and the uncertainties corresponding to the decision-making problem are recognized and accounted for using a probabilistic approach. After effectively incorporating the appropriate uncertainties, the decision maker can assign utility values to the consequences associated with each alternative. Lastly, an optimization procedure is carried out in order to find the alternative that maximizes the utility value.

Within the proposed decision support system for life-cycle maintenance planning of highway bridges, several attributes, including economic, societal, and environmental impacts, are considered in quantifying the consequences of structural

failure in terms of risk (i.e., probability of failure occurrence multiplied by its associated consequence). Previous research efforts have effectively performed risk analyses in a qualitative (Hessami 1999; Ellingwood 2001) and quantitative manner (Pedersen 2002; Decò and Frangopol 2011, 2012, 2013; Barone and Frangopol 2014a; Barone *et al.* 2014) under a multitude of hazards for various structures. In general, structural components that are under relatively high risk should receive priority for maintenance interventions. Although there have been a wide variety of studies investigating quantitative risk assessment, these studies do not attempt to quantify sustainability. In this chapter, risk assessment techniques are combined with multi-attribute utility theory to formulate an appropriate sustainability performance indicator.

Optimal maintenance planning is a widely investigated topic within the field of life-cycle engineering. Studies concerning the optimization of maintenance strategies based on reliability, risk, and/or redundancy have been conducted (Barone *et al.* 2014; Mori and Ellingwood 1994; Okasha and Frangopol 2009; Zhu and Frangopol 2013b). Additionally, lifetime distributions have also been used within maintenance optimization applications in (Yang *et al.* 2006) and (Okasha and Frangopol 2010b). In this chapter, structural performance is formulated in terms of multi-attribute utility that effectively represents the sustainability indicator. This novel utility-based sustainability metric is utilized as an objective within an optimization procedure that determines the best essential maintenance strategies for highway bridges. Additionally, a second objective that represents life-cycle maintenance costs is

integrated within the proposed framework. Therefore, a robust decision support system that simultaneously maximizes performance and minimizes cost is obtained.

The methodology utilized herein quantifies the sustainability of existing highway bridges and employs multi-criteria optimization techniques to find the best maintenance strategies. Within this approach, the desirability of each alternative (i.e., maintenance plan detailing the type and timing of interventions) depends on three risk-attributes (i.e., economic, social, and environmental impacts), measured with different units. Ultimately, there is a need to establish a consistent range of values that each attribute may take so that the attributes are directly comparable to each other. Utility theory is applied in order to normalize each risk-attribute value to a number between 0 and 1. The formulation of the utility function corresponding to each attribute greatly depends on the knowledge and preferential characteristics of the decision maker. Monotonically decreasing functions are employed to effectively depict the relative utility of detrimental consequences of the structural failure of deteriorating highway bridges. A final multi-attribute utility function is developed that considers the weighted relative utility value corresponding to each attribute involved. This function represents a sustainability metric that effectively weighs the contribution of impacts to the economy, society, and the environment.

The multi-attribute utility methodology adopted herein was first suggested in (Dong *et al.* 2015) where a sustainability performance indicator including the consequences of structural failure on the economy, society, and the environment was proposed. Besides the work reported in (Dong *et al.* 2015), there has been a lack of relevant studies that utilize multi-attribute utility theory within the structural

engineering field. Furthermore, little research has been carried out that includes optimization within multi-criteria decision making problems (Coello Coello 2000). Among this small pool of studies, (Papanikolaou *et al.* 2010) employed multi-objective optimization procedures to facilitate decision making regarding oil tanker design, (Grierson 2008) developed a multi-criteria decision making strategy that is applied to bridge maintenance-intervention protocol design, and (Dabous and Alkass 2008) proposed a multi-criteria decision support method for bridge deck management. In this chapter, multi-attribute utility theory is employed to effectively quantify the sustainability of highway bridges and determine optimal lifetime maintenance plans. This sustainability indicator quantifies the detrimental impacts of bridge failure due to increasing live loads and an aggressive corrosive environment, while the sustainability metric proposed by (Dong *et al.* 2015) was employed to assess the effects of seismic hazard on a network of multiple highway bridges. Overall, the main novelty of this work is the development of a sustainability performance indicator that has the ability to incorporate a wide variety of risks associated with structural failure of highway bridges. This performance indicator is integrated within a bi-objective optimization that determines optimal maintenance planning while balancing cost and performance.

Additionally, a four-objective optimization procedure is applied in this chapter to determine optimal maintenance schedules. The illustrative example contained herein examines the lifetime maintenance optimization problem that simultaneously maximizes utility associated with the maintenance cost and the utilities corresponding to economic, societal, and environmental risks. The results of this four-objective

optimization may be utilized in order to determine appropriate values of weighting factors for further use in the multi-attribute utility assignment.

The proposed methodology has the ability to quantify sustainability-based performance in terms of utility and effectively employs multi-criteria optimization procedures in order to determine optimum maintenance strategies that reduce the extent of detrimental consequences to the economy, society, and the surrounding environment, while simultaneously minimizing maintenance costs. The utility values of both the cost and performance corresponding to alternatives are utilized within an optimization procedure that determines optimal maintenance plans for highway bridges. The effects of the risk attitude and preferences of the decision maker, in addition to the number of maintenance interventions on the optimal maintenance strategies, are investigated. Furthermore, optimal maintenance strategies obtained considering the simultaneous maximization of four utility values are investigated as motivation for choosing appropriate weighting factors within the multi-attribute utility assessment. A genetic algorithm (GA) based optimization procedure is utilized to find the optimal maintenance interventions. The proposed approach provides optimal intervention strategies to the decision maker that ultimately allows for risk-informed decision making regarding maintenance of highway bridges. The capabilities of the presented decision support framework are illustrated on an existing highway bridge located in Colorado.

### 3.3 MULTI-ATTRIBUTE RISK ASSESSMENT OF HIGHWAY BRIDGES UNDER TRAFFIC LOADING

#### 3.3.1 Vulnerability analysis

The first step in the risk assessment is to evaluate the performance of a bridge considering the hazards that plague it. An increase in live loads associated with the average daily traffic and the effect of chloride contamination are the hazards considered herein for bridge superstructures. The time-variant performance function associated with a reinforced concrete bridge deck in bending  $g_{deck}$  is (Akgül 2002)

$$g_{deck}(t) = K_1 A_{sr}(t) \gamma_{mfs} \lambda_{deff} - K_2 \frac{A_{sr}(t)^2 \gamma_{mfs} f_y^2}{f'_{cs}} - K_3 \lambda_a - K_4 \lambda_c - K_5 \lambda_{trk}(t) \quad (3.1)$$

The random variables considered in Eq. (3.1) are:  $A_{sr}(t)$  = area of transverse steel reinforcing in the slab at time  $t$  ( $m^2$ ),  $f_y$  = yield strength of reinforcing steel in slab (MPa),  $f'_{cs}$  = compressive strength of the concrete slab (MPa),  $\gamma_{mfs}$  = modeling uncertainty for flexure in the slab,  $\lambda_{deff}$  = reinforcing depth uncertainty factor,  $\lambda_a$  = asphalt weight uncertainty factor,  $\lambda_c$  = concrete weight uncertainty factor, and  $\lambda_{trk}(t)$  = effect of the load. Deterministic quantities,  $K_1$ ,  $K_2$ ,  $K_3$ ,  $K_4$ , and  $K_5$ , take on specific values depending on bridge type and geometric properties. In addition to flexure in the deck, the most critical mode of failure for the girders is associated with flexure. Thus, the following performance function is assumed to describe the time-variant behavior of bending in the steel girders.

$$g_{girder}(t) = K_6 F_y S_p(t) \gamma_{mfg} - (K_7 + K_8) \lambda_s - K_9 \lambda_c - K_{10} \lambda_a - K_{11} - M_{trk}(t) I_f D_f \quad (3.2)$$

Random variables in Eq. (3.2) include:  $F_y$  = yield strength of steel girder (MPa),  $S_p(t)$  = plastic section modulus at time  $t$  ( $m^3$ ),  $I_f$  = impact factor,  $D_f$  = the distribution factor,  $\gamma_{mfg}$  = modeling uncertainty for flexure in girder,  $\lambda_s$  = structural steel weight uncertainty factor, and  $M_{trk}(t)$  = moment due to truck load (kN-m).  $K_6, K_7, K_8, K_9, K_{10}$ , and  $K_{11}$  are deterministic constants.

Time effects are simulated by applying an increasing live load to the bridge superstructure and simultaneously imposing a continuous reduction of the cross-sectional areas of the steel girders and reinforcing bars in the slab to reflect chloride contamination induced corrosion. The loading model utilized herein is based on a live load annual amplification approach proposed by (Okasha and Frangopol 2010d). The corrosion models applied to the steel girders (Eq. 3.3) and reinforced concrete deck (Eq. 3.4) are based Albrecht and Naeemi (1984) and Thoft-Christensen (1998), respectively. The section loss functions are defined as:

$$C(t) = At^B \quad (3.3)$$

$$A_s(t) = \begin{cases} n \frac{\pi D_0^2}{4} & \text{for } 0 \leq t \leq T_i \\ n \frac{\pi (D_0 - C_c \cdot i_c (t - T_i))^2}{4} & \text{for } t \geq T_i \end{cases} \quad (3.4)$$

where  $C(t)$  = corrosion penetration depth ( $\mu m$ ),  $A$  and  $B$  are parameters based on environmental aggressivity,  $A_s(t)$  = top transversal tensile steel reinforcement area ( $mm^2$ ),  $n$  = number of top transversal steel bars,  $D_0$  = initial top reinforcement diameter (mm),  $i_c$  = corrosion parameter ( $mA/cm^2$ ),  $C_c$  = corrosion coefficient, and  $T_i$  = corrosion initiation time (years). Failure probabilities associated with each component of a bridge superstructure (e.g., deck, exterior girders, and interior girders)

and the entire superstructure system are evaluated by the First Order Reliability Method (FORM) employing the RELSYS computer software (Estes and Frangopol 1998). Similar approaches have been adopted by Decò and Frangopol (2011), Zhu and Frangopol (2013), and Estes (1997) in order to calculate the system reliability. Note that the probability of system failure is considered as an input for the proposed optimization framework.

### ***3.3.2 Effects of maintenance actions***

The effects of maintenance actions may be evaluated by modifying particular parameters contained within the performance functions in Eqs. (3.1) and (3.2). In general, essential maintenance actions are typically applied when a performance indicator reaches a predefined threshold. The essential maintenance actions considered herein are the replacement of bridge superstructure components; more specifically, the replacement of the deck, exterior girders, interior girders, and the entire superstructure are the four maintenance actions considered. The time-variant cross sectional area of the reinforcement within the slab  $A_{s,r}$  and the plastic section modulus  $S_p$  associated with the steel girders are the specific parameters within the performance functions that are changed when maintenance is performed.

In addition to the effect of maintenance on a structure's performance, the cost of implementing maintenance to a bridge must also be considered within the multi-criteria decision support system. The total cost of a maintenance plan is calculated in terms of USD in the year the bridge was built. Therefore, the total cost of a lifetime maintenance strategy is determined as:

$$C_{maint} = \sum_{i=1}^{N_{EM}} \frac{C_{EM,i}(t)}{(1+r_m)^t} \quad (3.5)$$

where  $C_{EM,i}(t)$  = cost of a maintenance action  $i$  that is applied at year  $t$  (USD),  $r_m$  = discount rate of money, and  $N_{EM}$  = total number of essential maintenance actions considered through the lifetime of a structure.

### 3.3.3 *Evaluation of risk-attributes associated with highway bridges*

This section presents the risk assessment process involved in determining optimal maintenance plans for highway bridges considering multiple criteria. Risk, which combines the probability of occurrence of a specific event with the consequence associated with this event, is regarded as an important performance indicator. A simple formulation of risk is (Ang and De Leon 2005):

$$R = p \cdot \chi \quad (3.6)$$

where  $p$  = probability of occurrence of an adverse event and  $\chi$  = consequences of the event. Three main consequences or risk-attributes are investigated herein for highway bridges: economic, social, and environmental impacts. More specifically, these consequences include the rebuilding and repair costs (economic losses); extra travel time and distance that drivers must endure, in addition to any fatalities that may occur (social impact); and energy consumption and carbon dioxide (CO<sub>2</sub>) emissions (environmental consequences). Overall, the evaluation of a wide variety of consequences associated with structural failure plays a fundamental role in the decision making process regarding bridge maintenance planning.

The first risk-attribute investigated captures the economic consequences of structural failure associated with a bridge superstructure (i.e., the system). The economic impact (i.e., direct loss) is measured in terms of the risk associated with the rebuilding cost  $R_{RB}$  during a certain year for a bridge (Stein *et al.* 1999).

$$R_{RB}(t) = \frac{P_{f,sys}(t) \cdot C_1 \cdot W \cdot L}{(1 + r_m)^t} \quad (3.7)$$

where  $C_1$  = rebuilding cost per square meter ( $\$/m^2$ ),  $P_{f,sys}$  = probability of system failure,  $W$  = width of the bridge (m),  $L$  = length of the bridge (m),  $r_m$  = discount rate of money, and  $t$  = time (years).

Next, the indirect losses are investigated. These losses include the negative impacts of structural failure to society and the surrounding environment. The social impacts of bridge failure are explored first. The social consequences of bridge failure include the extra travel time and distance experienced by vehicle operators, in addition to any fatalities that may occur. The risk associated with the extra travel time for users that must use a detour may be expressed as a function of time (Stein *et al.* 1999):

$$R_{ETT}(t) = P_{f,sys}(t) \left[ O_r \left( 1 - \frac{TT_p}{100} \right) + \frac{TT_p}{100} \right] \frac{L_d \cdot ADT(t) \cdot D_d}{S_d} \quad (3.8)$$

where  $O_r$  = occupancy rate for non-truck vehicles,  $TT_p$  = percentage of average daily traffic that is trucks (%),  $L_d$  = detour length (km),  $ADT(t)$  = average daily traffic during year  $t$ ,  $D_d$  = duration of detour (days), and  $S_d$  = average detour speed (km/hour). Note that Eq. (3.8) is highly dependent upon the traffic volume on the bridge during year  $t$ .

Similarly, the risk attribute corresponding to the extra travel distance due to detour is computed (Stein *et al.* 1999).

$$R_{ETD}(t) = P_{f,sys}(t) \cdot L_d \cdot ADT(t) \cdot D_d \quad (3.9)$$

The last part of the social impact incorporates the total number of fatalities resulting from structural failure. The estimated annual expected number of fatalities is (Rackwitz 2002; Zhu and Frangopol 2013b):

$$R_{FT}(t) = P_{f,sys}(t) \left( \frac{L}{f_d} + 1 \right) \left[ O_r \left( 1 - \frac{TT_p}{100} \right) + \frac{TT_p}{100} \right] \quad (3.10)$$

where  $f_d$  is the safe following distance during driving (m).

The final risk attribute examined is the detrimental effects of structural failure on the environment. More specifically, the environmental metric accounts for two impacts: (a) carbon dioxide emissions, and (b) energy consumption associated with detour and bridge repair. The risk associated with carbon dioxide emissions resulting from detour is considered as one sub-attribute of the environmental metric. The annual expected amount of carbon dioxide emissions due to detour of a bridge is (Stein *et al.* 1999):

$$AER_{DET,C}(t) = P_{f,sys}(t) \cdot ADT(t) \cdot L_d \cdot D_d \left[ CPD_C \left( 1 - \frac{TT_p}{100} \right) + CPD_T \frac{TT_p}{100} \right] \quad (3.11)$$

where  $CPD_C$  and  $CPD_T$  represent carbon dioxide emissions per unit distance associated with cars and trucks, respectively (kg/km). The risk associated with the annual amount of energy consumption due to detour can also be computed as

$$AER_{DET,E}(t) = P_{f,sys}(t) \cdot ADT(t) \cdot L_d \cdot D_d \cdot EPD \quad (3.12)$$

where  $EPD$  = energy consumption per unit distance associated with any vehicle (MJ/km).

In addition to the environmental consequences resulting from detour, it is necessary to consider the environmental impacts produced from the repair or replacement of a highway bridge after experiencing major structural damage due to traffic loads and corrosion. For instance, carbon dioxide emissions resulting from repair or replacement actions are computed considering a fraction of the CO<sub>2</sub> emissions associated with rebuilding an entire bridge. The annual expected amount of carbon dioxide produced from the repair of a bridge can be computed as (based on Basöz and Mander 1999):

$$AER_{REP,C}(t) = P_{f,sys}(t) \cdot CD_{REB} \cdot W \cdot L \quad (3.13)$$

where  $CD_{REB}$  = amount of carbon dioxide associated with rebuilding (kg/m<sup>2</sup>). Similarly, the annual expected amount of energy consumption associated with the repair of a bridge can be calculated as

$$AER_{REP,E}(t) = P_{f,sys}(t) \cdot EC_{REB} \cdot W \cdot L \quad (3.14)$$

where  $EC_{REB}$  = total energy consumption associated with the rebuilding (GJ/m<sup>2</sup>).

In order to determine the total value of each environmental impact (i.e., CO<sub>2</sub> emissions and energy consumption) for a highway bridge, the annual environmental risk values associated with bridge detour and repair are added. The annual risk-attribute values corresponding to carbon dioxide emissions  $R_{EC}(t)$  and energy consumption  $R_{EE}(t)$  for a bridge during year  $t$  are

$$R_{EC}(t) = AER_{DET,C}(t) + AER_{REP,C}(t) \quad (3.15)$$

$$R_{EE}(t) = AER_{DET,E}(t) + AER_{REP,E}(t) \quad (3.16)$$

### 3.4 UTILITY ASSESSMENT FOR SUSTAINABILITY EVALUATION

Utility is defined as a measure of value (or desirability) to the decision maker. Utility theory provides a framework that can measure, combine, and consistently compare these relative values (Ang and Tang 1984). Utility theory is utilized herein in order to depict the relative desirability of lifetime maintenance strategies to the decision maker. This section outlines how multi-attribute utility theory is used to transfer the utility of each risk-attribute into one utility value that is representative of bridge sustainability. A utility function corresponding to the total cost of maintenance that considers the decision maker's risk attitude can also be formulated. Overall, the computational procedure adopted herein for the multi-attribute utility assessment of a bridge subjected to traffic loads and a corrosive environment is shown in Figure 3.1, where  $u_i$  and  $k_i$  are the utility function and associated weighting factor corresponding to the  $i$ th risk attribute. This flowchart outlines the process of calculating the utility associated with three risk-attributes as well as the multi-attribute utility value corresponding to the sustainability performance.

#### 3.4.1 *Utility function for maintenance cost*

Establishing a utility function that depicts the relative value of maintenance cost investment to the decision maker considering his/her particular risk attitude is crucial in the proposed decision support system. In general, the maintenance strategies

associated with high utility values correspond to relatively small maintenance costs and are usually preferred to those associated with small utility values (Howard and Matheson 1989). Given the maximum cost investment that the decision maker can tolerate, a utility function representative of maintenance cost considering the attitude of the decision maker may be formulated. The utility associated with a given maintenance cost is (Ang and Tang 1984):

$$u_c = \frac{1}{1 - \exp(-\gamma)} \left[ 1 - \exp\left(-\gamma \frac{C_{\max} - C_{\text{maint}}}{C_{\max}}\right) \right] \quad (3.17)$$

where  $C_{\text{maint}}$  = total maintenance cost,  $\gamma$  = risk attitude of the decision maker (i.e.,  $\gamma > 0$  indicates risk-aversion and  $\gamma < 0$  denotes risk-acceptance), and  $C_{\max}$  = maximum maintenance cost which is utilized to normalize the cost-utility so that it always takes values between 0 and 1. Considering the same maintenance strategy, a risk averse attitude will always yield a higher utility value than that produced from a risk accepting attitude.

### ***3.4.2 Utility function for risk-attributes***

The utility functions associated with each risk-attribute investigated within the sustainability assessment (economic, social, and environmental impacts) are formed considering the risk attitude of the decision maker (Keeney and Raiffa 1993). For the risk-attributes analyzed, each of the corresponding utility functions may be formulated as monotonically decreasing functions. Considering an exponential formulation, the utility associated with a single attribute (e.g., extra travel distance and carbon dioxide emissions) can be expressed as:

$$u_{RA} = \frac{1}{1 - \exp(-\gamma)} \left[ 1 - \exp\left(-\gamma \frac{RA_{\max} - RA}{RA_{\max} - RA_{\min}}\right) \right] \quad (3.18)$$

where  $RA$  = expected value of the risk-attribute value under investigation and  $RA_{\max}$  and  $RA_{\min}$  denote the maximum and minimum value of the risk-attribute, respectively. Overall, a monotonically decreasing function that has bounds of 0 and 1 must be utilized within the utility assignment procedure in order to accurately depict the relative utility of detrimental consequences. As indicated by (Keeney and Raiffa 1993), for a single attribute considered within the presented approach,  $u_{RA} = 1$  corresponds to the lowest possible loss while  $u_{RA} = 0$  is associated with the largest possible loss. The concavity of these utility functions is highly dependent on the risk attitude of the decision maker. Risk averse and risk accepting attitudes yield a concave and convex utility function, respectively.

### ***3.4.3 Multi-attribute utility assessment corresponding to sustainability***

After the utility function associated with each risk-attribute is appropriately established, multi-attribute utility theory may be employed to combine them into a single utility value that effectively represents a sustainability performance metric. Overall, the sustainability performance indicator may be quantified in terms of economic, social, and environmental consequences. Although there are various established types of multi-attribute utility functions, the additive formulation is utilized herein. Within the additive formulation for the multi-attribute utility function, marginal utility values associated with each attribute are multiplied by weighting factors and summed over all attributes investigated (Stewart 1996). The utility values corresponding to economic, social, and environmental risk-attributes are determined

by considering equal contributions of the sub-attributes involved. For example, the environmental utility associated with a particular solution is calculated considering equal contributions of two detrimental consequences: carbon dioxide emissions and energy consumption. Considering an additive formulation, the multi-attribute utility function utilized within the presented decision making framework is computed as (Jiménez *et al.* 2003)

$$u_s = k_{econ}u_{econ} + k_{soc}u_{soc} + k_{env}u_{env} \quad (3.19)$$

where  $u_s$  is the multi-attribute utility function associated with the sustainability performance metric;  $u_{econ}$ ,  $u_{soc}$ , and  $u_{env}$  represent the marginal utility values associated with economic, social, and environmental risk-attributes, respectively; and  $k_{econ}$ ,  $k_{soc}$ , and  $k_{env}$  are the weighting factors corresponding to the three metrics considered in the sustainability assessment such that  $k_{econ} + k_{soc} + k_{env} = 1$ . Typically, these weighting factors are not explicitly known or are difficult to assess for certain decision makers. However, within this chapter, a sensitivity study concerning these weighting factors is conducted in order to determine the effect of the decision maker's particular preference to which aspect of sustainability is most important.

### **3.5 OPTIMIZATION OF BRIDGE MAINTENANCE PLANNING**

The two utility functions investigated are: (a) the relative value of maintenance investment costs considering the risk attitude of the decision maker  $u_c$ , and (b) the sustainability of each alternative expressed in terms of the utility  $u_s$ . These utility functions are further used within a maintenance optimization process as the objective functions to be maximized. More specifically, the optimization herein maximizes the

minimum annual utility associated with sustainability while simultaneously maximizing the utility associated with the total maintenance cost. Generally, if the utility values of all the alternatives are available, the solution with the highest utility value is always preferred; thus, the two utility objectives are maximized within the presented optimization procedure.

The optimization approach embedded within the proposed maintenance methodology is shown in Figure 3.2. The optimization algorithm sends the candidates for the design variables (maintenance action and time of application) to the performance and cost modules which calculate the value of each objective function. The performance module has the capability to handle all computations associated with the system reliability assessment, consequences evaluation, probabilistic risk analysis, and utility value associated with the sustainability resulting from implementing maintenance. The main result of the performance module is the multi-attribute utility associated with sustainability considering maintenance; this objective value is maximized considering a specific bridge lifetime. Additionally, the cost module of the proposed computational framework calculates the total maintenance cost of a bridge. Next, the utility associated with this total maintenance cost is determined considering the risk attitude of the decision maker. Lastly, the utility value associated with both sustainability  $u_s$  and maintenance cost  $u_c$  is employed within the optimization module in order to find the set of Pareto optimum solutions outlining bridge maintenance planning. The set of Pareto optimum solutions for the multi-objective optimization problem is obtained utilizing GAs within an adequate number of generations (Okasha and Frangopol 2009, Frangopol 2001, Dong *et al.* 2014e).

The *bi-objective* optimization problem is formulated as follows:

***Given:***

- Bridge information including its geometry, physical characteristics, material properties, and time-variant system reliability (information associated with Eqs. 3.1 and 3.2)
- Consequences associated with structural failure (calculated using Eqs. 3.7 to 3.16)
- Risk attitude of the decision maker ( $\gamma$  in Eqs. 3.17 and 3.18)
- Sustainability multi-attribute utility function (Eq. 3.19) and weighting factors that represent the contribution of economic, social, and environmental risk-attributes ( $k_{econ}$ ,  $k_{soc}$ , and  $k_{env}$ , respectively in Eq. 3.19)
- Bridge lifetime under investigation ( $T_L$ )
- Total number of maintenance actions ( $N_{EM}$ )

***Find:***

- Bridge components to be replaced
- Time of application of maintenance actions

***So that:***

- Utility associated with the total maintenance cost  $u_c$  is maximized (Eq. 3.17)

- Annual minimum utility associated with sustainability  $u_s$  over the bridge lifetime is maximized (Eq. 3.19)

***Subjected to:***

- Total cost of maintenance should be less than a prescribed value
- Constraints on the allowable minimum and maximum values of each risk-attribute ( $RA_{min}$  and  $RA_{max}$ , respectively in Eq. 3.18)
- Constraints on the application times of maintenance

### **3.6 CASE STUDY**

The proposed multi-criteria optimization framework is applied to an existing highway bridge located in Broomfield, Colorado, USA. The E-16-FK Bridge is classified as a concrete on rolled I-beam continuous bridge (CIC) and consists of four spans. As shown in a transverse cross-section of the superstructure in Figure 3.3, the reinforced concrete slab is supported by five steel girders spaced evenly at 2.235 m apart. The bridge carries one lane of traffic in each direction (i.e., westbound and eastbound) and average daily traffic of 18,900 vehicles was reported in 2007 (FHWA 2013). The average daily traffic during the year the bridge was built (i.e.,  $t = 0$ ) is taken as 10,826 while the maximum predicted average daily traffic over the lifetime (i.e.,  $t = 75$  years) is 23,998 vehicles. The total length of the bridge  $L = 69.2$  m while the total width  $W = 10.4$  m.

The maintenance planning optimization problems based on risk reported in monetary terms associated with other bridges located in Colorado, USA have been previously investigated by Barone and Frangopol (2014a) and Zhu and Frangopol

(2013b). As stated previously, the ultimate aim of this illustrative example is to apply the proposed bi-objective optimization methodology considering multi-attribute utility theory to an existing highway bridge to determine optimal essential maintenance strategies. The effects of the risk attitude and preferences of the decision maker, in addition to the number of maintenance interventions on the optimal maintenance strategies are investigated herein. Furthermore, optimal maintenance strategies obtained considering the simultaneous maximization of four utility values (i.e.,  $u_c$ ,  $u_{econ}$ ,  $u_{soc}$ , and  $u_{env}$ ) are investigated as motivation for choosing appropriate weighting factors (i.e.,  $k_{econ}$ ,  $k_{soc}$ , and  $k_{env}$ ) within the assessment of the multi-attribute utility associated with sustainability.

### ***3.6.1 Evaluation of risk-attributes***

The initial step within this case study is to calculate the time-variant probability of failure associated with the components comprising the superstructure of the E-16-FK highway bridge. Eqs. (3.1) and (3.2) are utilized with the parameter values reported in Table 3.1 in order to determine time-variant component probabilities of failure. Note that all parameters listed in Table 3.1 follow the lognormal distribution. The following deterministic values are also considered in Eq. (3.1) for the investigated highway bridge's deck:  $K_1 = 4.0625 \times 10^{-1}$ ,  $K_2 = 4.0850 \times 10^{-3}$ ,  $K_3 = 1.9695 \times 10^{-1}$ ,  $K_4 = 4.1765 \times 10^{-1}$ ,  $K_5 = 4.6009$  (Akgül 2002). Additionally, the values of the constants contained in Eq. (3.2) considering exterior girders 1 and 5 are assumed as:  $K_6 = 8.3333 \times 10^{-2}$ ,  $K_7 = 32.070$ ,  $K_8 = 4.3860$ ,  $K_9 = 142.49$ ,  $K_{10} = 54.721$ , and  $K_{11} = 1.4940$ . Similarly, the deterministic parameters within Eq. (3.2) for interior girders 2, 3 and 4 take the following values:  $K_6 = 5.8 \times 10^{-1}$ ,  $K_7 = 5.24$ ,  $K_8 = 7.2527 \times 10^{-1}$ ,  $K_9 = 23.206$ ,

$K_{10} = 8.913$ ,  $K_{11} = 2.4333 \times 10^{-1}$  (Akgül 2002). The failure of the entire superstructure (i.e., the system) is modeled as a series-parallel system consisting of a failure of the deck or any two adjacent girders (see Figure 3.4). It is assumed that the substructure does require essential maintenance. Considering the above outlined system model configuration, component performance functions provided by Eqs. (3.1) and (3.2), deterministic parameters  $K_I - K_{II}$ , and probabilistic random variables listed in Table 3.1, the annual system reliability index and its corresponding annual probability of failure are computed using RELSYS (Estes and Frangopol 1998). The time-variant reliability profile (e.g., annual probability of failure) is considered as input for the maintenance optimization problem presented (see Figure 3.5). The four possible essential maintenance options and their associated costs considered herein are based on (Estes 1997); replacing the deck (D) has a maintenance cost of \$225,600, essential maintenance of the exterior girders ( $G_E$ ) costs \$104,600, essential maintenance of the interior girders ( $G_I$ ) costs \$156,900, and replacing the entire superstructure (S) costs \$487,100 (Estes 1997). It is assumed that the discount rate of money  $r_m$  is equal to 0.02 and the decision for implementing a particular optimal maintenance plan is made in 1996.

Next, the detrimental consequences of structural failure are evaluated. Based on Eqs. (3.5) to (3.14), the expected value of the sustainability sub-attributes are calculated in terms of their respective units. All probabilistic parameters utilized within computation of the risk-attributes are summarized in Table 3.2. The time-variant profile of the expected value corresponding to each sub-attribute of

sustainability considering no maintenance is shown in Figure 3.6 for a lifetime of  $T_L = 75$  years.

### ***3.6.2 Utility assessment for maintenance cost and sustainability performance***

Within the proposed optimization procedure, for each alternative, it is necessary to evaluate both the utility associated with total maintenance cost  $u_c$  and the utility value that is representative of the minimum annual sustainability performance metric  $u_s$ . The utility value associated with the total maintenance cost is obtained utilizing Eq. (3.17) with  $C_{max} = \$1M$ . The formulation of the cost utility employed herein effectively captures the decision maker's preference to investing money in the face of risk.

The multi-attribute utility value corresponding to the annual sustainability performance metric in terms of economic, social, and environmental attributes must be determined, in addition to the utility associated with the maintenance cost for each alternative considered within the optimization framework. Once the expected value of each sustainability sub-attribute is determined, it may be transferred to utility considering the exponential formulation in Eq. 3.18). The annual utility value corresponding to each sub-attribute is calculated considering the range of risk-attribute values shown in Table 3.3. Within this specific example, these minimum and maximum risk-attribute values are obtained considering the no maintenance case;  $RA_{min}$  and  $RA_{max}$  are the expected risk-attribute values at  $t = 0$  and  $t = T_L$  (i.e., 75 years) assuming that no maintenance is performed. In other cases, the decision maker may directly assign values to  $RA_{min}$  and  $RA_{max}$  in order to reflect personal risk tolerances. Furthermore, the annual utility values associated with each attribute of

sustainability (i.e.,  $u_{econ}$ ,  $u_{soc}$ , and  $u_{env}$ ) are computed considering a weighted average of its sub-attributes. Each sub-attribute's utility value is weighted equally (i.e., 1/3) in order to determine a single utility value associated with each attribute (i.e., economic, social, and environmental) of sustainability. The final step of this stage of the analysis involves calculating an annual utility value corresponding to the entire sustainability metric; the multi-attribute utility associated with the bridge's total sustainability considering the effects of maintenance is determined using Eq. (3.19). Figure 3.7 depicts the annual economic, social, and environmental utility values, and the time-variant multi-attribute utility corresponding to the sustainability performance metric considering no maintenance. With no maintenance, the utility associated with sustainability decreases from 1 to 0 over the lifetime of the structure. The implementation of maintenance interventions restores the sustainability of the structure; lifetime maintenance planning can effectively mitigate a variety of risks while simultaneously ensuring that sustainability performance is always within acceptable levels.

### ***3.6.3 Optimal maintenance planning***

The bi-objective maintenance planning problem is solved using a GA-based optimization approach. MATLAB's Global Optimization Toolbox (MathWorks 2013) is employed herein in order to obtain optimal lifetime maintenance strategies for the highway bridge investigated. The problem presented was solved using MATLAB on a Dell Precision R5500 rack workstation equipped with two six cores X5675 Intel Xeon processors with 3.06 GHz clock speed and 24 GB DDR3 memory.

Considering the framework outlined previously, there are several inputs that influence the results of the proposed decision support system. For the specific life-cycle maintenance problems investigated herein, the sustainability multi-attribute utility function considering the no maintenance case, depicted in Figure 3.7 for Colorado highway bridge E – 16 – FK, is employed. The optimization is performed by simultaneously maximizing the utility associated with total maintenance cost  $u_c$  and the annual minimum utility corresponding to the sustainability  $u_s$  over the lifetime of the bridge (i.e.,  $T_L = 75$  years). The main results of the optimization procedure are the maintenance actions performed on the bridge components and their respective times of application. The following constraints are also considered herein: (a) total maintenance cost should not exceed  $C_{max} = \$1M$ , (b) constraints on the allowable minimum and maximum values of each risk-attribute (see Table 3.3), (c) first essential maintenance may not be performed before  $t = 5$  years, and (d) consecutive maintenance actions must be performed at least 3 years apart.

The Pareto optimal solutions obtained considering three maintenance actions (i.e.,  $N_{EM} = 3$ ) with a risk accepting (e.g.,  $\gamma = -1$ ) and risk averse (e.g.,  $\gamma = 1$ ) decision maker are shown in Figure 3.8. The weighting factors  $k_{econ}$ ,  $k_{soc}$ , and  $k_{env}$  are all assumed to be equal to one third for this example, representing equal contribution of detrimental economic, societal, and environmental impacts. The risk averse decision maker will always assign larger utility to the same alternatives as compared to a decision maker that is risk accepting. The essential maintenance strategies corresponding to solutions A1, A2, A3, B1, B2, and B3 in Figure 3.8 are detailed within Table 3.4. The solutions associated with the risk averse decision maker, B1,

B2, and B3, represent maintenance strategies that correspond to different values of utility associated with cost and sustainability. Compared to the other Pareto alternatives obtained for a risk averse decision maker, Solution B1 is a high-cost, high-performance solution with a cost utility of 0.5613 and minimum annual sustainability utility of 0.8705. The maintenance plan outlined for Solution B1 entails replacing the entire superstructure at years 33, 52, and 65. Conversely, Solution B3 is a low-cost, low-performance solution with  $u_c = 0.9044$  and  $u_s = 0.1800$ . The maintenance plan associated with Solution B3 includes replacing the interior girders at year 50, the deck at year 69, and again the interior girders at year 74. Solutions B2 and B3 are summarized in Table 3.4.

Furthermore, the cost utility, minimum annual utilities corresponding to the economic, social, and environmental risk attributes, and the minimum annual multi-attribute utility associated with the sustainability performance for representative solutions marked in Figure 3.8 are shown in Table 3.5. The profiles of the annual utility associated with sustainability for solutions B1, B2, and B3 are shown in Figure 3.9. In addition to the specific maintenance plan and utility values, the maximum annual expected risk-attributes corresponding to each Pareto alternative may also be investigated. Table 3.6 summarizes the maximum annual risk attributes values corresponding to the representative optimal maintenance strategies. Amongst the selected Pareto alternatives obtained for a risk averse decision maker, Solution B3 is the highest cost alternative; however, it yields relatively low consequences in terms of economic, social, and environmental impacts. In order to illustrate time effects, the

annual risk profiles associated with CO<sub>2</sub> emissions  $R_{EC}$  corresponding to Solutions B1, B2, and B3 are shown in Figure 3.10.

In addition to the effect of the decision maker's risk attitude on the Pareto optimal solutions, the influence of the number of essential maintenance actions is also investigated. Figure 3.11 depicts Pareto optimal solutions considering a variable number of essential maintenance actions (i.e.,  $N_{EM} = 1, 2, \text{ or } 3$ ), a risk averse decision maker, and weighting factors all equal to one third. The maintenance plans corresponding to the three representative solutions on the Pareto front in Figure 3.11, Solutions C1, C2, and C3, are shown in Table 3.7. It is evident that maintenance plans that consider only one intervention have the lowest cost (i.e., high cost utility) but, as a limit, can only achieve a certain level of sustainability utility. Intervention strategies that contain two or more essential maintenance actions can achieve higher levels of utility associated with sustainability but possess higher maintenance costs (i.e., lower cost utility) when compared to the plans containing only one maintenance action. This trend can also be observed in Figure 3.12, which plots the annual sustainability utility values corresponding to the representative solutions marked as C1, C2, and C3 within Figure 3.11. Solution C3 dictates maintenance that frequently restores the sustainability performance and allows it to remain large throughout the lifetime, while Solution C1 only contains one intervention that dramatically increases the sustainability performance but is unable to keep it at high levels throughout the entire lifetime.

The weighting factors contained within the multi-attribute utility equation have a great effect on the shape of the final Pareto front. Figure 3.13 depicts the Pareto

optimal solutions for the bi-objective optimization problem considering three maintenance actions, a risk averse decision maker, and three separate sets of weighting factors. The combination of weighting factors that produces the largest utility values associated sustainability is  $(k_{econ}, k_{soc}, k_{env}) = (0.1, 0.8, 0.1)$ , while the weighting factor combination of  $(0.8, 0.1, 0.1)$  yields relatively smaller performance utility values. The maintenance strategies corresponding to representative Solutions D1, D2, and D3 are outlined within Table 3.8.

The final part of this illustrative example includes the examination of the Pareto front obtained by carrying out a four-objective optimization procedure that maximizes the utility associated with maintenance cost  $u_c$  while simultaneously maximizing the minimum annual economic  $u_{econ}$ , social  $u_{soc}$ , and environmental  $u_{env}$  utilities. The motivation behind performing this optimization is to determine the sensitivity of the Pareto front to change in the values of the weighting factors for future use in the decision support framework. Figure 3.14 presents the output of the four-objective optimization procedure considering a risk averse decision maker (i.e.,  $\gamma = 1$ ) in a 3D plot with utility associated with economic, social, and environmental risks represented on each of the axes. The fourth objective, the utility associated with maintenance cost, is segmented into four separate ranges and the solutions falling into each of these ranges are plotted in Figure 3.14(a) – (d). Selected points from this four-objective Pareto front and their respective values of minimum annual utility values are indicated in Table 3.9. Overall, the results obtained for the four-objective optimization problem may be employed to determine the effect of the utility associated with maintenance cost  $u_c$  on the other three utilities.

### 3.7 CONCLUSIONS

This chapter presents a framework for life-cycle maintenance optimization of highway bridges that utilizes multi-attribute utility theory to quantify the sustainability performance metric. The ultimate aim of implementing maintenance throughout the lifetime of a bridge is to mitigate the detrimental impacts of structural failure to the economy, society, and the environment. Optimum maintenance plans are obtained by carrying out a multi-criteria optimization procedure where the utility associated with total maintenance cost and utility corresponding to sustainability performance are considered as conflicting objectives.

Overall, this chapter proposes a comprehensive approach for the life-cycle maintenance optimization of highway bridges considering the decision maker's risk attitude and preferential characteristics. The presented methodology can be used to assist decision making regarding maintenance actions and, ultimately, maintain the life-cycle sustainability of highway bridges.

The following conclusions are drawn:

1. All three aspects of sustainability (i.e., economic, social, and environmental) are crucial to the performance assessment of highway bridges. Multi-attribute utility theory allows for the quantification of a structure's sustainability performance considering weighting factors that define the relative contribution of each aspect of sustainability. In general, utility theory can be employed to determine the desirability of a particular

alternative considering a decision maker's risk attitude towards consequences of structural failure.

2. Optimum maintenance plans for highway bridges can be obtained by employing a multi-objective optimization approach that results in a set of Pareto optimal solutions. Ultimately, a decision maker is able to make informed decisions based on their particular preferences and the decision support system provided by the Pareto set of optimal solutions. Depending on the maintenance cost, level of sustainability, and in turn, maximum annual risk-attribute values desired, a decision maker can choose a Pareto optimal intervention plan that best satisfies his/her needs.
3. The risk attitude of the decision maker has a large impact on the optimal solutions resulting from the proposed decision support system.
4. The maximum number of essential maintenance actions considered throughout a bridge's lifetime has great effects on the final Pareto optimal solutions. Alternatives with very few maintenance actions are associated with significantly larger cost utilities as compared to maintenance plans that implement more intervention actions.
5. The weighting factors considered within the multi-attribute utility assessment of sustainability have a significant impact on the resulting Pareto optimal solutions. Thus, it is crucial to determine appropriate values for them. The four-objective optimization process that is presented herein acts as a preliminary investigation in determining the sensitivity of optimum solutions to changes in the values of the weighting factors.

Further research is needed to properly select appropriate weighting factors within the multi-attribute utility assessment process.

Table 3.1. Random variables and their corresponding parameters used within the reliability analysis of the E-16-FK highway bridge.

Random Variable	Mean	COV	References
Area of transverse steel reinforcing in the slab $A_{sr}$	Varies (m <sup>2</sup> )	Varies	Akgül (2002)
Yield strength of reinforcing steel in slab $f_y$	308.9 MPa	0.11	Akgül (2002)
Compressive strength of the concrete slab $f'_{cs}$	19.03 MPa	0.18	Akgül (2002)
Modeling uncertainty for flexure in the slab $\gamma_{mfs}$	1.02	0.06	Akgül (2002)
Slab reinforcing depth uncertainty factor $\lambda_{deff}$	1.00	0.02	Akgül (2002)
Asphalt weight uncertainty factor $\lambda_a$	1.00	0.025	Akgül (2002)
Concrete weight uncertainty factor $\lambda_c$	1.05	0.01	Akgül (2002))
Effect of the load on the slab $\lambda_{trk}$	Varies	0.20	Akgül (2002); Okasha and Frangopol (2010d)
Yield strength of steel girders $F_y$	252.6 MPa	0.12	Akgül (2002)
Plastic section modulus of steel girders $S_p$	Varies (m <sup>3</sup> )	Varies	Akgül (2002)
Impact factor for steel girders $I_f$	1.12	0.10	Akgül (2002)
Distribution factor for steel girders $D_f$	1.44	0.12	Akgül (2002)
Modeling uncertainty for flexure in girder $\gamma_{mfg}$	1.11	0.11	Akgül (2002)
Structural steel weight uncertainty factor $\lambda_s$	1.03	0.08	Akgül (2002)
Moment due to truck load on steel girders $M_{trk}$	Varies (kN-m)	0.20	Akgül (2002); Okasha and Frangopol (2010d)

Table 3.2. Variables and their corresponding parameters used in the evaluation of the risk-attributes associated with the investigated highway bridge.

Random Variable	Mean	COV	Distribution type	Reference
Rebuilding cost parameter $C_I$	\$1292/m <sup>2</sup>	--	Deterministic	Dong <i>et al.</i> (2014f)
Width of the bridge $W$	10.4 m	--	Deterministic	FHWA (2013)
Length of the bridge $L$	69.2 m	--	Deterministic	FHWA (2013)
Occupancy rate for non-truck vehicles $O_r$	1.56	--	Deterministic	Stein <i>et al.</i> (1999)
Percentage of average daily traffic that is trucks $TT_p$	4%	--	Deterministic	FHWA (2013)
Detour length $L_d$	7.9 km	0.20	LN	Based on local transportation network; Google Maps (2014)
Average daily traffic $ADT$	Varies	0.20	LN	FHWA (2013)
Duration of detour $D_d$	180 days	0.20	LN	Stein <i>et al.</i> (1999)
Average detour speed $S_d$	104 km/hr	0.20	LN	Based on local transportation network
Safe following distance $f_d$	55 m	0.20	LN	Colorado State Patrol (2011)
Carbon dioxide emissions associated with cars $CPD_C$	0.22 kg/km	0.20	LN	Dong <i>et al.</i> (2014f)
Carbon dioxide emissions associated with trucks $CPD_T$	0.56 kg/km	0.20	LN	Dong <i>et al.</i> (2014f)
Energy consumption associated with each vehicle $EPD$	3.80 MJ/km	0.20	LN	Dong <i>et al.</i> (2014f)
Carbon dioxide emissions associated with rebuilding $CD_{REB}$	159 kg/m <sup>2</sup>	0.20	LN	Dequidt (2012)
Energy consumption associated with rebuilding $EC_{REB}$	2.05 GJ/m <sup>2</sup>	0.20	LN	Dequidt (2012)

Table 3.3. Minimum and maximum values of risk-attributes.

Attribute type	Attribute	Minimum $RA_{min}$	Maximum $RA_{max}$
Economic	Rebuilding cost $R_{RB}$ (USD)	171	172,572
Social	Extra travel time $R_{ETT}$ (hr)	41	364,895
	Extra travel distance $R_{ETD}$ (km)	2827	24,824,743
	Fatalities $R_{FT}$ (no.)	$6.375 \times 10^{-4}$	2.655
Environmental	CO <sub>2</sub> emissions $R_{EC}$ (kg)	691	5,975,918
	Energy consumption $R_{EE}$ (MJ)	11,012	95,462,023

Table 3.4. Maintenance plans corresponding to the representative risk solutions on the Pareto front shown in Figure 3.8.

Solution	Maintenance actions	Time of application (years)
A1	[D, S, S]	[32, 43, 61]
A2	[D, G <sub>I</sub> , D]	[40, 57, 71]
A3	[D, G <sub>I</sub> , G <sub>I</sub> ]	[50, 70, 74]
B1	[S, S, S]	[33, 52, 65]
B2	[D, G <sub>I</sub> , G <sub>I</sub> ]	[40, 58, 73]
B3	[G <sub>I</sub> , D, G <sub>I</sub> ]	[50, 69, 74]

Note: D = replace the deck; G<sub>I</sub> = replace all interior girders; S = replace the entire superstructure

Table 3.5. Minimum annual utility values corresponding to six solutions within the Pareto front in Figure 3.8.

Solution	Cost utility	Minimum annual utility			
	$u_c$	Economic $u_{econ}$	Social $u_{soc}$	Environmental $u_{env}$	Sustainability $u_s$
A1	0.4037	0.5636	0.6769	0.6768	0.6840
A2	0.7026	0.3219	0.5711	0.5757	0.5527
A3	0.7671	0.1107	0.4158	0.4531	0.3265
B1	0.5613	0.7570	0.8708	0.8707	0.8705
B2	0.8790	0.5634	0.7426	0.7426	0.7500
B3	0.9044	0.0950	0.2081	0.2311	0.1800

Table 3.6. Maximum annual utility risk-attribute values corresponding to solutions A and B within the Pareto front in Figure 3.8.

Solution	Maximum annual risk-attribute values					
	Economic		Social	Environmental		
	Rebuilding cost $R_{RB}$ (USD)	Extra travel time $R_{ETT}$ (hr)	Extra travel distance $R_{ETD}$ (km)	Fatalities $R_{FT}$ (no.)	CO <sub>2</sub> emissions $R_{EC}$ (kg)	Energy consumption $R_{EE}$ (MJ)
A1	55,894	83,158	5,657,427	0.605	1,361,880	21,755,288
A2	96,798	113,552	7,725,250	0.871	1,860,760	29,721,230
A3	14,274	15,376	10,461,001	1.435	2,528,629	40,361,388
B1	60,408	72,990	4,965,703	0.533	1,195,365	19,095,305
B2	96,798	133,247	9,065,123	0.969	2,182,195	34,859,373
B3	162,103	306,079	20,823,333	2.364	5,017,196	80,133,059

Table 3.7. Maintenance plans corresponding to solutions C1, C2, and C3 on the Pareto front shown in Figure 3.11.

Solution	Maintenance actions	Time of application (years)	Cost utility $u_c$	Minimum annual performance utility $u_s$
C1	[D]	[55]	0.9541	0.4175
C2	[D, G <sub>I</sub> ]	[41, 71]	0.9134	0.6939
C3	[S, S, G <sub>I</sub> ]	[33, 54, 69]	0.6595	0.8559

Note: D = replace the deck; G<sub>I</sub> = replace all interior girders; S = replace the entire superstructure

Table 3.8. Maintenance plans corresponding to solutions D1, D2, and D3 on the Pareto front shown in Figure 3.13 considering various weighting factors.

Solution	Weighting factors	Maintenance actions	Time of application (years)	Cost utility $u_c$	Minimum annual performance utility $u_s$
D1	(0.8, 0.1, 0.1)	[S, S, S]	[30, 43, 58]	0.4879	0.8449
D2	(0.1, 0.8, 0.1)	[D, G <sub>I</sub> , S]	[39, 52, 65]	0.8005	0.8308
D3	(1/3, 1/3, 1/3)	[D, G <sub>I</sub> , G <sub>I</sub> ]	[40, 58, 73]	0.8790	0.7500

Note: D = replace the deck; G<sub>I</sub> = replace all interior girders; S = replace the entire superstructure

Table 3.9. Maintenance plans and associated utility values corresponding to the representative solutions on the four-dimensional Pareto front contained in Figure 3.14.

Solution	Maintenance actions	Respective time of application (years)	Cost utility $u_c$	Minimum annual utility		
				Economic $u_{econ}$	Social $u_{soc}$	Environmental $u_{env}$
E1	[D, G <sub>I</sub> , S]	[40, 52, 64]	0.8001	0.5634	0.8397	0.8540
E2	[D, G <sub>I</sub> , S]	[34, 49, 61]	0.7805	0.7303	0.8496	0.8506
E3	[S, S, G <sub>I</sub> ]	[32, 56, 71]	0.6623	0.7783	0.8546	0.8566
E4	[S, S, S]	[37, 56, 67]	0.5991	0.6532	0.8796	0.8812

Note: D = replace the deck; G<sub>I</sub> = replace all interior girders; S = replace the entire superstructure

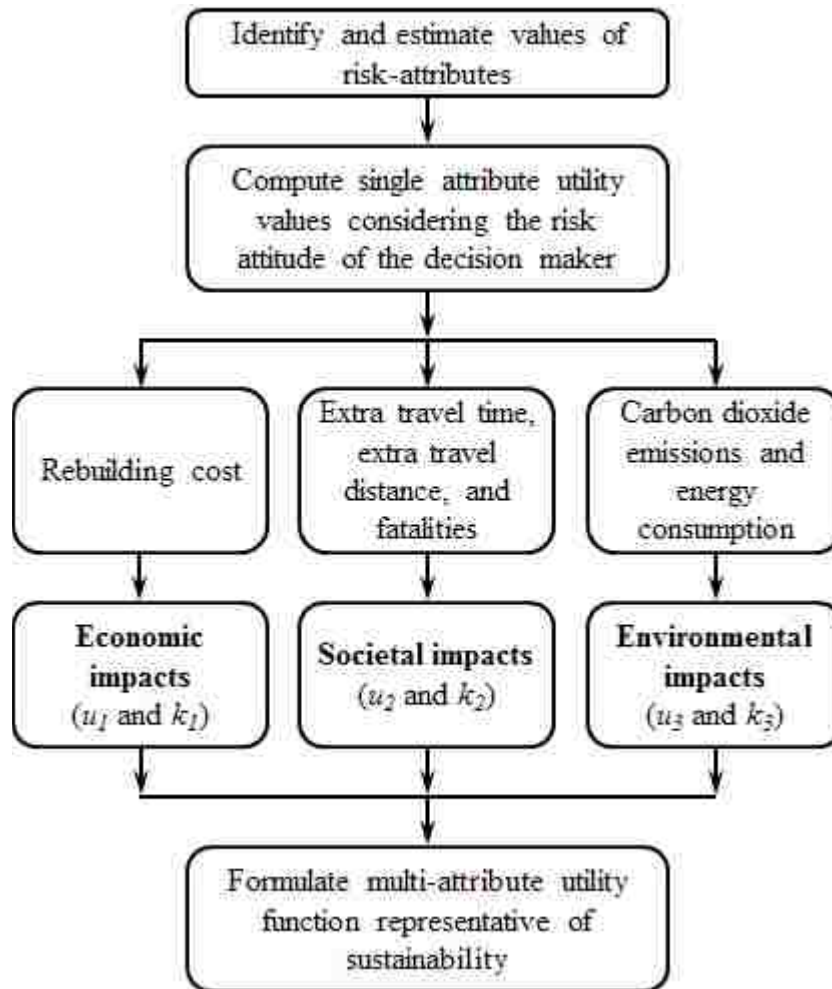


Figure 3.1. Flowchart describing the multi-attribute utility performance assessment.

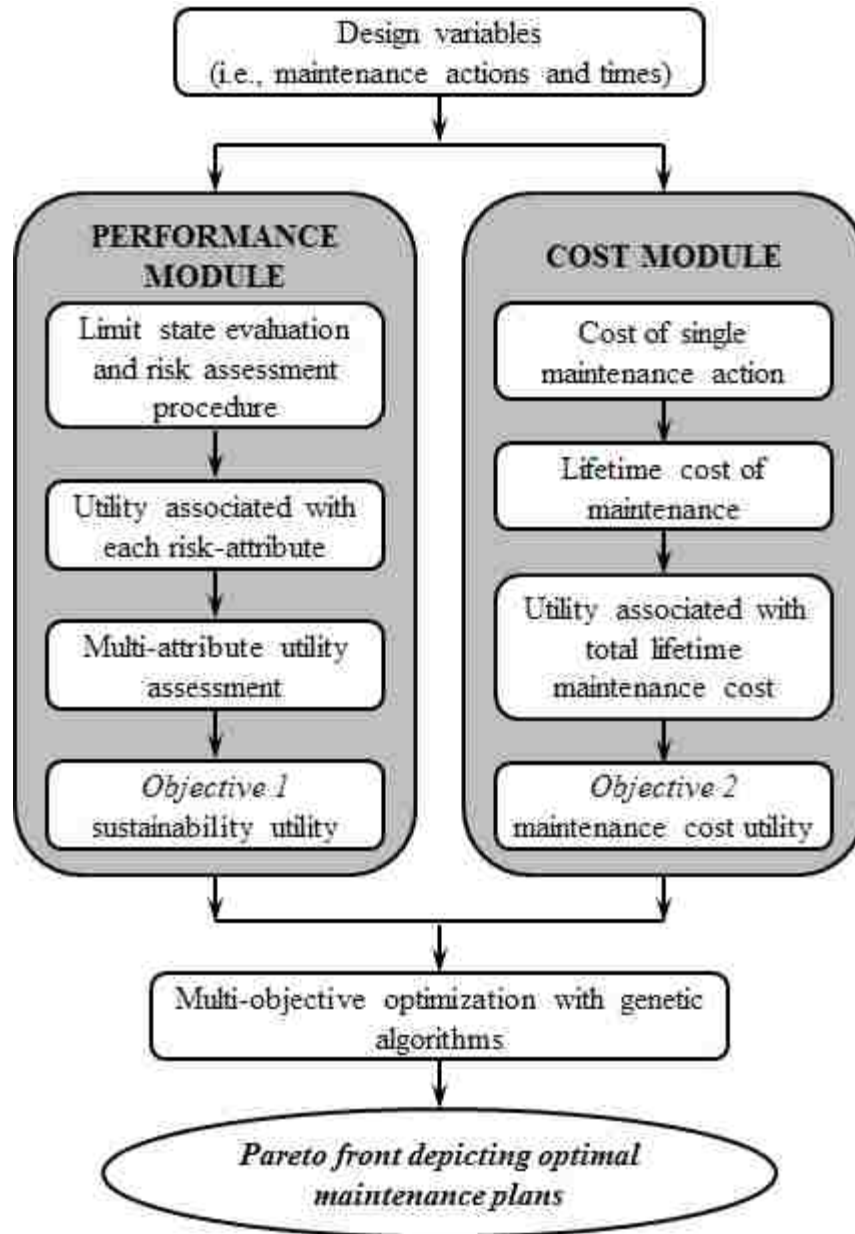


Figure 3.2. Flowchart describing the bi-objective optimization procedure.

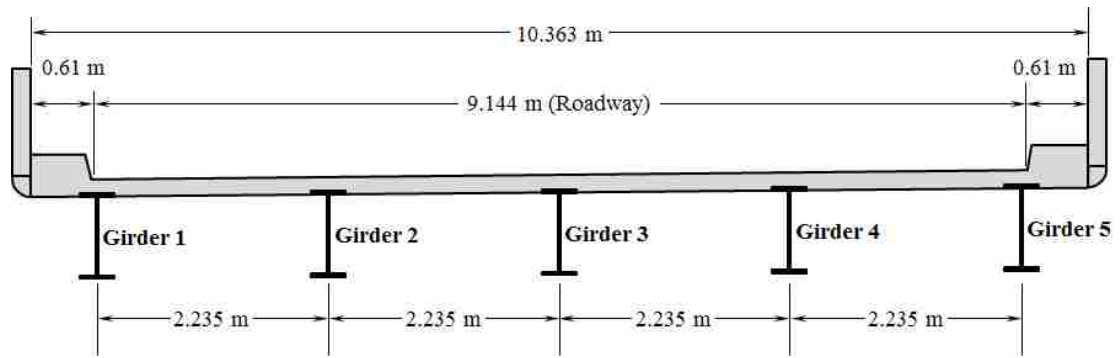
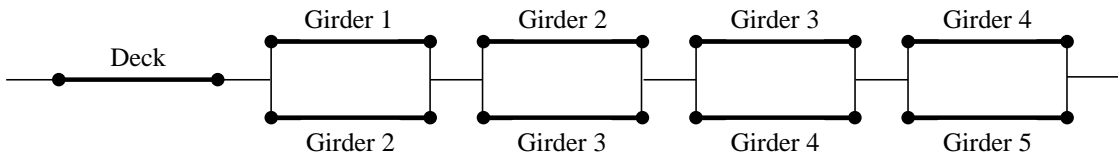


Figure 3.3. Transverse cross-section of the superstructure of bridge E-16-FK.



Girder 1 and 5: exterior girders  
Girders 2, 3, and 4: interior girders

Figure 3.4. System reliability model for the investigated bridge superstructure.

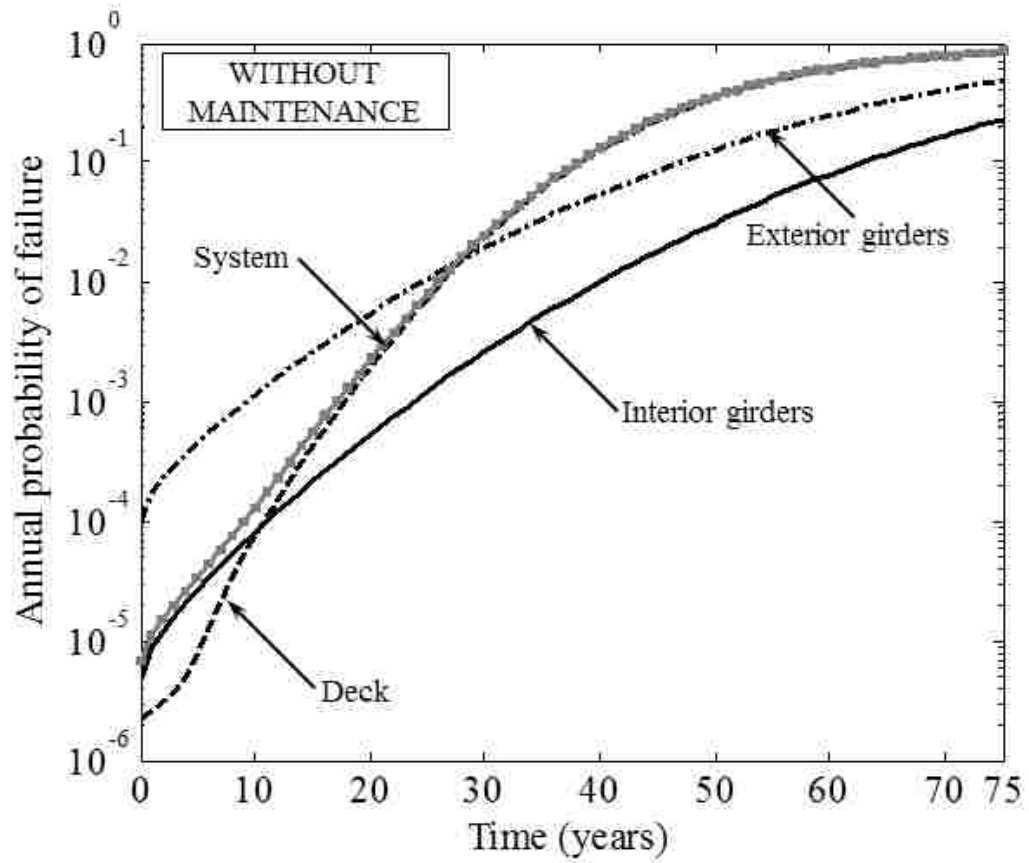


Figure 3.5. Evolution of annual probability of failure over time of the elements of the superstructure and the system, as a whole.

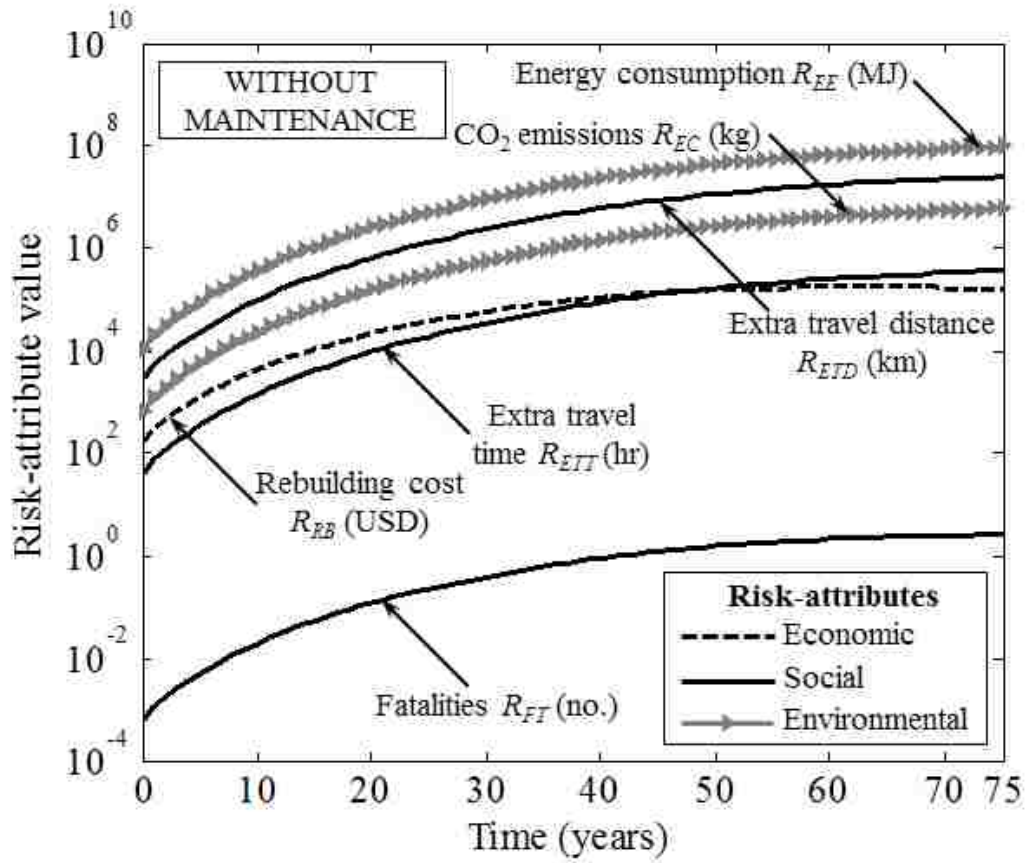


Figure 3.6. Time-variant risk attributes considering no maintenance.

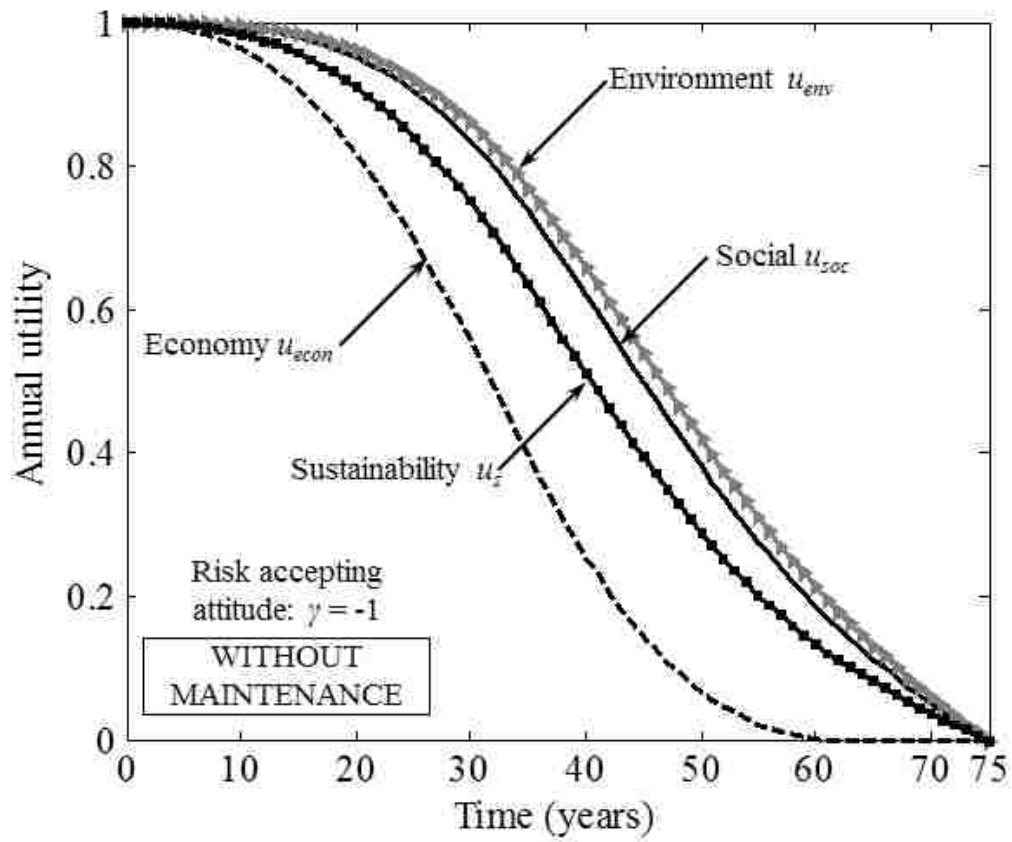


Figure 3.7. Profiles of annual utility associated with economic, social, and environmental sustainability metrics considering no maintenance and a risk averse attitude ( $\gamma = -1$ ).

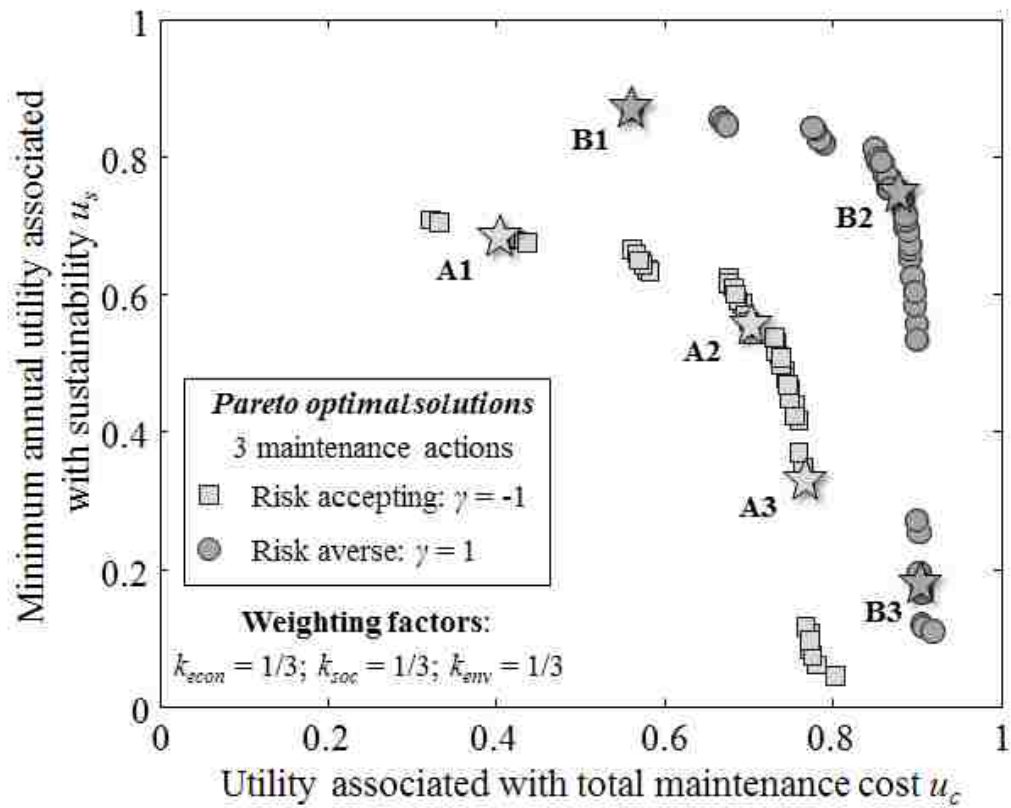


Figure 3.8. Pareto optimal solutions for three maintenance actions considering risk accepting and risk averse attitudes.

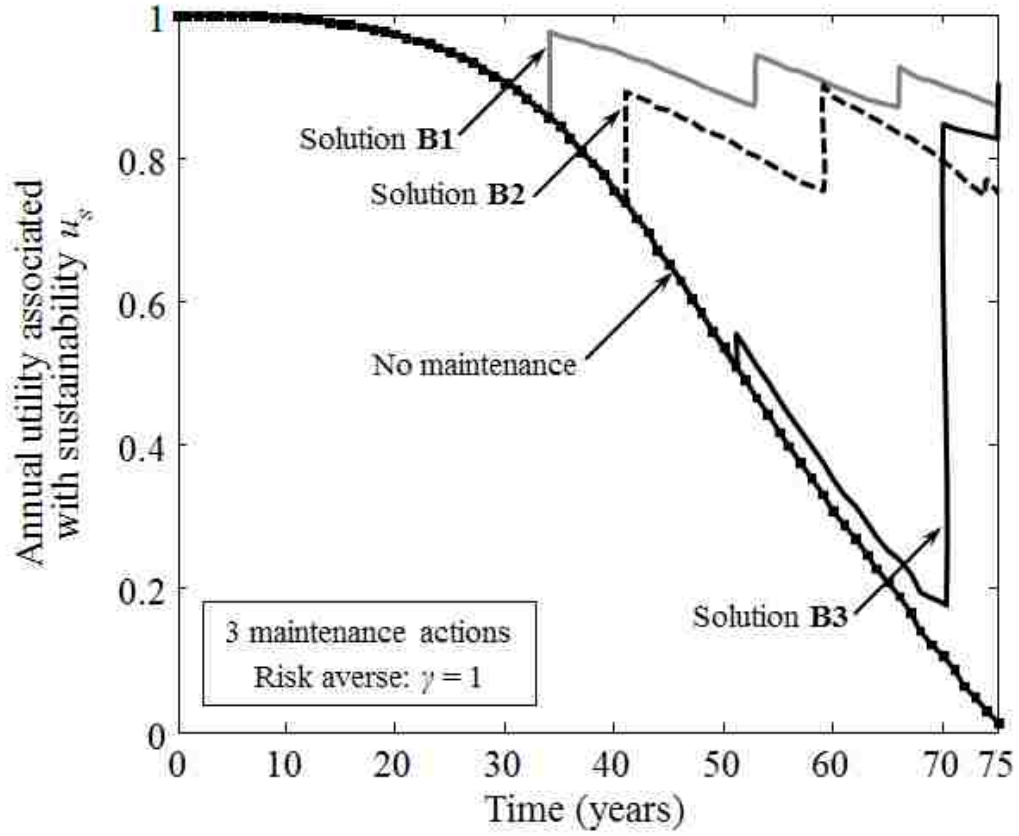


Figure 3.9. Profiles of annual utility associated with sustainability corresponding to three (B1, B2, B3) optimal solutions considering a risk averse decision maker as shown in Figure 3.8.

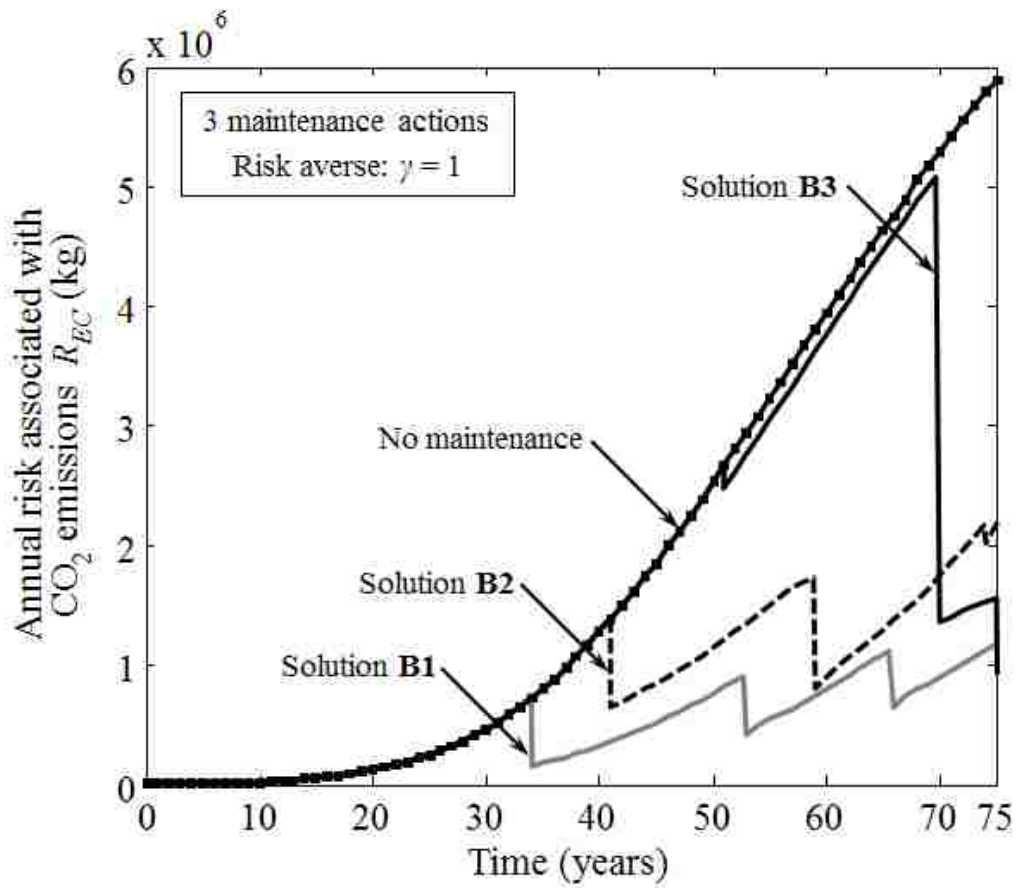


Figure 3.10. Time-variant annual risk associated with CO<sub>2</sub> emissions  $R_{EC}$  corresponding to representative optimal solutions considering a risk accepting decision maker as shown in Figure 3.8.

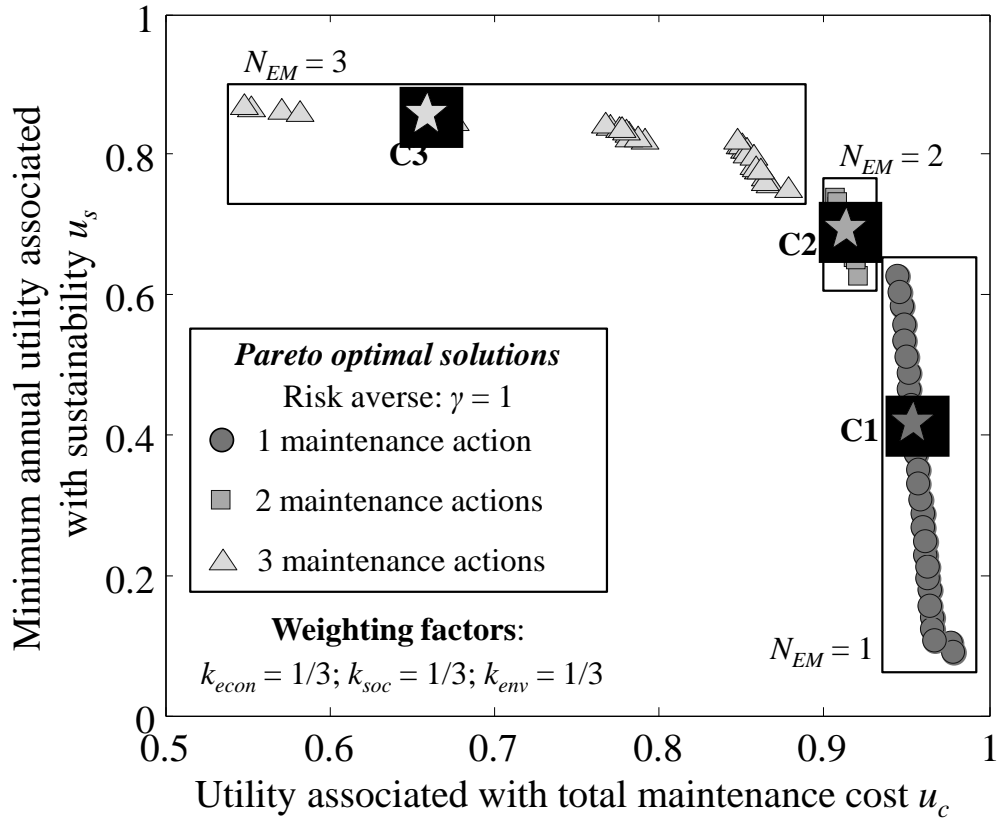


Figure 3.11. Pareto optimal solutions considering a variable number of essential maintenance actions and a risk averse decision maker.

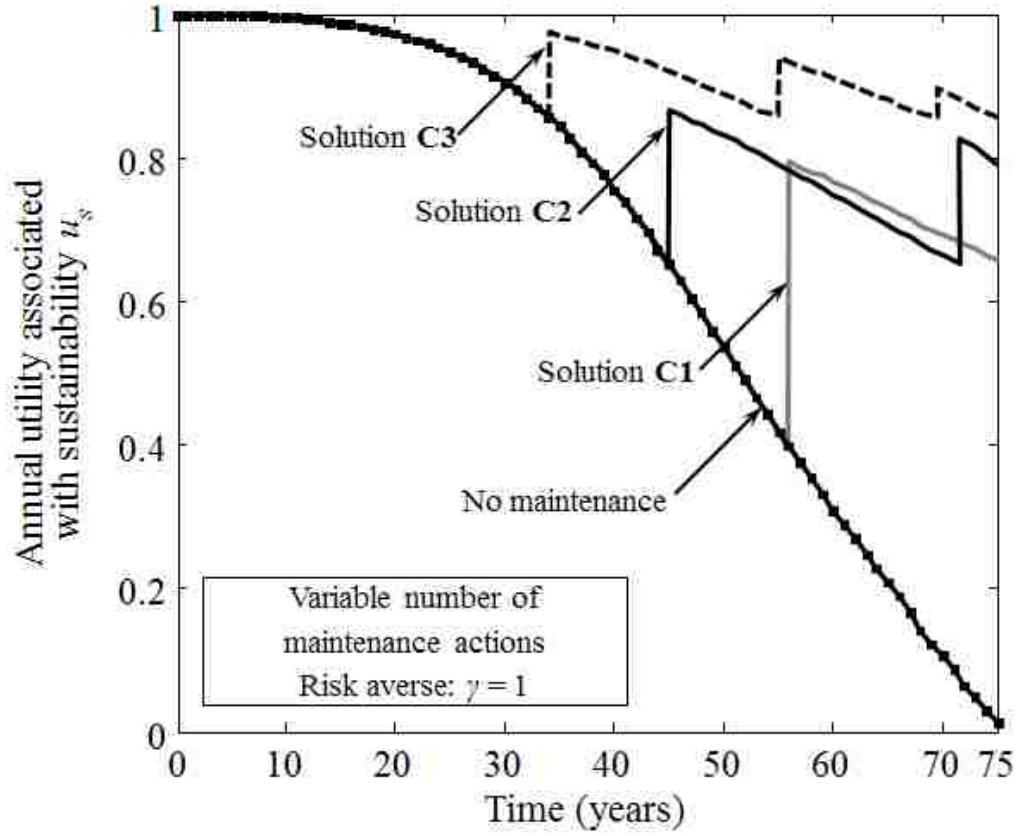


Figure 3.12. Annual utility associated with sustainability corresponding to representative solutions on the Pareto front in Figure 3.11.

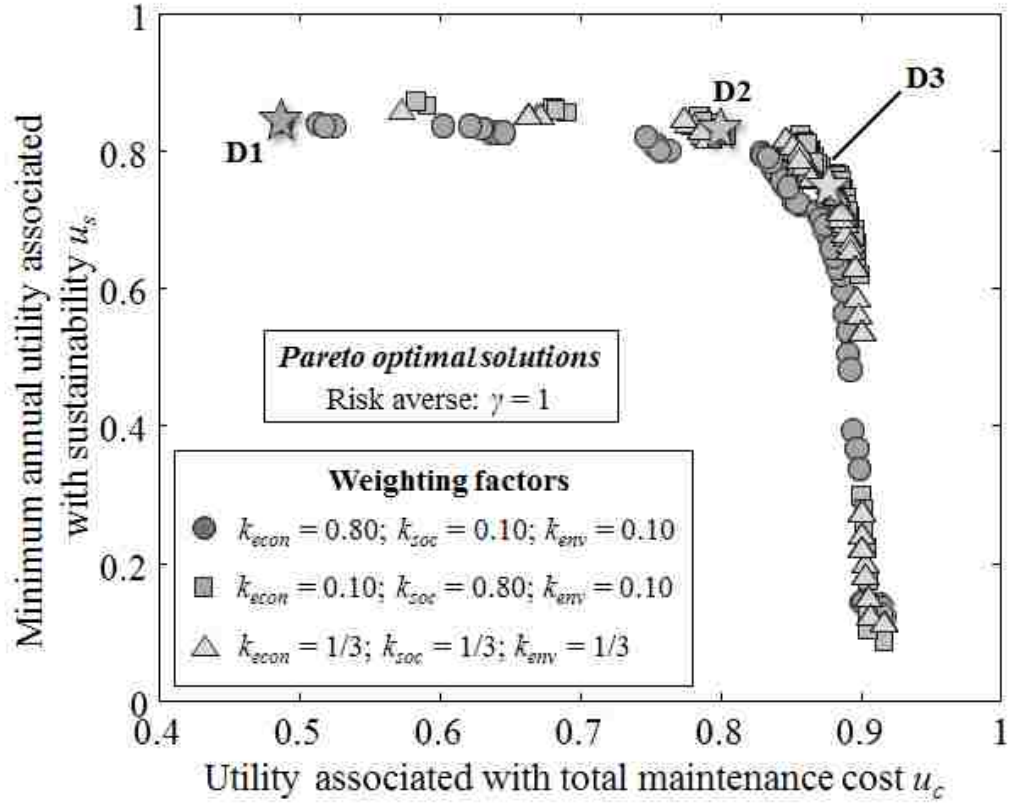


Figure 3.13. Pareto optimal solutions considering variable multi-attribute utility weighting factors and a risk averse decision maker.

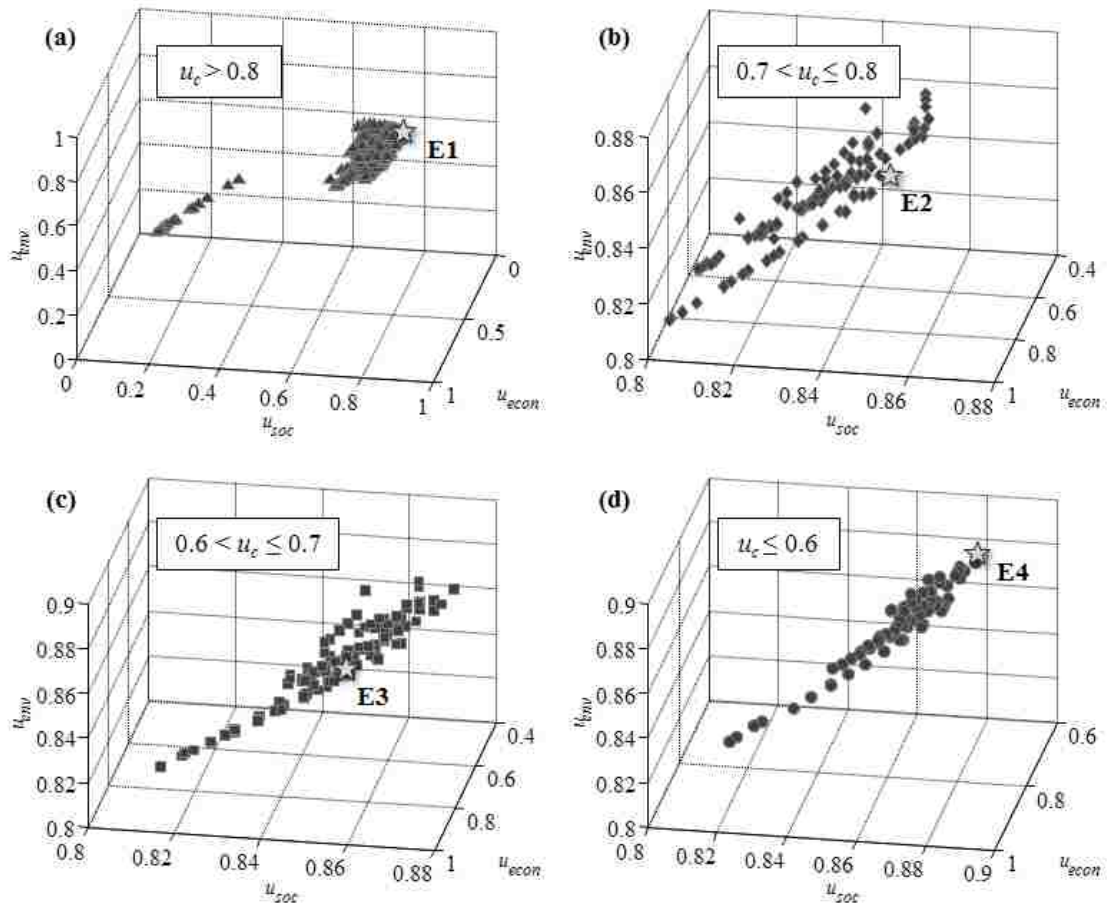


Figure 3.14: Pareto optimal solutions for the four-objective optimization problem that simultaneously maximizes  $u_c$ ,  $u_{econ}$ ,  $u_{soc}$ , and  $u_{env}$  considering a risk averse attitude ( $\gamma = 1$ ).

# **CHAPTER 4 LIFE-CYCLE UTILITY-INFORMED MAINTENANCE PLANNING BASED ON LIFETIME FUNCTIONS: OPTIMUM BALANCING OF COST, FAILURE CONSEQUENCES AND PERFORMANCE BENEFIT**

## **4.1 OVERVIEW**

Decision making regarding the optimum maintenance of civil infrastructure systems under uncertainty is a topic of paramount importance. This topic is experiencing growing interest within the field of life-cycle structural engineering. Embedded within the decision making process and optimum management of engineering systems is the structural performance evaluation, which is facilitated through a comprehensive life-cycle risk assessment. Lifetime functions are utilized herein to model, using closed form analytical expressions, the time-variant effect of intervention actions on the performance of civil infrastructure systems. Multi-attribute utility theory is used to incorporate the influence of the decision maker's risk attitude on the relative desirability of lifetime maintenance strategies. The presented decision-support framework has the ability to quantify maintenance cost, failure consequences, and performance benefit in terms of utility. This framework effectively employs tri-objective optimization procedures in order to determine optimum maintenance strategies under uncertainty. It provides optimum lifetime intervention plans allowing for utility-informed decision making regarding maintenance of civil infrastructure systems. The effects of the risk attitude, correlation among components, and the number of maintenance interventions on the optimum maintenance strategies are

investigated. The capabilities of the proposed decision support framework are illustrated on an existing highway bridge.

The work presented in this chapter is based upon the research published in Sabatino *et al.* (2016); Frangopol and Sabatino (2016a,b); and Frangopol *et al.* (2016a,2017).

## **4.2 INTRODUCTION**

In 2013, the American Society of Civil Engineers reported, within the Report Card for America's Infrastructure, that the average age of the United States' 607,380 bridges was 42 years (ASCE 2013). Additionally, nearly a quarter of these highway bridges were classified as either structural deficient or functionally obsolete (FHWA 2013). These staggering statistics highlight the dire need to implement rational mitigation strategies that maintain structural performance within acceptable levels through the life-cycle of deteriorating civil infrastructure. Throughout their service lives, highway bridges may be subjected to various stressors that cause their structural performance to decrease over time, ultimately leading to failure. The consequences associated with structural failure can be widespread and significant. In order to avoid the detrimental effects of structural failure, lifetime functions, paired with risk and sustainability indicators, are utilized within an efficient life-cycle maintenance optimization procedure to find intervention strategies that balance maintenance cost, failure consequences, and performance benefit.

Decision making regarding the optimum maintenance of civil and marine infrastructures is a topic of paramount importance and is experiencing growing interest

within the field of life-cycle structural engineering. In general, decision making may be divided into five separate stages: the pre-analysis, problem set-up, uncertainty quantification, utility assignment, and optimization (Keeney and Raiffa 1993). First, all possible solution alternatives are identified and the uncertainties associated with the investigated decision-making problem are accounted for using a probabilistic approach. Since technical and economic uncertainties are both expected and unavoidable in the life-cycle assessment of civil structures, decisions regarding infrastructure must consider all relevant uncertainties associated with the probability of structural failure and its corresponding consequences (Ang 2011). For deteriorating highway bridges, uncertainties are present within modeling the structural resistance (e.g., material properties and element dimensions), the occurrence and magnitude of hazards that may impact the structure (e.g., corrosion, fatigue, earthquakes, floods, and hurricanes), operating conditions, and loading cases (Stewart 2001).

After effectively incorporating the appropriate uncertainties, the decision maker may assign utility values to the attributes associated with each alternative considering his/her risk attitude. Utility theory is applied to normalize each attribute to a number between 0 and 1 so that all attributes corresponding to a solution alternative can be directly compared. The formulation of the utility function corresponding to each attribute greatly depends on the knowledge, preferential characteristics, and risk attitude of the decision maker. The attributes investigated herein include cost (i.e., cost of essential maintenance), failure consequences (i.e., direct and indirect risks), and performance benefit (i.e., improvement in lifetime functions). In this chapter, these attributes are identified as cost, risk, and benefit, respectively. In order to effectively

combine certain attributes for further use in a tri-objective optimization procedure, a multi-attribute utility function is developed that considers the weighted relative utility value corresponding to each attribute involved. In the last step of the decision making process, optimization is performed in order to find the alternative that maximizes the utility value. The proposed framework incorporates three conflicting and inter-related objectives into a maintenance optimization procedure that has the capability of determining the best intervention schedules (i.e., maintenance plans detailing the components to be maintained and timing of interventions) that simultaneously balance cost, risk, and benefit.

Within the proposed decision support system for life-cycle maintenance planning of civil structures, several separate detrimental impacts are considered in quantifying the consequences of structural failure to the economy, society, and surrounding environment in terms of risk. In its most basic form, risk is calculated as the probability of occurrence of a specific event multiplied by the consequence associated with this event. Previous research efforts have included risk analyses in both qualitative (Hessami 1999; Ellingwood 2001) and quantitative manners (Pedersen 2002; Decò and Frangopol 2011, 2012, 2013; Barone and Frangopol 2014a; Barone *et al.* 2014) considering a wide variety of hazards and many different structures (Arunraj and Maiti 2007).

In this chapter, risk assessment techniques are combined with multi-attribute utility theory to establish appropriate risk and performance benefit indicators that incorporate different attributes. The utility values associated with risk and benefit are computed considering the difference between the risk and benefit attributes after and

before maintenance is applied. A similar approach for the risk and benefit assessment was employed by Sabatino *et al.* (2015), in which a decision making support tool was developed for the maintenance of existing highway bridges considering multi-attribute utility theory within a bi-objective optimization process that balances the utility values associated with maintenance cost and sustainability. Multi-attribute utility theory was also employed by Dong *et al.* (2014e) to determine optimum retrofit actions for a network of bridges subjected to seismic hazard. Although previous studies employed multi-attribute utility to represent the risks that plague structures, the work herein focuses on establishing a comprehensive decision support framework that (a) utilizes computationally efficient lifetime functions, (b) incorporates a large variety of criteria within a tri-objective optimization procedure that balances maintenance cost, risks, and benefit, and (c) may be applied to a wide array of engineering systems.

Lifetime distributions are used to represent the performance of a structural system over its life-cycle through functions that probabilistically characterize the system's time-to-failure, which is regarded as a continuous, non-negative random variable (Leemis 1995). These functions have been utilized to model the time-variant effect of intervention actions on the performance of structural systems in several studies including van Noortwijk and Klatter (2004), Yang *et al.* (2004, 2006a,b), Okasha and Frangopol (2009, 2010c); Orcesi and Frangopol (2011), and Barone and Frangopol (2013, 2014a,b). Moreover, research regarding lifetime functions has emphasized their power as an effective tool in quantifying the lifetime reliability of highway bridges (Yang *et al.* 2004). Barone and Frangopol (2014a,b) used system hazard and availability to quantify structural performance and determine optimum

maintenance schedules for an existing highway bridge. However, lifetime functions were not used to calculate risk. Lifetime functions are employed herein to determine the benefit provided by optimized lifetime maintenance plans based upon minimum lifetime system availability and maximum lifetime system hazard. Furthermore, these functions are directly incorporated within risk calculations herein in order to compute both direct and indirect risks.

As indicated previously, the proposed decision-support framework has the ability to quantify cost, risk, and benefit in terms of utility and effectively employs tri-objective optimization procedures in order to determine optimum maintenance strategies. The effects of the risk attitude and preferences of the decision maker, in addition to the number of maintenance interventions on the optimum maintenance strategies, are investigated. A genetic algorithm (GA) based optimization procedure is employed to find optimum maintenance schedules. The proposed approach provides optimum lifetime intervention strategies to the decision maker that ultimately allows for risk-informed decision making regarding maintenance of civil infrastructure. The capabilities of the presented decision support framework are illustrated on five representative 4-component series-parallel systems and an existing highway bridge located in Colorado.

### **4.3 LIFETIME FUNCTIONS**

The main advantage of employing lifetime distributions within reliability calculations is the extreme mathematical flexibility that is provided by their closed-formulation expression of the distribution of time-to-failure. Due to their mathematical versatility,

computations involving lifetime distributions are efficient; thus, these distributions are particularly suitable for problems involving optimization (Okasha and Frangopol 2010b). Generally, lifetime distributions are used to represent time-variant structural performance through continuous functions that are established in closed-form by considering the time-to-failure of components as a continuous random variable (Okasha and Frangopol 2010c). More specifically, the time-to-failure random variable is defined as the time elapsing from the time a component is put into operation until it fails for the first time (Hoyland and Rausand 1994). The type of distribution used to represent the probability density function (PDF) associated with the time-to-failure of a particular component is determined based upon its failure characteristics and historical material behavior. Commonly employed distributions used to represent the PDF of time-to-failure are the Weibull and exponential distributions (Jiang and Murthy 1995; Lai and Murthy 2003; van Noortwijk and Klatter 2004; Okasha and Frangopol 2010c). With knowledge of the PDFs describing the times-to-failure of the components comprising an engineering system, the distribution of the system time-to-failure can be calculated considering the type and configuration (e.g., series, parallel, or series-parallel) of the system.

#### ***4.3.1 Component analysis***

The most commonly used lifetime functions include the PDF of the time-to-failure and survivor, availability, and hazard functions. The Weibull PDF of component time-to-failure is (Leemis 1995):

$$f(t) = k \cdot \lambda \cdot (\lambda \cdot t)^{k-1} \exp\left[-(\lambda \cdot t)^k\right] \text{ for } t > 0 \quad (4.1)$$

where  $k$  and  $\lambda$  are the shape and scale parameter of the Weibull distribution, respectively. In general, the shape and scale parameters used in the Weibull PDF of the time-to-failure associated with the components of a structural system are determined based upon failure data related to specific materials and deterioration mechanisms. Next, the probability that the time-to-failure  $T_F$  of the investigated component is less than a given time instant  $t$ , denoted as the cumulative-time failure probability  $F(t)$ , is:

$$F(t) = P[t > T_F] = \int_0^t f(x)dx \quad (4.2)$$

where  $T_F$  = time-to-failure of the investigated component or system. The complement of  $F(t)$  is the survivor function  $S(t)$ , which expresses the probability of a component or system surviving (i.e., not failed) before the time instant  $t$ .  $S(t)$  has been utilized to assess bridge lifetime performance and to facilitate the implementation of maintenance strategies to an existing structure (Yang *et al.* 2004, 2006a,b). The survivor function, in its most general form, is (Leemis 1995):

$$S(t) = 1 - F(t) = P[t \leq T_F] = \int_t^{\infty} f(x)dx \quad (4.3)$$

If  $f(t)$  follows a Weibull distribution, the associated survivor function is:

$$S(t) = 1 - F(t) = \exp\left[-(\lambda \cdot t)^k\right] \quad (4.4)$$

The survivor function may be used as a basis to calculate other lifetime functions. For example, the availability of a component  $A(t)$ , which is defined as the probability that the component is functioning at a given time instant, coincides with  $S(t)$  when no maintenance is considered (Ang and Tang 1984; Leemis 1995). The availability

function has been employed in assessing the effects of implementing intervention strategies to existing civil infrastructure (Biswas *et al.* 2003; Barone and Frangopol 2014a,b).

In addition to availability, the hazard function  $h(t)$  is also investigated as a suitable performance indicator in the context of lifetime functions. This function provides information regarding how fast a component becomes non-functional over time. Overall, the hazard metric is representative of the occurrence of failure as a function of time for any component. There are several other common terms utilized to describe the hazard function including hazard rate, failure rate, rate function, and intensity function. The hazard function has been successfully applied to several areas of science and engineering, including biological sciences (Tanner and Wong 1984; Heidenreich *et al.* 1997; Horová *et al.* 2009), performance assessment of engineering systems (Zhang and Li 2010; Amari *et al.* 2012; Thies *et al.* 2012), fatigue analysis (Lawson and Chen 1995), and optimum maintenance planning of complex systems (Cui *et al.* 2004; Barone and Frangopol 2014a,b).

The hazard function  $h(t)$  for a particular component is calculated by considering the probability of failure between  $t$  and  $t + \Delta t$  conditioned on the event that the component is functioning at time  $t$  (Leemis 1995):

$$h(t) = \lim_{\Delta t \rightarrow 0} \frac{P[t \leq T_F \leq t + \Delta t \mid t \leq T_F]}{\Delta t} = -\frac{S'(t)}{S(t)} = \frac{f(t)}{S(t)} = \frac{f(t)}{1 - F(t)} \quad (4.5)$$

The units of  $h(t)$  are typically given in failures per time unit. Therefore, in order to determine the number of expected failures within a certain interval,  $h(t)$  is multiplied by that time interval. The shape of the hazard function is indicative of how a

component ages. In general, when the hazard function is large, the component is subject to a significant risk of failure, and when the hazard function is small, the component has less chance of experiencing failure. Considering the assumption that the PDF of time-to-failure  $f(t)$  follows the Weibull distribution, the expression for  $h(t)$  is:

$$h(t) = k \cdot \lambda^k \cdot t^{k-1} \quad (4.6)$$

### ***4.3.2 System analysis***

Thus far, the mathematical relations for the survivor  $S(t)$ , availability  $A(t)$ , and hazard  $h(t)$  functions for the component level have been presented. In order to formulate system-level expressions, the configuration of the system must be considered. For systems comprised of components with known lifetime distributions, the closed-form system survivor  $S_{\text{sys}}(t)$ , availability  $A_{\text{sys}}(t)$ , and hazard  $h_{\text{sys}}(t)$  functions may be obtained for both statistically independent (i.e.,  $\rho = 0$ ) and perfectly correlated (i.e.,  $\rho = 1$ ) components based upon cut set techniques (Leemis 1995) considering the system configuration (e.g., series, parallel, or series-parallel).

### ***4.3.3 Effects of essential maintenance***

The main advantage of employing lifetime functions to facilitate efficient maintenance planning lies in the fact that it is possible to perform direct computations in analytical form. In general, the type of maintenance applied to structural components greatly depends upon the deterioration mechanisms and their evolution in time. Accordingly, different maintenance measures may be applied during the lifetime of a structural

component. Assuming that only essential maintenance (i.e., full replacement of component(s)) is implemented and that interventions are performed  $N$  times during the lifetime of a deteriorating system, the resulting change to component lifetime functions may be evaluated.  $S_i(t) = 1 - F_i(t)$ ,  $A_i(t)$ , and  $h_i(t)$  represent the  $i$ th's component lifetime functions with no maintenance, while  $S_{i,m}(t) = 1 - F_{i,m}(t)$ ,  $A_{i,m}(t)$ , and  $h_{i,m}(t)$  denote the same component's lifetime functions considering maintenance. Assuming essential maintenance is implemented at times  $T_1, \dots, T_N$  on the  $i$ th component and  $T_0 = 0$  (i.e., the initial observation time), the  $i$ th component's resulting survivor function adjusted for maintenance  $S_{i,m}(t)$ , is:

$$S_{i,m}(t) = \begin{cases} S_i(t) & \text{for } t < T_1 \\ S_i(t - T_N) \prod_{j=1}^N S_i(T_j - T_{j-1}) & \text{for } T_N \leq t \leq T_{N+1}, j \geq 1 \end{cases} \quad (4.7)$$

where  $S_i(t) = 1 - F_i(t)$  = survivor function associated with component  $i$  considering no maintenance. Each time essential maintenance is applied to component  $i$ , the magnitude of the slope corresponding to  $S_{i,m}(t) = 1 - F_{i,m}(t)$  decreases. Although the survivor function is a continuous, monotonically decreasing function of time, the availability function abruptly increases in value whenever maintenance is performed. More specifically, it is assumed that component availability is restored to its original value (i.e.,  $A_{i,m}(t) = 1$ ) when essential maintenance (i.e., full replacement) is performed on a particular component. The availability function corresponding to a maintained component  $i$ ,  $A_{i,m}(t)$ , is obtained from the unmaintained component survivor function as (Okasha and Frangopol 2010b):

$$A_{i,m}(t) = \begin{cases} S_i(t) & \text{for } t < T_1 \\ S_i(t - T_N) & \text{for } T_N \leq t \leq T_{N+1} \end{cases} \quad (4.8)$$

In a similar way, component hazard is restored to its initial value (i.e.,  $h_{i,m}(t) = 0$ ) after each replacement. The hazard function for the maintained component  $i$  is:

$$h_{i,m}(t) = h_i(t - T_N) \quad \text{for } T_N \leq t \leq T_{N+1} \quad (4.9)$$

where  $h_i(t)$  = hazard function associated with component  $i$  without maintenance.

After component lifetime functions are established for a particular maintenance plan, the lifetime functions at the system-level can provide information regarding the structural system performance considering maintenance. Calculations of system survivor  $S_{sys,m}(t)$ , availability  $A_{sys,m}(t)$ , and hazard  $h_{sys,m}(t)$  are highly dependent upon system configuration and the correlation among components (i.e., statistically independent  $\rho = 0$  or perfectly correlated  $\rho = 1$ , where  $\rho$  = correlation coefficient).

#### 4.4 ATTRIBUTES EVALUATION

This section highlights the three separate objectives utilized within the optimization procedure embedded within the proposed decision support framework for lifetime maintenance planning. Maintenance *cost*, *failure consequences* quantified via *risk* metrics, and performance *benefit* measured by the improvement in minimum annual system availability and maximum annual system hazard are regarded as the three objectives investigated herein.

#### 4.4.1 Cost

The cost of a lifetime maintenance plan is computed in terms of USD in the year the structure was built. The total cost of a lifetime essential maintenance strategy is determined as:

$$C_{maint} = \sum_{j=1}^N \frac{C_{EM,j}(t)}{(1+r_m)^t} \quad (4.10)$$

where  $C_{EM,j}$  = cost of maintenance action  $j$  applied at year  $t$  (USD),  $r_m$  = annual discount rate of money, and  $N$  = total number of essential maintenance actions considered throughout the lifetime of a structure.

#### 4.4.2 Consequences

Risk, which combines the probability of occurrence of a specific event with the consequence associated with this event, is a crucial performance indicator for civil infrastructure. A simple formulation of risk is (Ang and De Leon 2005):

$$R = p \cdot \chi \quad (4.11)$$

where  $p$  = probability of occurrence of an adverse event and  $\chi$  = consequences of the event. Three main consequences are investigated herein for highway bridges: economic, social, and environmental impacts. More specifically, these consequences include the rebuilding and repair costs (economic losses); extra travel time and distance that drivers must endure, in addition to any fatalities that may occur (social impact); and energy consumption and carbon dioxide (CO<sub>2</sub>) emissions (environmental consequences). Both the effects of direct (i.e., economic impacts) and indirect (i.e., social and environmental losses) consequences may be incorporated into the

calculation of the total risk. Overall, the evaluation of a wide variety of consequences associated with structural failure plays a fundamental role in the decision making process regarding infrastructure management planning. Time-variant direct and indirect risk attributes are calculated considering the following expressions:

$$RA_{direct}(t) = P_{f,sys}(t) \cdot C_{direct}(t) \quad (4.12)$$

$$RA_{indirect}(t) = P_{f,sys}(t) \cdot C_{indirect}(t) \quad (4.13)$$

where  $P_{f,sys}(t)$  = probability of system failure during year  $t$ ,  $C_{direct}(t)$  = direct consequences associated with system failure, and  $C_{indirect}(t)$  = indirect consequences. The total risk associated with a particular system is calculated considering the sum of its direct and indirect risks. In this chapter, the annual probability of system failure  $P_{f,sys}(t)$  is calculated using the system hazard function  $h_{sys}(t)$  and the cumulative-time failure probability is calculated using the complement of the survivor system function  $F_{sys}(t) = 1 - S_{sys}(t)$ . These two ways of calculating the system probability of failure (i.e., annual and cumulative) yield distinctly different optimum maintenance plans considering all other parameters remain the same. In fact, the illustrative highway bridge example presented herein investigates the sensitivity of the optimum solutions to which form of the probability of system failure is utilized within risk calculations.

Although specific risks related to the economic, social, and environmental impacts are considered herein, the decision maker may include his/her desired number of risk attributes within the related lifetime maintenance optimization procedure. For example, if the most dire concern of the decision maker is the effects of structural

failure on the surrounding environment and local society, then he/she may decide to employ only the indirect consequences within the developed risk calculation approach.

#### **4.4.3 Benefit**

The performance benefit utilized within the proposed tri-objective maintenance optimization framework is calculated based on the improvement in lifetime function values when essential maintenance strategies are implemented. Two indicators are utilized as benefit attributes herein: (a) an increase in the minimum lifetime availability and (b) a decrease in the maximum lifetime hazard when comparing the no maintenance case with the optimum maintenance case. Therefore, when considering just the increase in minimum lifetime availability as the sole benefit, the difference between minimum lifetime availability offered by the cases without and with maintenance serves as the index employed to measure the performance benefit. A similar procedure may be carried out to determine the performance benefit in terms of system hazard. Although the benefits included herein are related to availability and hazard, other benefits of implementing lifetime maintenance strategies may be included in the proposed decision making framework.

#### **4.5 UTILITY ASSESSMENT**

Utility functions that depict the relative value of each attribute to the decision maker considering his/her particular risk attitude play vital roles within the proposed decision making support system. Maintenance strategies associated with relatively high utility values are typically the most desirable solutions. This section provides the process for formulating single and multi-attribute utility functions that effectively depict the

decision maker's value of lifetime maintenance schedules in terms of cost, risk, and benefit. Overall, the computational procedure adopted herein for computing attributes and their corresponding utility values, in relation to decision making, is shown in Figure 4.1.

#### 4.5.1 *Single attribute utility assignment*

Two types of attributes are considered: (a) one that possesses decreased desirability when its attribute value is increased, and (b) another that exhibits increased desirability as the attribute value increases. The investigated attributes that fall into the first category are maintenance cost, direct and indirect risk, and system hazard. The system availability is the only attribute herein that causes an increase in desirability as the attribute value is increased. Figure 4.2(a) depicts a qualitative representation of typical exponential utility functions that are monotonically decreasing for the attributes that experience a decrease in utility (i.e., desirability) as the attribute value increases. Conversely, Figure 4.2(b) shows representative exponential utility functions that are monotonically increasing for the system availability; as the system availability increases, the utility also increases. The governing equation for the utility functions shown in Figure 4.2(a) is (Ang and Tang 1984):

$$u_{a,dec} = \frac{1}{1 - \exp[-\gamma]} \left( 1 - \exp \left[ -\gamma \frac{a_{\max} - a}{a_{\max} - a_{\min}} \right] \right) \quad (4.14)$$

where  $\gamma$  = risk attribute of the decision maker (i.e.,  $\gamma > 0$  indicates risk aversion and  $\gamma < 0$  denotes risk acceptance),  $a$  = expected value of the attribute value under investigation,  $a_{\min}$  = minimum value of the attribute, and  $a_{\max}$  = maximum value of the attribute. The minimum and maximum values of the investigated attribute are utilized

to normalize the utility so that it always takes values between 0 and 1. Considering the same solution alternative, a risk averse attitude will produce yield a higher utility than that yielded from a risk accepting attitude. Similarly, the monotonically increasing utility functions shown in Figure 4.2(b) are governed by the following equation.

$$u_{a,inc} = \frac{1}{1 - \exp[-\gamma]} \left( 1 - \exp \left[ -\gamma \frac{a - a_{\min}}{a_{\max} - a_{\min}} \right] \right) \quad (4.15)$$

For a single attribute,  $u_a = 1$  and  $u_a = 0$  correspond to the most and least desirable value that the investigated attribute may take, respectively. In general, a risk averse attitude produces a concave utility function, while a risk accepting attitude is exhibited by a convex utility function.

#### **4.5.2 Multi-attribute utility**

Once the utility function associated with each attribute is appropriately established, multi-attribute utility theory may be employed to combine them into single utility values that effectively represent each of the three separate utility objectives employed in the optimization procedure presented herein (i.e., cost  $u_{cost}$ , risk  $u_{risk}$ , and benefit  $u_{benefit}$ ). Although there are various types of multi-attribute utility functions, the additive formulation is employed herein. This formulation is obtained by multiplying marginal utility values associated with each attribute by weighting factors and summing over all attributes investigated (Stewart 1996). The utility associated with indirect risk  $u_{r,i}$  is computed considering equal contributions of social and environmental consequences. Subsequently, the utility associated with the total risk is quantified as:

$$u_{r,tot} = \frac{1}{2}(u_{r,d} + u_{r,i}) \quad (4.16)$$

where  $u_{r,d}$  = utility associated with direct risk, and  $u_{r,i}$  = utility associated with indirect risk.

Similarly, the first step in formulating the multi-attribute utility function representative of the performance benefit considering maintenance is calculating the utility of the minimum lifetime system availability and maximum lifetime system hazard. If the decision maker would like the multi-criteria optimization procedure to include the effects of both system availability and hazard, then the following formulation of the benefit utility under maintenance is used:

$$u_{b,m} = \frac{1}{2}(u_A + u_h) \quad (4.17)$$

where  $u_{b,m}$  = utility associated with the performance benefit considering maintenance,  $u_A$  = utility associated with minimum lifetime system availability, and  $u_h$  = utility associated with maximum lifetime system hazard. Additionally, if the decision maker desires only the effect of system availability or hazard to be included within the performance benefit utility, then  $u_{b,m} = u_A$  or  $u_{b,m} = u_h$ , respectively.

The utility associated with cost  $u_{cost}$  is calculated using the exponential form of the single attribute utility function. Cost attributes can easily be incorporated within the decision making process if reliable data regarding these cost metrics are available.

### ***4.5.3 Utility associated with performance benefit***

The total utility associated with the performance benefit,  $u_{benefit}$ , is:

$$u_{benefit} = u_{b,m} - u_{b,0} \quad (4.18)$$

where  $u_{b,0}$  = performance utility without maintenance.

#### **4.6 TRI-OBJECTIVE OPTIMIZATION FRAMEWORK FOR LIFETIME MAINTENANCE PLANNING**

Overall, the three utility functions integrated within the presented multi-criteria optimization framework represent the relative value of solution alternatives to the decision maker, considering his/her risk attitude. The three objectives that are all simultaneously maximized are: (a) utility corresponding to lifetime maintenance investment cost  $u_{cost}$ , (b) utility associated with risk  $u_{risk}$ , and (c) utility associated with performance benefit  $u_{benefit}$ . The general methodology embedded within the proposed optimization procedure is shown in Figure 4.1. Within the proposed framework, three separate modules compute the objective values utilized within the multi-criteria optimization process, whose results come in the form of Pareto optimum solutions outlining bridge maintenance planning. Although the numerical examples presented herein address the life-cycle essential maintenance planning problem, the proposed multi-criteria decision support system has the capability to optimize non-essential maintenance interventions (e.g., preventive measures which may delay deterioration or temporarily reduce the rate of deterioration) if information regarding the effect of these actions becomes available. A set of Pareto optimum solutions is obtained utilizing GAs within an adequate number of generations (Okasha and Frangopol 2009; Frangopol 2011; Dong *et al.* 2014e).

The *tri-objective* optimization problem is formulated as follows:

**Given:**

- Lifetime functions representing time-variant structural performance of components comprising an engineering system (information associated with Eqs. 4.1 – 4.6)
- Monetary cost associated with specific essential maintenance actions (input to Eq. 4.10)
- Risk associated with structural failure (Eqs. 4.11– 4.13)
- Risk attitude of the decision maker ( $\gamma$  in Eqs. 4.14 and 4.15)
- Desired attributes to be included (e.g., direct, indirect, or total risk within the formulation of  $u_{risk}$ )
- Lifetime under investigation ( $T_L$ )
- Total number of maintenance actions ( $N$ )

***Find:***

- Components to be maintained
- Time of application of maintenance actions

***So that:***

- Utility associated with the total maintenance cost  $u_{cost}$  is maximized
- Minimum utility associated with risk  $u_{risk}$  over the system's lifetime is maximized
- Minimum utility associated with performance benefit  $u_{benefit}$  over the system's lifetime is maximized

***Subjected to:***

- Maximum allowable total maintenance cost
- Constraints on the allowable minimum and maximum values of each attribute ( $a_{min}$  and  $a_{max}$ , respectively, in Eqs. 4.14 and 4.15)
- Constraints on the application times of maintenance actions

#### 4.7 ILLUSTRATIVE EXAMPLE

In order to illustrate the capabilities of the proposed decision support system, the presented methodology is demonstrated on five systems consisting of the four same components, as shown in Figure 4.3. For these five configurations, the utility assignment is carried out and the evaluation of the no maintenance case is conducted in order to determine the effect of system configuration on the utility profiles. The shape  $k_i$  and scale  $\lambda_i$  parameters corresponding to the Weibull distribution are used to define the PDF of time-to-failure of the four components investigated in this example, as follows: component 1,  $k_1 = 2.6$  and  $\lambda_1 = 8 \times 10^{-3}$ ; component 2,  $k_2 = 2.4$  and  $\lambda_2 = 6 \times 10^{-3}$ ; component 3,  $k_3 = 2.4$  and  $\lambda_3 = 5 \times 10^{-3}$ ; and component 4,  $k_4 = 2.1$  and  $\lambda_4 = 6 \times 10^{-3}$ . For the systems in Figure 4.3, the closed-form system survivor  $S_{sys}(t)$ , availability  $A_{sys}(t)$ , and hazard  $h_{sys}(t)$  functions are obtained for both statistically independent (i.e.,  $\rho = 0$ ) and perfectly correlated (i.e.,  $\rho = 1$ ) components. The cumulative-time failure probability,  $F(t)$ , hazard  $h(t)$ , and availability  $A(t)$  of each of the four components in Figure 4.3 are shown in Figure 4.4(a), Figure 4.5(a), and Figure 4.6(a), respectively. Considering the five system configurations shown in Figure 4.3, the system cumulative-time failure probability  $F_{sys}(t) = 1 - S_{sys}(t)$ , availability  $A_{sys}(t)$ , and hazard  $h_{sys}(t)$  for the extreme correlation cases are shown in Figure 4.4(b), Figure 4.5(b), and

Figure 4.6(b), respectively. Since the calculation of the probability of failure may use either  $F_{sys}(t)$  or  $h_{sys}(t)$ , Figure 4.7 depicts the effects of correlation among components on both the cumulative-time system failure probability and annual system failure probability of systems A and E. The most conservative cases are associated with the cumulative-time failure probability for the independence and full correlation assumptions, for systems A and E, respectively.

Next, the consequences of structural failure are examined and the corresponding risk attributes are evaluated for Systems A to E. The economic impact (i.e., direct loss) is measured in terms of the risk associated with the rebuilding cost  $C_{direct}$  during a certain year. Similarly, the indirect losses (i.e., consequences to local society and environment) are measured in terms of the risk associated with the monetary indirect consequences  $C_{indirect}$ . For illustrative purposes, in this example,  $C_{direct}$  and  $C_{indirect}$  are assumed as 400,000 USD and 1,000,000 USD, respectively. Considering these assumptions, direct, indirect, and total risk profiles for systems A and E are shown in Figure 4.8.

The last step involves formulating the time-variant utility values associated with risk and benefit. Once the time-variant risk and benefit attributes are determined, they may be transferred to utility considering the exponential formulations in Eqs. (4.14) and (4.15). For example, the utility corresponding to each attribute is calculated considering the range of risk attribute values shown in Table 4.1. In this table,  $a_{min}$  and  $a_{max}$  are the expected attribute values at  $t = 0$  and  $t = T_L$  (i.e., 60 years).  $u_{risk}$  and  $u_{benefit}$  are computed using Eqs. (4.16) to (4.18). Figure 4.9 depicts utility profiles for system A with risk averse and risk taking attitudes. It is evident from this figure that risk

averse and risk taking attitudes yield convex and concave utility functions, respectively. Furthermore, time-variant total risk and benefit utilities of the five systems A to E are shown in Figure 4.10 and Figure 4.11, respectively. The effect of system configuration is quite significant. For systems with a high level of redundancy (i.e., systems B and E), both total risk and benefit utilities tend to remain at high levels for a longer period of time than those associated with the other systems.

#### **4.8 CASE STUDY**

The case study presented herein applies the developed framework to the E-17-HS bridge, an existing reinforced concrete highway bridge located in Adams County, Colorado. The bridge deck is supported by four reinforced concrete T-girders, as detailed in Akgül (2002). The superstructure of bridge (i.e., the system) is modeled with a series-parallel model that defines system failure as either failure of the deck or any two adjacent girders.

It is assumed that the PDFs of time-to-failure of the three main components of the bridge superstructure, the deck (D), exterior girders ( $G_E$ ), and interior girders ( $G_I$ ), follow the Weibull distribution with the following shape  $k_i$  and scale  $\lambda_i$  parameters: (a) deck,  $k_1 = 2.4$  and  $\lambda_1 = 8 \times 10^{-3}$ ; (b) exterior girders,  $k_2 = 2.3$  and  $\lambda_2 = 8 \times 10^{-3}$ ; and (c) interior girders,  $k_3 = 2.1$  and  $\lambda_3 = 6 \times 10^{-3}$  (Barone and Frangopol 2014a). The functions  $F(t)$ ,  $h(t)$  and  $A(t)$  associated with no maintenance considering extreme correlations and a lifetime  $T_L = 75$  years are reported in Figure 4.12. Figure 4.13 depicts the annual and cumulative system probability of failure profiles under extreme correlation conditions. The five possible maintenance options and their associated

costs considered herein are (Barone and Frangopol 2014a,b); replacing the deck (D), 100,000 USD; replacing the two exterior ( $G_E$ ) or the two interior ( $G_I$ ) girders, 80,000 USD; replacing all girders (G), 140,000 USD; and replacing the entire superstructure (S), 200,000 USD. An annual discount rate of money  $r_m = 0.02$  is assumed unless otherwise noted.

The next step includes evaluating the detrimental consequences associated with structural failure of the system. Based on Dong *et al.* (2015), the expected value of all the risk attributes are calculated in terms of their respective units. Namely, the economic impact (i.e., direct loss) is measured in terms of the risk associated with the rebuilding cost  $R_{RB}$  during a certain year, while the social consequences of bridge failure include the extra travel time  $R_{ETT}$  and distance  $R_{ETD}$  experienced by vehicle operators, in addition to any fatalities that may occur  $R_{FT}$ . The third type of risk examined encompasses the detrimental effects of structural failure on the environment. More specifically, the environmental metric accounts for two impacts: (a) carbon dioxide emissions  $R_{EC}$ , and (b) energy consumption associated with detour and bridge repair  $R_{EE}$ . In general, indirect risks integrate the effects of both social and environmental consequences of structural failure.

Within this chapter, the investigated risk attribute values may be computed in two different ways: one in which the annual probability of failure (i.e.,  $P_{f,sys}$  in Eqs. 4.12 and 4.13) is derived directly from the system hazard and one that utilizes the system cumulative distribution function (CDF) as a measure of system failure (i.e.,  $F_{sys}(t) = 1 - S_{sys}(t)$ ). Considering the parameters in Table 4.2, the time-variant consequences considering the no maintenance case are determined. The time-variant

profile of the expected value corresponding to each risk attribute considering statistical independence among components ( $\rho = 0$ ) is shown in Figure 4.14.

Within the proposed tri-objective optimization procedure, for each alternative, it is necessary to evaluate the utilities associated with total maintenance cost  $u_{cost}$ , risk  $u_{risk}$ , and benefit  $u_{benefit}$ . The value associated with  $u_{cost}$  is obtained from Eq. (4.14) with minimum cost  $a_{min} = 0$  and maximum budget  $a_{max} = 400,000$  USD. Once the time-variant risk and benefit attributes are determined, they may be transferred to utility considering the exponential formulations in Eqs. (4.14) and (4.15). The utility value corresponding to each attribute is calculated considering the range of risk attribute values shown in Table 4.3, with the system hazard utilized as the probability of failure. Within this case study, these minimum and maximum attribute values are obtained considering the no maintenance case;  $a_{min}$  and  $a_{max}$  are the expected attribute values at  $t = 0$  and  $t = T_L$  (i.e., 75 years) assuming no maintenance. In other cases, the decision maker may directly assign values to  $a_{min}$  and  $a_{max}$  in order to reflect personal risk tolerances. Furthermore,  $u_{risk}$  and  $u_{benefit}$  are computed considering Eqs. (4.16) to (4.18). Figure 4.15 depicts the time-variant utility profiles corresponding to the risk and benefit considering no maintenance. In this case, all utilities decrease continuously over the lifetime of the structure. The application of essential maintenance interventions improves the performance of the structure and reduces risk; lifetime maintenance planning can effectively mitigate a variety of risks while simultaneously ensuring that performance is within acceptable levels.

There are several inputs that influence the final results of the proposed decision support tool. For this case study, the optimization is performed by simultaneously

maximizing the utility associated with total maintenance cost  $u_{cost}$ , the minimum utility corresponding to the risk  $u_{risk}$ , and the minimum utility associated with the benefit  $u_{benefit}$  over the lifetime of the bridge (i.e.,  $T_L = 75$  years). The main output of this optimization procedure are the bridge components to be maintained and their respective times of application. The following constraints are also considered herein: (a) total maintenance cost should not exceed 400,000 USD, (b) constraints on the allowable minimum  $a_{min}$  and maximum  $a_{max}$  values of each risk and benefit attribute are defined in Table 4.3, (c) essential maintenance may not be performed before  $t = 5$  years or after  $t = 70$  years, and (d) consecutive maintenance actions must be performed at least 3 years apart. The tri-objective maintenance planning problem is solved using a genetic algorithm-based optimization approach. MATLAB's Global Optimization Toolbox (MathWorks 2013) is utilized in order to determine optimum lifetime maintenance strategies for the highway bridge investigated. The problem presented was solved using MATLAB on a Dell Precision R5500 rack workstation equipped with two six cores X5675 Intel Xeon processors with 3.06 GHz clock speed and 24 GB DDR3 memory.

The first set of optimum solutions presented herein employs an annual risk formulation that incorporates the system hazard function. In this particular example, both the hazard and availability improvements experienced from maintenance are used to establish the utility associated with benefit. Three-dimensional Pareto fronts obtained considering different risk attitudes  $\gamma$ , correlations among components  $\rho$ , number of maintenance actions  $N_{EM}$ , and discount rates of money  $r_m$  are shown in Figure 4.16.

Considering the two Pareto fronts depicted in Figure 4.16a (i.e.,  $N_{EM} = 3$ ,  $\rho = 0$ ,  $r_m = 2\%$ , and variable risk attitude  $\gamma$ ), the maintenance strategies corresponding to solutions A1, A2, A3, B1, B2, and B3 are detailed in Table 4.4. The optimum solutions associated with a risk averse (i.e.,  $\gamma = 2$ ) and risk taking ( $\gamma = -2$ ) decision maker are A1, A2, A3 and B1, B2, B3, respectively. They represent maintenance strategies that correspond to different values of utility associated with cost, risk, and benefit. The maintenance plan for solution A1 entails replacing the interior girders at years 24 and 70, and replacing the exterior girders at year 47. The maintenance plan associated with Solution A3 includes replacing the entire superstructure at years 16 and 57, and the deck at year 36.

Furthermore, the optimum values of the utilities associated with the six representative solutions in Figure 4.16a are indicated in Table 4.5. The profiles of the utility associated with total risk  $u_{risk}$  and performance benefit  $u_{benefit}$  for the representative solutions A1, A2, A3 and B1, B2, B3 are shown in Figure 4.17a and Figure 4.17b, respectively. In addition to the specific optimum maintenance plans and utility values, the maximum and minimum lifetime risk and benefit attributes corresponding to each Pareto alternative are also examined; Table 4.6 summarizes the maximum and minimum attributes values corresponding to the representative optimum maintenance strategies highlighted in Figure 4.16a. In order to illustrate time effects associated with the optimum solution A2 for the cases with and without maintenance, the risk utility and economic risk profiles are shown in Figure 4.18. Furthermore, for the same solution, the performance benefit utility, survival

probability, availability, and hazard associated with bridge components and the bridge system are indicated in Figure 4.19.

The Pareto fronts contained within Figure 4.16a are further detailed in Figure 4.20 for the case  $0.5 \leq u_{benefit} \leq 0.6$ . As shown, for Pareto solutions exhibiting a benefit utility between 0.5 and 0.6, the risk utility for a risk averse (i.e.,  $\gamma = 2$ ) and risk accepting (i.e.,  $\gamma = -2$ ) decision maker always falls in the range of  $0.55 \leq u_{risk} \leq 0.62$  and  $0.37 \leq u_{risk} \leq 0.45$ , respectively. Similarly, the cost utilities associated with the specific solutions outlined in Figure 4.20 fall in the range  $0.81 \leq u_{cost} \leq 0.82$  and  $0.31 \leq u_{cost} \leq 0.36$  for a risk averse and risk accepting attitude, respectively.

In addition to the effect of the decision maker's risk attitude on the Pareto solutions, the influence of the assumed correlation among components  $\rho$ , the discount rate of money  $r_m$ , and the number of essential maintenance actions  $N_{EM}$  are investigated. Figure 4.16b depicts Pareto fronts for a risk averse decision maker considering two extreme cases of correlation among the components of the system. The Pareto fronts associated with statistical independence and perfect correlation are examined and two representative solutions C1 and C2 from these fronts are highlighted in Figure 4.16b. Similarly, the influence of the discount rate of money on Pareto solutions is indicated in Figure 4.16c. The optimum solutions C3 and C4 in Figure 4.16c are compared to solutions C1 and C2 within Table 4.7. In this table, the cost utilities, corresponding minimum lifetime risk and benefit utilities, and maintenance schedules associated with solutions C1, C2, C3, and C4 are summarized.

Next, the effect of the number of essential maintenance actions on the Pareto solutions is examined. Figure 4.16d shows Pareto solutions considering a variable number of essential maintenance actions (i.e.,  $N_{EM} = 1, 2, \text{ or } 3$ ), a discount rate of 2%, and a variable risk attitude. The maintenance plans corresponding to the three representative solutions on each of the Pareto fronts in Figure 4.16d, solutions D1, D2, D3, E1, E2, and E3, in addition to their associated cost, risk, and benefit utilities, are detailed in Table 4.8. In general, maintenance plans that consider only one intervention have the lowest cost (i.e., high cost utility) but, as a limit, can only achieve a certain levels of risk and benefit utilities. Intervention strategies that contain two or more essential maintenance actions can achieve higher levels of utilities associated with risk and benefit but possess higher maintenance costs (i.e., lower cost utility) when compared to the plans containing only one maintenance action. This trend can also be observed in Figure 4.21, which contains the time-variant risk and benefit utilities corresponding to solutions D1, D2, and D3. Solution D3 dictates maintenance that frequently restores the performance benefit and risk utilities and allows them to remain relatively large throughout the lifetime, while Solution D1 only contains one intervention that dramatically increases the risk and performance benefit utilities but is unable to sustain high levels throughout the entire lifetime.

The final part of this case study includes the comparison of the Pareto fronts obtained by carrying out the lifetime maintenance optimization considering annual or time-cumulative system failure probability, calculated with  $h_{sys}(t)$  and  $F_{sys}(t)$ , respectively. Figure 4.22 presents the output of these two optimizations assuming a risk averse decision maker (i.e.,  $\gamma = 2$ ), a 2% discount rate of money, and three

essential maintenance actions. The maintenance plans and utility values associated with two representative solutions associated with annual and cumulative-time system failure probability, F1 and F2, respectively, are reported in Table 4.9. In general, the optimum maintenance plans considering cumulative-time system failure probability exhibit smaller utilities than those associated with annual system failure probability.

#### **4.9 CONCLUSIONS**

This chapter presents a decision-support framework that has the ability to quantify cost, risk, and benefit in terms of utility and effectively employs tri-objective optimization procedures in order to determine the best maintenance strategies for structures with deteriorating components characterized by lifetime functions. The effects of the risk attitude and preferences of the decision maker, number of maintenance interventions, discount rate of money, correlation among components, and computational type of system failure probability (i.e., annual or cumulative-time) on the optimum maintenance strategies are investigated. The flexibility of the multi-attribute utility evaluation process is demonstrated by examining five systems with different configurations comprised of four components. Additionally, the capabilities of the presented optimization and decision support framework are illustrated on an existing highway bridge located in Colorado.

Overall, a comprehensive approach for the multi-objective life-cycle maintenance optimization of deteriorating structural systems based on multi-attribute utility theory considering lifetime functions and the decision maker's risk attitude is developed. The presented methodology can be used to assist decision making

regarding maintenance actions and, ultimately, maintain optimum performance of civil structures during their life-cycle by balancing the utility values associated with maintenance cost, risk, and performance benefits.

The following conclusions are drawn:

1. It is crucial to consider a variety of risks that plague civil infrastructure systems when quantifying their lifetime performance. Economic, social, and environmental consequences of structural failure are incorporated within the proposed methodology by employing multi-attribute utility theory. By taking into account a wide variety of risks, the decision maker can ensure that the maintenance plans resulting from the optimization were calculated in a robust and comprehensive manner.
2. Optimum essential maintenance strategies are determined using a multi-criteria optimization algorithm that balances three objectives: the utilities associated with maintenance cost, risk, and performance benefit. Ultimately, a decision maker is able to make utility-informed decisions based on his/her particular preferences and the decision support system provided by the Pareto set of optimum solutions.
3. The risk attitude of the decision maker can have significant influence on the optimum solutions resulting from the proposed decision support system. Additionally, the number of essential maintenance actions considered throughout a structural system's lifetime has an important effect on the final Pareto solutions.

4. The way system failure probability is calculated, annual or cumulative-time, influences the final Pareto solutions.
5. System modeling greatly influences the optimum maintenance plans. Depending upon how system failure is modeled, the optimum time-variant utilities can vary significantly.
6. Employing lifetime functions within risk and life-cycle optimization under uncertainty assessment provides mathematical flexibility due to their closed-form expression of the distribution of time-to-failure.

Table 4.1. Minimum and maximum annual values of attributes involved in the risk and benefit assessment of the five four-component systems shown in Figure 4.3.

System configuration (see Figure 4.3)	Attribute	Independence ( $\rho = 0$ )		Full correlation ( $\rho = 1$ )	
		Minimum	Maximum	Minimum	Maximum
		$a_{min}$	$a_{max}$	$a_{min}$	$a_{max}$
System A	Direct risk (USD)	0	1,974	0	784
	Indirect risk (USD)	0	4,935	0	1,959
	System hazard $h_{sys}$	0	0.0162	0	0.0064
	System availability $A_{sys}$	0.6656	1	0.8621	1
System B	Direct risk (USD)	0	1	0	271
	Indirect risk (USD)	0	3	0	678
	System hazard $h_{sys}$	0	$1 \times 10^{-5}$	0	0.0022
	System availability $A_{sys}$	0.999	1	0.9459	1
System C	Direct risk (USD)	0	790	0	783
	Indirect risk (USD)	0	1,976	0	1,959
	System hazard $h_{sys}$	0	0.0065	0	0.0064
	System availability $A_{sys}$	0.8617	1	0.8621	1
System D	Direct risk (USD)	0	508	0	501
	Indirect risk (USD)	0	1,270	0	1,252
	System hazard $h_{sys}$	0	0.0042	0	0.0041
	System availability $A_{sys}$	0.8890	1	0.8896	1
System E	Direct risk (USD)	0	152	0	420
	Indirect risk (USD)	0	381	0	1,050
	System hazard $h_{sys}$	0	0.0012	0	0.0034
	System availability $A_{sys}$	0.9385	1	0.9175	1

Table 4.2. Parameters used in the evaluation of the risk attributes associated with the E-17-HS bridge.

Parameter	Mean value	Reference
Rebuilding cost parameter $C_I$	1292 USD/m <sup>2</sup>	(Dong <i>et al.</i> 2014f)
Width of the bridge $W$	10.4 m	(Akgül 2002)
Length of the bridge $L$	64.5 m	(Akgül 2002)
Occupancy rate for non-truck vehicles $O_r$	1.56	(Stein <i>et al.</i> 1999; Barone and Frangopol 2014a,b)
Percentage of average daily traffic that is trucks $TT_p$	4%	(Barone and Frangopol 2014a,b)
Detour length $L_d$	10 km	(Barone and Frangopol 2014a,b)
Average daily traffic $ADT$	400 vehicles	(Barone and Frangopol 2014a,b)
Duration of detour $D_d$	365 days	(Barone and Frangopol 2014a,b)
Average detour speed $S_d$	64 km/hr	(Barone and Frangopol 2014a,b)
Safe following distance $f_d$	55 m	(Colorado State Patrol. 2011)
Carbon dioxide emissions associated with cars $CPD_C$	0.22 kg/km	(Dong <i>et al.</i> 2014f)
Carbon dioxide emissions associated with trucks $CPD_T$	0.56 kg/km	(Dong <i>et al.</i> 2014f)
Energy consumption associated with each vehicle $EPD$	3.80 MJ/km	(Dong <i>et al.</i> 2014f)
Carbon dioxide emissions associated with rebuilding $CD_{REB}$	159 kg/m <sup>2</sup>	(Dequidt 2012)
Energy consumption associated with rebuilding $EC_{REB}$	2.05 GJ/m <sup>2</sup>	(Dequidt 2012)

Table 4.3. Minimum and maximum annual values of attributes involved in the risk and benefit assessment of the E-17-HS bridge

Attribute type	Attribute	Independence ( $\rho = 0$ )		Full correlation ( $\rho = 1$ )	
		Minimum	Maximum	Minimum	Maximum
		$a_{min}$	$a_{max}$	$a_{min}$	$a_{max}$
Risk (economic)	Rebuilding cost $R_{RB}$ (USD)	0	3,105	0	1,848
	Extra travel time $R_{ETT}$ (hr)	0	555	0	329
Risk (social)	Extra travel distance $R_{ETD}$ (km)	0	23,094	0	13,711
	Fatalities $R_{FT}$	0	0.0528	0	0.0314
	CO <sub>2</sub> emissions $R_{EC}$ (kg)	0	7,165	0	4,939
Risk (environmental)	Energy consumption $R_{EE}$ (MJ)	0	109,510	0	65,015
Benefit	System hazard $h_{sys}$	0	0.0158	0	0.0094
Benefit	System availability $A_{sys}$	0.6599	1	0.7457	1

Table 4.4. Maintenance plans corresponding to the six optimum solutions on the Pareto fronts shown in Figure 4.16a.

Solution (see Figure 4.16a)	Maintenance actions	Time of application (years)
A1	[G <sub>I</sub> , G <sub>E</sub> , G <sub>I</sub> ]	[24, 47, 70]
A2	[D, G <sub>I</sub> , D]	[29, 46, 64]
A3	[S, S, D]	[16, 36, 57]
B1	[G <sub>I</sub> , G <sub>I</sub> , G <sub>I</sub> ]	[23, 46, 70]
B2	[D, G, D]	[23, 41, 52]
B3	[D, S, S]	[18, 33, 54]

Note: D = replace the deck; G<sub>I</sub> = replace all interior girders;  
G<sub>E</sub> = replace all exterior girders; G = replace all girders;  
S = replace the entire superstructure

Table 4.5. Optimum utility values corresponding to the six optimum solutions within the Pareto fronts in Figure 4.16a.

Solution (see Figure 4.16a)	Cost utility $u_{cost}$	Optimum utility					
		Direct risk $u_{r,d}$	Indirect risk $u_{r,i}$	Total risk $u_{risk}$	Hazard $u_h$	Availability $u_A$	Benefit $u_{benefit}$
A1	0.8232	0.5291	0.6061	0.5676	0.6061	0.4581	0.5347
A2	0.7648	0.7756	0.8729	0.8508	0.8729	0.9471	0.9010
A3	0.2725	0.9088	0.9424	0.9377	0.9424	0.9829	0.9626
B1	0.3865	0.1313	0.1609	0.1515	0.1609	0.1023	0.1316
B2	0.1886	0.4219	0.6222	0.5842	0.6222	0.8153	0.7393
B3	0.0439	0.5269	0.7302	0.6730	0.7302	0.9067	0.8184

Table 4.6. Attribute values corresponding to the six optimum solutions within the Pareto fronts in Figure 4.16a.

Solution	Maximum values						Minimum value	
	Economic attribute	Social attributes			Environmental attributes		System hazard	System availability
	$R_{RB}$ (USD)	$R_{ETD}$ (km)	$R_{ETT}$ (hr)	$R_{FT}$	$R_{EC}$ (kg)	$R_{EE}$ (MJ)	$h_{sys}$	$A_{sys}$
A1	2,155	14,521	349	0.0332	4,505	68,858	0.0099	0.7456
A2	1,381	6,865	165	0.0157	2,130	32,554	0.0047	0.9505
A3	712	3,621	87	0.0083	1,123	17,170	0.0025	0.9823
B1	2,159	14,928	359	0.0342	4,632	70,788	0.0102	0.7454
B2	1,076	4,567	110	0.0105	1,417	21,656	0.0031	0.9704
B3	817	3,067	74	0.0070	952	14,544	0.0021	0.9857

Note:  $R_{RB}$ ,  $R_{ETD}$ ,  $R_{ETT}$ ,  $R_{FT}$ ,  $R_{EC}$ , and  $R_{EE}$  are defined in Table 4.3

Table 4.7. Maintenance plans corresponding to the four optimum solutions within the Pareto fronts in Figure 4.16b,c.

Solution (see Figure 4.16b,c)	Correlation coefficient $\rho$	Discount rate $r_m$	Maintenance actions	Time of application (years)	Cost utility $u_{cost}$	Minimum utility	
						Total risk $u_{risk}$	Benefit $u_{benefit}$
C1	0	2%	[G <sub>I</sub> , G <sub>E</sub> , G <sub>I</sub> ]	[24, 48, 70]	0.8231	0.5676	0.5353
C2	1	2%	[D, G <sub>I</sub> , D]	[22, 31, 53]	0.7388	0.8684	0.9078
C3	0	0%	[D, G <sub>E</sub> , G <sub>I</sub> ]	[37, 53, 59]	0.5822	0.8818	0.9103
C4	0	2%	[D, G <sub>I</sub> , D]	[28, 42, 62]	0.7611	0.8565	0.9157

Table 4.8. Maintenance plans corresponding the six optimum solutions within the two Pareto fronts shown in Figure 4.16d.

Solution (see Figure 4.16d)	Maintenance actions	Time of application (years)	Cost utility $u_{cost}$	Optimum utility	
				Total risk $u_{risk}$	Benefit $u_{benefit}$
D1	[D]	[50]	0.9680	0.6056	0.7574
D2	[D, D]	[40, 68]	0.8870	0.7367	0.8162
D3	[D, D, D]	[35, 58, 70]	0.7472	0.7942	0.8210
E1	[D]	[56]	0.8039	0.1374	0.2449
E2	[D, D]	[42, 68]	0.5148	0.2906	0.3817
E3	[D, D, D]	[27, 53, 70]	0.2913	0.3326	0.3866

Table 4.9. Maintenance plans corresponding to the two optimum solutions within the two Pareto fronts shown in Figure 4.22.

Solution (see Figure 4.22)	Maintenance actions	Time of application (years)	Cost utility $u_{cost}$	Minimum utility	
				Total risk $u_{risk}$	Benefit $u_{benefit}$
F1	[D, G <sub>I</sub> , D]	[29, 46, 64]	0.7648	0.8508	0.9010
F2	[G <sub>I</sub> , G <sub>E</sub> , G <sub>I</sub> ]	[23, 46, 70]	0.8232	0.3688	0.5338

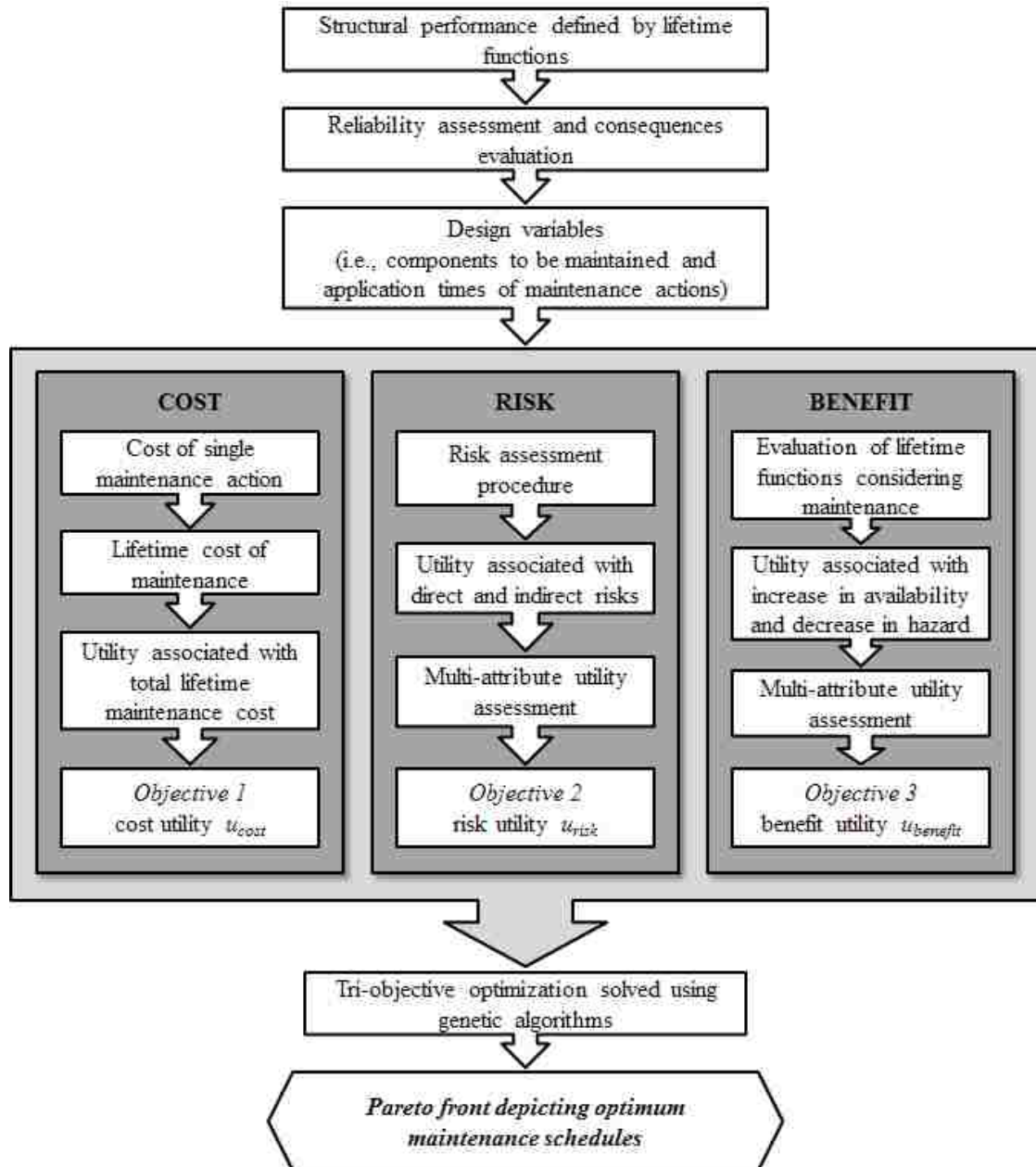


Figure 4.1. Flowchart outlining the computations involved in the decision support tool.

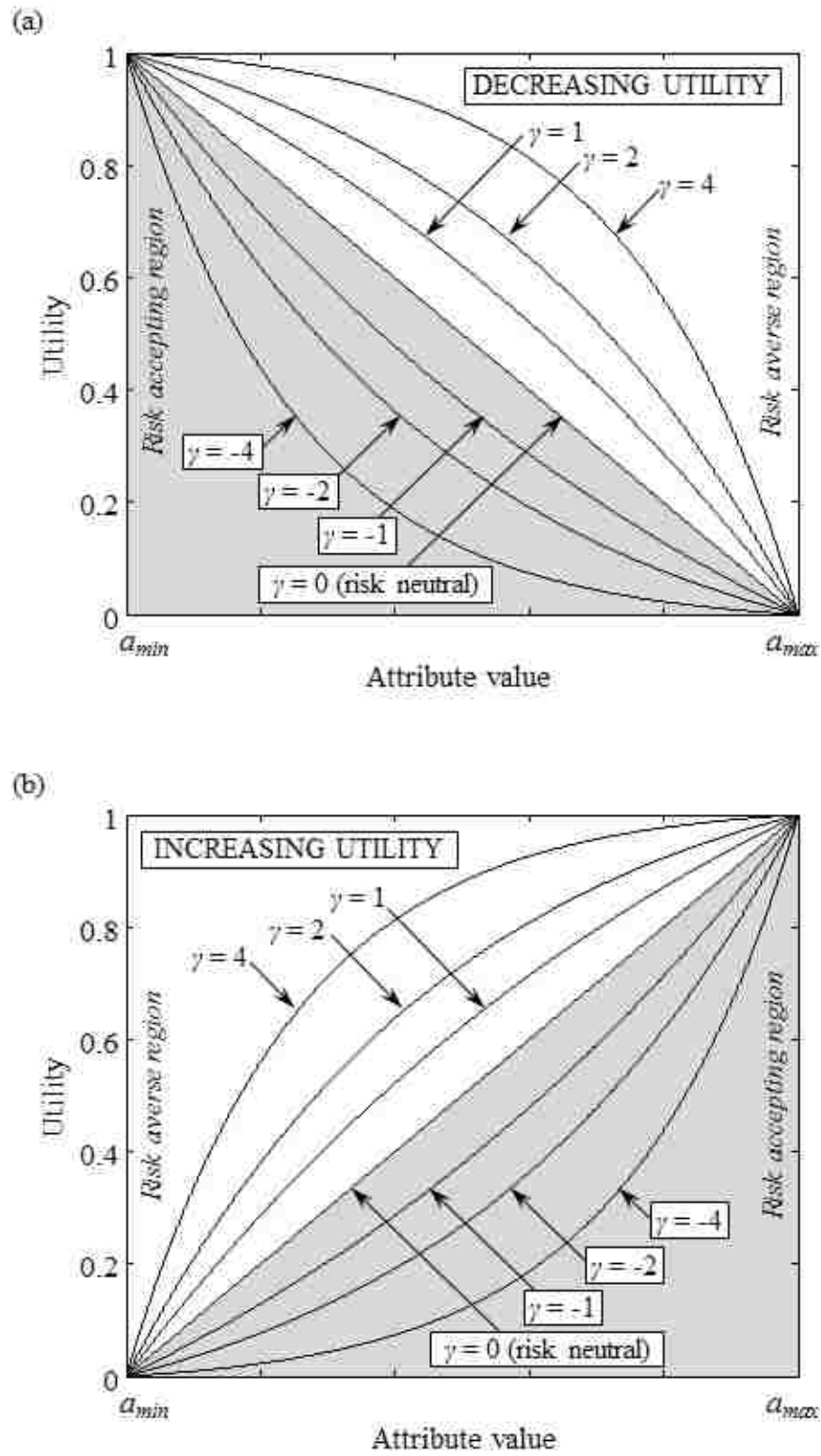


Figure 4.2. Exponential utility functions that are monotonically (a) decreasing and (b) increasing as the attribute value increase.

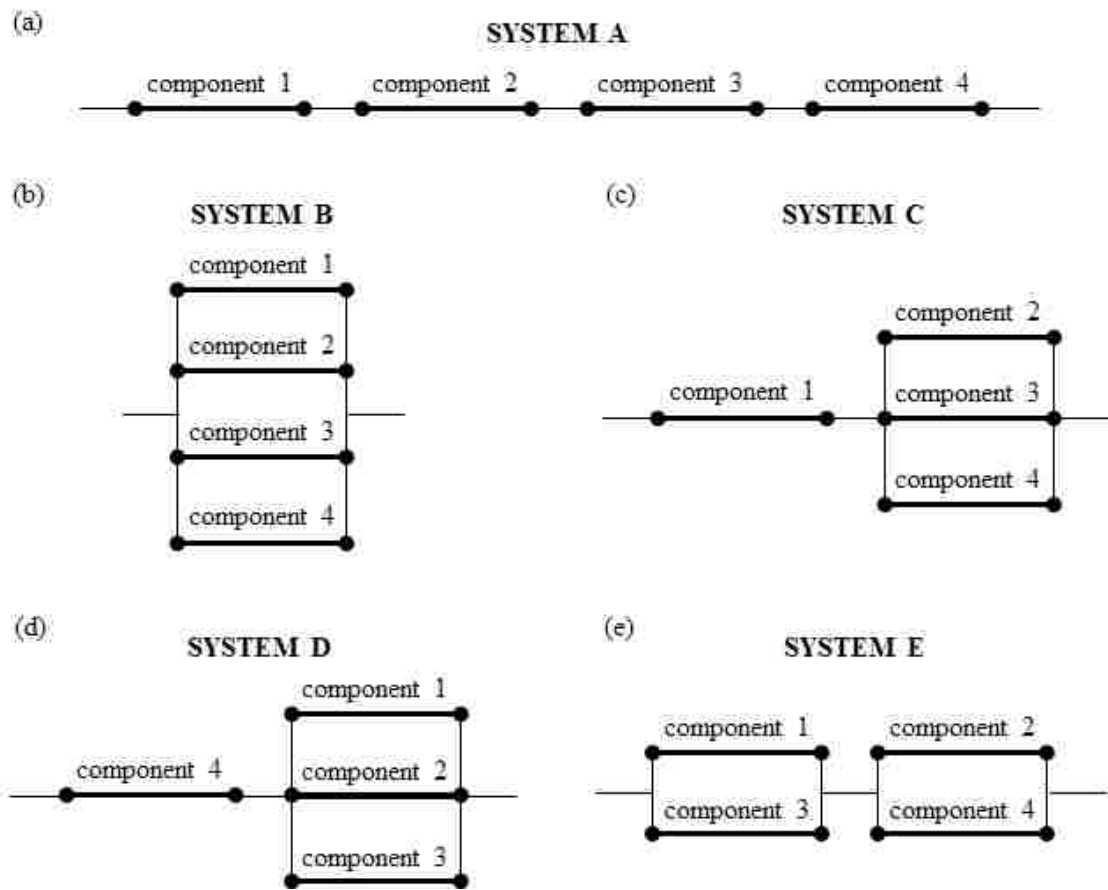


Figure 4.3. Five configurations of a four-component system

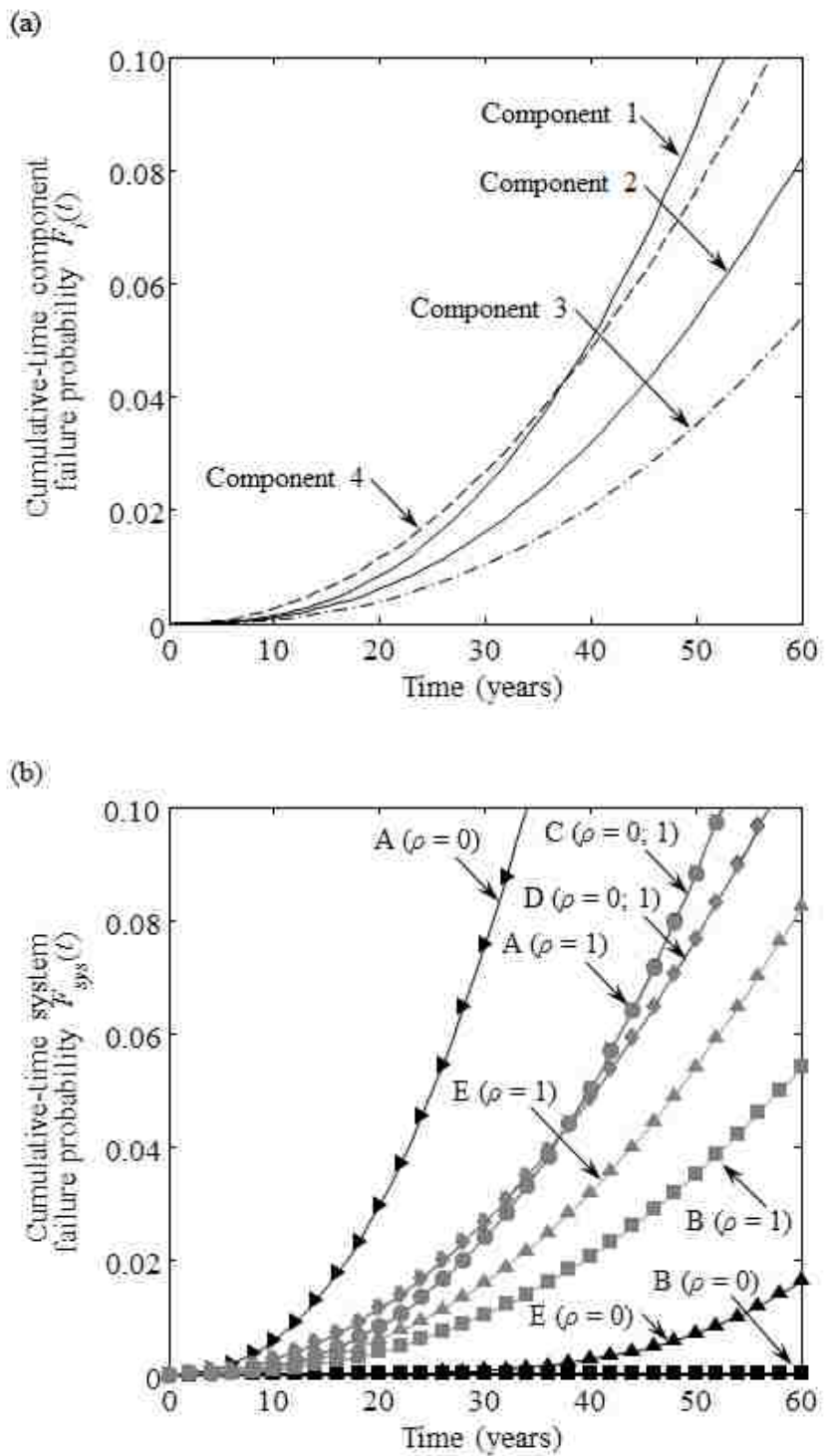


Figure 4.4. Cumulative-time failure probability associated with (a) components and (b) systems in Figure 4.3 considering independence ( $\rho = 0$ ) and full correlation ( $\rho = 1$ ) among components.

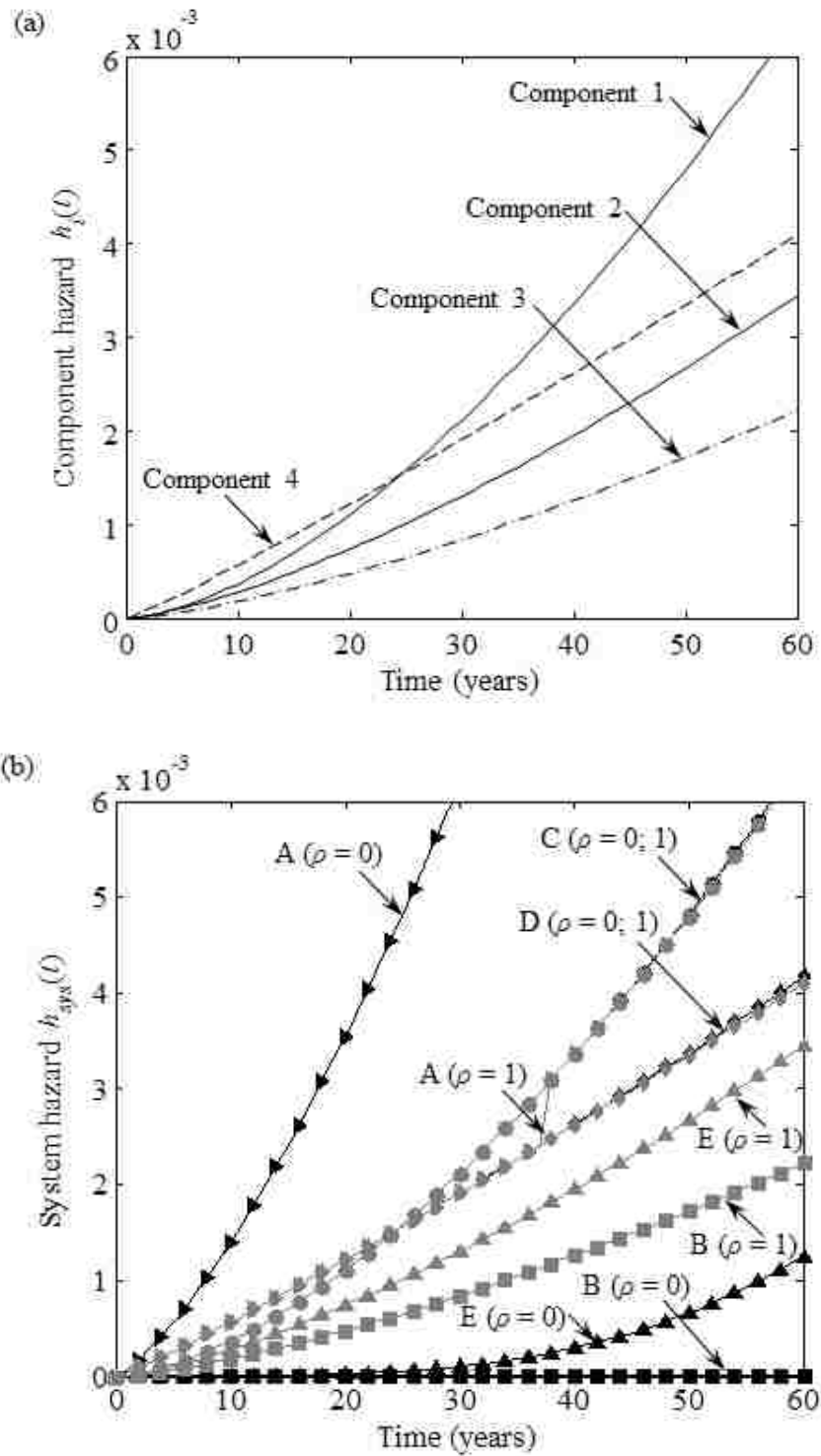


Figure 4.5. Hazard associated with (a) components and (b) systems in Figure 4.3 considering independence ( $\rho = 0$ ) and full correlation ( $\rho = 1$ ) among components.

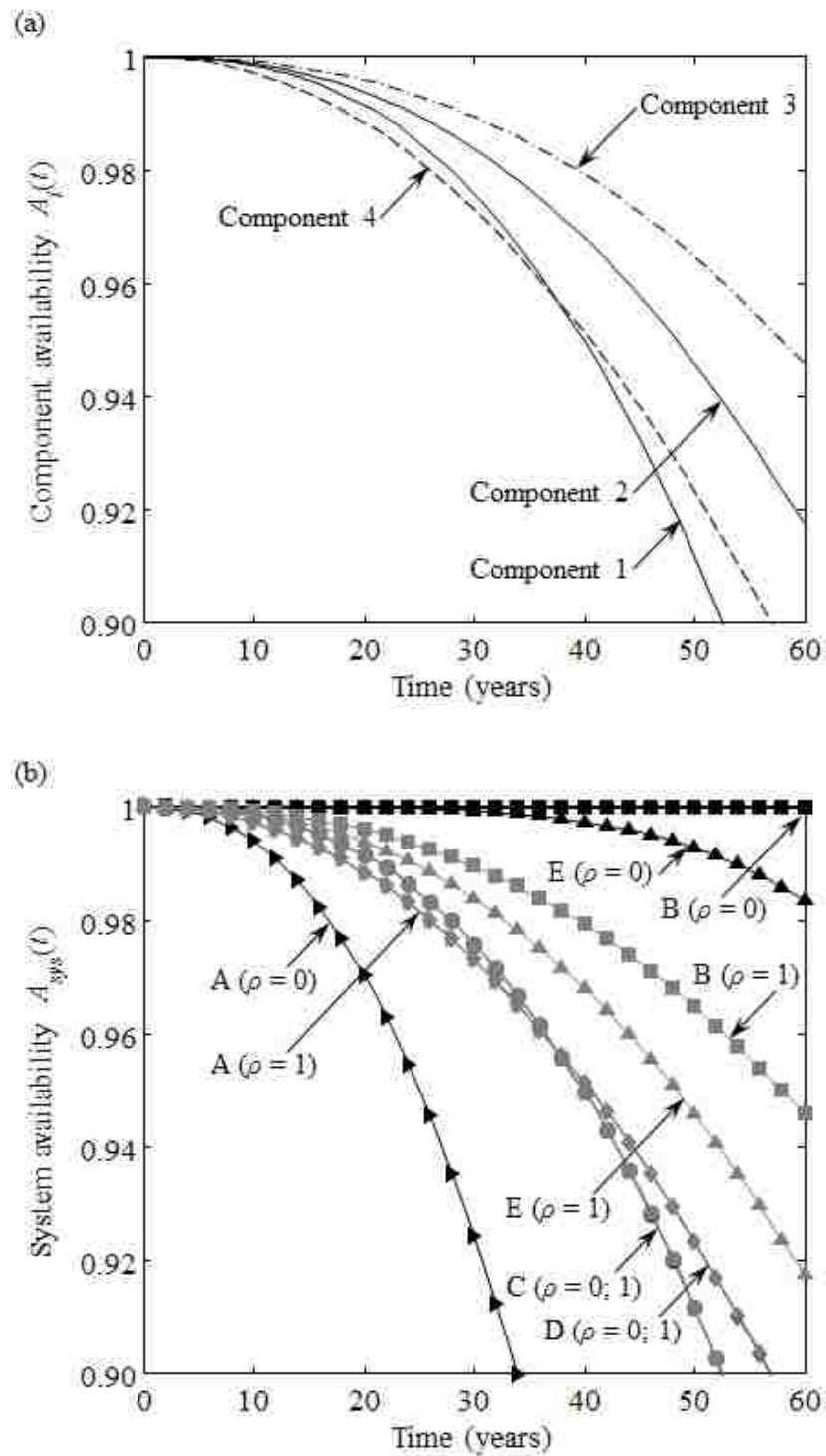


Figure 4.6. Availability associated with (a) components and (b) systems in Figure 4.3 considering independence ( $\rho = 0$ ) and full correlation ( $\rho = 1$ ) among components.

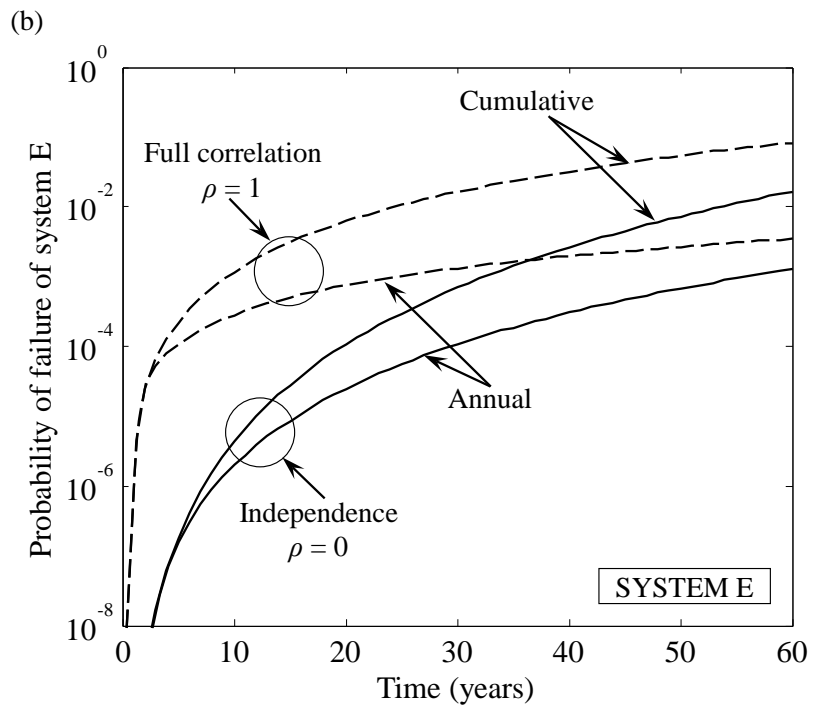
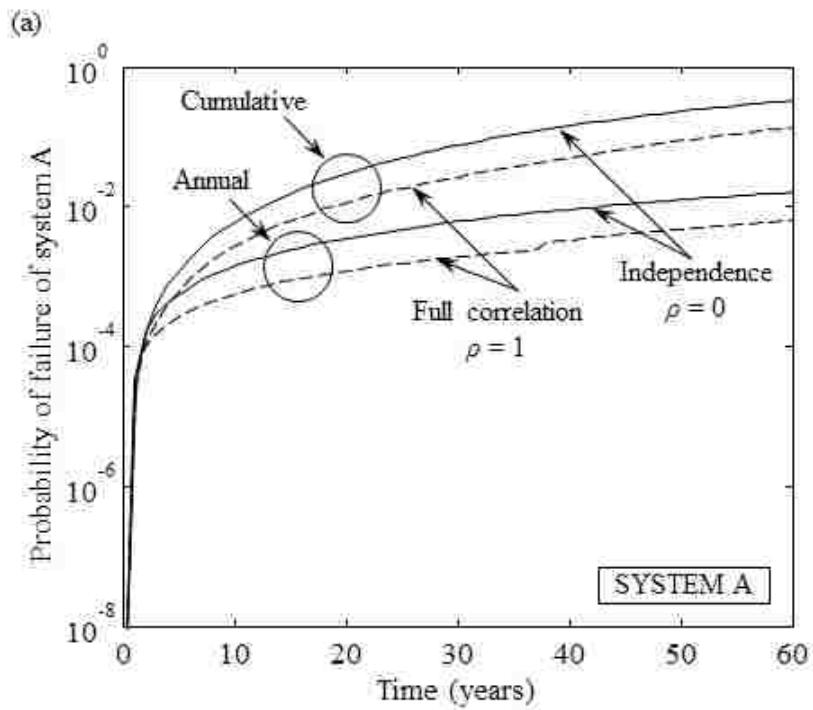


Figure 4.7. Cumulative and annual probability of system failure considering extreme correlation cases among components of (a) System A and (b) System E.

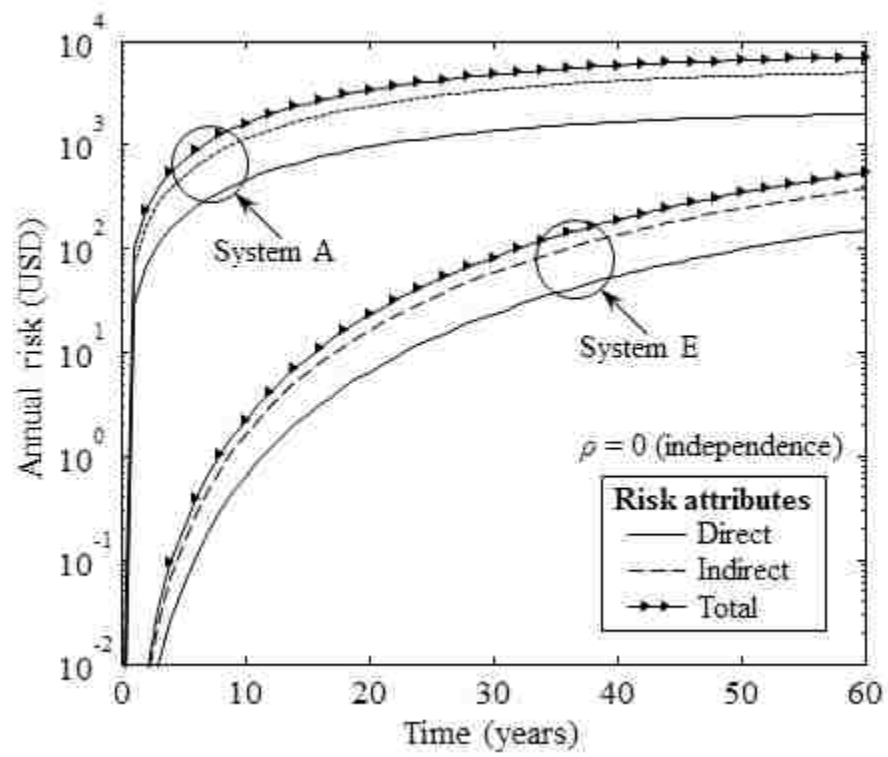


Figure 4.8. Time-variant profiles of annual direct, indirect, and total risk attributes for systems A and E, considering statistical independence among components ( $\rho = 0$ ).

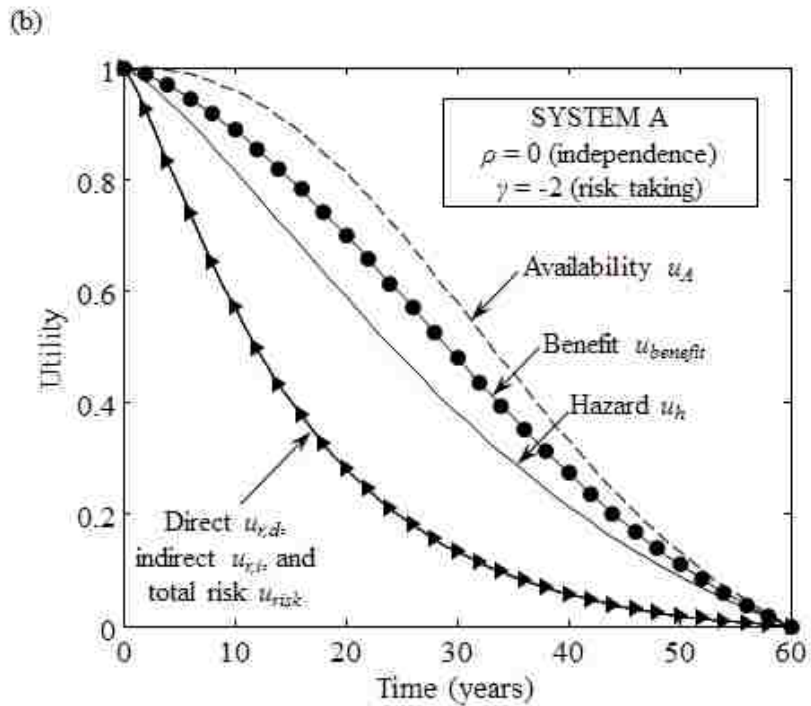
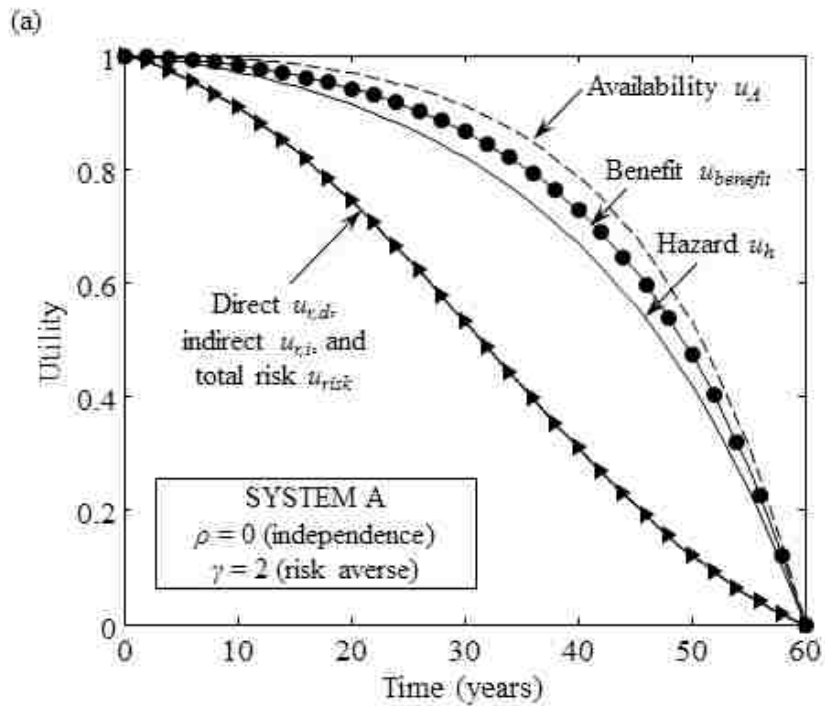


Figure 4.9. Time-variant profiles of availability, hazard, risk, and benefit utilities considering system A, independence among components ( $\rho = 0$ ), and (a) risk averse ( $\gamma = 2$ ) or (b) risk taking attitude ( $\gamma = -2$ ).

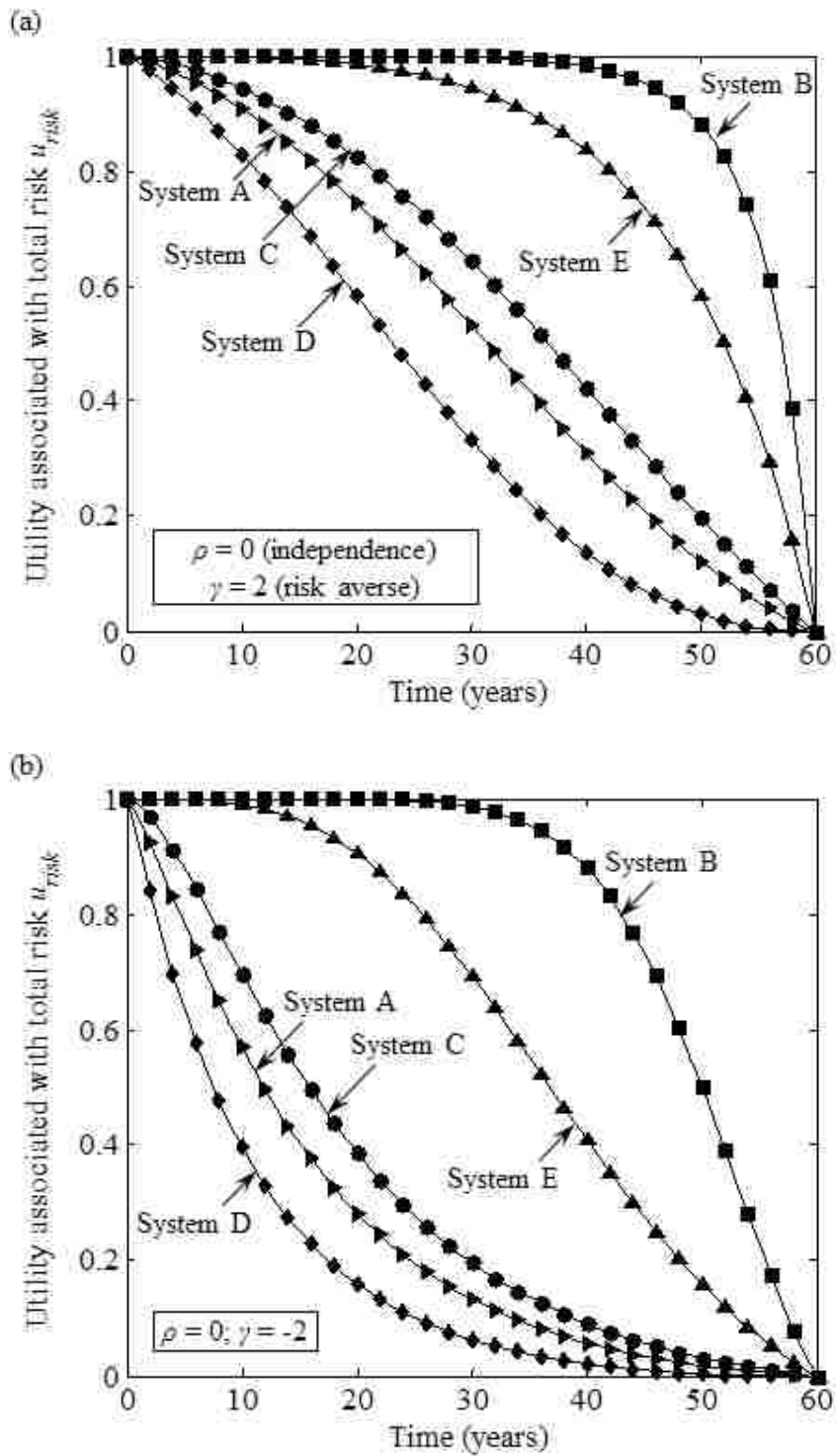


Figure 4.10. Time-variant profiles of total risk utilities considering all systems in Figure 4.3, independence among components ( $\rho = 0$ ), and (a) risk averse ( $\gamma = 2$ ) or (b) risk taking attitude ( $\gamma = -2$ ).

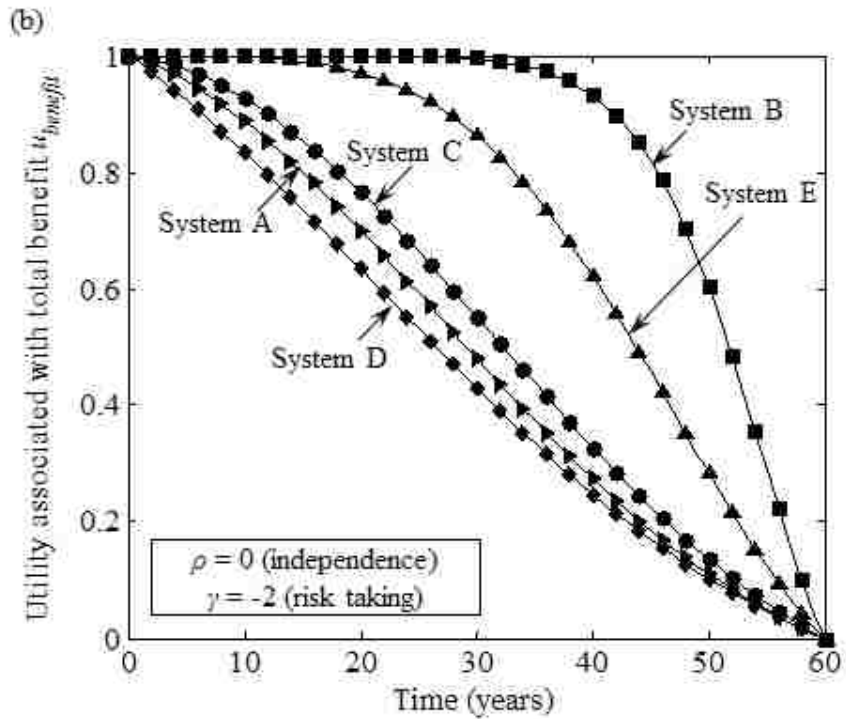
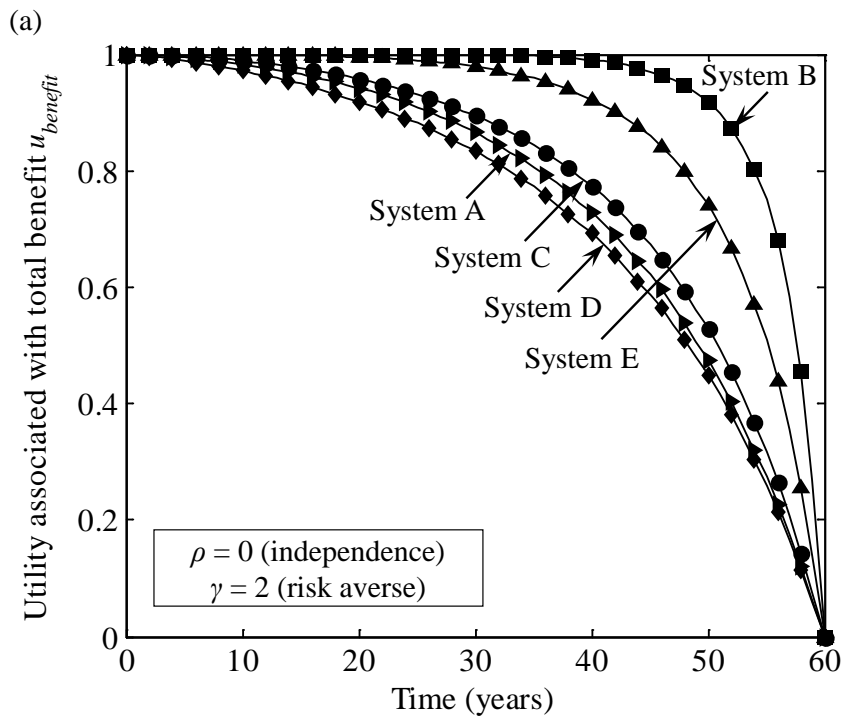


Figure 4.11. Time-variant profiles of benefit utilities considering all systems in Figure 4.3, independence among components ( $\rho = 0$ ), and (a) risk averse ( $\gamma = 2$ ) or (b) risk taking attitude ( $\gamma = -2$ ).

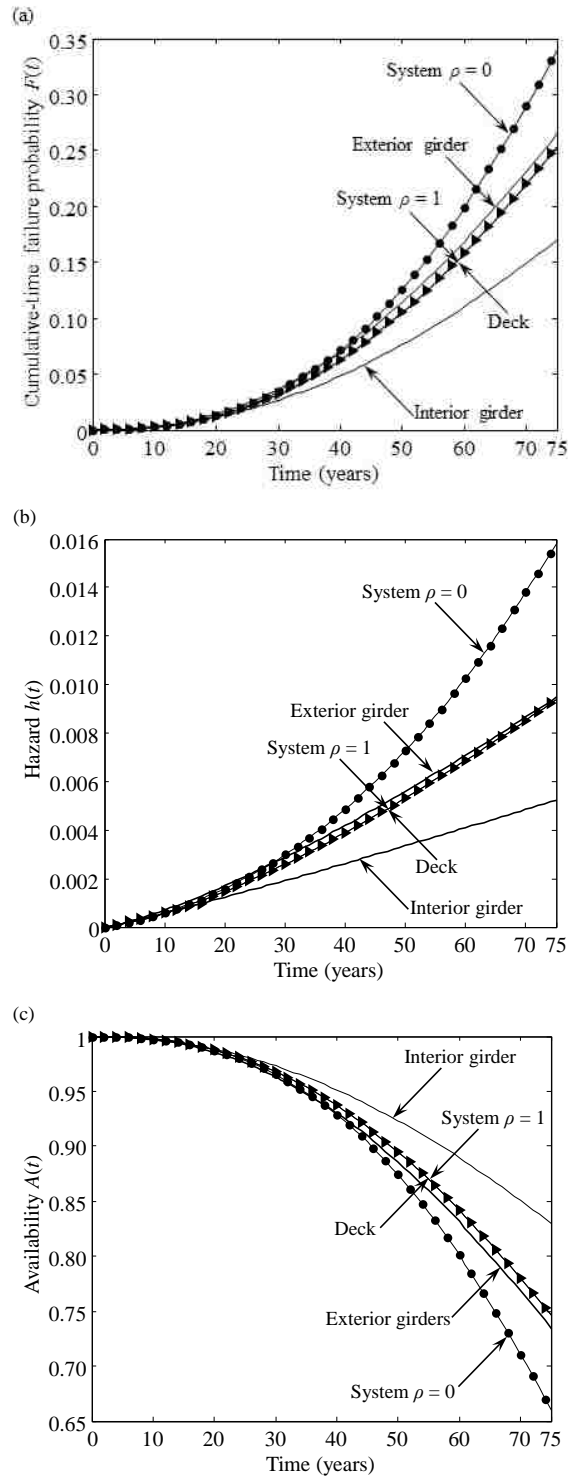


Figure 4.12. (a) Cumulative-time failure probability, (b) hazard, and (c) availability associated with both the components and the system (i.e., superstructure of the bridge E-17-HS) considering no maintenance and extreme correlation cases.

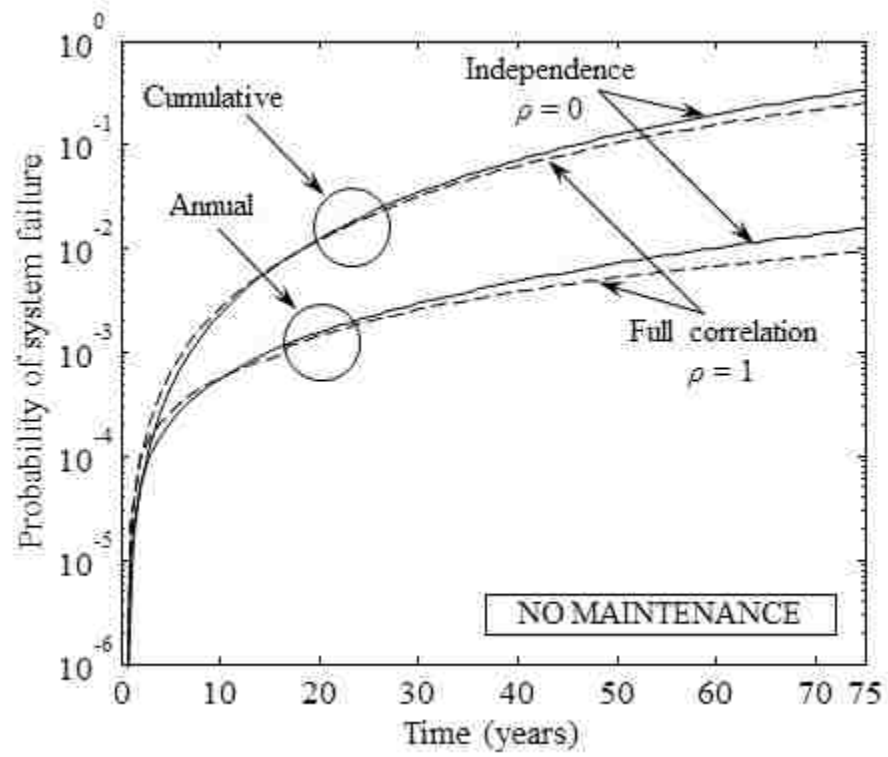


Figure 4.13. Cumulative and annual probability of system (i.e. superstructure of bridge E-17-HS) failure considering extreme correlation cases among components

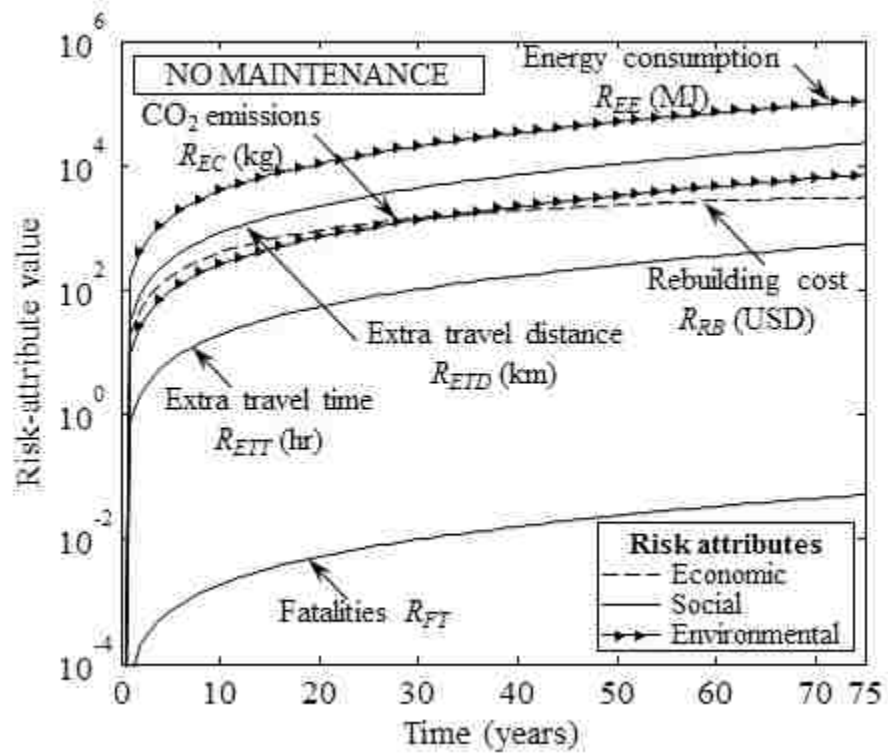


Figure 4.14. The time-variant profile of each risk attribute considering no maintenance, statistical independence among components ( $\rho = 0$ ), and the annual probability of system failure.

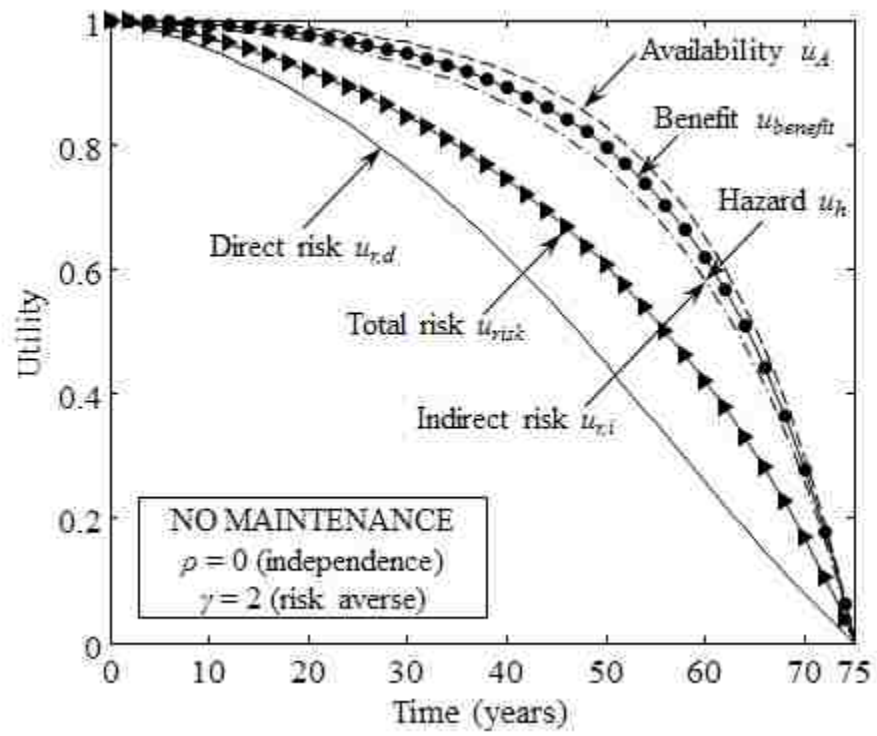
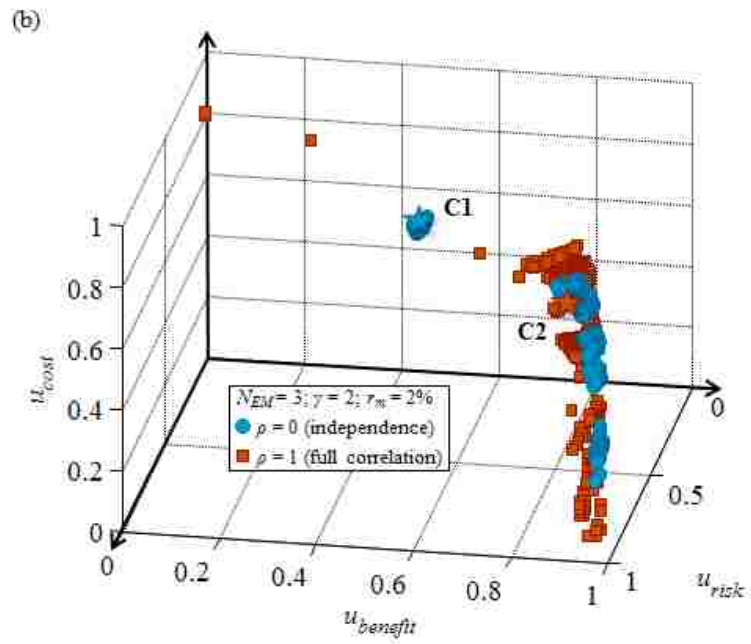
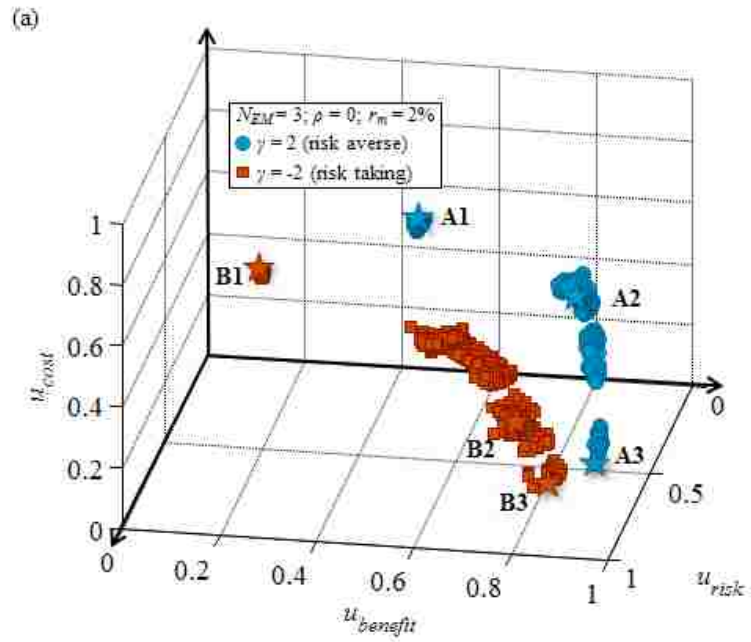


Figure 4.15. The time-variant profile of risk and benefit utilities considering independence among components ( $\rho = 0$ ) and a risk averse attitude ( $\gamma = 2$ ).



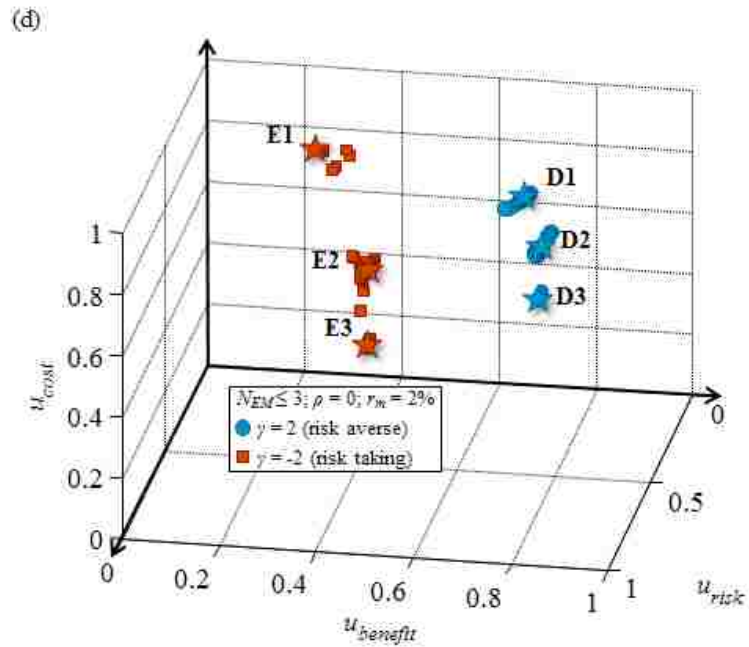
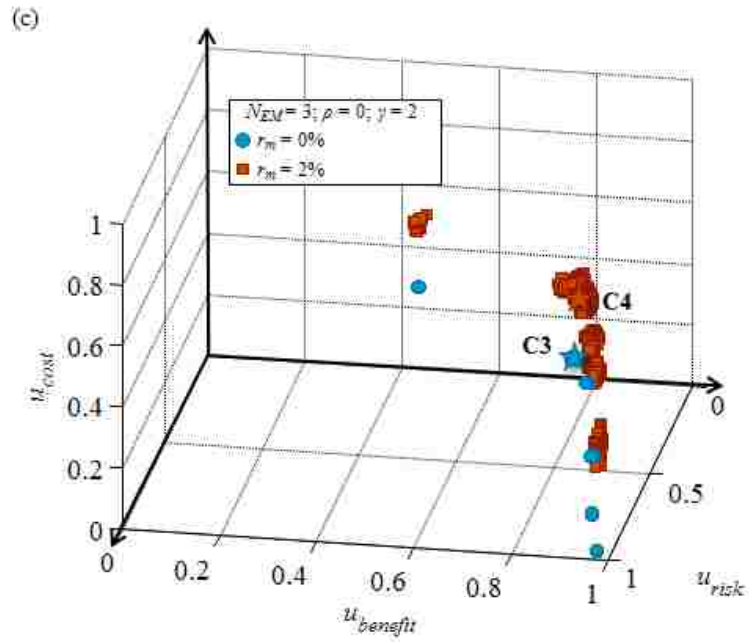


Figure 4.16. Pareto optimum solutions considering the effects of (a) risk attitude  $\gamma$ , (b) correlation among components  $\rho$ , (c) discount rate of money  $r_m$ , and (d) number of maintenance actions  $N_{EM}$ .

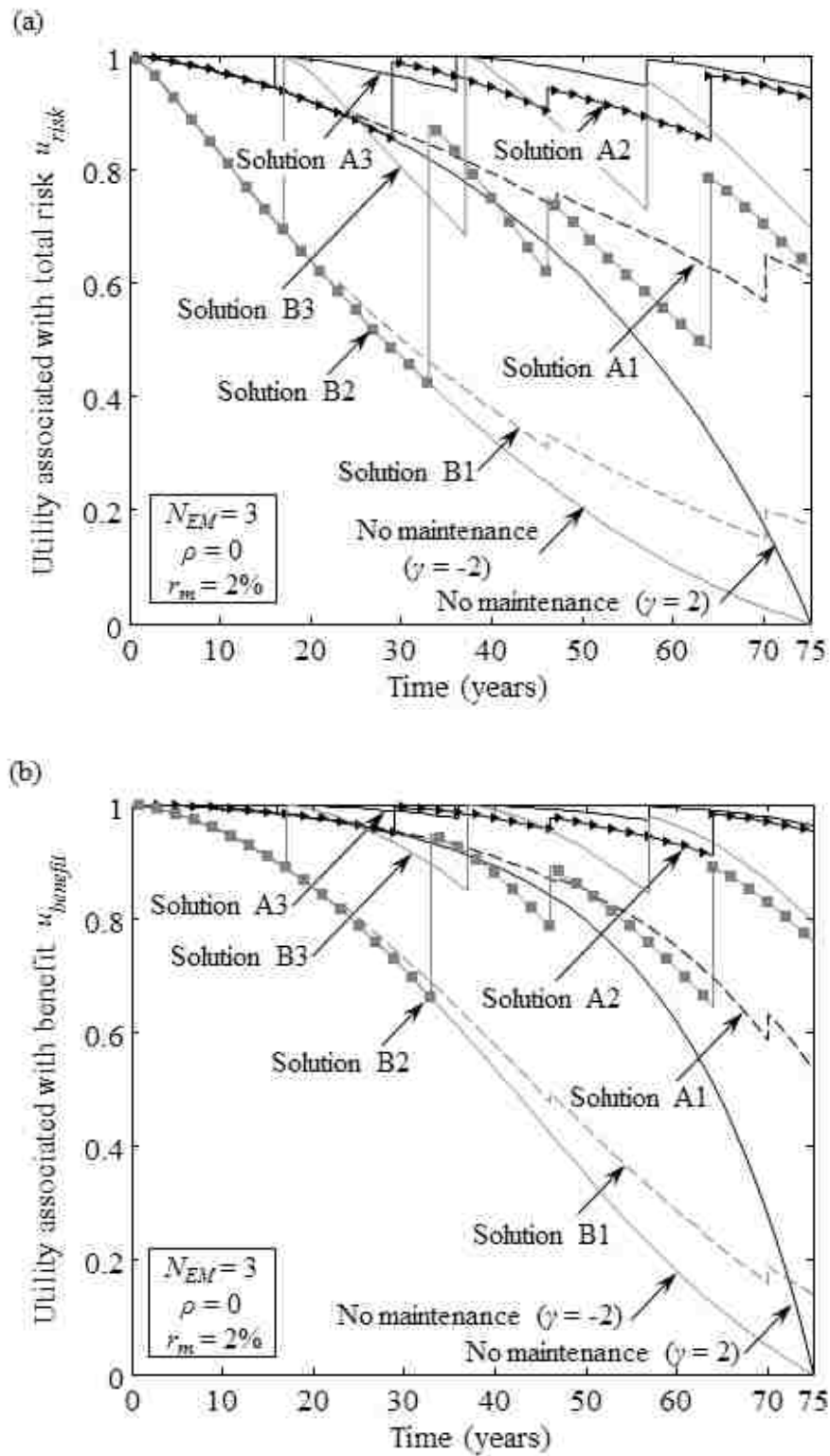


Figure 4.17. (a) Risk and (b) benefit utility profiles associated with the six optimum solutions shown in Figure 4.16a

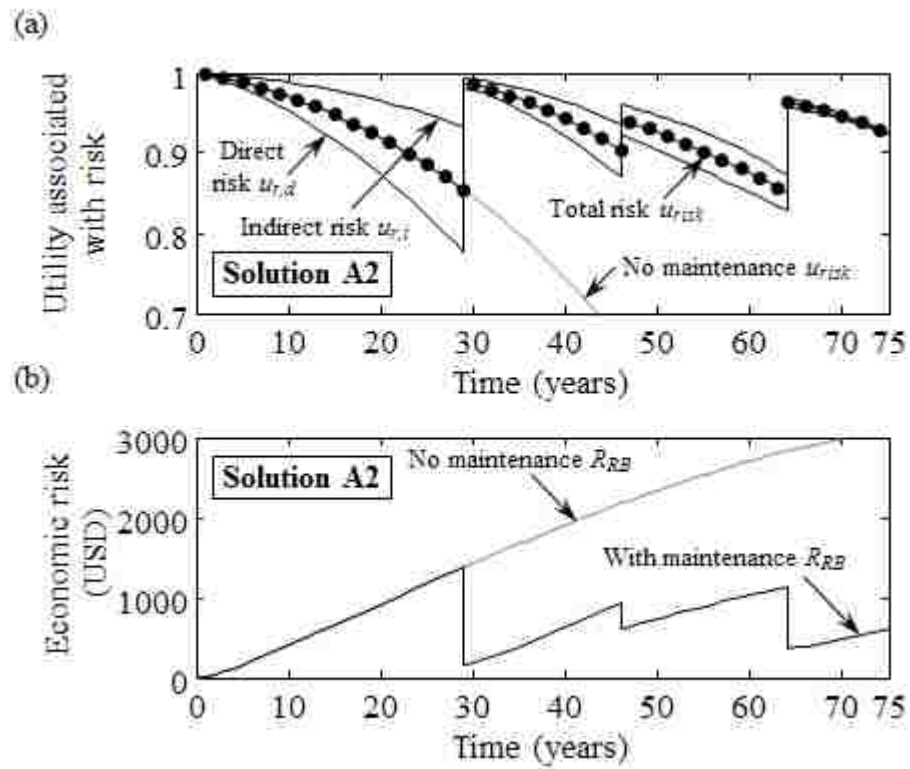


Figure 4.18. Time-variant (a) risk utilities and (b) economic risk values associated with the optimum solution A2 in Figure 4.16a.

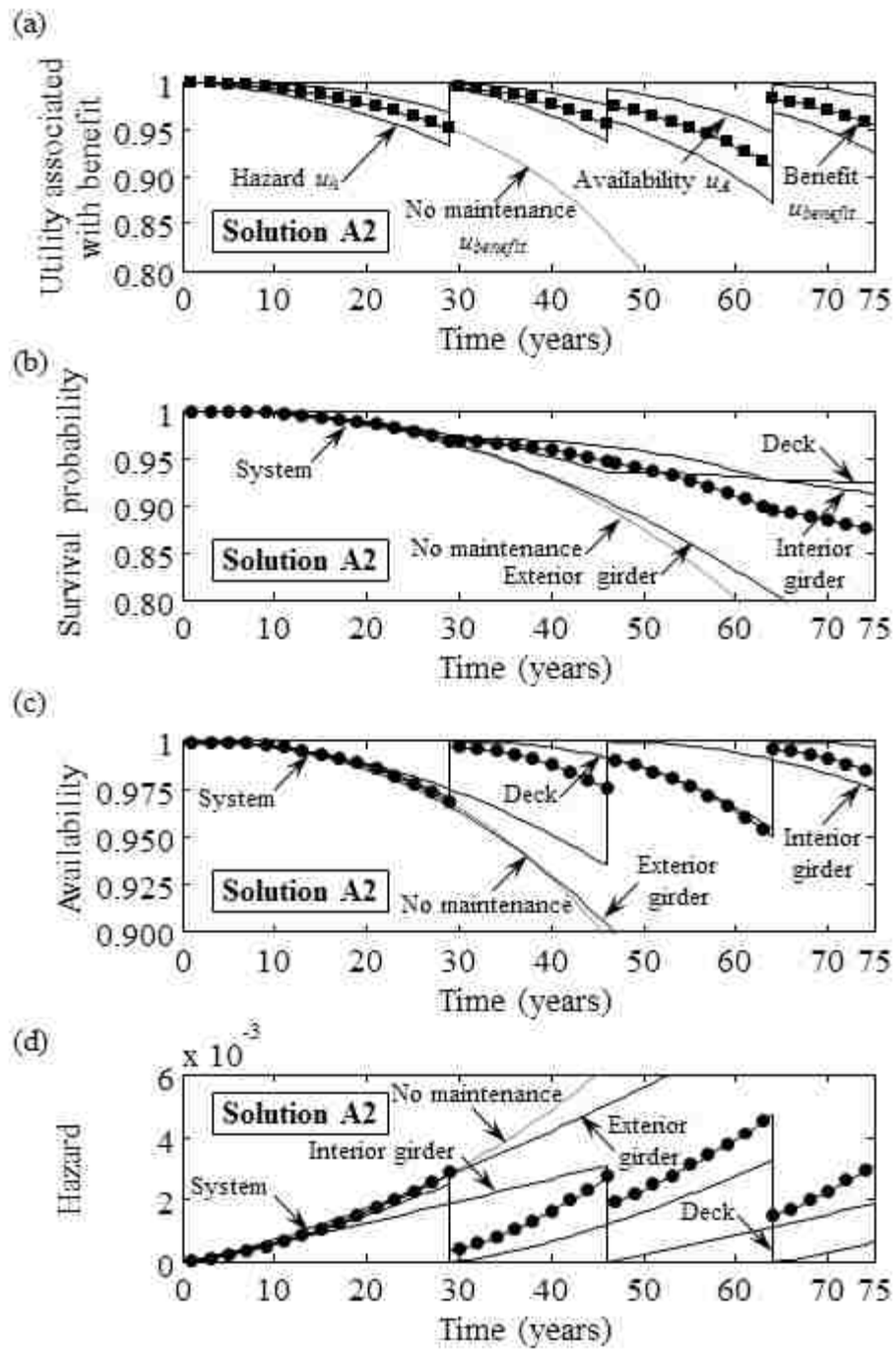


Figure 4.19. Time-variant (a) utilities associated with benefit, (b) survival probability, (c) availability, and (d) hazard associated with the optimum solution A2 in Figure 4.16a.

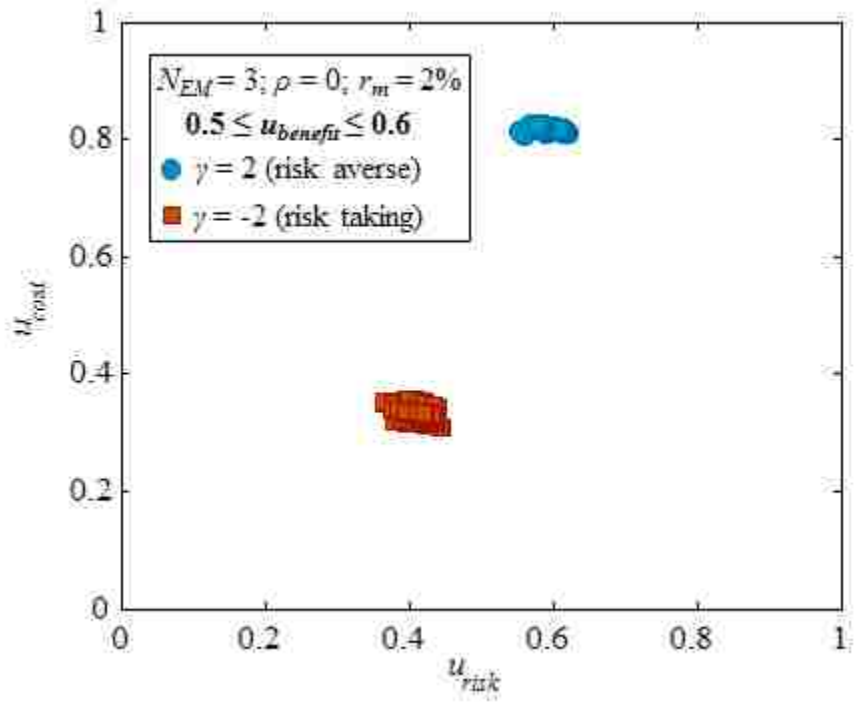


Figure 4.20. Pareto optimum solutions associated with benefit utilities  $u_{benefit}$  within the range 0.5 – 0.6 associated with Figure 4.16a.

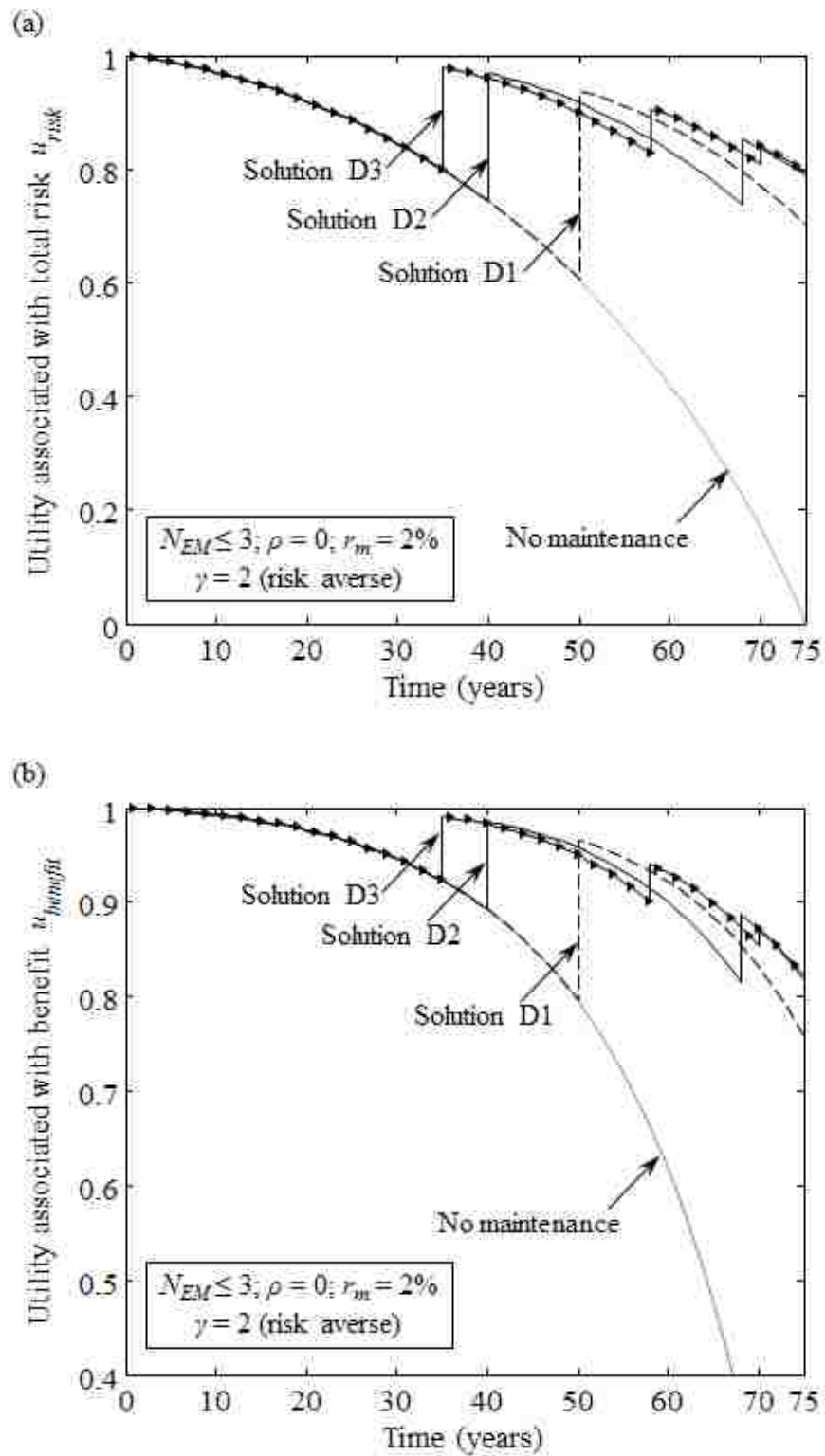


Figure 4.21. Time-variant (a) risk and (b) benefit utilities corresponding to optimum solutions D1, D2, and D3 in Figure 4.16d.

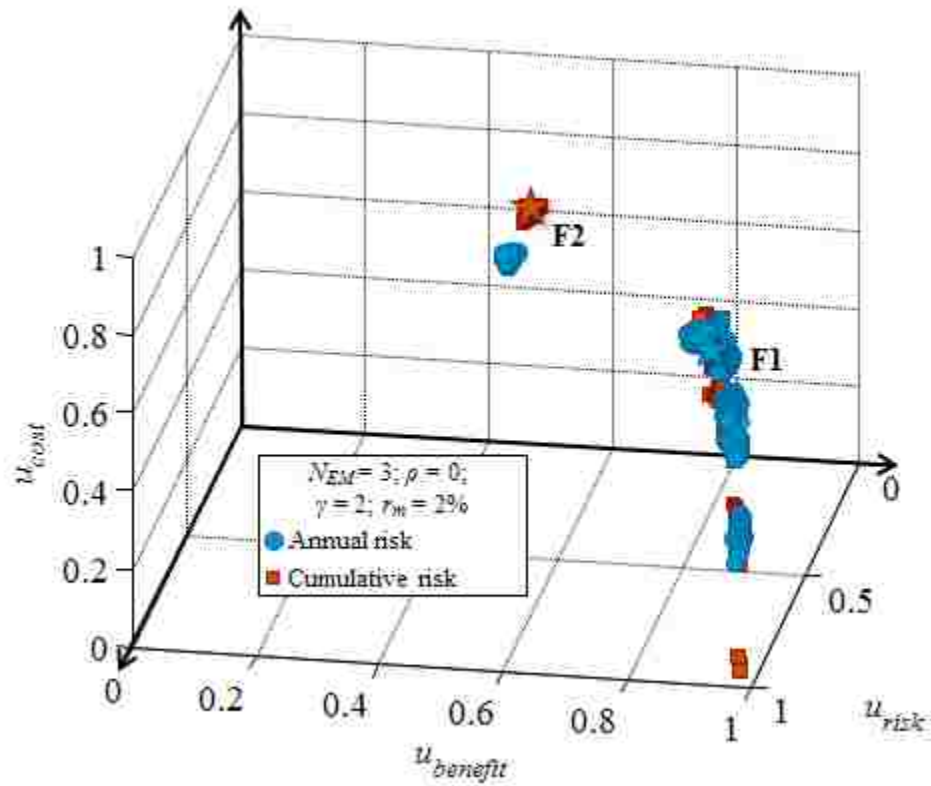


Figure 4.22. Pareto optimum solutions associated with both annual failure probability and cumulative-time failure probability considering a risk averse attitude ( $\gamma = 2$ ), independence among components ( $\rho = 0$ ), discount rate of money of 2% ( $r_m = 0.02$ ), and three maintenance actions ( $N_{EM} = 3$ ).

## **CHAPTER 5 DECISION MAKING FRAMEWORK FOR OPTIMAL SHM PLANNING OF SHIP STRUCTURES CONSIDERING AVAILABILITY AND UTILITY**

### **5.1 OVERVIEW**

Uncertainties associated with modeling and performance prediction of structures may be addressed and subsequently reduced by including, within the performance assessment, information collected from inspections and structural health monitoring (SHM). Under ideal conditions, continuous monitoring is required to accurately assess and predict the performance of deteriorating systems; however, in general, this is neither practical nor financially efficient. Presented herein is an approach that determines cost-effective SHM plans that consider the probability that the performance prediction model based on monitoring data is suitable throughout the life-cycle of ship structures. This probability is used to compute the expected average availability of monitoring data for prediction during the life-cycle of a system. Utility theory is employed to incorporate the influence of the decision maker's risk attitude on the relative desirability of SHM plans. Optimization techniques are utilized to simultaneously maximize the utilities associated with monitoring cost and expected average availability in order to determine optimal monitoring strategies under uncertainty. The effects of the formulation of the utility function, risk attitude of the decision maker and number of uniform and non-uniform time monitoring intervals on optimal SHM plans are investigated. The capabilities of the proposed decision support framework are illustrated on a naval ship.

The work presented in this chapter is based upon the research published in Sabatino and Frangopol (2017a); Sabatino and Frangopol (2017b,c); and Dong *et al.* (2016).

## **5.2 INTRODUCTION**

Due to the ever-changing state of an engineering system subjected to deterioration, it is imperative to consider both aleatory and epistemic uncertainties within structural performance assessment procedures. In general, aleatory and epistemic uncertainties are associated with the randomness of the underlying phenomenon and the models used to predict reality, respectively (Ang and Tang 2007). Although aleatory uncertainties are not reducible, epistemic uncertainties may be reduced by including information collected from inspections and structural health monitoring (Peil 2005; Frangopol and Messervey 2009a, 2009b).

The structural performance prediction of naval vessels is affected by various uncertainties inherent in the load conditions, damage propagation, among others (Soliman *et al.* 2015). Utilizing SHM within the performance assessment of ship structures is an effective tool to reduce uncertainties in the analysis and derive crucial information on the real-time structural response (Paik and Frieze 2001). Since SHM can provide reliable information regarding the future state of a structure, the collected data associated with optimized SHM plans will, in general, reduce epistemic uncertainties associated with structural performance prediction. The overall goals of SHM, in relation to civil and marine infrastructure, include: (a) assessing structural performance, (b) predicting remaining service life, and (c) providing a decision tool

for optimal life-cycle management of deteriorating infrastructure (Frangopol 2011). The first two objectives outlined above were explored in depth by Okasha and Frangopol (2010a), Okasha *et al.* (2010; 2011), Zhu and Frangopol (2013a), Frangopol and Kim (2014), Decò and Frangopol (2015), Soliman *et al.* (2015), and Mondoro *et al.* (2016). For instance, Soliman *et al.* (2015) used SHM to evaluate fatigue structural performance and assess serviceability of deteriorating ship structures. Within this chapter, the third objective outlined above is emphasized by determining cost-efficient SHM plans that provide crucial information regarding ship performance.

In an ideal situation, continuous monitoring is required to accurately assess and predict the performance of deteriorating naval vessels; however, in general, this is neither practical nor financially efficient. Thus, SHM plans that balance cost and performance objectives must be established (Kim and Frangopol 2011b). Presented in this chapter is a computational framework that has the ability to determine cost-effective SHM plans considering the probability that the performance prediction model based on monitoring data is suitable throughout the life-cycle of a naval vessel. This probability is used to calculate the expected average availability of monitoring data for performance prediction of a ship structure during the investigated time horizon. Within this context, the expected average availability associated with a SHM plan is representative of the overall quality of the collected data and its usefulness in predicting future performance (Kim and Frangopol 2011b). The proposed computational approach employs SHM data collected during seakeeping trials and normal ship operation to determine the future state of ships and ultimately cost-effective SHM plans. With very few exceptions (e.g., Kim and Frangopol 2011b),

there is a lack of studies that determine optimal SHM plans considering the availability of the data collected. The approach presented by Kim and Frangopol (2011b) considers only uniform time monitoring planning and does not include the effect of the decision maker's attitude on optimal monitoring plans. The methodology presented herein provides both uniform and non-uniform optimal monitoring plans based on utility functions that integrate the effect of the risk attitude of a decision maker.

Embedded within the presented decision support system for the optimal planning of SHM for marine structures is the performance prediction modeling, which is accomplished using statistics of the extremes and availability theory. Utility theory is employed herein to incorporate the influence of the decision maker's risk attitude on the relative desirability of lifetime SHM plans (Keeney and Raiffa 1993, Dong *et al.* 2016, Sabatino *et al.* 2016). In general, utility is defined as a measure of desirability to the decision maker (Ang and Tang 1984). Three different formulations of utility functions, always bounded by 0 and 1, are employed to express the relative desirability of lifetime SHM schedules.

Overall, utility theory is a powerful tool used to conduct rational multi-criteria decision making analyses considering uncertain information (Thurston 2001, Malak *et al.* 2009, Sabatino *et al.* 2015, 2016, Sabatino and Frangopol 2016a,b,c). Benefits of implementing decision based design with utility analysis include: avoiding biases of the decision maker, identifying alternatives worth further analysis, determining which tradeoffs are most desirable, avoiding irrationality under uncertainty, and communicating preference information to non-technical team members (Thurston

2001). Research efforts have been conducted regarding the use of utility theory in decision making problems. Keeny and Wood (1977) used multi-attribute utility theory to evaluate water resource development plans; twelve attributes were employed in their robust decision making analysis. Yang and Xu (2002) employed a utility-based approach to analyze the performance of four types of motorcycles considering three separate performance attributes to represent overall desirability. Fernández *et al.* (2005) presented a utility-based selection decision support methodology for aiding human judgment in making critical selection decisions. In addition to the technical advantages of employing utility theory in decision making analysis, this theory provides a mechanism to bridge the communication barrier between engineers and decision makers (Ross *et al.* 2004).

Genetic algorithm-based optimization techniques are utilized to simultaneously maximize the utilities associated with monitoring cost and expected average availability in order to determine optimal SHM plans under uncertainty. The effects of the formulation of the utility function, risk attitude of the decision maker, number of monitoring intervals, and assumptions in calculating the expected average availability of the prediction model on the optimal SHM strategies are investigated. Furthermore, both uniform and non-uniform monitoring interval SHM plans are explored. The capabilities of the proposed decision support framework are illustrated on an aluminum wave piercing catamaran.

### **5.3 PERFORMANCE PREDICTION CONSIDERING SHM DATA**

In order to manage SHM data effectively and reduce the overall amount of recorded information, the data associated with extreme physical quantities should be considered (Mahmoud *et al.* 2005). In the context of deteriorating structural systems under fatigue, SHM can be used to evaluate fatigue structural performance and assess their serviceability. A prediction function based on monitored extreme data can provide accurate information regarding the effective stress range and the number of cycles a deteriorating system may experience during its service life. The future state of a system and whether it conforms to the prediction function is based on the relation among the variation of monitored extreme data in time, the effective stress range, and the number of cycles. Overall, the prediction function based on monitored extreme data serves as an effective tool in assessing and predicting fatigue structural performance of deteriorating systems (Frangopol *et al.* 2008a,b, Strauss *et al.* 2008). Figure 5.1 presents the flowchart of the performance prediction, expected average availability, and cost of implementing monitoring. Detailed explanations regarding Figure 5.1 can be found in this section.

#### **5.3.1 SHM data analysis**

The formulation of the prediction function is based on statistics of the extremes. The extreme values of measured quantities can be treated as random variables. The probability density functions (PDFs) corresponding to these extreme values can be derived from the statistical data associated with the initial sample values. The extreme data is assumed to follow the asymptotic distributions established by Gumbel (1958):

Type I, Type II, and Type III. For instance, when the monitored data follow either normal or exponential distributions that have exponential tails, the largest monitored value may be effectively captured by a Type I asymptotic PDF (Ang and Tang 1984).

### 5.3.2 *Exceedance probability*

Next, regression techniques are utilized to establish an appropriate prediction function based upon the monitoring data. The residuals between this prediction function and actual extreme recorded data can be assumed normally distributed with a mean value of zero (Ang and Tang 1984). In this case, the extreme values may be modeled by the Type I asymptotic form. For this type of problem, the probability that the maximum positive residual in  $Y$  future monitored samples will be larger than the maximum positive residual among  $z$  already observed samples is given as (Ang and Tang 1984)

$$P_e = 1 - \exp\left[-\frac{Y}{z}\right] \quad (5.1)$$

Considering Eq. (5.1), in which  $z$  = number of daily maximum positive residuals and  $Y$  = number of daily maximum positive residuals in the future, the probability that the largest positive residual in the future  $t$  days will exceed the largest positive residual during the monitoring period  $\tau_m$  (days) is (Ang and Tang 1984)

$$P_e = 1 - \exp\left[-\frac{t}{\tau_m}\right] \quad (5.2)$$

Future down- and up-crossings, subsequently called exceedances, of the minimum negative residuals and the maximum positive residuals, respectively, may also be considered simultaneously. In this case, the probability that the maximum residual during  $t$  future days will exceed the largest positive residual during  $\tau_m$  monitoring days

or the minimum residual in  $t$  days will be less than the minimum negative residual during  $\tau_m$  days is (Ang and Tang 1984)

$$P_e = 1 - \exp\left[-\frac{2 \cdot t}{\tau_m}\right] \quad (5.3)$$

Next, the probability associated with the number of future exceedances  $ex$  can be formulated considering the equations for a single exceedance (i.e., Eqs. 5.2 and 5.3) and the Poisson process. For instance, the probability of future exceedances  $Y_{ex} = ex$  considering the largest positive residual within the prediction model is (Ang and Tang 1984)

$$P(Y_{ex} = ex) = \frac{(t/\tau_m)^{ex}}{ex!} \cdot \exp\left[-\frac{t}{\tau_m}\right] \quad (5.4)$$

Furthermore, considering the probability of future exceedances  $P(Y_{ex} = ex)$ , the probability of observing at least  $ex$  exceedances  $P_{ex}$  is calculated as

$$P_{ex} = P(Y_{ex} \geq ex) = 1 - \sum_{k=0}^{ex-1} P(Y_{ex} = k) \quad (5.5)$$

As an example, when examining only the positive residual, the probability of observing at least  $ex$  exceedances is derived using Eqs. (5.4) and (5.5).

$$P_{ex} = P(Y_{ex} \geq ex) = 1 - \sum_{k=0}^{ex-1} \left( \frac{(t/\tau_m)^k}{k!} \cdot \exp\left[-\frac{t}{\tau_m}\right] \right) \quad (5.6)$$

### 5.3.3 *Expected average availability*

Once the probability associated with residual exceedances is established, the expected average availability of the monitoring data for prediction may be derived. In general,

the availability of a system is defined as the probability that the system is in an operating state. The availability of SHM data for performance prediction can be characterized by the probability that the prediction model based on monitoring data can be usable in the future. The average availability of the prediction model during a time period  $\tau$  is calculated considering two mutually exclusive and collectively exhaustive events (i.e., the prediction model is usable and the prediction model is not usable) as (Kim and Frangopol 2011b)

$$\bar{A} = A_{pm}(\tau) + \frac{t_l}{\tau} \cdot U_{pm}(\tau) \quad (5.7)$$

where  $A_{pm}(\tau)$  = availability of the prediction model during  $\tau$ ,  $U_{pm}(\tau)$  = unavailability of the prediction model during  $\tau$ ,  $A_{pm}(\tau) + U_{pm}(\tau) = 1$ , and  $t_l$  = time to lose the usability of the adopted prediction model. The prediction model adopted herein utilizes the maximum residual between values from prediction model and monitoring data for future performance prediction. For instance, during monitoring period  $\tau_m$ , if this residual exceeds the maximum residual observed, then the prediction model is considered no longer usable. Within this context, the expected average availability associated with a SHM plan is representative of the overall quality of the collected data and its usefulness in predicting future performance.

The expected average availability of the prediction model during a time period  $\tau$  is developed considering Eq. (5.7) and the exceedance probability  $P_{ex}$  formulated in Eq. (5.5) as (Ang and Tang 1984; Kim and Frangopol 2011b)

$$E(\bar{A}) = \frac{1}{\tau} \int_0^{\tau} (1 - P_{ex}) dt \quad (5.8)$$

Table 5.1 summarizes the expected average availability values associated with various combinations of number of exceedances and residual(s) considered in the prediction model.

Two types of SHM plans are included within the analyses herein: those that exhibit regular monitoring periods and plans that possess non-uniform monitoring periods. Figure 5.2 outlines the typical monitoring plan associated with regular and non-uniform interval monitoring periods. For SHM plans with uniform monitoring periods, the relationship between the monitoring period  $\tau_m$  (days), time  $\tau$  in days that the system is not monitored, an initial unmonitored time period  $\tau_{ini}$ , which is assumed to begin immediately after the end of the reference monitoring period, and the time horizon  $T_h$  is illustrated in Figure 5.2a. Similarly, SHM plans with non-uniform time monitoring intervals are defined by an initial unmonitored time period  $\tau_{ini}$ , the duration of each monitoring period  $\tau_{m1}, \tau_{m2}, \dots, \tau_{mn}$ , and the duration of each non-monitoring interval  $\tau_1, \tau_2, \dots, \tau_n$ . Although two different types of SHM plans are considered herein, the calculation of expected average availability is quite similar for both cases. The expected average availability of SHM data considering uniform interval monitoring periods is directly calculated using Eq. (5.8). However, the expected average availability associated with SHM plans possessing irregular duration monitoring intervals is calculated by considering the expected average availability of each full cycle (e.g.,  $\tau_{m1} + \tau_1$ ). First, the integral contained in Eq. (5.8) is computed considering each cycle separately, then the resulting values are multiplied by the ratio of the full cycle duration to the total time horizon (e.g.,  $(\tau_{m1} + \tau_1)/T_h$ ), and added together to determine the expected average availability of SHM plans with non-

uniform monitoring intervals. Overall, the number of exceedances allowed, residuals examined in the prediction process, and type of SHM plan are presented as inputs to the presented SHM decision support framework.

#### 5.3.4 Monitoring cost

Monitoring costs are associated with the overall data collection procedure. More specifically, general preparation, project coordination, placement of sensors, wiring, data acquisition setup and maintenance, continuous review of collected data, analysis of SHM data, and preparation of the associated reports activities are all included within monitoring costs estimations (Frangopol *et al.* 2008a,b). Considering that the total monitoring cost of a SHM plan is proportional to the monitoring duration and that all actions related to the monitoring program are implemented only during the monitoring durations, the cumulative monitoring cost  $C_m$  over a total time horizon can be calculated for plans that include uniform and non-uniform monitoring periods. For uniform monitoring intervals, the total monitoring cost is calculated as:

$$C_m = \left( \frac{C_{m0} \cdot \tau_{m0}}{\tau_m} + C_p \right) \cdot \sum_{i=1}^n \left( (1 + r_m)^{(\tau + \tau_m)(i-1)} \right)^{-1} \quad (5.9)$$

where  $C_{m0}$  = reference monitoring cost during  $\tau_{m0}$  days,  $r_m$  = daily discount rate of money,  $n$  = total number of cycles investigated, and  $C_p$  = cost of initializing monitoring. Similarly, the cumulative monitoring cost associated with SHM plans with non-uniform monitoring periods is:

$$C_m = \left( \frac{C_{m0} \cdot \tau_{m0}}{\tau_m} + C_p \right) \cdot \sum_{i=1}^n \left( (1 + r_m)^{\tau_{mi} + \sum_{j=1}^i (\tau_j + \tau_{mj})} \right)^{-1} \quad (5.10)$$

## 5.4 UTILITY ASSESSMENT

Utility is a measure of value (or desirability) of a certain alternative for the decision maker. In this context, utility depicts the relative desirability of lifetime SHM strategies to the decision maker. The computational procedure adopted for the utility assessment of SHM planning is shown as a part of Figure 5.3. Overall, this flowchart outlines the process of calculating the utility associated monitoring costs and expected average availability. In addition, it is shown how these utility functions are incorporated into a bi-objective optimization framework that facilitates optimal decision making concerning SHM planning.

### 5.4.1 Risk attitude

Utility functions associated with cost and expected average availability are computed considering the risk attitude of the decision maker  $Att$ , defined herein as the negative ratio of the second derivative of a utility function to its first derivative (Pratt 1964; Arrow 1965). The risk attitude is calculated as follows:

$$Att = -\frac{u''}{u'} \quad (5.11)$$

where  $u$  is the utility function investigated, and  $u'$  and  $u''$  are the first and second derivative, respectively.. Negative and positive risk attitude indicate risk acceptance and risk aversion, respectively. Two types of attributes are considered within this chapter: (a) one that exhibits decreased desirability when increased (i.e., monitoring cost), and (b) one that possesses increased desirability when increased (i.e., expected

average availability). A normalized value  $x$  may be established for each type of attribute considering decreasing  $x_{dec}$  or increasing  $x_{inc}$  desirability as follows:

$$x_{dec} = \frac{a_{\max} - a}{a_{\max} - a_{\min}} \quad (5.12)$$

$$x_{inc} = \frac{a - a_{\min}}{a_{\max} - a_{\min}} \quad (5.13)$$

where  $a$  = attribute value under investigation,  $a_{\min}$  = minimum value of the attribute, and  $a_{\max}$  = maximum value of the attribute. The minimum and maximum values of the investigated attribute are utilized to normalize the utility so that it always takes values between 0 and 1. Within the proposed framework, the minimum and maximum attribute values corresponding to the monitoring cost in USD are  $a_{\min} = 0$  and  $a_{\max} = C_{m,max}$ , respectively. Similarly, the minimum and maximum attribute values associated with availability are  $a_{\min} = 0$  and  $a_{\max} = 1$ , respectively.

#### 5.4.2 Formulations

Three types of monotonic utility function formulations are considered within the proposed approach: (a) exponential, (b) quadratic, and (c) logarithmic. The governing equations corresponding to these utility formulations are (Keeney and Raiffa 1993; Ang and Tang 1984):

$$u_{\text{exp}} = \frac{1 - \exp[-\rho \cdot x]}{1 - \exp[-\rho]} \quad (5.14)$$

$$u_{\text{quad}} = \frac{1}{1 - \alpha/2} \cdot \left( x - \frac{1}{2} \cdot \alpha \cdot x^2 \right) \quad (5.15)$$

$$u_{\text{log}} = \frac{1}{\ln\left[\frac{1+\beta}{\beta}\right]} \cdot (\ln[x + \beta] - \ln[\beta]) \quad (5.16)$$

where  $\rho$ ,  $\alpha$ , and  $\beta$  are the parameters associated with exponential, quadratic, and logarithmic utility functions, respectively. Considering the definition of risk attitude  $Att$  outlined in Eq. (5.11) and the utility formulations detailed in Eqs. (5.14), (5.15), and (5.16), the risk attitude, as a function of attribute value, is calculated and expressions for the most extreme value of coefficient  $\gamma$  over all attribute values (i.e., smallest negative or largest positive value) are derived. The coefficients  $\gamma$  represent the smallest negative and largest positive risk attitude  $Att$  associated with the utility formulations. These coefficients are representative of the risk attitude of the decision maker and are considered as given within the proposed optimization approach. Given  $\gamma$ , appropriate values of the parameters  $\rho$ ,  $\alpha$ , and  $\beta$  in the exponential, quadratic, and logarithmic utility equations, respectively, can be calculated as (Pratt 1964; Arrow 1965)

$$\rho = \gamma \quad (5.17)$$

$$\alpha = \frac{\gamma}{1 + |\gamma|} \quad (5.18)$$

$$\beta = \begin{cases} 1 \times 10^{10} & \text{if } \gamma = 0 \\ \frac{1}{\gamma} & \text{if } \gamma < 0 \text{ or } \gamma > 0 \end{cases} \quad (5.19)$$

Plots of the utility function corresponding to an attribute, considering the exponential, quadratic, and logarithmic formulation, are provided in Figure 5.4, Figure 5.5, and Figure 5.6, respectively.  $u = 1$  corresponds to the best case scenario while  $u = 0$  is associated with the worst possible case. Alternatives associated with large utility values are preferred to those associated with small utility values (Howard and Matheson 1989). The concavity of the utility functions is highly dependent on the risk attitude of the decision maker. Risk averse and risk accepting attitudes yield concave

and convex utility functions, respectively. Additionally, the relationship between the parameters  $\rho$ ,  $\alpha$ , and  $\beta$  and the extreme risk attitude coefficient  $\gamma$  are depicted in Figure 5.4, Figure 5.5, and Figure 5.6. The exponential formulation exhibits constant risk attitude as a function of attribute value, the logarithmic form is associated with decreasing risk aversion, and the quadratic utility formulation corresponds to increasing risk aversion (Keeney and Raiffa 1993).

## 5.5 OPTIMIZATION FRAMEWORK

Considering  $a_{min}$  and  $a_{max}$  for both attributes investigated, the risk attitude of the decision maker characterized by the extreme risk attitude coefficient  $\gamma$ , and the utility function formulation, appropriate utility functions corresponding to monitoring cost  $u_c$  and expected average availability  $u_a$  may be established and ultimately employed within the optimization procedure outlined in Figure 5.3. Within the proposed decision support framework, utility values corresponding to monitoring cost  $u_c$  and expected average availability  $u_a$  are calculated for each SHM plan alternative. Genetic algorithms are employed to iteratively search for and determine optimal SHM plans that simultaneously maximize  $u_c$  and  $u_a$ . Finally, a Pareto front depicting optimal monitoring plans in the objective space is determined. Embedded within this trade-off set of solutions are SHM plans that are characterized by  $\tau_m$ ,  $\tau$ , and  $\tau_{ini}$  for uniform monitoring intervals and  $\tau_{m1}$ ,  $\tau_{m2}$ , ...,  $\tau_{mn}$ ,  $\tau_1$ ,  $\tau_2$ , ...,  $\tau_n$ , and  $\tau_{ini}$  for non-uniform monitoring durations. The outputs of the optimization procedure are the durations of the monitoring periods, in days, as outlined in Figure 5.2.

The optimization formulation is outlined as follows:

*Given:*

- SHM data for a duration of  $\tau_{m0}$  days
- Cost of reference SHM data  $C_{m0}$
- Target life  $T_h$
- Discount rate of money  $r_m$
- Total number of monitoring cycles  $n$
- Case (determined by residuals examined and number of exceedances  $ex$  considered in the prediction process, please refer to Table 5.1)
- Coefficient  $\gamma$  representative of risk attitude

*Find:*

- Monitoring duration ( $\tau_m$  for uniform intervals;  $\tau_{m1}, \tau_{m2}, \dots, \tau_{mn}$  for non-uniform intervals)
- Prediction duration ( $\tau$  and  $\tau_{ini}$  for uniform intervals;  $\tau_{ini}$  and  $\tau_1, \tau_2, \dots, \tau_n$  for non-uniform intervals)

*So that:*

- Utility associated with monitoring cost  $u_c$  is maximized
- Utility associated with expected average availability  $u_a$  is maximized

*Subjected to:*

- Maximum allowable budget for cumulative monitoring cost  $C_{m,max}$
- Duration of each non-monitoring period  $\tau$  must be greater than or equal to  $\tau_{min}$  and less than or equal to  $\tau_{max}$ ,  $\tau_{min} \leq \tau \leq \tau_{max}$
- Duration of each monitoring period  $\tau_m$  must be greater than or equal to  $\tau_{m,min}$  and less than or equal to  $\tau_{m,max}$ ,  $\tau_{m,min} \leq \tau_m \leq \tau_{m,max}$
- Duration of SHM plan, including the last monitoring period, must be less than  $T_h$
- Duration of SHM plan, including the last non-monitoring period, must be at least  $T_h$

Ultimately, the decision maker will use the outputs of the optimization, (i.e., the Pareto set of solutions that outline optimal SHM plans), to make the best informed choices regarding cost-effective SHM planning.

## **5.6 CASE STUDY**

The SHM planning optimization procedure presented within this chapter is applied to the HSV-2 swift, an aluminum wave piercing catamaran. The ship measures 98 m in length and is capable of achieving speeds of 38–47 knots (Incat 2003). A three dimensional schematic of the ship is shown in Figure 5.7a (Incat 2003; Brady 2004a,b; Salvino and Brady 2008; Soliman *et al.* 2015).

Upon completion of the construction of the naval vessel in December 2003, it was instrumented with various types of sensors to measure the primary load response, stress concentrations, and behavior under secondary loading (Brady 2004a). More specifically, the HSV-2 swift was instrumented with foil strain gages and piezoelectric accelerometers that were wired and connected to remote junction boxes and an instrumentation trailer (Brady 2004a). This monitoring plan was deployed with several main goals, including determining the safe operating limits of the HSV-2 swift based on responses measured in both calm and rough water seakeeping trials (Brady 2004a). In order to determine the response under a wide array of operational conditions, seakeeping trials were carried out that varied the ship speed, wave heading, and sea state.

As a part of the monitoring program, 16 sensors (i.e., sensors T1-1 to T1-16) were used to measure the structural response of the ship to global loading in terms of

global bending stresses, pitch connecting moments, and split responses. A second set of sensors (i.e., T2-1 to T2-9 and T2-12 to T2-21) were placed in order to determine stress concentrations at various locations. The locations at which T1 and T2 sensors were installed were selected based on detailed finite element analysis and previous experience with similar ships (Brady 2004a). An example of sensor placement is depicted in Figure 5.7b for sensor T2-4 of frame 26; this sensor was placed to measure the bending response on the keel at frame 26 on the port side. This sensor and its counterpart sensor T2-5, installed on the same frame but on the starboard side, exhibited the largest strain response among all the T2 sensors (Soliman *et al.* 2015).

The strain data was filtered and then used to obtain the stress range bin histograms and average number of cycles for each operational condition (Soliman *et al.* 2015). The resulting stress range histograms are utilized herein as input for the presented SHM planning framework. Complete information regarding the data collection, signal analyses, and stress range histograms can be found in Soliman *et al.* (2015) and Mondoro *et al.* (2016). Based upon the total run-time of the initial SHM data, optimal SHM plans are developed for the HSV-2 swift considering an initial monitoring time of  $\tau_{m0} = 3$  days. For the uniform monitoring interval problem, the outputs of the optimization algorithm are the monitoring period  $\tau_m$  (days) and the time  $\tau$  in days that the vessel is not monitored. Note that the SHM plans reported within this chapter include an initial unmonitored time period  $\tau_{ini}$ , which is assumed to occur directly after the reference monitoring period. Similarly, the outputs of the optimization procedure for the non-uniform monitoring interval problem are the

monitoring durations (i.e.,  $\tau_{m1}, \tau_{m2}, \dots, \tau_{mn}$ ) and prediction durations (i.e.,  $\tau_{ini}$  and  $\tau_1, \tau_2, \dots, \tau_n$ ).

For all the optimizations carried out within this chapter, unless otherwise noted, a total time horizon  $T_h$  of the HSV-2 swift of 10 years (i.e., 3650 days) is assumed and each SHM plan consists of 4 monitoring cycles (i.e.  $n = 4$ ). Additionally, for each alternative (i.e., SHM plan), it is necessary to evaluate both the utility associated with total monitoring cost  $u_c$  and the utility that is representative of the expected average availability  $u_a$ . The utility value associated with the total monitoring cost is obtained utilizing Eqs. (5.12), (5.14), (5.15), and (5.16) with  $a_{max} = \$500,000$  (i.e., 500 times the reference monitoring cost  $C_{m0} = \$1,000$ ) and  $a_{min} = \$0$ , and the cost of initializing monitoring  $C_p = \$500$  (i.e., 0.5 times  $C_{m0}$ ). Similarly, the utility value associated with expected average availability  $u_a$  is calculated considering Eqs. (5.13), (5.14), (5.15), and (5.16) with  $a_{max} = 1$  and  $a_{min} = 0$ .

The following constraints on the design variables involved in the optimization are also considered: (a)  $150 \text{ days} \leq \tau_{ini} \leq 500 \text{ days}$ , (b)  $60 \text{ days} \leq \tau_m \leq 1500 \text{ days}$ , (c)  $60 \text{ days} \leq \tau \leq 1500 \text{ days}$ , (d) duration of a SHM, plan including the last monitoring period, is less than  $T_h$ , and (e) duration of the SHM, plan including the last non-monitoring period, is at least  $T_h$ . The last two constraints are included to ensure that the optimal SHM plans cover the entirety of the time horizon investigated. Considering the non-uniform monitoring interval problem, constraints (b) and (c) listed above are modified to include all monitoring durations (i.e.,  $\tau_{m1}, \tau_{m2}, \dots, \tau_{mn}$ ) and prediction durations (i.e.,  $\tau_1, \tau_2, \dots, \tau_n$ ).

### 5.6.1 *Uniform time intervals*

This section contains the results of several optimization problems, considering a variety of inputs to the optimal SHM framework outlined previously and uniform monitoring intervals. First, the effects of the type of utility formulation on optimal SHM plans are investigated. Considering the exponential, quadratic, and logarithmic utility formulations, three separate optimization procedures are carried out for a risk accepting decision maker (i.e.,  $\gamma = -1$ ) considering case LS4 in Table 5.1 (i.e., at least 4 exceedances of the minimum negative and maximum positive extreme values) and an annual discount rate of money  $r_m = 2\%$ . The Pareto optimal solutions for this problem are shown in Figure 5.8 for all three utility types considered. Six representative solutions in the objective space (i.e., A1, A2, ... , A6) are highlighted as five-point stars in Figure 5.8.

Representative solutions A1, A2, A3, and A4 correspond to SHM plans obtained considering the exponential utility formulation, while solutions A5 and A6 are associated with quadratic and logarithmic utility formulations, respectively. SHM plans embedded within the Pareto front corresponding to the exponential utility formulation are outlined, in the design space, in Figure 5.9. Note that this figure details the SHM plans with monitoring periods denoted by thick lines with round caps at each end and non-monitoring durations indicated by thin, dashed lines (please refer to Figure 5.2a). As shown, a solution that exhibits relatively large cost utility  $u_c$  will usually possess a relatively small utility associated with availability  $u_a$ . Figure 5.10 depicts SHM plans corresponding to solutions A2, A5, and A6 within Figure 5.8; these SHM plans all exhibit availability utility  $u_a$  values equal to 0.4. Although the

plans shown in Figure 5.10 are similar in terms of monitoring durations and timings, they possess different cost utilities  $u_c$  and cumulative monitoring costs  $C_m$ .

Next, the effects of the residuals examined in the prediction process and number of exceedances  $ex$  considered on the Pareto optimal solutions are investigated. An optimization is carried out for a risk averse decision maker (i.e.,  $\gamma = 2$ ) considering the quadratic utility formulation and an annual discount rate of money  $r_m = 2\%$ . This optimization procedure is conducted for several combinations of residuals examined in the prediction process and number of exceedances  $ex$ . Figure 5.11a depicts Pareto optimal solutions considering the maximum positive residual, denoted by case L (see Table 5.1) while Figure 11b shows Pareto optimal solutions associated with both the minimum negative residual and the maximum positive residual, named herein as case LS (see Table 5.1). Representative SHM plans B1, B2, B3, C1, C2, and C3 are highlighted in Figure 5.11 and depicted in the design space in Figure 5.12. By comparing the Pareto fronts shown in Figure 5.11a and Figure 5.11b, for the same number of exceedances  $ex$ , it is evident that optimal solutions considering case L exhibit larger availability utility  $u_a$  than those associated with case LS. For instance, if the Pareto fronts contained in Figure 5.11 associated with  $ex = 3$  for both cases L and LS are plotted together, it could be observed that the optimal solutions on separate Pareto fronts with equal cost utility  $u_c$  possess different availability utilities  $u_a$ . More specifically, considering optimal SHM plans on each front that correspond to the same cost utility  $u_c$ , the solution corresponding to case L exhibits larger availability utility  $u_a$  than that associated with case LS. Figure 5.12 shows that solutions corresponding to case L possess shorter monitoring durations than those associated with case LS.

Additionally, the SHM plans associated with relatively small number of exceedances (e.g.,  $ex = 1$ ) exhibit longer monitoring durations than those considering larger number of exceedances (e.g.,  $ex = 5$ ) for both cases L and LS.

The last uniform monitoring interval SHM problem presented herein investigates the effect of the number of monitoring cycles  $n$  on the Pareto optimal SHM obtained for the HSV-2 swift. Thus far, the optimizations presented within this chapter have assumed a fixed number of monitoring cycles (i.e.,  $n = 4$ ); however, this constraint may be relaxed and the number of monitoring cycles may be included as a design variable within the optimization by introducing the parameter  $n_{max}$ , the maximum number of cycles. Assuming  $n_{max} = 8$  cycles, a risk averse decision maker (i.e.,  $\gamma = 1$ ), the logarithmic utility formulation, and case L3 in Table 5.1 (i.e., at least 3 exceedances of the maximum positive residual), an optimization is carried out to determine SHM plans with a varying number of monitoring cycles over a ten year period. The results of this optimization are presented, in the form of a Pareto front, in Figure 5.13. Within this figure, the fill-shade of each solution within the objective space denotes the number of monitoring intervals embedded within that particular SHM solution. Five representative solutions, D1, D2, D3, D4, and D5, possessing availability utility  $u_a$  values of 0.2, 0.4, 0.6, 0.8, and 0.95, are highlighted in Figure 5.13. The SHM plans, including monitoring interval durations, are depicted in Figure 5.14 for optimal solutions D1, D2, D3, D4, and D5. As shown, optimal SHM plans with a relatively small number of monitoring cycles (e.g.,  $n = 2$ ) possess high cost utilities  $u_c$ , but relatively low availability utilities  $u_a$ . Conversely, SHM plans with relatively large number of monitoring cycles (e.g.,  $n = 8$ ) are high in cost but are very

effective in ensuring accurate performance prediction. For example, optimal SHM plans like Solution D5 exhibit large utility associated with availability (i.e.,  $u_a = 0.95$ ) but relatively small cost utility (i.e.,  $u_c = 0.251$ ).

### 5.6.2 *Non-uniform time intervals*

Similarly, the optimization procedure outlined previously is also applied to non-uniform time monitoring (see Figure 5.2b). The effects of utility formulation, risk attitude, and the discount rate of money on the final Pareto optimal solutions obtained are examined in detail.

First, the effects of the utility formulation on optimal, non-uniform interval SHM plans are investigated. Considering the exponential, quadratic, and logarithmic utility formulations, three separate optimization procedures are carried out for a risk accepting decision maker (i.e.,  $\gamma = -2$ ) considering case LS4 in Table 5.1 (i.e., at least 4 exceedances of the minimum negative and maximum positive extreme values), an annual discount rate of money  $r_m = 2\%$ , and  $n = 4$  monitoring cycles. The Pareto optimal solutions for this problem are shown in Figure 5.15. Five representative solutions in the objective space are highlighted as five-point stars in Figure 5.15. Representative solutions E1, E2, E3, and E4 are associated with SHM plans obtained considering the exponential utility formulation, while solutions E5 and E6 are associated with quadratic and logarithmic utility formulations, respectively. SHM plans embedded within the Pareto front corresponding to the exponential utility formulation are shown, in the design space, in Figure 5.16. From Figure 5.16 it is observed that solutions exhibiting low availability utility  $u_a$  (e.g., Solution E1) have a

total monitoring duration (i.e.,  $\tau_{m1} + \tau_{m2} + \tau_{m3} + \tau_{m4}$ ) that is shorter than those plans with relatively higher availability utility  $u_a$  (e.g., Solution E4). In addition to analyzing the variation of SHM plans along the Pareto front corresponding to just one utility formulation, SHM plans that have the same availability utility (i.e.,  $u_a = 0.4$ ) but are obtained considering different utility formulations are compared in Figure 5.17. Although there are visual differences between the three optimal SHM plans corresponding to solutions E2, E5, and E6, their cost utilities do not differ greatly, especially considering solutions E5 and E6 associated with quadratic and logarithmic utility formulations, respectively.

Next, the effect of the risk attitude of the decision maker on optimal SHM plans is investigated. Two separate optimizations are performed for a risk accepting and risk averse decision maker (i.e.,  $\gamma = -2$  and  $\gamma = 2$ , respectively) considering the exponential utility formulation, an annual discount rate of money  $r_m = 2\%$ ,  $n = 4$  monitoring cycles, and case LS3 (i.e., at least 3 exceedances of the minimum negative and maximum positive residuals, see Table 5.1). The two Pareto fronts resulting from this optimization are presented, in the objective space, in Figure 5.18. According to this figure, in general, optimal SHM plans associated with a risk averse decision maker exhibit higher cost and availability utilities than those corresponding to a risk accepting decision maker. Representative solution sets F and G contain optimal SHM plans associated with a risk accepting and risk averse decision maker, respectively; the monitoring timelines corresponding to solution set F and G are depicted in Figure 5.19 and Figure 5.20, respectively. SHM plans corresponding to a risk averse decision maker have short duration monitoring periods that occur late during the investigated

time horizon, while the solutions associated with a risk accepting decision maker exhibit longer monitoring durations that occur toward the beginning of the investigated time horizon.

The final sensitivity analysis conducted herein studies the effect of the annual discount rate of money  $r_m$  on the optimal SHM plans for the HSV-2 swift. Considering  $r_m = 6\%$ ,  $2\%$ , and  $0\%$ , three optimization procedures are conducted. The resulting Pareto fronts are depicted in Figure 5.21 considering a risk averse decision maker (i.e.,  $\gamma = 2$ ), the quadratic utility formulation,  $n = 4$  monitoring cycles, and case LS3 (i.e., at least 3 exceedances of the minimum negative and maximum positive residuals). A representative solution on each Pareto front in Figure 5.21 is highlighted with a five point star; these solutions, Solution H1, H2, and H3, all possess availability utility  $u_a = 0.8$ , indicating that collected data will be extremely useful in providing predictions for future performance. The monitoring plans corresponding to Solutions H1, H2, and H3 are detailed in Figure 5.22. The optimal SHM plans are quite sensitive to the annual discount rate of money  $r_m$ . For instance, as evidenced in Figure 5.22, Solution H3, which considers  $r_m = 0\%$ , possesses monitoring periods that are relatively uniform and occur toward the beginning of the investigated time horizon; however, Solution H1, where  $r_m = 6\%$ , has monitoring periods that vary in duration and occur toward beginning, middle, and end of the investigated time horizon.

## 5.7 CONCLUSIONS

Overall, optimal SHM plans, the output of the presented decision support framework, allow for availability-informed decision making regarding monitoring of ship

structures. Optimal SHM plans are obtained by simultaneously maximizing the utilities associated with monitoring cost and expected average availability of the prediction model. Three formulations of the utility function are considered herein: exponential, quadratic, and logarithmic. The effects of the formulation of the utility function, risk attitude of the decision maker, number of monitoring intervals, and assumptions in calculating the expected average availability of the prediction model on the optimal SHM strategies are investigated. Given the risk attitude, the decision maker can employ the proposed decision-support system to make cost- and availability- informed choices regarding the monitoring of ship structures.

The following conclusions are drawn:

1. SHM plans are determined using a multi-criteria optimization algorithm that balances two objectives: the utilities associated with monitoring cost and expected average availability. Ultimately, a decision maker is able to make informed decisions based on the decision support system provided by the Pareto set of optimal solutions.
2. The risk attitude of the decision maker can have great influence on the optimal solutions resulting from the proposed decision support system. In general, risk averse decision makers, will assign larger utility values to the same alternative as compared to risk accepting decision makers.
3. The number of monitoring cycles considered throughout the time horizon investigated has an important effect on the Pareto solutions. Both the cumulative monitoring cost and overall effectiveness of the SHM data, represented by expected average availability are sensitive to changes in the

proposed number of cycles and in the discount rate of money. The effect of the time horizon considered on the Pareto solutions also has to be investigated.

4. Further and continued research and promotion of an integrated utility-based approach as the rational basis for optional structural health monitoring planning of ship structures considering uncertainties is required.

Table 5.1. Expected average availability corresponding to various combinations of number of exceedances and the residual(s) examined in the prediction process

Case	Number of exceedances $ex$	Residual(s) examined	Expected average availability $E(\bar{A})$
L1	$ex \geq 1$	Maximum positive	$\frac{\tau_m}{t} \cdot (1 - \exp[-t/\tau_m])$
L2	$ex \geq 2$	Maximum positive	$\frac{1}{t} \cdot (2 \cdot \tau_m - (t + 2 \cdot \tau_m) \cdot \exp[-t/\tau_m])$
L3	$ex \geq 3$	Maximum positive	$\frac{1}{t} \cdot \left( 3 \cdot \tau_m - \frac{\exp[-t/\tau_m]}{2 \cdot \tau_m} \cdot (t^2 + 4 \cdot t \cdot \tau_m + 6 \cdot \tau_m^2) \right)$
L4	$ex \geq 4$	Maximum positive	$\frac{1}{t} \cdot \left( 4 \cdot \tau_m - \frac{\exp[-t/\tau_m]}{6 \cdot \tau_m^2} \cdot (t^3 + 6 \cdot t^2 \cdot \tau_m + 18 \cdot t \cdot \tau_m^2 + 24 \cdot \tau_m^3) \right)$
L5	$ex \geq 5$	Maximum positive	$\frac{1}{t} \cdot \left( 5 \cdot \tau_m - \frac{\exp[-t/\tau_m]}{24 \cdot \tau_m^3} \cdot (t^4 + 8 \cdot t^3 \cdot \tau_m + 36 \cdot t^2 \cdot \tau_m^2 + 96 \cdot t \cdot \tau_m^3 + 120 \cdot \tau_m^4) \right)$
LS1	$ex \geq 1$	Minimum negative and maximum positive	$\frac{\tau_m}{2 \cdot t} \cdot (1 - \exp[-(2 \cdot t)/\tau_m])$
LS2	$ex \geq 2$	Minimum negative and maximum positive	$\frac{1}{t} \cdot (\tau_m - (t + \tau_m) \cdot \exp[-(2 \cdot t)/\tau_m])$
LS3	$ex \geq 3$	Minimum negative and maximum positive	$\frac{1}{t} \cdot \left( \exp[-(2 \cdot t)/\tau_m] \cdot \left( \frac{-2 \cdot t - t^2/\tau_m}{-(3 \cdot \tau_m)/2} \right) + (3 \cdot \tau_m)/2 \right)$
LS4	$ex \geq 4$	Minimum negative and maximum positive	$\frac{1}{t} \cdot \left( 2 \cdot \tau_m - \frac{\exp[-(2 \cdot t)/\tau_m]}{3 \cdot \tau_m^2} \cdot (2 \cdot t^3 + 6 \cdot t^2 \cdot \tau_m + 9 \cdot t \cdot \tau_m^2 + 6 \cdot \tau_m^3) \right)$
LS5	$ex \geq 5$	Minimum negative and maximum positive	$\frac{1}{t} \cdot \left( \frac{5 \cdot \tau_m}{2} - \frac{\exp[-(2 \cdot t)/\tau_m]}{6 \cdot \tau_m^3} \cdot (2 \cdot t^4 + 8 \cdot t^3 \cdot \tau_m + 18 \cdot t^2 \cdot \tau_m^2 + 24 \cdot t \cdot \tau_m^3 + 15 \cdot \tau_m^4) \right)$

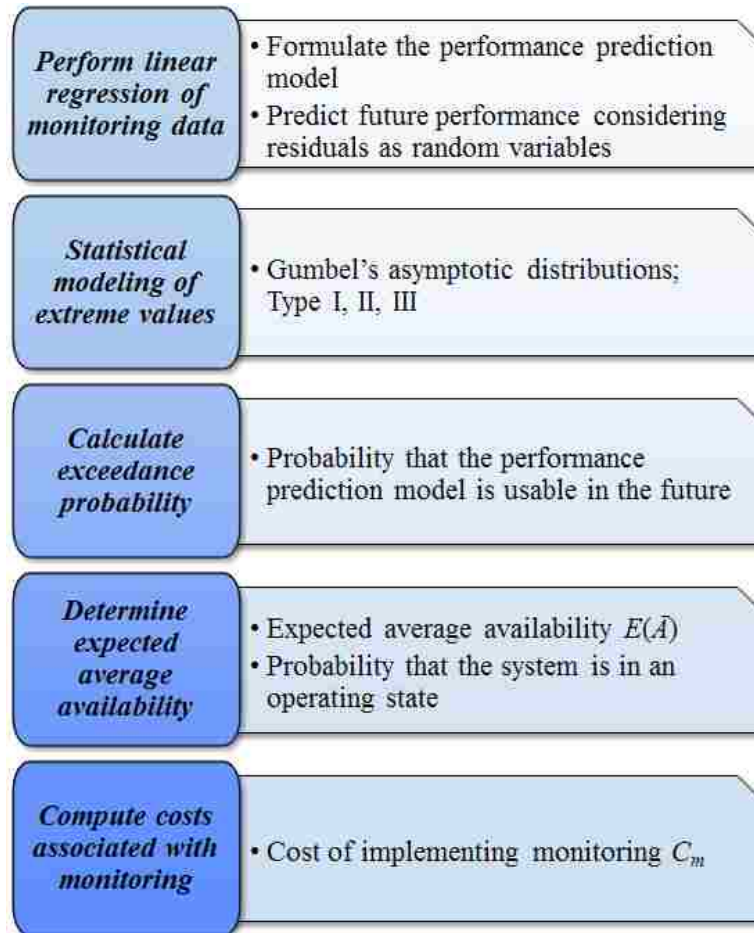


Figure 5.1. Flowchart describing the performance prediction, expected average availability, and cost of implementing monitoring.

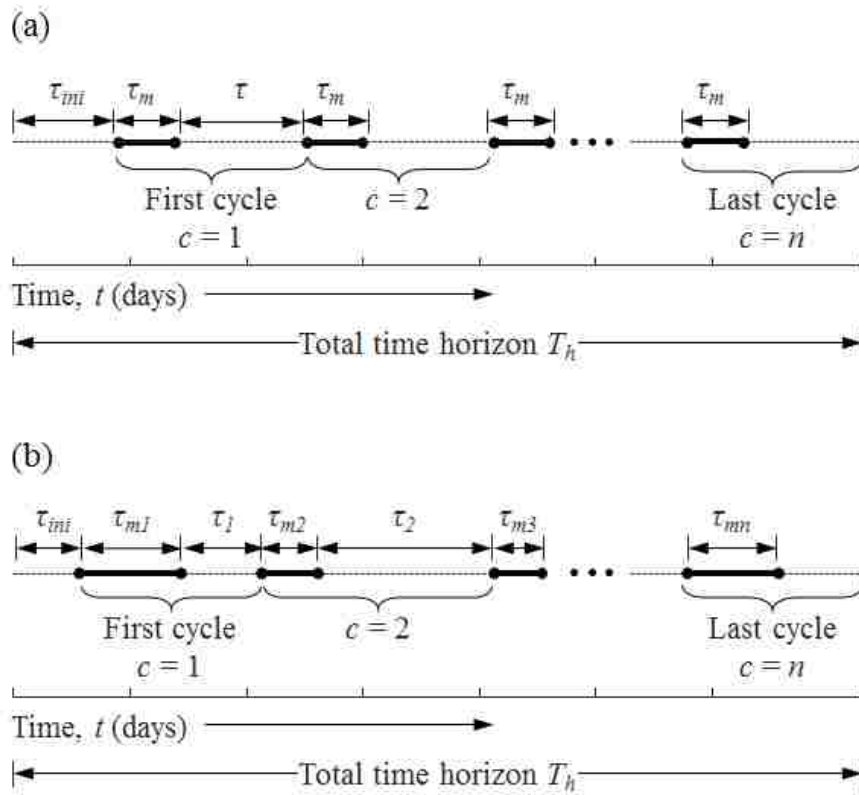


Figure 5.2. Timeline of monitoring at (a) uniform time and (b) non-uniform time intervals.

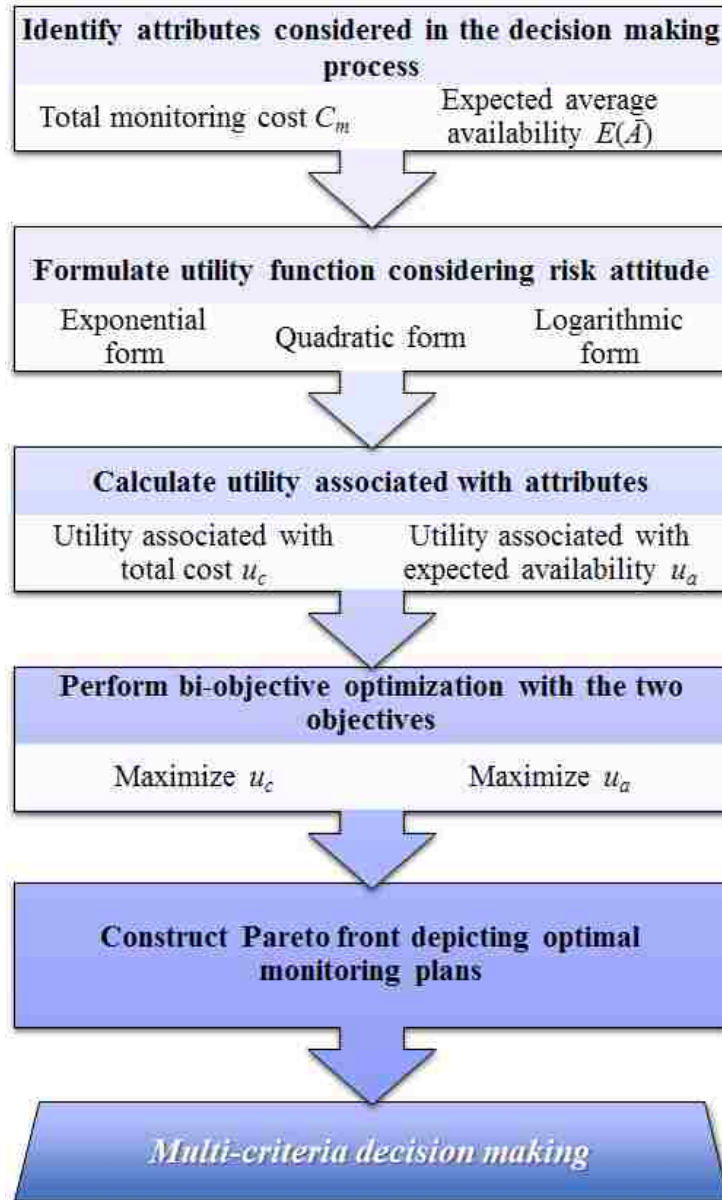


Figure 5.3. Flowchart describing the utility assessment and optimization procedure.

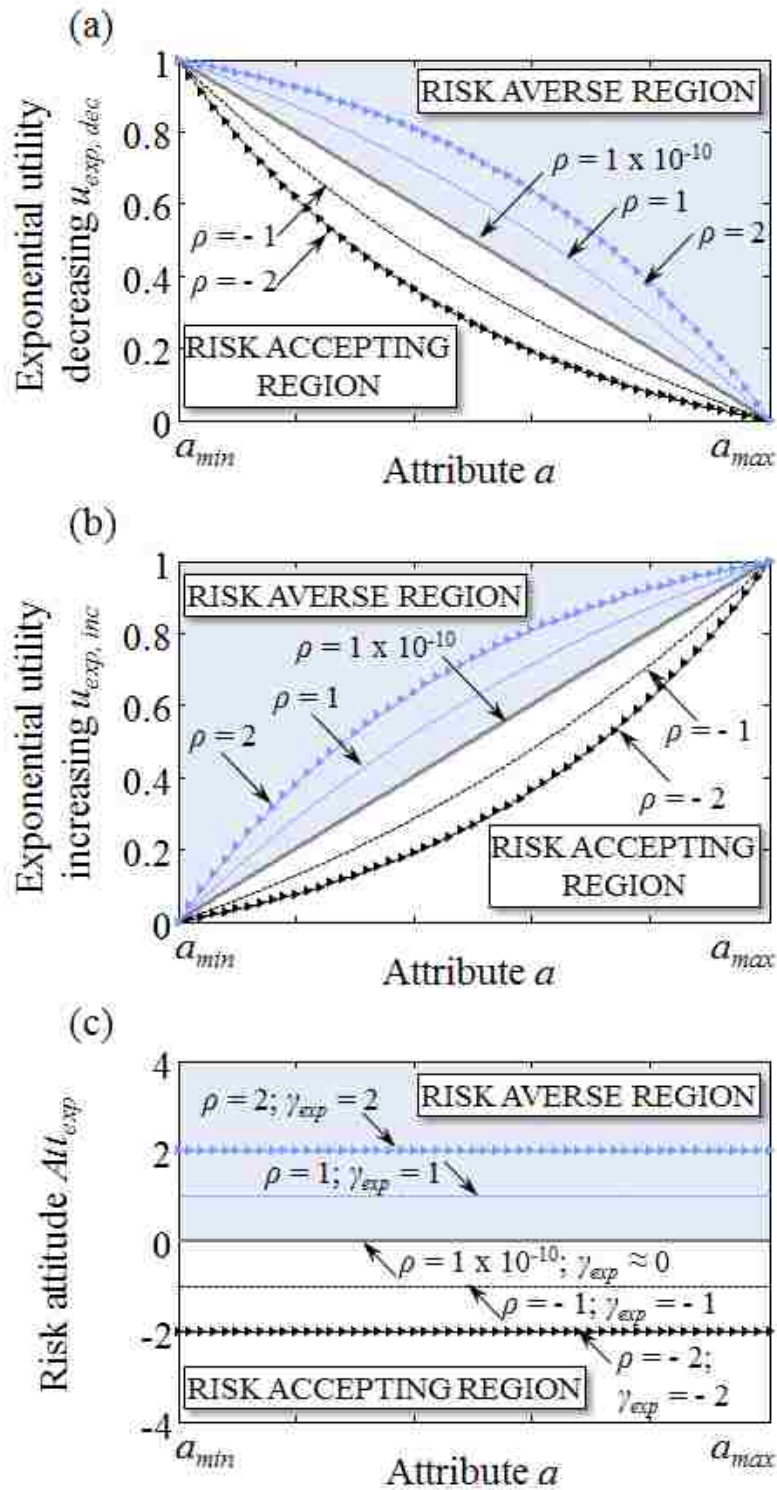


Figure 5.4. (a) Exponential utility decreasing, (b) exponential utility increasing, and (c) risk attitude as functions of attribute  $a$  for different values of  $\rho$  and  $\gamma_{exp}$ .

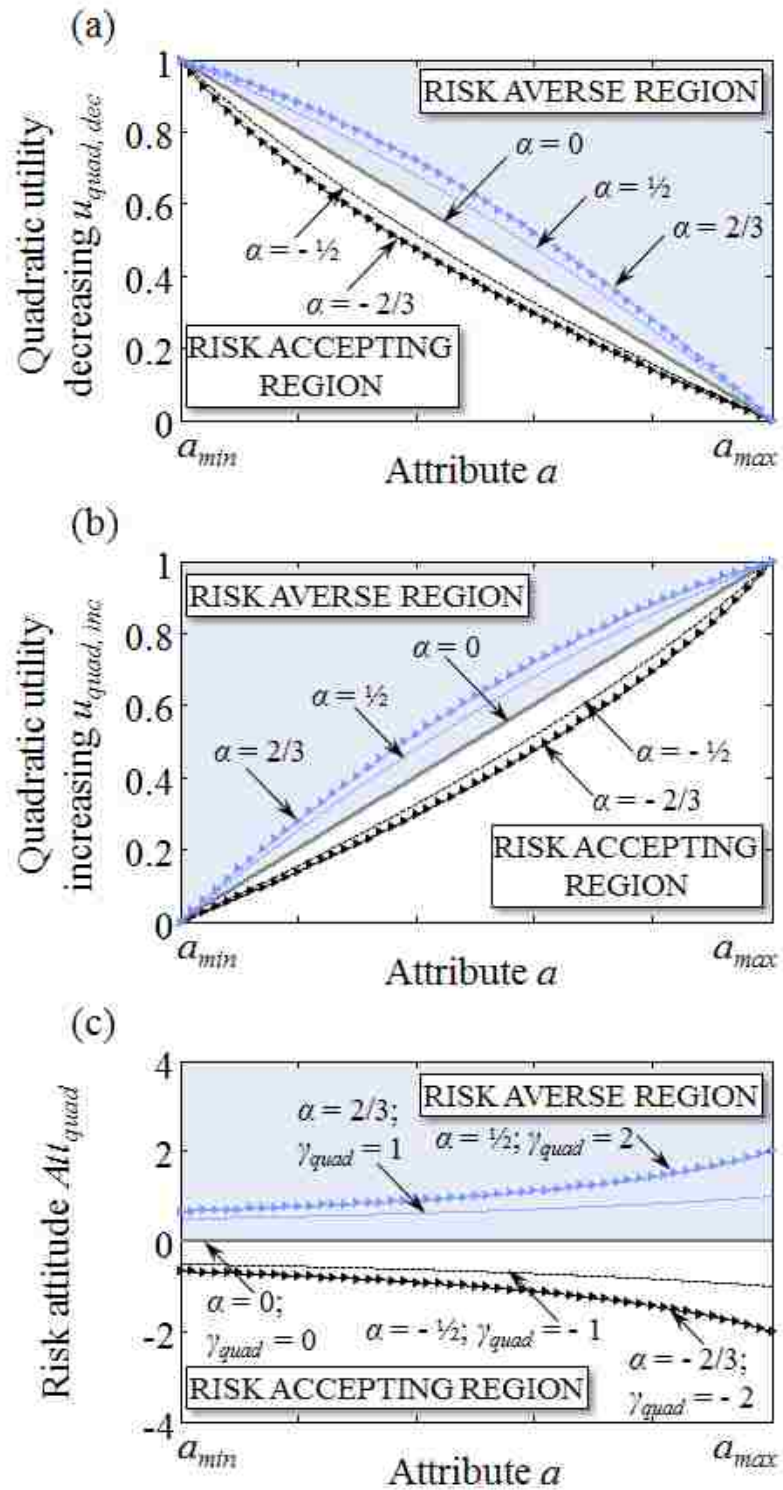


Figure 5.5. (a) Quadratic utility decreasing, (b) quadratic utility increasing, and (c) risk attitude as functions of attribute  $a$  for different values of  $\alpha$  and  $\gamma_{quad}$ .

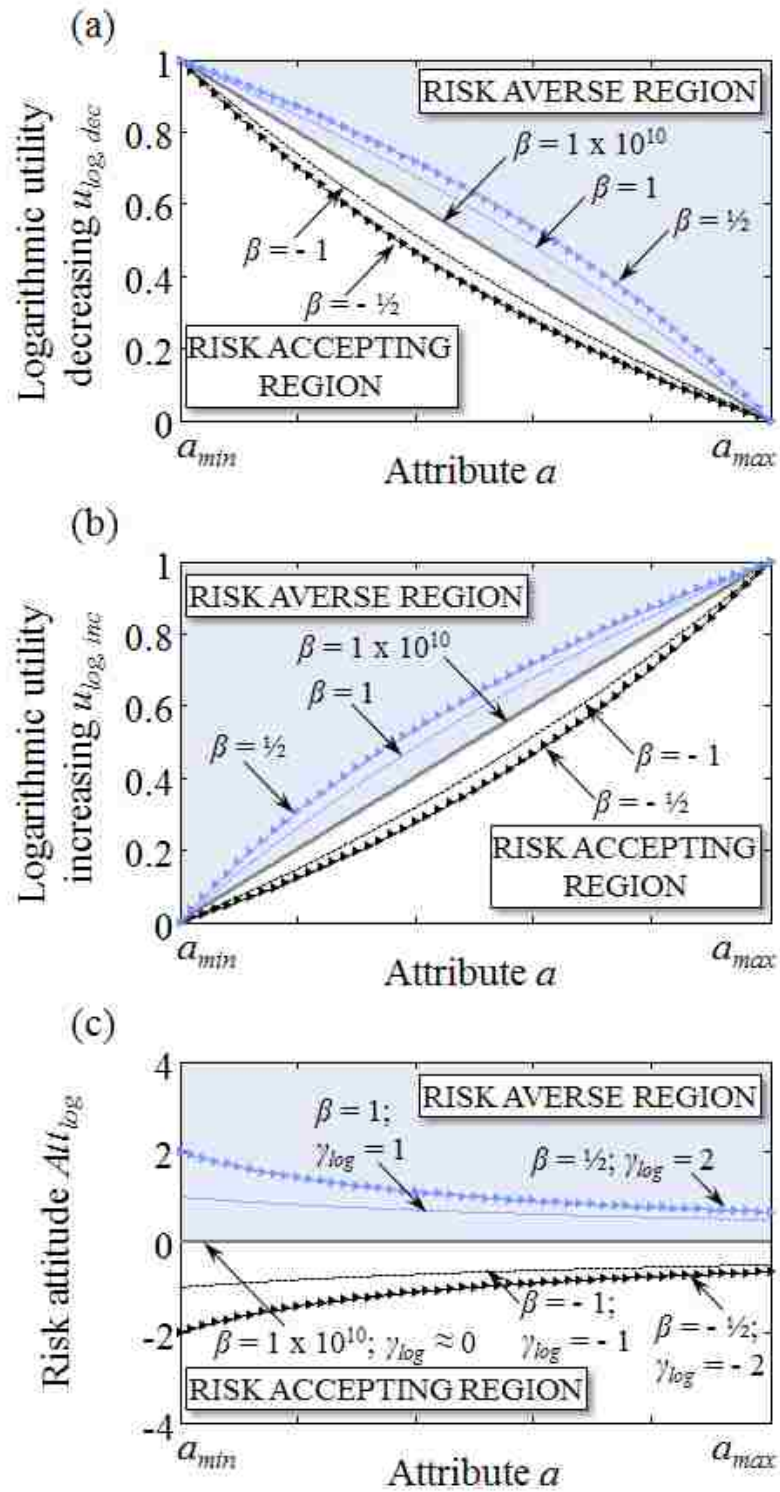


Figure 5.6. Logarithmic utility decreasing, (b) logarithmic utility increasing, and (c) risk attitude as functions of attribute  $a$  for different values of  $\beta$  and  $\gamma_{log}$ .

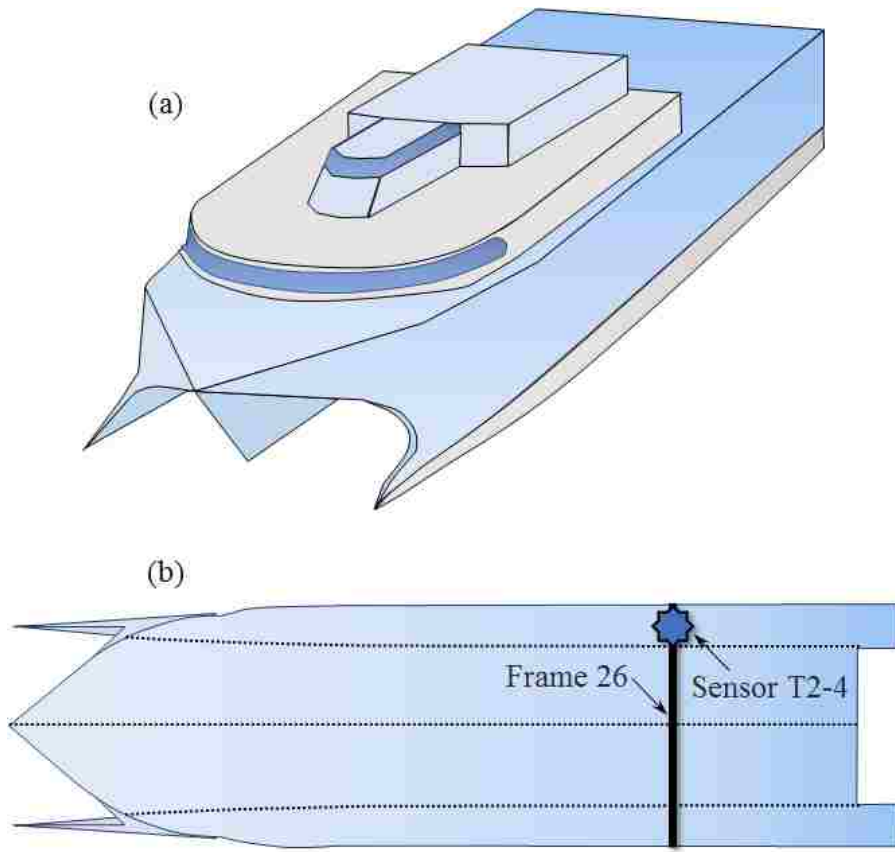


Figure 5.7. (a) HSV-2 swift and (b) plan view detailing the location of an example sensor, T2-4 on frame 26 (adapted from Soliman *et al.* 2015).

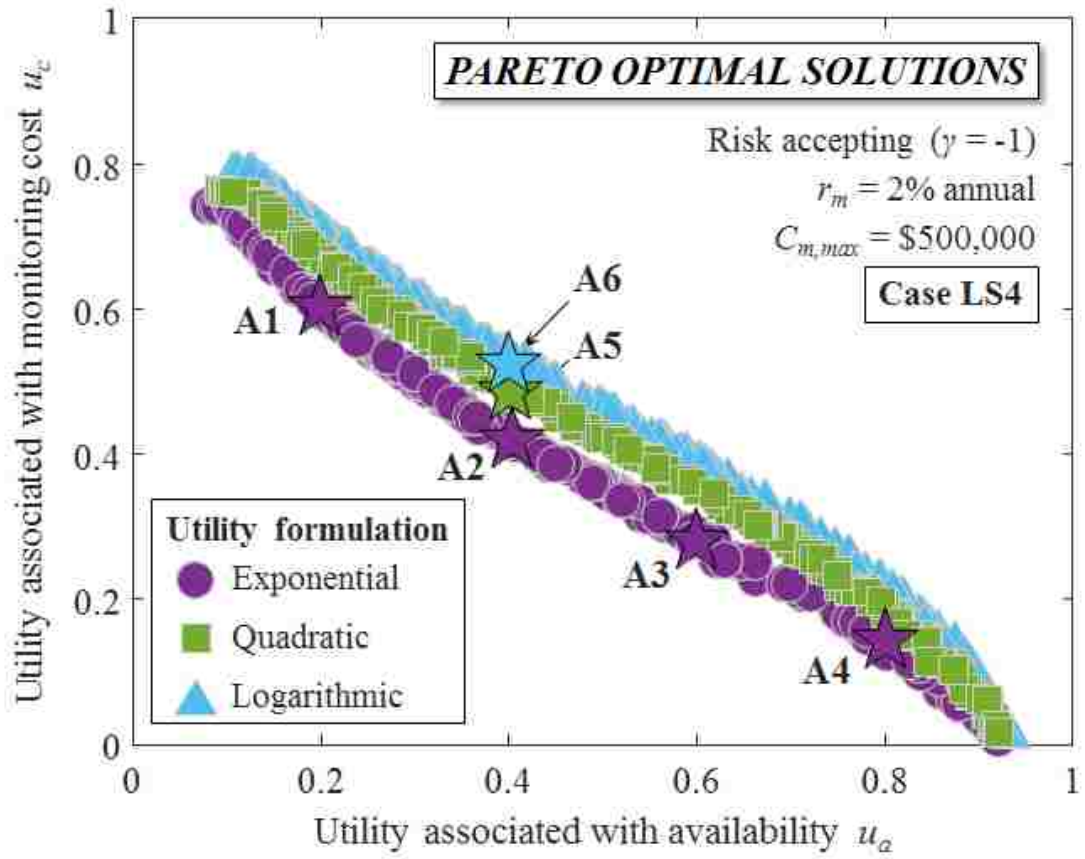


Figure 5.8. Pareto optimal solutions considering uniform monitoring time intervals, a risk accepting attitude, and three utility formulations.

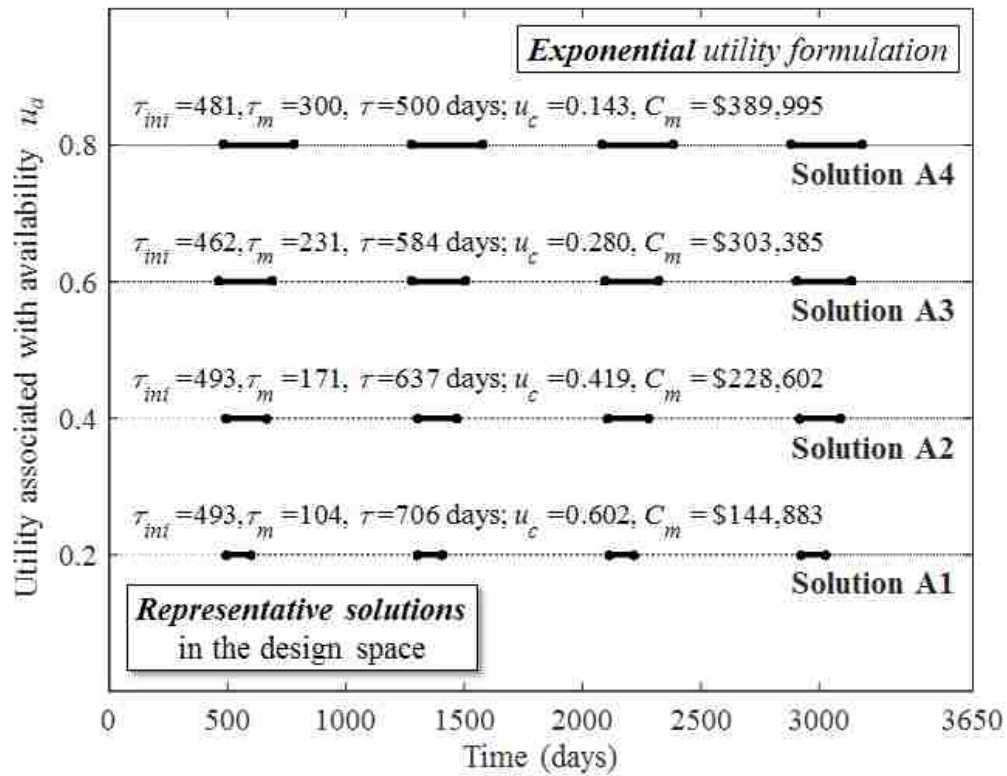


Figure 5.9. Uniform monitoring time interval SHM plans corresponding to four representative solutions on the Pareto front associated with the exponential utility formulation shown in Figure 5.8.

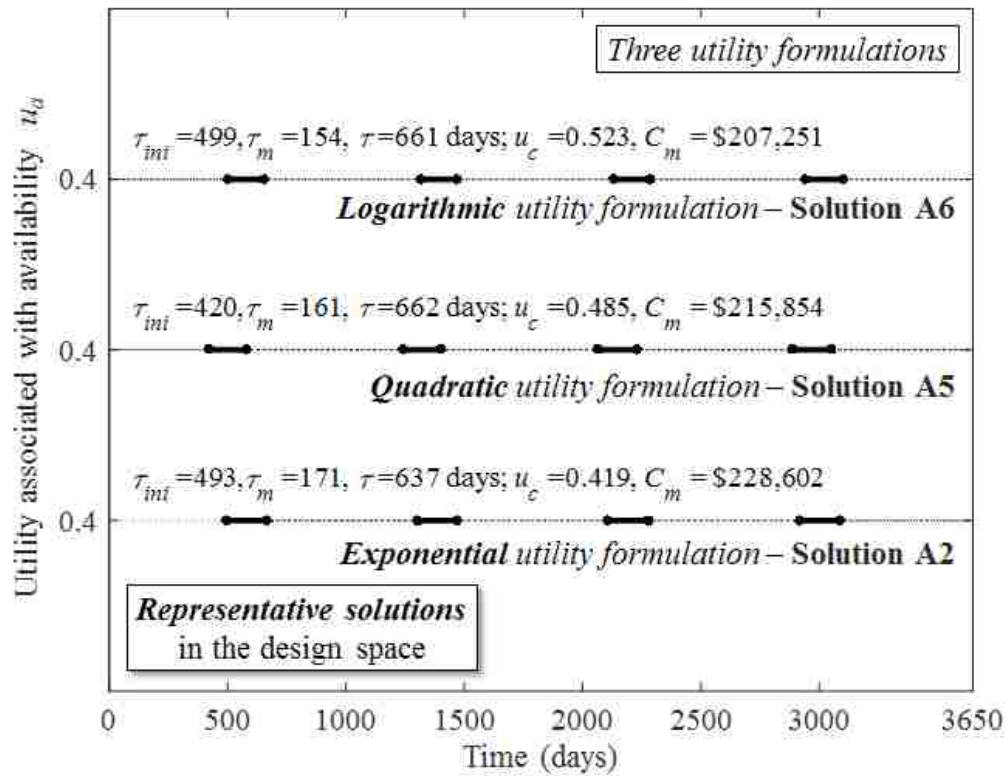


Figure 5.10. Uniform monitoring time interval SHM plans corresponding to three representative solutions associated with  $u_a = 0.4$  on the Pareto fronts in Figure 5.8.

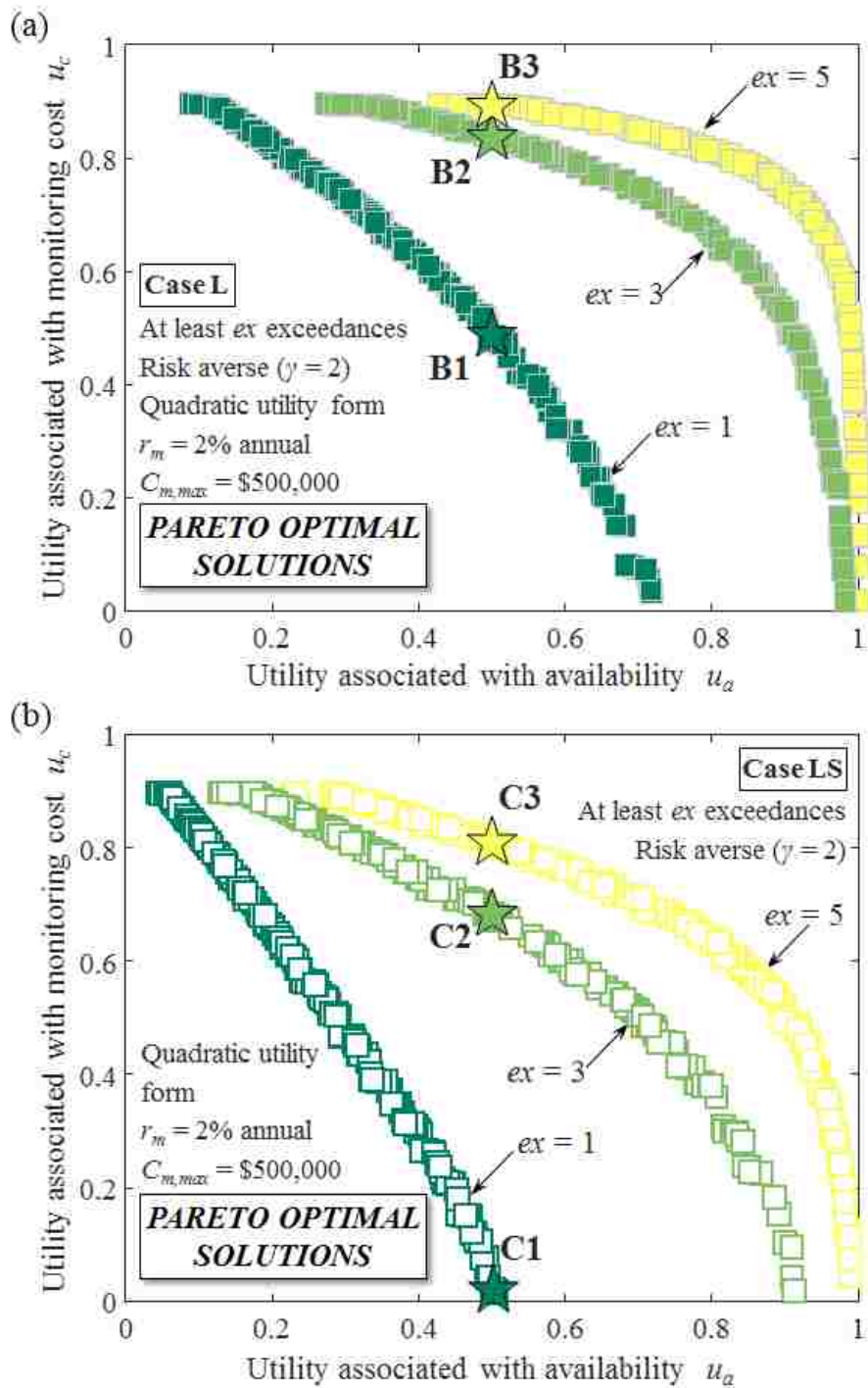


Figure 5.11. Pareto optimal solutions considering uniform monitoring time intervals, a risk averse attitude, and different number of exceedances (i.e.,  $ex = 1$ ,  $ex = 3$ ,  $ex = 5$ ) for residuals associated with cases (a) L and (b) LS.

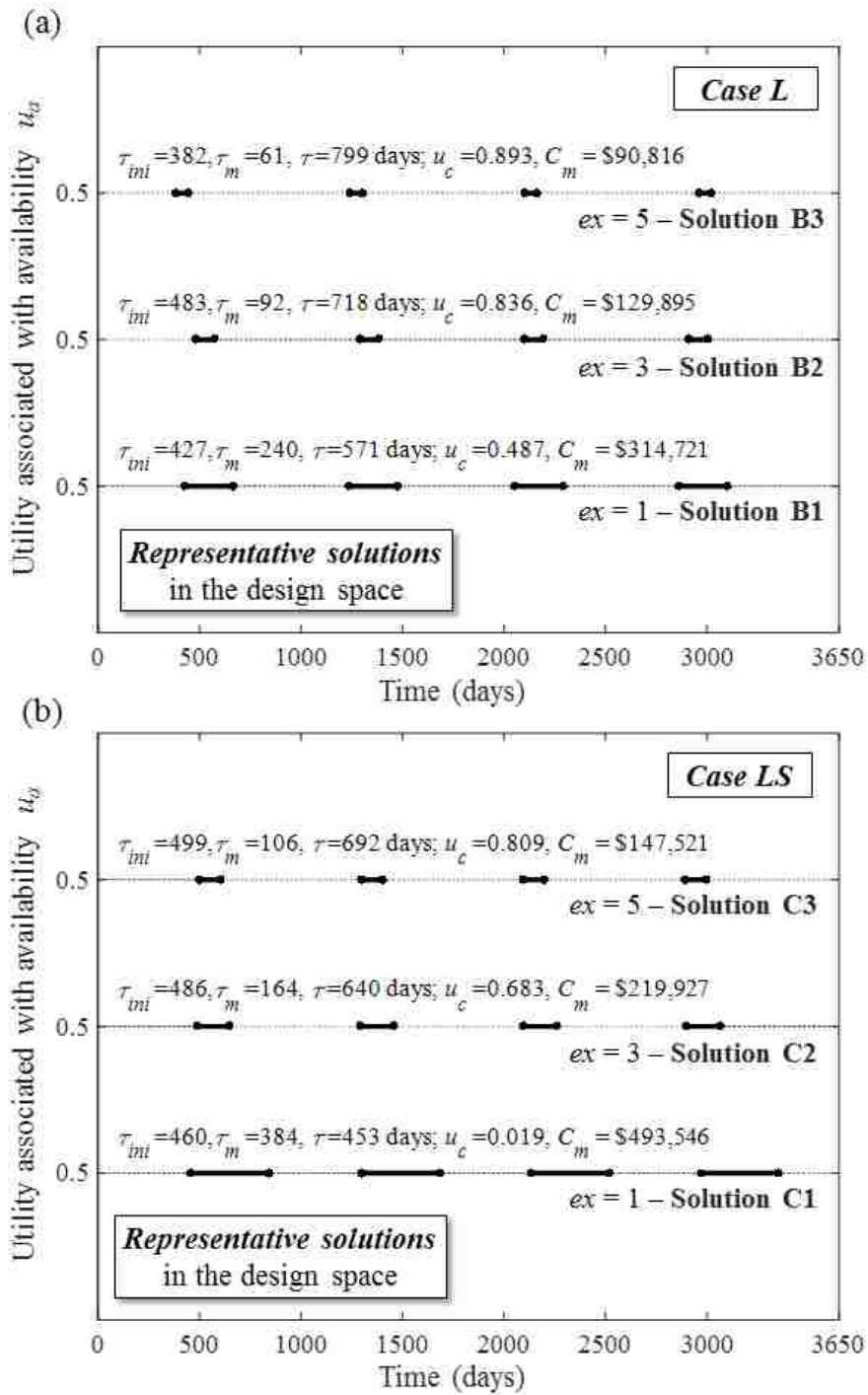


Figure 5.12. Uniform monitoring interval SHM plans corresponding to three representative solutions on the Pareto fronts contained in (a) Figure 5.11a and (b) Figure 5.11b.

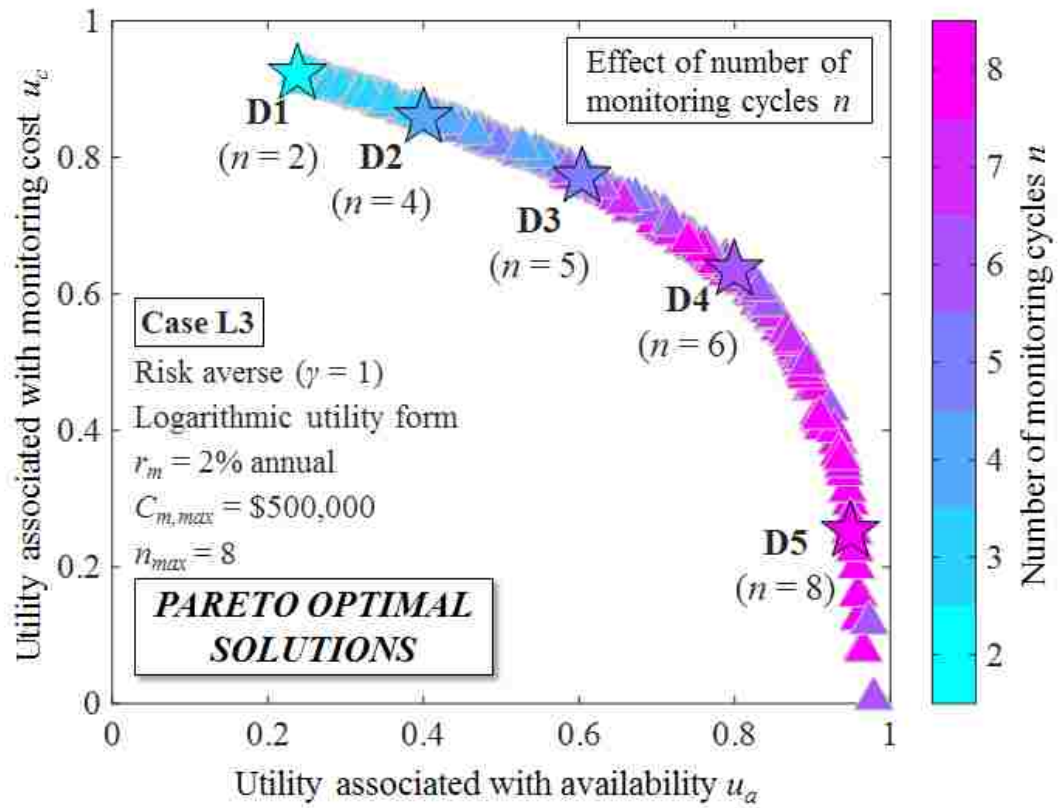


Figure 5.13 Pareto optimal solutions considering uniform monitoring time intervals, a risk averse attitude, and variable number of monitoring cycles.

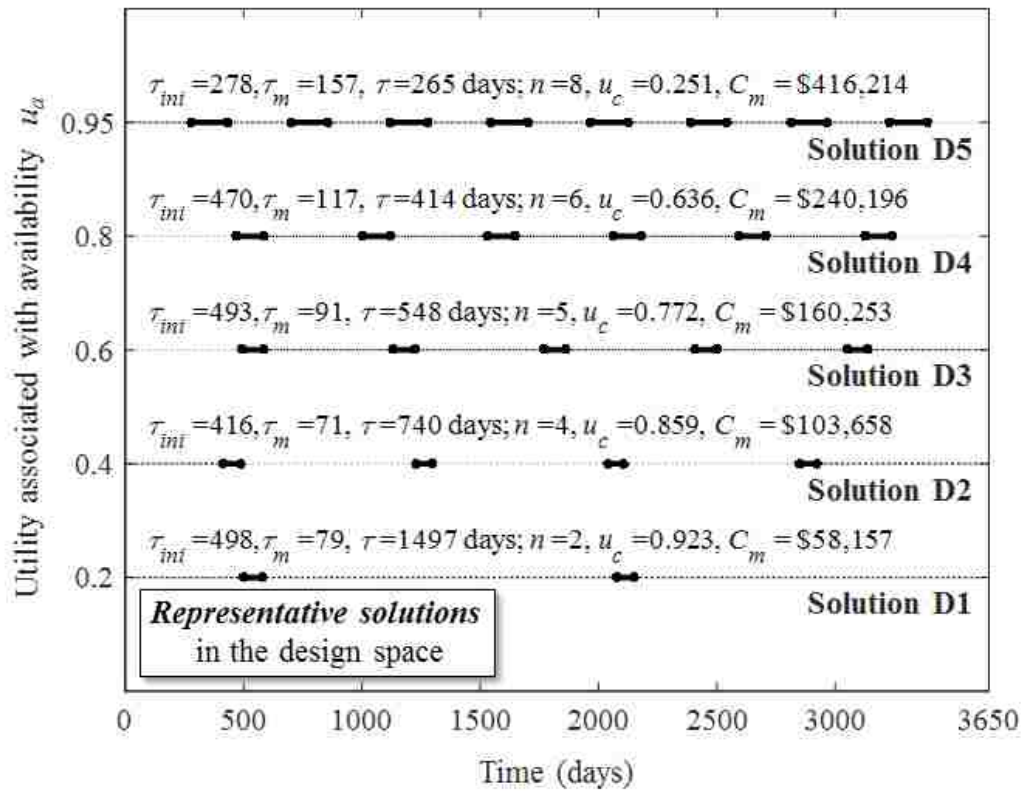


Figure 5.14. Uniform interval SHM plans corresponding to five representative solutions on the Pareto front in Figure 5.13.

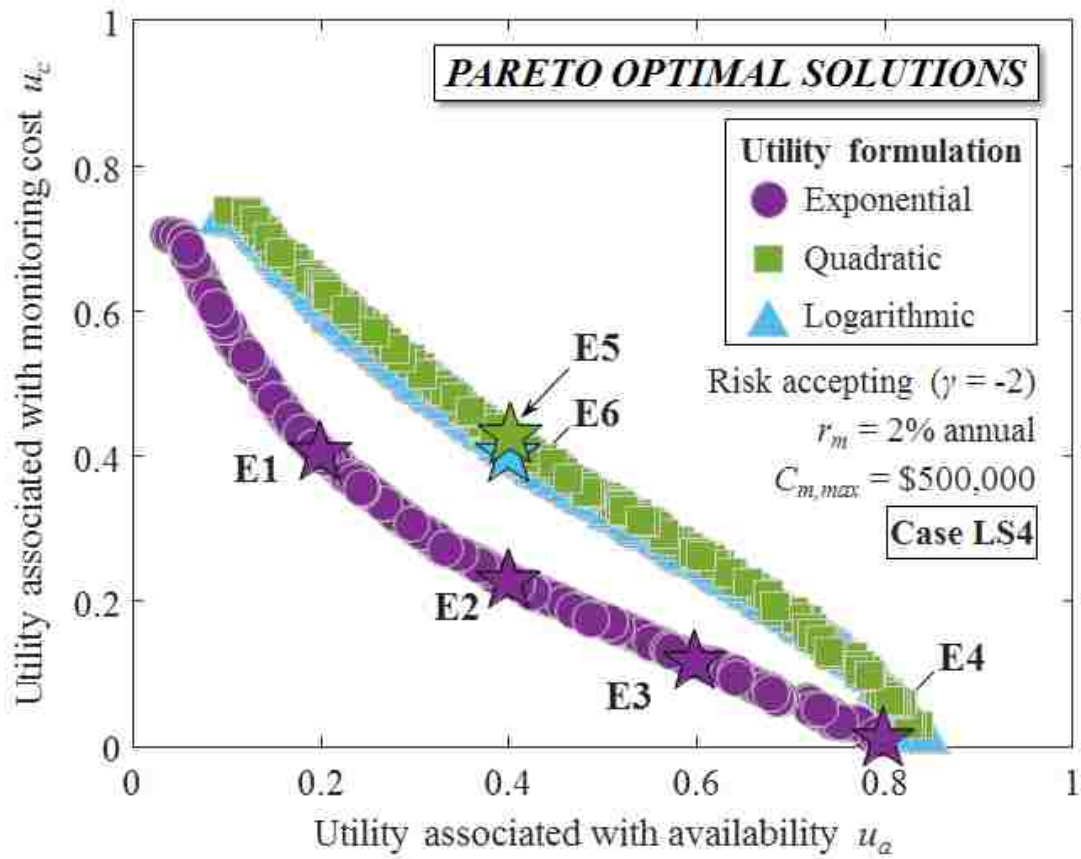


Figure 5.15. Effect of the utility formulation on the Pareto optimal solutions considering non-uniform time monitoring intervals and a risk accepting attitude.

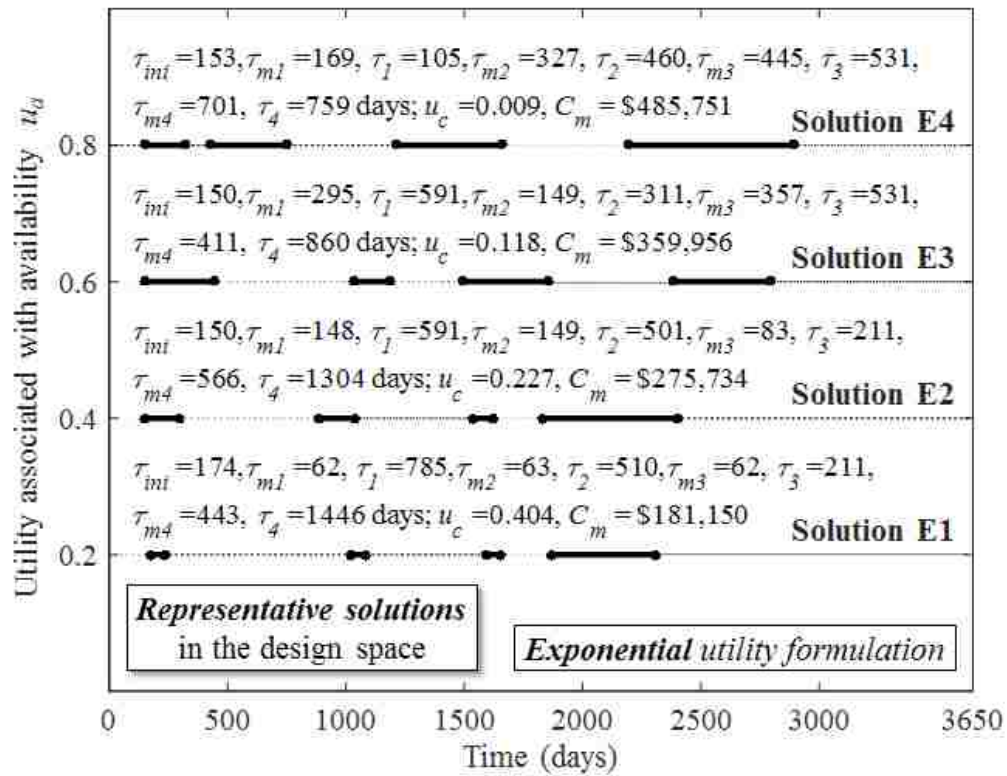


Figure 5.16. Non-uniform interval SHM plans corresponding to four representative solutions on the Pareto front corresponding to the exponential utility formulation shown in Figure 5.15.

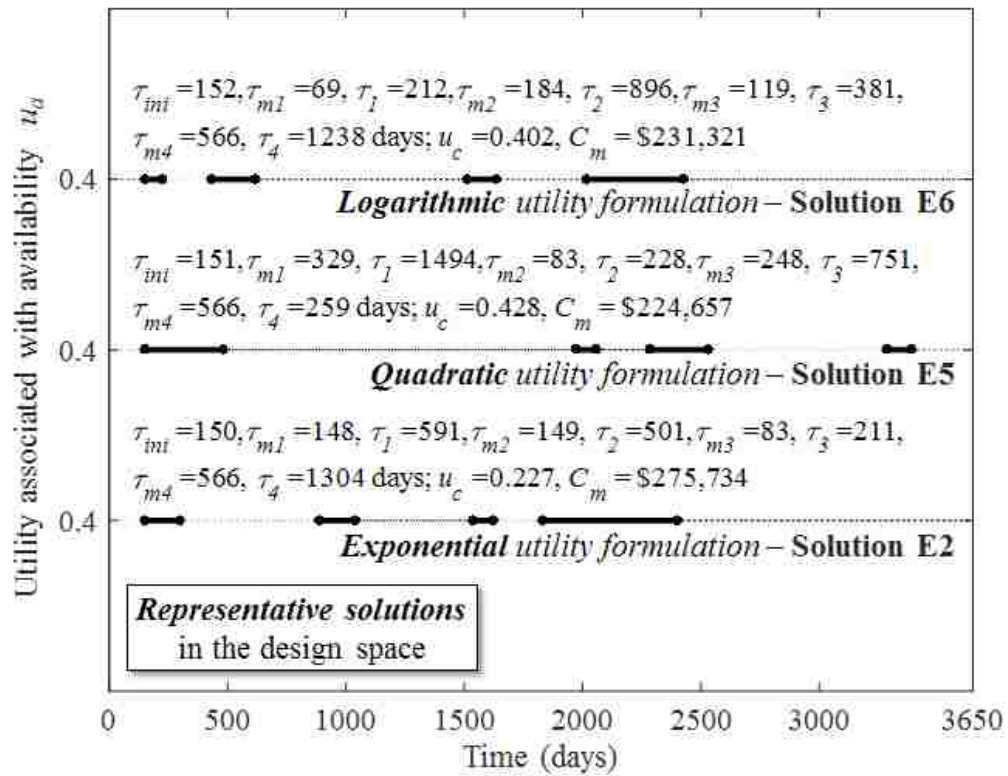


Figure 5.17. Non-uniform interval SHM plans corresponding to three representative solutions associated with  $u_a = 0.4$  on the Pareto fronts in Figure 5.15.

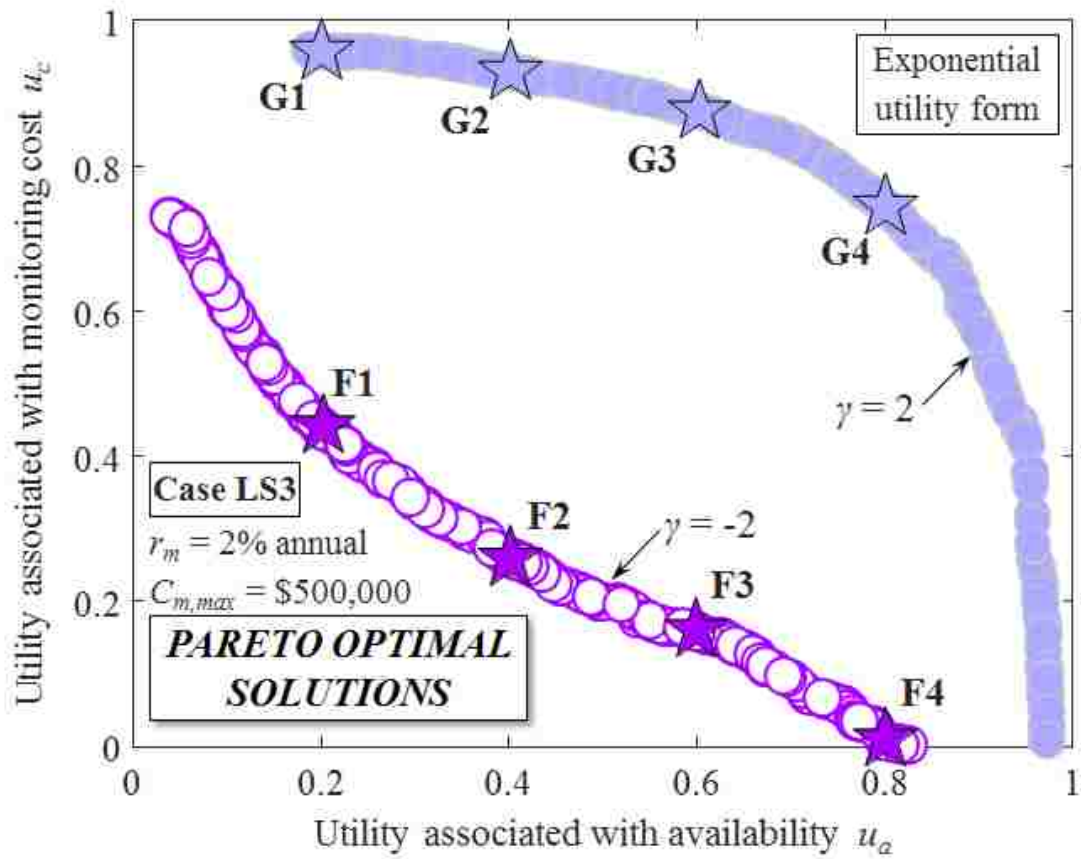


Figure 5.18. Pareto optimal solutions considering non-uniform monitoring intervals, the exponential utility formulation, and two risk attitudes

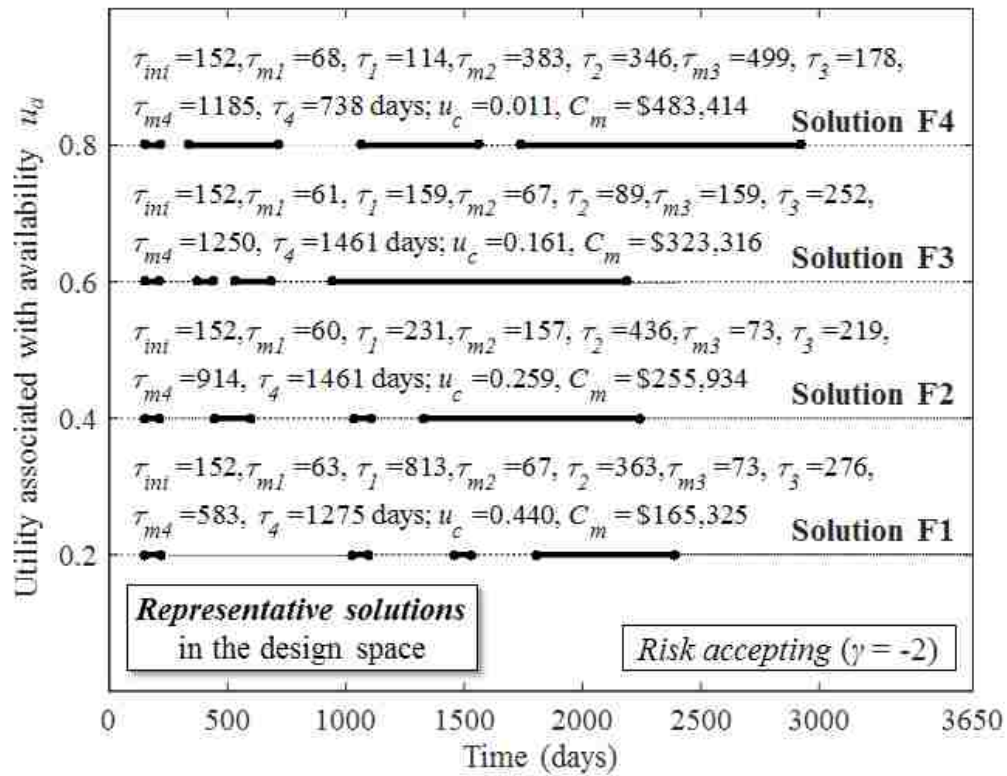


Figure 5.19. Non-uniform interval SHM plans corresponding to four representative solutions on the Pareto front corresponding to a risk accepting attitude shown in Figure 5.18.

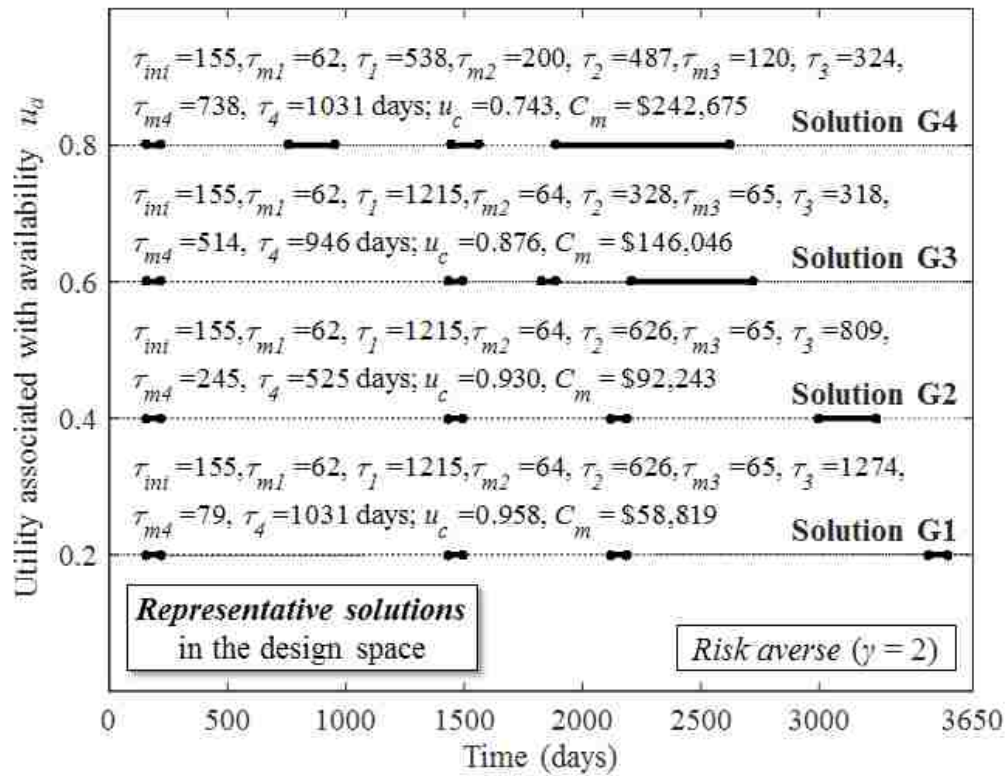


Figure 5.20. Non-uniform interval SHM plans corresponding to four representative solutions on the Pareto front corresponding to a risk averse attitude shown in Figure 5.18.

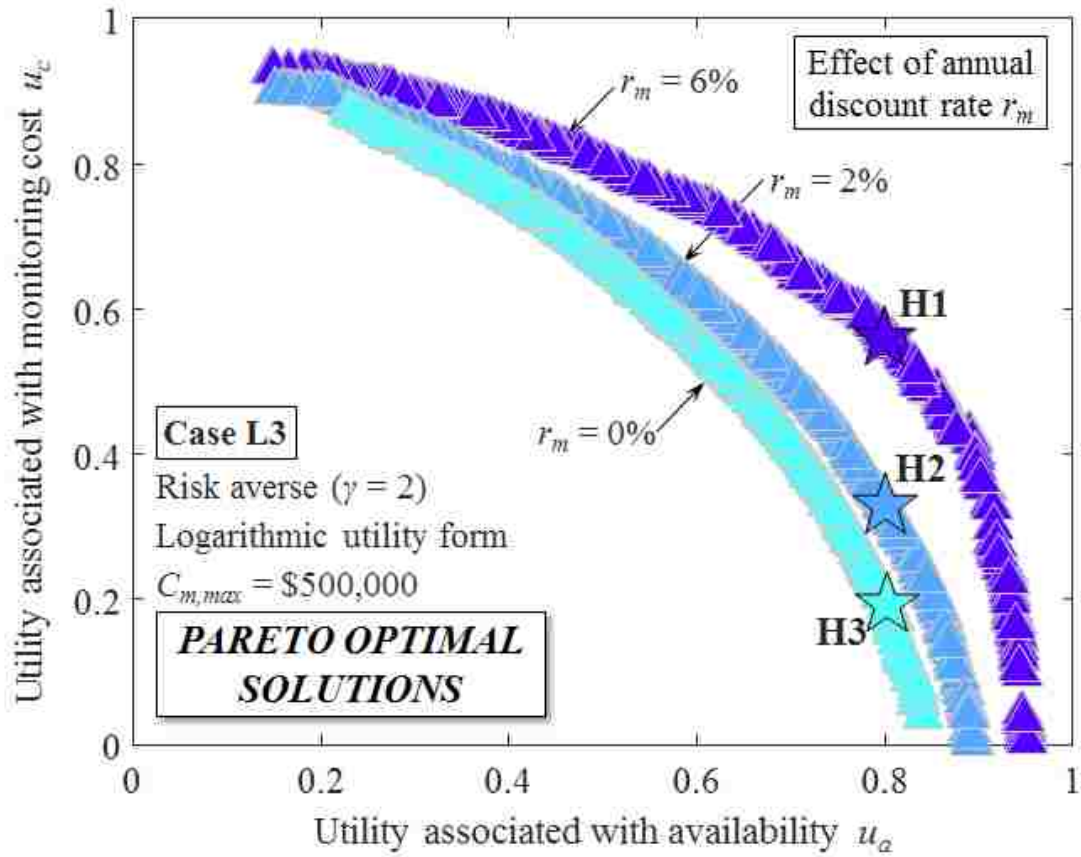


Figure 5.21. Effect of the discount rate of money on the Pareto optimal solutions considering non-uniform monitoring intervals, the logarithmic utility formulation, and a risk averse attitude

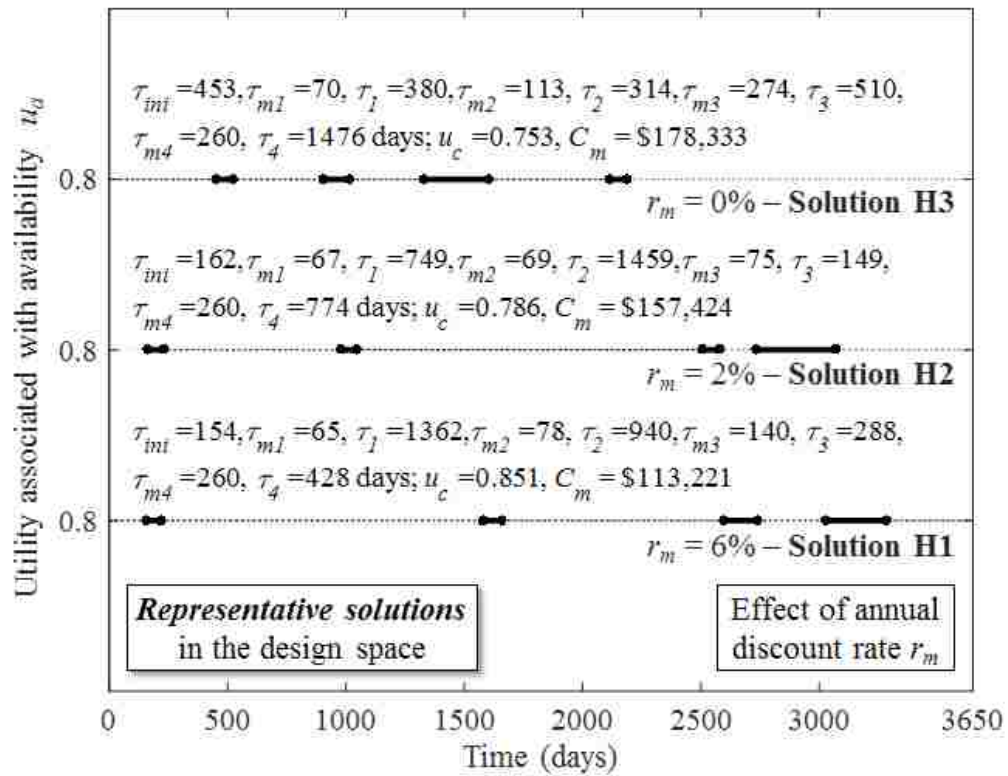


Figure 5.22. Non-uniform interval SHM plans corresponding to three representative solutions associated with  $u_a = 0.8$  on the Pareto fronts in Figure 5.21.

## **CHAPTER 6 SUMMARY, CONCLUSIONS, AND FUTURE WORK**

### **6.1 SUMMARY**

This study presented, from a life-cycle perspective, various aspects pertaining to the maintenance and safety of deteriorating infrastructure systems. A utility and sustainability-based methodology to carry out probabilistic optimization of lifetime intervention actions regarding deteriorating structural systems was presented. The roles of probabilistic performance indicators including reliability, risk, and sustainability, within the context of decision making for infrastructure systems, were highlighted. Furthermore, utility theory was introduced and a multi-attribute utility value representative of sustainability, established in order to effectively combine the effect of economic, social, and environmental risks, was proposed. Multi-objective optimization procedures, with cost and sustainability-based utilities as the objectives to be maximized, were used to determine the best maintenance plans for highway bridges.

Cost- and availability-informed decision making regarding monitoring of ship structures can be carried out considering the approach developed in this study. A bi-objective optimization process was performed that simultaneously maximizes the utilities associated with monitoring cost and availability. Several different utility formulations (e.g., exponential, quadratic, and logarithmic) formulations are considered. Overall, given the risk attitude of the decision maker and a maximum budget, the approach may be used to facilitate cost- and availability-informed choices regarding the monitoring of ships and other structures. Although the proposed

framework was applied to bridge and ship structures herein, it can be employed to facilitate informed decision making for other types of engineering systems if information regarding the structural properties, loading, and relevant performance indicators is provided.

Chapter 1 contained an introduction and overview of the topics covered within this study. Objectives of the study, summary of the approach, contributions, and an outline of the document were also presented.

Chapter 2 discussed fundamental topics related to the life-cycle performance assessment and lifetime management of deteriorating infrastructure systems under uncertainty. Methods regarding the quantification of the life-cycle performance, system reliability, risk, and sustainability of infrastructure systems at the component and systems levels were discussed. Additionally, life-cycle management planning and optimization under a constrained budget and performance constraints were presented through a probabilistic management framework.

Chapter 3 and 4 presented methodologies for determining optimal maintenance strategies for highway bridges, considering utility-based performance and cost as conflicting objectives. Within Chapter 3, utility theory was employed to effectively capture the sustainability performance of highway bridges and the impact of the decision maker's risk attitude. Chapter 4 emphasized the use of lifetime functions to quantify structural performance. The presented decision-support framework in Chapter 4 was used to quantify maintenance cost, failure consequences, and performance benefit in terms of utility. Overall, Chapters 3 and 4 provided optimum lifetime

intervention plans allowing for utility-informed decision making regarding maintenance of highway bridges.

Chapter 5 proposed a decision making framework for optimal SHM planning of ship structures considering availability and utility. Utility theory was employed to incorporate the influence of the decision maker's risk attitude on the relative desirability of SHM plans. Optimization techniques were utilized to simultaneously maximize the utilities associated with monitoring cost and expected average availability in order to determine optimal monitoring strategies under uncertainty.

Chapter 6 presented a general summary, conclusions, and ideas for future research work.

Appendix A summarized approaches for modeling the system reliability of bridge systems. Appendix B and C presented a list of notations for each chapter and a list of acronyms for the entire document.

Overall, Chapters 3, 4 and 5 of this study directly fit into the framework presented within Figure 1.1. Multi-attribute utility theory was used to formulate a utility-based sustainability index which offers a measure of desirability of a given management alternative to the decision maker. The computational framework developed in this study incorporated utility theory, which provides the basis to quantify, combine, and consistently compare the relative values of different alternatives while taking into account the decision maker's attitude. Overall, a generalized framework for probabilistic optimal decision making and life-cycle

management considering risk, sustainability, and utility was developed and applied to bridges and ships.

## **6.2 CONCLUSIONS**

The following conclusions are drawn from the optimal, utility-based, lifetime management of bridges:

- It is crucial to consider a variety of risks that plague civil and marine infrastructure systems when quantifying their lifetime performance. By taking into account a wide variety of risks, the decision maker can ensure that the maintenance plans resulting from the optimization were calculated in a robust and comprehensive manner.
- All three aspects of sustainability (i.e., economic, social, and environmental) are crucial to the performance assessment of highway bridges. Multi-attribute utility theory allows for the quantification of a structure's sustainability performance considering weighting factors that define the relative contribution of each aspect of sustainability.
- Employing lifetime functions within risk and life-cycle optimization under uncertainty assessment provides mathematical flexibility due to their closed-form expression of the distribution of time-to-failure.
- Optimum maintenance plans for highway bridges can be obtained by employing a multi-objective optimization approach that results in a set of Pareto optimal solutions. Ultimately, a decision maker is able to make informed decisions based on their particular preferences and the decision

support system provided by the Pareto set of optimal solutions. The risk attitude of the decision maker has a large impact on the optimal solutions resulting from the proposed decision support system.

- System modeling greatly influences the optimum maintenance plans. Depending upon how system failure is modeled, the optimum time-variant utilities can vary significantly.
- The way system failure probability is calculated, annual or cumulative-time, influences the final Pareto solutions.
- The maximum number of essential maintenance actions considered throughout a bridge's lifetime has great effects on the final Pareto optimal solutions.
- The weighting factors considered within the multi-attribute utility assessment of sustainability have a significant impact on the resulting Pareto optimal solutions. Thus, it is crucial to determine appropriate values for them.

Based on the decision support tool developed to optimize the SHM scheduling on ship structures, the following conclusions are drawn:

- SHM plans are determined using a multi-criteria optimization algorithm that balances two objectives: the utilities associated with monitoring cost and expected average availability. Ultimately, a decision maker is able to make informed decisions based on the decision support system provided by the Pareto set of optimal solutions.
- The risk attitude of the decision maker can have great influence on the optimal solutions resulting from the proposed decision support system. In general, risk

averse decision makers, will assign larger utility values to the same alternative as compared to risk accepting decision makers.

- The number of monitoring cycles considered throughout the time horizon investigated has an important effect on the Pareto solutions.

### **6.3 FUTURE WORK**

- The performance assessment and prediction processes are the building blocks of a life-cycle management framework. The prediction process greatly depends on the accuracy of the performance prediction model and the descriptors of its probabilistic parameters. However, in some cases, accurate information regarding some model parameters does not exist; therefore, future efforts to quantify these parameters are imperative. For instance, the equations developed for the risk attributes calculated in section 3.3.3 of this study may be improved to more accurately depict actual environmental and societal consequences of structural failure.
- The effect of different types of maintenance on the sustainability performance of bridges needs to be further developed. The examples provided in Chapters 3 and 4 consider crude essential maintenance actions of replacing entire elements of a bridge superstructure. Therefore, further research is needed to establish the relationship among various maintenance types including essential and preventive maintenance.
- An approach that incorporates multi-attribute utility theory provides a framework which can quantify, combine, and consistently compare the relative

values of different alternatives while taking into account the decision maker's attitude. However, sensitivity studies aimed to quantify the weighing factors which represent the effect of the decision maker's particular preference to which aspect of sustainability is most important are still needed. The weighing factors considered within the multi-attribute utility assessment of sustainability have a significant impact on the resulting Pareto optimal solutions. Thus, it is crucial to determine appropriate values for them. Although the four-objective optimization process that was presented in Chapter 3 acts as a preliminary investigation in determining the sensitivity of optimum solutions to changes in the values of the weighing factors, further research is needed to properly select appropriate weighing factors within the multi-attribute utility assessment process.

- Employing lifetime functions within risk and life-cycle optimization under uncertainty assessment provides mathematical flexibility due to their closed-form expression of the distribution of time-to-failure. Further study on implementing lifetime functions as probabilistic performance indicators for structural components and systems needs to be conducted. There is considerable computational advantage to using this closed formulation, time-dependent expressions.
- There is a great need for more research regarding establishing appropriate utility functions to utilize within decision support tools for infrastructure systems. Although it is outside the scope of this study, an entire area of research could be dedicated to developing appropriate utility functions for

lifetime management of civil infrastructure. Overall, it is necessary to derive accurate predictions regarding how decision makers invest their money in the face of risk.

- The number of monitoring cycles considered throughout the time horizon investigated has an important effect on the Pareto solutions within illustrative example presented in Chapter 5. Both the cumulative monitoring cost and overall effectiveness of the SHM data, represented by expected average availability are sensitive to changes in the proposed number of cycles and in the discount rate of money. The effect of the time horizon considered on the Pareto solutions also has to be investigated. In general, further research and promotion of an integrated utility-based approach as the rational basis for optimal structural health monitoring planning of ship structures considering uncertainties is required.

## REFERENCES

- Adams, W.M. (2006). *The future of sustainability: re-thinking environment and development in the twenty-first century*. Report of the IUCN Renowned Thinkers Meeting, 29–31.
- Adey, B., Hajdin, R. and Bruhwiler, E. (2003). Supply and demand system approach to development of bridge management strategies. *Journal of Infrastructure Systems*, 9(3), 117.
- Akgül, F. (2002). *Lifetime system reliability prediction for multiple structure types in a bridge network*. Ph.D. Thesis, Dept. of Civil, Environmental, and Architectural Engineering, University of Colorado, Boulder, CO.
- Albrecht, P. and Naeemi, A. (1984). *Performance of weathering steel in bridges*, NCHRP Report 272, Washington, DC.
- Amari, S.V., Pham, H., and Misra, R.B. (2012). Reliability characteristics of k-out-of-n warm standby systems. *IEEE Transactions on Reliability*, 61(4), 1007-1018.
- Ang, A. H-S. (2011). Life-cycle considerations in risk-informed decisions for design of civil infrastructures. *Structure and Infrastructure Engineering*, 7(1-2), 3-9.
- Ang, A. H-S. and De Leon, D. (2005). Modeling and analysis of uncertainties for risk-informed decisions in infrastructures engineering. *Structure and Infrastructure Engineering*, 1(1), 19-21.
- Ang, A. H-S. and Tang, W.H. (1984). *Probability concepts in engineering planning and design: decision, risk and reliability*. Vol. II. New York: Wiley.
- Ang, A. H-S. and Tang, W.H. (2007). *Probability concepts in engineering: emphasis on applications to civil and environmental engineering*, 2nd edition, Wiley, New York.
- Arrow, K.J. (1965). *Aspects of the theory of risk-bearing*. Helsinki: Yrjö Jahnssonin Säätiö.
- Arunraj, N. S. and Maiti, J. (2007). Risk-based maintenance—Techniques and applications. *Journal of Hazardous Materials*, 142(3), 653-661.
- ASCE. (2013). *2013 Report card for America's infrastructure*. American Society of Civil Engineers, Reston, VA.  
<http://www.infrastructurereportcard.org/a/documents/2013-Report-Card.pdf>.
- ASCE. (2016). ASCE Grand Challenge. *American Society of Civil Engineers*.  
<http://www.asce.org/grand-challenge/>
- ASCE. (2017). *2017 Report card for America's infrastructure*. American Society of Civil Engineers, Reston, VA. <http://www.infrastructurereportcard.org/>

- Augusti, G., Ciampoli, M., and Frangopol, D.M. (1998). Optimal planning of retrofitting interventions on bridges in a highway network. *Engineering Structures*, 20(11), 933-939.
- Barone, G. and Frangopol, D.M. (2013). Hazard-based optimum lifetime inspection and repair planning for deteriorating structures. *Journal of Structural Engineering*, 139(12), 1-12.
- Barone, G. and Frangopol, D.M. (2014a). Life-cycle maintenance of deteriorating structures by multi-objective optimization involving reliability, risk, availability, hazard and cost. *Structural Safety*, 48, 40-50.
- Barone, G. and Frangopol, D.M. (2014b). Reliability, risk and lifetime distributions as performance indicators for life-cycle maintenance of deteriorating structures. *Reliability Engineering & System Safety*, 123, 21-37.
- Barone, G., Frangopol, D.M., and Soliman, M. (2014). Optimization of life-cycle maintenance of deteriorating bridges with respect to expected annual system failure rate and expected cumulative cost. *Journal of Structural Engineering*, 140(2), 1-13.
- Basöz, N. and Mander, J. (1999). Enhancement of the highway transportation lifeline module in HAZUS, *National Institute of Building Sciences (NIBS)*, Washington, D.C.
- Biondini, F., Camnasio, E., and Palermo, A. (2014). Lifetime seismic performance of concrete bridges exposed to corrosion. *Structure and Infrastructure Engineering*, 10, 880-900.
- Biondini, F., Frangopol, D.M. and Malerba, P.G. (2008). Uncertainty effects on lifetime structural performance of cable stayed bridges. *Probabilistic Engineering Mechanics*, 23(4), 509-522.
- Biswas, A., Sarkar, J., and Sarkar, S. (2003). Availability of a periodically inspected system, maintained under an imperfect-repair policy. *IEEE Transactions on Reliability*, 52(3), 311-318.
- Bocchini, P., and Frangopol, D.M. (2013). Connectivity-based optimal scheduling for maintenance of bridge networks. *Journal of Engineering Mechanics*, 139, 170-769.
- Brady T.F. (2004a). *HSV-2 swift instrumentation and technical trials plan*. NSWCCD-65-TR-2004/18, 1 July 2004. West Bethesda, MD: Naval Surface Warfare Center, Carderock Division.
- Brady T.F. (2004b). *Global structural response measurement of SWIFT (HSV-2) from JLOTS and blue game rough water trials*. NSWCCD-65-TR-2004/33, 1 December 2004. West Bethesda, MD: Naval Surface Warfare Center, Carderock Division.
- Cesare, M., Santamarina, J. C., Turkstra, C. J., and Vanmarcke, E. (1993). Risk-based bridge management. *Journal of Transportation Engineering*, 119(5), 742-750.

- Chang, S.E. and Shinozuka, M. (1996). Life-cycle cost analysis with natural hazard risk. *Journal of Infrastructure Systems*, 2(3), 118-126.
- CIB (2001). *Risk assessment and risk communication in civil engineering*. TG 32 Report 259, Rotterdam: Council for Research and Innovation in Building and Construction.
- Coello Coello, C.A. (2000). Handling preferences in evolutionary multiobjective optimization: a survey. *Proceedings of the Congress on Evolutionary Computation*, July 2000, 30–37.
- Colorado State Patrol. (2011). *Colorado driver handbook*, Denver, CO.
- Cui, L., Kuo, W., Loh, H.T., and Xie, M. (2004). Optimal allocation of minimal & perfect repairs under resource constraints. *IEEE Transactions on Reliability*, 53(2), 193-199.
- Czarnecki, A.A. and Nowak, A.S. (2007). Reliability-based evaluation of steel girder bridges. *Bridge Engineering, Proceedings of the Institution of Civil Engineers*, 160, Issue BE1, 9–15.
- Dabous, S.A. and Alkass, S. (2008). Decision support method for multi-criteria selection of bridge rehabilitation strategy. *Construction Management and Economics*, 26(8), 883-893.
- Davis, L. (Ed.). (1991). *Handbook of genetic algorithms*. New York: Van Nostrand Reinhold.
- Deb, K. (2001). *Multi-Objective Optimization Using Evolutionary Algorithms*. John Wiley and Sons, UK.
- Deb, K., Pratap, A., Agrawal, S., and Meyarivan, T. (2002). A fast and elitist multiobjective genetic algorithm: NSGA-II. *Transaction on Evolutionary Computation*, 6(2), 182–97.
- Decò A. and Frangopol, D.M. (2011). Risk assessment of highway bridges under multiple hazards. *Journal of Risk Research*, 14(9), 1057-1089.
- Decò A. and Frangopol, D.M. (2012). Lifetime risk assessment of bridges affected by multiple hazards. *The Sixth International Conference on Bridge Maintenance, Safety and Management*, Stresa, Lake Maggiore, Italy. 2922-2929.
- Decò A. and Frangopol, D.M. (2013). Life-cycle risk assessment of spatially distributed aging bridges under seismic and traffic hazards. *Earthquake Spectra*, 29(1), 127-153.
- Decò A. and Frangopol, D.M. (2015). Real-time risk of ship structures integrating structural health monitoring data: Application to multi-objective optimal ship routing. *Ocean Engineering*, 96, 312-329
- Dequidt, T. (2012). *Life cycle assessment of a Norwegian bridge*. M.S. Thesis, Department of Civil and Transport Engineering, Norwegian University of Science and Technology, Trondheim, Norway.

- Ditlevsen, O. and Bjerager, P. (1986). Methods of structural systems reliability. *Structural Safety*, 3(3), 195-229
- Dong Y., Frangopol D.M., and Sabatino, S. (2014a). Risk-informed decision making for bridges under mainshock and aftershocks seismic sequence, *The 7th International Conference on Bridge Maintenance, Safety and Management (IABMAS 2014)*, Shanghai, China, July 7-11, 2014.
- Dong Y., Frangopol D.M., and Sabatino, S. (2014b). Risk-informed decision making for disaster recovery incorporating sustainability and resilience, *The 3rd International Conference on Urban Disaster Reduction (3ICUDR 2014)*, Boulder, Colorado, September 28-October 1, 2014.
- Dong Y., Frangopol D.M., and Sabatino, S. (2014c). Sustainability-based pre-earthquake probabilistic retrofit optimization of highway bridges considering risk attitudes, *The 7th International Conference on Bridge Maintenance, Safety and Management (IABMAS 2014)*, Shanghai, China, July 7-11, 2014.
- Dong Y., Frangopol D.M., and Sabatino, S. (2014d). Sustainability-based bi-objective optimization for seismic retrofit of bridge networks considering risk attitudes, *The 4th International Conference on Life-Cycle Civil Engineering (IALCCE 2014)*, Tokyo, Japan, November 16-19, 2014.
- Dong Y., Frangopol D.M., and Saydam, D. (2013). Time-variant sustainability assessment of seismically vulnerable bridges subjected to multiple hazards. *Earthquake Engineering and Structural Dynamics*, 42, 1451–1467.
- Dong Y., Frangopol D.M., and Saydam, D. (2014e). Pre-earthquake probabilistic retrofit optimization of bridge networks based on sustainability. *Journal of Bridge Engineering*, 19(6), 1-10.
- Dong Y., Frangopol D.M., and Saydam, D. (2014f). Sustainability of highway bridge networks under seismic hazard. *Journal of Earthquake Engineering*, 18, 41–66.
- Dong, Y., Frangopol, D.M., and Sabatino, S. (2015). Optimizing bridge network retrofit planning based on cost-benefit evaluation and multi-attribute utility associated with sustainability. *Earthquake Spectra*, 31(4), 2255-2280.
- Dong, Y., Frangopol, D.M., and Sabatino, S. (2016). A decision support system for mission-based ship routing considering multiple performance criteria. *Reliability Engineering & System Safety*, 150, 190-201.
- Elkington, J. (2004). *Enter the Triple Bottom Line*. Adrian Henriques and Julie Richardson (Eds.), The triple bottom line: does it all add up? Earthscan, Sterling, VA.
- Ellingwood, B.R. (2001). Acceptable risk bases for design of structures. *Progress in Structural Engineering and Materials*, 3(2), 170-179.

- Ellingwood, B.R. (2005). Risk-informed condition assessment of civil infrastructure: state of practice and research issues. *Structure and Infrastructure Engineering*, 1(1), 7-18.
- Enright, M.P. and Frangopol, D.M. (1999a). Condition prediction of deteriorating concrete bridges. *Journal of Structural Engineering*, 125(10), 1118-1125.
- Enright, M.P. and Frangopol, D.M. (1999b). Reliability-based condition assessment of deteriorating concrete bridges considering load redistribution. *Structural Safety*, 21, 159-195.
- Enright, M.P. and Frangopol, D.M. (2000). RELTSYS: A computer program for life prediction of deteriorating system. *Structural Engineering and Mechanics*, 9(6), 557-568
- Estes, A.C. (1997). *A system reliability approach to the lifetime optimization of inspection and repair of highway bridges*. Ph.D. Thesis, Dept. of Civil, Environmental, and Architectural Engineering, University of Colorado, Boulder, CO.
- Estes, A.C. and Frangopol, D.M. (1998). RELSYS: A computer program for structural system reliability. *Structural Engineering and Mechanics*, 6(8), 901-999.
- Estes, A.C. and Frangopol, D.M. (1999). Repair optimization of highway bridges using system reliability approach. *Journal of Structural Engineering*, 125(7), 766-775.
- Estes, A.C. and Frangopol, D.M. (2001). Bridge lifetime system reliability under multiple limit states. *Journal of Bridge Engineering*, 6(6), 523-528.
- Estes, A.C. and Frangopol, D.M. (2005). *Life-cycle evaluation and condition assessment of structures*. Chapter 36 in *Structural Engineering Handbook*, 2nd Edition, W-F. Chen and E. M. Lui (Eds.), CRC Press, 36-51.
- Estes, A.C., Frangopol, D.M., and Foltz, S.D. (2004). Updating reliability of steel miter gates on locks and dams using visual inspection results. *Engineering Structures*, 26, 319-333.
- Fernández, M.G., Seepersad, C.C., Rosen, D.W., Allen, J.K., and Mistree, F. (2005). Decision support in concurrent engineering – the utility-based selection decision support problem. *Concurrent Engineering: Research and Applications*, 13(1), 13-27.
- FHWA. (2013). *National Bridge Inventory (NBI) database*. US Department of Transportation, Federal Highway Administration, Washington, DC. [www.fhwa.dot.gov/bridge/nbi.htm](http://www.fhwa.dot.gov/bridge/nbi.htm). (accessed December 2015).
- Frangopol, D.M. (1997). *Application of life-cycle reliability based criteria to bridge assessment and design*. P.C. Das (ed.), *Safety of Bridges*. Thomas Telford, London, 151-157.

- Frangopol, D.M. (2011). Life-cycle performance, management, and optimization of structural systems under uncertainty: accomplishments and challenges, *Structure and Infrastructure Engineering*, 7(6), 389-413.
- Frangopol, D.M. and Bocchini, P. (2012). Bridge network performance, maintenance and optimisation under uncertainty: accomplishments and challenges. *Structure and Infrastructure Engineering* 8, 341–356.
- Frangopol, D.M. and Curley, J.P. (1987). Effects of damage and redundancy on structural reliability. *Journal of Structural Engineering*, 113(7), 1533-1549.
- Frangopol, D.M. and Furuta, H., eds. (2001). *Life-Cycle Cost Analysis and Design of Civil Infrastructure Systems*, ASCE, Reston, Virginia.
- Frangopol, D.M. and Kim, S. (2014). Prognosis and life-cycle assessment based on SHM information. Chapter 5 in *Sensor Technologies for Civil Infrastructures: Applications in Structural Health Monitoring*. M.L. Wang, J.P. Lynch, and H. Sohn, eds., *Woodhead Publishing Series in Electronic and Optical Materials*, Vol 2, Woodhead Publishing-Elsevier, Cambridge, U.K., 145-171.
- Frangopol, D.M. and Liu, M. (2007). Maintenance and management of civil infrastructure based on condition, safety, optimization, and life-cycle cost. *Structure and Infrastructure Engineering*, 3(1), 29-41.
- Frangopol, D.M. and Messervey, T.B. (2009a). Life-cycle cost and performance prediction: Role of structural health monitoring. Chapter 16 in *Frontier Technologies for Infrastructures Engineering*, S-S, Chen and A.H-S. Ang, eds., *Structures and Infrastructures Book Series*, Vol. 4, D. M. Frangopol, Book Series Editor, CRC Press/Balkema, Boca Raton, London, New York, Leiden, 361-381.
- Frangopol, D.M. and Messervey, T.B. (2009b). Maintenance principles for civil structures. Chapter 89 in *Encyclopedia of Structural Health Monitoring*, C. Boller, F-K. Chang, and Y. Fujino, eds., John Wiley & Sons Ltd, Chichester, UK, Vol. 4, 1533-1562.
- Frangopol, D.M. and Okasha, N.M. (2009). Lifetime-oriented multi-objective optimization of structural maintenance considering system reliability, redundancy and life-cycle cost using GA. *Structural Safety*, 31(6), 460-474.
- Frangopol, D.M. and Sabatino, S. (2016a). Risk-informed decision making for sustainable infrastructure, *The 5th International Symposium on Reliability Engineering and Risk Management (ISRERM 2016)*, Seoul, Korea, August 17-20, 2016.
- Frangopol, D.M. and Sabatino, S. (2016b). The role of structural reliability, risk, and utility-based performance indicators in informed decision making for sustainable infrastructure, *International Symposium on Sustainability and Resiliency of Infrastructure ISSRI 2016*, Taipei, Taiwan, November 9-12, 2016.

- Frangopol, D.M. and Soliman, M. (2015). Application of soft computing techniques in life-cycle optimization of civil and marine structures. Chapter 2 in *Computational Techniques for Civil and Structural Engineering*, J. Kruis, Y. Tsompanakis and B.H.V. Topping, eds., Saxe-Coburg Publications, Stirlingshire, Scotland, 43-58.
- Frangopol, D.M. and Soliman, M. (2016). Life-cycle of structural systems: recent achievements and future directions. *Structure and Infrastructure Engineering*, 12(1), 1-20.
- Frangopol, D.M., Dong, Y., and Sabatino, S. (2017). Bridge life-cycle performance and cost: analysis, prediction, optimization and decision making. *Structure and Infrastructure Engineering*, 1-19.
- Frangopol, D.M., Kallen, M-J., and van Noortwijk, J. (2004). Probabilistic models for life-cycle performance of deteriorating structures: review and future directions. *Progress in Structural Engineering and Materials*, 6(4), 197-212.
- Frangopol, D.M., Kong, J.S., and Gharaibeh, E.S. (2001). Reliability- based life-cycle management of highway bridges. *Journal of Computing in Civil Engineering*, 15(1), 27-34.
- Frangopol, D.M., Lin, K-Y., and Estes, A.C. (1997). Life-cycle cost design of deteriorating structures. *Journal of Structural Engineering*, 123(10), 1390-1401.
- Frangopol, D.M., Sabatino, S., and Dong, Y. (2015a). Life-cycle management of infrastructure systems considerations reliability, risk, and sustainability, *Engineering Mechanics Institute Conference 2015 (EMI 2015)*, Stanford, USA, June 16-19, 2015.
- Frangopol, D.M., Sabatino, S., and Dong, Y. (2016a). Bridge life-cycle performance and cost: analysis, prediction, optimization and decision making, *The 8th International Conference on Bridge Maintenance, Safety and Management (IABMAS 2016)*, Foz do Iguaçu, Brazil, June 26-30, 2016.
- Frangopol, D.M., Sabatino, S., and Dong, Y. (2016b). Life-cycle performance-based assessment and management of civil infrastructure considering reliability, redundancy, risk, sustainability, and utility, *The 6th Asian-Pacific Symposium on Structural Reliability and its Applications (APSSRA 6)*, Shanghai, China, May 28-30, 2016.
- Frangopol, D.M., Sabatino, S., and Soliman, M. (2015b). Maintenance and safety of deteriorating systems: a life-cycle perspective, *The 2nd International Conference on Performance-based and Life-cycle Structural Engineering (PLSE 2015)*, Brisbane, Australia, December 9-11, 2015.
- Frangopol, D.M., Strauss, A., and Kim, S. (2008a). Bridge reliability assessment based on monitoring. *Journal of Bridge Engineering*, 13(3), 258-270.

- Frangopol, D.M., Strauss, A., and Kim, S. (2008b). Use of monitoring extreme data for the performance prediction of structures: General approach. *Engineering Structures*, 30(12), 3644–3653.
- Galambos, T.V. (1989). System reliability and structural design, in: D.M. Frangopol, ed., *New Directions in Structural System Reliability*, University of Colorado Press, Boulder, CO, 158-166.
- Gharaibeh, E.S. and Frangopol, D.M. (2000). Safety assessment of highway bridges based on system reliability and redundancy. *Congress Report, 16th Congress of IABSE*, Lucerne, Switzerland, 274-275.
- Ghosn, M. and Moses, F. (1998). *Redundancy in highway bridge superstructures*. Washington, DC: National Academy Press, National Cooperative Highway Research Program, NCHRP Report 406, Transportation Research Board.
- Goldberg, D.E. (1989). *Genetic Algorithms in Search, Optimization and Machine Learning*. Addison-Wesley, MA.
- Google Maps. (2014). E-16-FK highway bridge [street map]. Retrieved from [www.google.com/maps/@39.9176763,-105.0934651,15z?hl=en](http://www.google.com/maps/@39.9176763,-105.0934651,15z?hl=en). (accessed September 2014).
- Grierson, D.E. (2008). Pareto multi-criteria decision making. *Advanced Engineering Informatics*, 22(3), 371–384.
- Gumbel, E. J. (1958). *Statistics of extremes*, Columbia University Press, New York.
- Hawk, H., and Small, P. (1998). The BRIDGIT bridge management system. *Structural Engineering International*, 8(4), 309-314
- Heidenreich, W.F., Luebeck, E.G., and Moolgavkar, S.H. (1997). Some properties of the hazard function of the two-mutation clonal expansion model. *Risk Analysis*, 17(3), 391-399.
- Hendawi, S. and Frangopol, D.M. (1994). System reliability and redundancy in structural design and evaluation. *Structural Safety*, 16, 47-71.
- Hessami, A.G. (1999). Risk management: a systems paradigm. *Systems Engineering*, 2(3), 156-167.
- Horová, I., Pospíšil, Z., and Zelinka, J. (2009). Hazard function for cancer patients and cancer cell dynamics. *Journal of Theoretical Biology*, 258(3), 437-443.
- Howard, R.A. and Matheson, J.E. (1989). *Readings on the principles and applications of decision analysis*. Strategic Decisions Group, Menlo Park, CA.
- Hoyland A. and Rausand, M. (1994). *System Reliability Theory: Models and Statistical Methods*, Wiley-Interscience publication, John Wiley & Sons, NY.
- Incat. (2003). 98 Metre wave piercing catamaran, <http://www.incat.com.au/domino/incat/incatweb.nsf/0/76457AADD2C1A987CA2571AF0019EC66?OpenDocument> (accessed 21 June 2016).

- Jiang, R. and Murthy, D.N.P. (1995). Reliability modeling involving two weibull distributions. *Reliability Engineering & System Safety*, 47(3), 187-198.
- Jiménez, A., Ríos-Insua, S., and Mateos, A. (2003). A decision support system for multiattribute utility evaluation based on imprecise assignments. *Decision Support Systems*, 36, 65–79.
- Keeney, R.L. and Raiffa, H. (1993). *Decisions with Multiple Objectives: preferences and value tradeoffs*. Cambridge University Press.
- Kim, S. and Frangopol, D.M. (2011a). Cost-based optimum scheduling of inspection and monitoring for fatigue sensitive structures under uncertainty. *Journal of Structural Engineering*, 137(11), 1319–1331.
- Kim, S. and Frangopol, D.M. (2011b). Cost-effective lifetime structural health monitoring based on availability. *Journal of Structural Engineering*, 137(1), 22–33.
- Kim, S. and Frangopol, D.M. (2011c). Inspection and monitoring planning for RC structures based on minimization of expected damage detection delay. *Probabilistic Engineering Mechanics*, 26, 308–320.
- Kim, S. and Frangopol, D.M. (2017). Efficient multi-objective optimization of probabilistic service life management, *Structure and Infrastructure Engineering*, 13(1), 147-159.
- Kong, J.S. and Frangopol, D.M. (2003). Life-cycle reliability based maintenance cost optimization of deteriorating structures with emphasis on bridges, *Journal of Structural Engineering*, 129(6), 818–828.
- Kong, J.S. and Frangopol, D.M. (2005). Sensitivity analysis in reliability- based lifetime performance prediction using simulation. *Journal of Materials in Civil Engineering*, 17(3), 296-306.
- Kong, J.S., Ababneh, A.N., Frangopol, D.M. and Xi, Y. (2002). Reliability analysis of chloride penetration in saturated concrete. *Probabilistic Engineering Mechanics*, 17(3), 305-315.
- Lai, C.D and Murthy, D.N.P. (2003). A modified weibull distribution. *IEEE Transactions on Reliability*, 52(1), 33-37.
- Lawson, L. and Chen, E.Y. (1995). Microcracks: The hazard function and reliability inspection. *Journal of Testing and Evaluation*, 23(4), 315–318.
- Leemis, L.M. (1995). *Reliability, Probabilistic Models and Statistical Methods*. Prentice Hall, NJ.
- Liu, D., Ghosn, M., Moses, F. and Neuenhoffer, A. (2001). *Redundancy in Highway Bridge Substructures*. National Cooperative Highway Research Program, NCHRP Report 458, Transportation Research Board, National Academy Press, Washington D.C.

- Liu, M. and Frangopol, D.M. (2006a). Optimizing bridge network maintenance management under uncertainty with conflicting criteria: Life-cycle maintenance, failure, and user costs. *Journal of Structural Engineering*, 131(11), 1835-1845.
- Liu, M. and Frangopol, D.M. (2006b). Probability-based bridge network performance evaluation. *Journal of Bridge Engineering*, 11(5), 633-641.
- Lounis, Z. (2004). Risk-based maintenance optimization of bridge structures. <http://irc.nrc-cnrc.gc.ca/fulltext/nrcc47063/nrcc47063.pdf> (Dec. 2004).
- Lundie, S., Peters, G.M., and Beavis, P.C. (2004). Life cycle assessment for sustainable metropolitan water systems planning. *Environmental Science and Technology*, 38, 3465–3473.
- Mahmoud, H.N., Connor, R.J., and Bowman, C.A. (2005). Results of the fatigue evaluation and field monitoring of the I-39 Northbound Bridge over the Wisconsin River. ATLSS Rep. No. 05-04, Lehigh Univ., Bethlehem, PA.
- Malak, R.J., Aughenbaugh, J.M., and Paredis, C.J.J. (2009). Multi-attribute utility analysis in set-based conceptual design. *Computer-Aided Design*, 41(3), 214-227.
- Marsh, P.S., and Frangopol, D.M. (2007). Lifetime multi-objective optimization of cost and spacing of corrosion rate sensors embedded in a deteriorating reinforced concrete bridge deck. *Journal of Structural Engineering*, 133(6), 777-787.
- Marzouk, M.M. and Hisham, M. (2011). Bridge information modeling in sustainable bridge management. ICSDC 2011: Integrating Sustainability Practices in the Construction Industry - Proceedings of the *International Conference on Sustainable Design and Construction 2011*, 457-466.
- MathWorks (2013). *Statistics Toolbox™ 7 User's Guide*. Natick, MA: The Math Works, Inc.
- Mondoro, A., Soliman, M., and Frangopol, D.M. (2016). Prediction of structural response of naval vessels based on available structural health monitoring data. *Ocean Engineering* (in press).
- Morcous, G. and Lounis, Z. (2005). Maintenance optimization of infrastructure networks using genetic algorithms. *Automation in Construction*, 14, 129-142.
- Morcous, G., Lounis, Z., and Cho, Y. (2010). An integrated system for bridge management using probabilistic and mechanistic deterioration models: Application to bridge decks. *KSCE Journal of Civil Engineering*, 14(4), 527-537.
- Mori, Y., and Ellingwood, B. (1994). Maintaining reliability of concrete structures. II: Optimum Inspection/Repair. *Journal of Structural Engineering*, 120(3), 846-862.

- Moses, F., Khedekar, N. and Ghosn, M. (1993). System reliability of redundant structures using response functions. *Proceedings of the Offshore Mechanics and Arctic Engineering Symposium*, ASCE.
- Neves, L.C. and Frangopol, D.M. (2005). Condition, safety and cost profiles for deteriorating structures with emphasis on bridges. *Reliability Engineering & System Safety*, 89(2), 185-198.
- Neves, L.C., Frangopol, D.M., and Cruz, P.J. (2004). Cost of reliability improvement and deterioration delay of maintained structures. *Computers & Structures*, 82(13-14), 1077-1089.
- Neves, L.C., Frangopol, D.M., and Cruz, P.J. (2006). Probabilistic lifetime-oriented multi-objective optimisation of bridge maintenance: Single maintenance type. *Journal of Structural Engineering*, 132, 991–1005.
- Okasha, N.M. and Frangopol, D.M. (2009). Lifetime-oriented multi-objective optimization of structural maintenance considering system reliability, redundancy and life-cycle cost using GA. *Structural Safety*, 31(6), 460-474.
- Okasha, N.M. and Frangopol, D.M. (2010a). Integration of structural health monitoring in a system performance based life-cycle bridge management framework. *Structure and Infrastructure Engineering*, 8(11), 999-1016.
- Okasha, N.M. and Frangopol, D.M. (2010b). Novel approach for multi-criteria optimization of life-cycle preventive and essential maintenance of deteriorating structures. *Journal of Structural Engineering*, 136(8), 1009-1022.
- Okasha, N.M. and Frangopol, D.M. (2010c). Redundancy of structural systems with and without maintenance: An approach based on lifetime functions. *Reliability Engineering & System Safety*, 95(5), 520-533.
- Okasha, N.M. and Frangopol, D.M. (2010d). Time-variant redundancy of structural systems. *Structure and Infrastructure Engineering*, 6(1-2), 279-301
- Okasha, N.M. Frangopol, D.M., and Decò, A. (2010). Integration of Structural Health Monitoring in Life-Cycle Performance Assessment of Ship Structures under Uncertainty. *Marine Structures*, 23(3) 303-321.
- Okasha, N.M. Frangopol, D.M., Saydam, D., and Salvino, L.W. (2011). Reliability Analysis and Damage Detection in High Speed Naval Crafts Based on Structural Health Monitoring Data. *Structural Health Monitoring*, 10(4), 361-379.
- Orcesi, A. and Frangopol, D.M. (2011). Use of lifetime functions in the optimization of nondestructive inspection strategies for bridges. *Journal of Structural Engineering*, 137(4), 531-539.
- Paik, J. K. and Frieze, P.A. (2001). Ship structural safety and reliability. *Progress in Structural Engineering and Materials*, 3(2): 198-21
- Paliou, C., Shinozuka, M., and Chen, Y-N. (1990). Reliability and redundancy of offshore structures. *Journal of Engineering Mechanics*, 116(2), 359-378.

- Papanikolaou, A., Zaraphonitis, G., Boulougouris, E., Langbecker, U., Matho, S., Sames, P. (2010). Multi-objective optimization of oil tanker design. *Journal of Marine Science and Technology*, 15(4), 359-373.
- Pedersen, P.T. (2002). Collision risk for fixed offshore structures close to high-density shipping lanes. *Proceedings of the Institution of Mechanical Engineers, Part M: Journal of Engineering for the Maritime Environment*, 216(1), 29-44.
- Peil, U. (2005). Assessment of bridges via monitoring. *Structure and Infrastructure Engineering*, 1(2), 101-117.
- Pratt, J.W. (1964). Risk aversion in the small and in the large. *Econometrica*, 32(1/2), 122-136.
- Rackwitz, R. (2002). Optimization and risk acceptability based on the life quality index. *Structural Safety*, 24(2-4), 297-331.
- Rashedi, M.R. and Moses, F. (1988). Identification of failure modes in system reliability. *Journal of Structural Engineering*, 114(2), 292-313.
- Ross, A.M., Hastings, D.E., Warmkessel, J.M., and Diller, N.P. (2004). Multi-attribute tradespace exploration as front end for effective space system design, *Journal of Spacecraft and Rockets*, 41(1), 20-28.
- Sabatino, S. and Frangopol, D.M. (2016a). Life-cycle sustainability of highway bridges, *The 8th International Conference on Bridge Maintenance, Safety and Management IABMAS 2016*, Foz do Iguacu, Brazil, June 26-30, 2016.
- Sabatino, S. and Frangopol, D.M. (2016b). Structural health monitoring planning of ship structures in a life-cycle perspective. *Proceedings of the Fifth International Symposium on Life -Cycle Civil Engineering, IALCCE2016*, Delft, Netherlands.
- Sabatino, S. and Frangopol, D.M. (2016c). Treating system reliability, redundancy, risk, and sustainability as performance-based design and assessment requirements in a life-cycle context, *The 7th Probabilistic Mechanics and Reliability Conference (PMC 2016)*, Nashville, Tennessee, May 22-26, 2016.
- Sabatino, S. and Frangopol, D.M. (2017a). Decision making framework for optimal SHM planning of ship structures considering availability and utility. *Ocean Engineering*, 135, 194-206.
- Sabatino, S. and Frangopol, D.M. (2017b). Decision support system for optimum lifetime sustainability-based maintenance planning of highway bridges, *International Conference on Sustainable Infrastructure (ICSI 2017)*, New York, New York, October 26-28, 2017
- Sabatino, S. and Frangopol, D.M. (2017c). Optimum utility-informed SHM planning of ship structures considering uniform and non-uniform monitoring time intervals, *The 12th International Conference on Structural Safety & Reliability (ICOSSAR 2017)*, Vienna, Austria, August 6-10, 2017.

- Sabatino, S., Frangopol, D.M., and Dong, Y. (2015). Sustainability-informed maintenance optimization of highway bridges considering multi-attribute utility and risk attitude. *Engineering Structures*, 102, 310-321.
- Sabatino, S., Frangopol, D.M., and Dong, Y. (2016). Life-cycle utility-informed maintenance planning based on lifetime functions: Optimal balancing of cost, failure consequences, and performance benefit. *Structure and Infrastructure Engineering*, 12(7), 830-847.
- Salvino L.W., and Brady, T.F. (2008). Hull monitoring system development using hierarchical framework for data and information management. In: *Proceedings of the 7<sup>th</sup> international conference on computer and IT applications in the marine industries (COMPIT'08)*, Liège, April 2008, 21–23.
- Saydam, D. and Frangopol, D.M. (2011). Time-dependent performance indicators of damaged bridge superstructures. *Engineering Structures*, 33, 2458–2471.
- Saydam, D., Bocchini, P., and Frangopol, D.M. (2013a). Time-dependent risk associated with deterioration of highway bridge networks. *Engineering Structures*, 54(0), 221-233.
- Saydam, D., Frangopol, D.M., and Dong, Y. (2013b). Assessment of Risk using Bridge Element Condition Ratings, *Journal of Infrastructure Systems*, 19(3), 252-265.
- Shinozuka, M. (2008). Resilience and sustainability of infrastructure systems. Proceedings of the *International Workshop on Frontier Technologies for Infrastructures Engineering*, Taipei, Taiwan, October 24-25, 2008, S-S. Chen and A.H-S. Ang, eds., Taiwan Building Technology Center, National Taiwan University of Science and Technology, Taipei, Taiwan, 225-244.
- Soliman, M. and Frangopol, D.M. (2014). Life-cycle management of fatigue sensitive structures integrating inspection information. *Journal of Infrastructure Systems*, 20, 04014001.
- Soliman, M., Barone, G., and Frangopol, D.M. (2015). Fatigue reliability and service life prediction of aluminum naval ship details based on monitoring data. *Structural Health Monitoring*, 14(1), 3-19.
- Soliman, M., Frangopol, D.M., and Kim, S. (2013). Probabilistic optimum inspection planning of steel bridges with multiple fatigue sensitive details. *Engineering Structures*, 49, 996–1006.
- Stein, S. and Sedmera, K. (2006). *Risk-based management guidelines for scour at bridges with unknown foundations*. Final Report for NCHRP Project 24-25.
- Stein, S.M., Young, G.K., Trent, R.E., and Pearson, D.R. (1999). Prioritizing scour vulnerable bridges using risk. *Journal of Infrastructure Systems*, 5(3), 95-101.
- Stewart, M.G. (2001). Reliability-based assessment of ageing bridges using risk ranking and life cycle cost decision analyses. *Reliability Engineering and System Safety*, 74(3), 263-273.

- Stewart, M.G. and Rosowsky, D.V. (1998). Time-dependent reliability of deteriorating reinforced concrete bridge decks. *Structural Safety*, 20, 91-109.
- Stewart, T.J. (1996). Robustness of additive value function methods in MCDM. *Journal of Multi-Criteria Decision Analysis*, 5(4), 301-309.
- Strauss, A., Frangopol, D.M., and Kim, S. (2008). Use of monitoring extreme data for the performance prediction of structures; Bayesian updating. *Engineering Structures*, 30(12), 3654–3666.
- Tang, K. and Melchers, R.E. (1988). Incremental formulation for structural reliability analysis. *Civil Engineering Systems*, 153-158.
- Tanner, M.A. and Wong, W.H. (1984). Data-based nonparametric estimation of the hazard function with applications to model diagnostics and exploratory analysis. *Journal of the American Statistical Association*, 79(385), 174-182.
- Thies, P.R., Smith, G.H., and Johanning, L. (2012). Addressing failure rate uncertainties of marine energy converters. *Renewable Energy*, 44(0), 359-367.
- Thoft-Christensen, P. (1998). Assessment of the reliability profiles for concrete bridges. *Engineering Structures* 20(11), 1004–1009.
- Thoft-Christensen, P. and Murotsu, Y. (1986). *Application of Structural Systems Reliability Theory*. , Springer, Berlin.
- Thompson, P.D., Small, E.P., Johnson, M., and Marshall, A.R. (1998). The Pontis bridge management system. *Structural Engineering International*, 8(4), 303-308.
- Thurston, D. (2001). Real and misconceived limitations to decision based design with utility analysis. *Journal of Mechanical Design*, 123(2), 176-182.
- van Noortwijk, J.M. and Klatter, H.E. (2004). The use of lifetime distributions in bridge maintenance and replacement modelling. *Computers & Structures*, 82(13–14), 1091-1099.
- Vu, K. and Stewart, M.G. (2000). Structural reliability of concrete bridges including improved chloride-induced corrosion models. *Structural Safety*, 22, 313-333.
- Wen, Y.K. and Kang, Y.J. (2001). Minimum building life-cycle cost design criteria I. Methodology, and II. Applications. *Journal of Structural Engineering*, 127(3), 330-346.
- Yang, J.-B. and Xu, D.-L. (2002). On the evidential reasoning algorithm for multiple attribute decision analysis under uncertainty. *IEEE Transactions on Systems, Man, and Cybernetics - Part A: Systems and Humans*, 32(3), 289-304.
- Yang, S., Frangopol, D.M., and Neves, L.C. (2004). Service life prediction of structural systems using lifetime functions with emphasis on bridges. *Reliability Engineering & System Safety*, 86(1), 39-51.

- Yang, S., Frangopol, D.M., and Neves, L.C. (2006). Optimum maintenance strategy for deteriorating bridge structures based on lifetime functions. *Engineering Structures*, 28(2), 196-206.
- Yang, S., Frangopol, D.M., and Neves, L.C. (2006a). Optimum maintenance strategy for deteriorating bridge structures based on lifetime functions. *Engineering Structures*, 28(2), 196-206.
- Yang, S-I, Frangopol, D.M., Kawakami, Y., and Neves, L.C. (2006b). The use of lifetime functions in the optimization of interventions on existing bridges considering maintenance and failure costs. *Reliability Engineering & System Safety*, 91(6), 698-705.
- Zhang, Z. and Li, X. (2010). Some new results on stochastic orders and aging properties of coherent systems. *IEEE Transactions on Reliability*, 59(4), 718-724.
- Zhu, B. and Frangopol, D.M. (2013a). Incorporation of structural health monitoring data on load effects in the reliability and redundancy assessment of ship cross-sections using Bayesian updating. *Structural Health Monitoring*, 12(4), 377-392.
- Zhu, B. and Frangopol, D.M. (2013b). Risk-based approach for optimum maintenance of bridges under traffic and earthquake loads. *J Structural Engineering*, 139(3), 422-434.
- Zhu, B. and Frangopol, D.M. (2013c). Reliability, redundancy and risk as performance indicators of structural systems during their life-cycle. *Engineering Structures*, 41, 34-49.

# APPENDIX A SYSTEM RELIABILITY MODELING OF BRIDGES

## A.1 OVERVIEW

This appendix summarizes methodologies for modeling the system reliability of bridge systems. In particular, when building a system reliability model, several fundamental engineering principles are integrated into the approach, including identification of relevant failure modes, uncertainty quantification, and probabilistic considerations. This commentary was provided to the Federal Highway Administration in 2017 to augment a report on the application of redundancy factors to highway bridge systems.

## A.2 NOTATIONS

CDF = cumulative distribution function

$E(X)$  = mean value of the random variable  $X$

$E_c(R)$  = mean resistance of a single component

$E_{cs}(R)$  = mean resistance of a component in a system

$F_j$  = failure of component  $j$

$g$  = performance function

$M$  = safety margin

$P$  = load

PDF = probability density function

$P_f$  = probability of failure

$P_s$  = probability of survival

$Q$  = load effect

$R$  = resistance of a component

$V(X)$  = coefficient of variation of the random variable  $X$

$X$  = random variable

$\beta_c$  = reliability index of a single component

$\beta_{cs}$  = reliability index of a component in a system

$\beta_{sys}$  = reliability index of a system

$\delta$  = post-failure behavior factor

$\eta_R$  = component redundancy factor

$\mu_M$  = mean of the safety margin

$\mu_Q$  = mean of the load effect

$\mu_R$  = mean of the component resistance

$\rho(X_1, X_2)$  = correlation coefficient between random variables  $X_1$  and  $X_2$

$\sigma_M$  = standard deviation of the safety margin

$\sigma_Q$  = standard deviation of the load effect

$\sigma_R$  = standard deviation of the component resistance

$\Phi^{-1}(\cdot)$  = inverse of the standard normal cumulative distribution

$\cap$  = union of events

$\cup$  = intersection of events

### **A.3 RELEVANT TERMS**

Bridge component

Bridge component reliability

Bridge component redundancy

Bridge failure modes

Bridge modeling

Bridge sub-system

Bridge sub-system redundancy

Bridge sub-system reliability

Bridge system

Bridge system reliability

Bridge system redundancy

Brittle component

Correlation among bridge component resistances

Correlation among bridge failure modes

Correlation among bridge loads

Correlation between two random variables

Ductile component

Post-failure behavior

Semi-brittle component

## A.4 DEFINITIONS

### A.4.1 Bridge component

According to AASHTO, a bridge component may be regarded as a physical piece of material that comprises a bridge. For example, structural bridge components include girders, decks, and piers. In this report, the word component is encountered when analyzing system reliability block diagrams; the components are arranged in specific configurations within the system reliability block diagram. A girder can fail in many ways (e.g., bending, shear) and in various locations. A component in the reliability model used in this study is a place where a limit state could occur. For example, a bridge girder can fail in many ways (e.g., bending, shear) and in various locations.

Component  $j$ , representing a specific bridge part (e.g., girder) is idealized in Figure A.1

### A.4.2 Bridge system

The bridge system is the combination of all the components comprising the bridge structure. An example of an eight-component bridge system is shown in Figure A.2.

### A.4.3 Bridge sub-system

A bridge sub-system is considered a group of components within the bridge system. As an example, three sub-systems (i.e., A, B, and C) of the bridge system in Figure A.2 are highlighted in Figure A.3. If  $F_j$  represents the failure of component  $j$ , the failure of sub-system A requires the failure of component 1 *or* component 2, *or both*, expressed mathematically as the event  $F_1 \cup F_2$ . Similarly, sub-system B fails when both component 3 *and* 4 fail (i.e.,  $F_3 \cap F_4$ ). The failure of sub-system C occurs when

component 5 fails or components 6, 7, and 8 fail simultaneously (i.e.,  $F_5 \cup (F_6 \cap F_7 \cap F_8)$ ).

#### ***A.4.4 Bridge failure modes***

A failure occurs when a component or system stops performing its required function. A failure mode is defined as the mechanism that is responsible for the non-operation of a component, sub-system, or system. For structural components within bridge systems, failure modes investigated include shear, bending, fatigue, yielding, rupture, and cracking, among others.

#### ***A.4.5 Bridge modeling***

Bridge modeling refers to the configuration of the system reliability block diagram, including series, parallel, and series-parallel. An example of each type of these systems is shown in Figure A.4. Systems A, B, C, D, and E contain the same four components arranged in different configurations. Series, parallel, and series-parallel systems are depicted in Figure A.4a, Figure A.4b, and Figure A.4c-e, respectively.

In order to provide guidance for the discretization of superstructure continuums, the process of system modeling associated with different types of bridges is discussed herein. For a box girder bridge, it can be assumed that the critical sections are arranged in either series, parallel, or a series-parallel. Additionally, for a bridge that consists of steel girders that support a reinforced concrete deck, the girders' and deck's failure modes may be arranged in a series-parallel configuration; this type of bridge is modeled in Figure A.7.

#### ***A.4.6 Bridge component redundancy***

Component redundancy is a measure of how much its failure contributes the failure of the bridge system. AASHTO defines component redundancy as “the quality of a bridge component that enables it to perform its design function in a damaged state.” As an example, rupture or yielding of an individual component may not cause collapse or failure of the whole bridge system (AASHTO 2010).

#### ***A.4.7 Bridge system redundancy***

If a system is redundant, there exists more than one way of fulfilling the requirements of system operation (i.e., non-failure). Similarly, bridge redundancy is defined as “the capability of a bridge structural system to carry loads after damage or the failure of one or more of its members” in The Manual for Bridge Evaluation (AASHTO 2008).

#### ***A.4.8 Bridge sub-system redundancy***

Similar to the definition of bridge system redundancy, if a sub-system is redundant, there exists more than one way of fulfilling the requirements of sub-system operation (i.e., non-failure).

#### ***A.4.9 Bridge component reliability***

In general, bridge component reliability can be defined as the probability that this component will adequately perform its purpose for a period of time under specified environmental conditions. The reliability assessment of bridge components can be expressed as a problem of supply and demand, which is modeled by means of random variables. For instance, if  $R$  and  $Q$  are the resistance and the load effect corresponding to a specific bridge component respectively, the probability that  $Q$  will not exceed  $R$

represents the reliability of the structural component investigated. The resistance of a bridge component greatly depends upon the material it is composed of, the environmental conditions, in addition to its dimensions. In contrast, the load effect depends upon hazards that the bridge component is subject to and also on the bridge characteristics.

The probability of failure of a component is defined as the probability of violating any of the limit state functions that define its failure modes. Limit states associated with bridge components are expressed with equations relating the resistance of the structural component to the load effects acting on this component. The safety margin is expressed as follows:

$$M = R - Q \quad (\text{A.1})$$

where  $M$  is the safety margin,  $R$  represents the resistance, and  $Q$  denotes the load effect. Another way of expressing the safety margin is called the performance function  $g$ . For example, the structural behavior of a bridge component may be described by the following performance function:

$$g = R - Q \quad (\text{A.2})$$

The safety margin  $M$  is a random variable with probability density function (PDF)  $f_M(m)$ . As shown in Figure A.5, the area under the PDF upper bounded by  $m = 0$  represents the probability of failure. The reliability index of a component is defined as (see Figure A.5):

$$\beta_c = \frac{\mu_M}{\sigma_M} \quad (\text{A.3})$$

where  $\mu_M$  and  $\sigma_M$  are the mean and standard deviation of the safety margin, respectively.

If  $R$  and  $Q$  are independent, the reliability index of a component becomes

$$\beta_c = \frac{\mu_R - \mu_Q}{\sqrt{\sigma_R^2 + \sigma_Q^2}} \quad (\text{A.4})$$

where  $\mu_R$ ,  $\mu_Q$  and  $\sigma_R$ ,  $\sigma_Q$  are the means and standard deviations, respectively.

Furthermore, on the assumption that the safety margin  $M$  is normally distributed, the reliability index can be expressed as:

$$\beta_c = \Phi^{-1}(P_s) = \Phi^{-1}(1 - P_f) \quad (\text{A.5})$$

where  $\Phi^{-1}(\cdot)$  is the inverse of the standard normal cumulative distribution function (CDF),  $P_f$  is the probability of failure, and  $P_s = 1 - P_f$  is the probability of safety.

#### **A.4.10 Bridge system reliability**

Bridge system reliability is calculated considering the system reliability model (also called the system reliability block diagram). Bridge systems that are composed of multiple components can be classified as series, parallel, or combined series-parallel. In general, the failure events comprising the system reliability model may be represented as events in series (defined as union,  $\cup$ ) or in parallel (denoted as intersection,  $\cap$ ).

Systems whose components are connected in series are such that the failure of *any* of these components constitutes the failure of system. These types of systems (i.e., series systems) have no redundancy and are also known as “weakest link” systems; the

reliability of this type of system requires that none of the components fail. An idealized series system is shown in Figure A.6a. For series systems, the domain  $\Omega$ , representing system failure, is expressed in terms of component failure events as:

$$\Omega = \bigcup_{k=1}^n \{g_k(\mathbf{X}) < 0\} \quad (\text{A.6})$$

Conversely, if system failure requires the failure of *all* its components, then the system may be idealized as a parallel system. If any of the components survive in a parallel system, the system will not fail. Clearly, a parallel system is a redundant system and may be represented as shown in Figure A.6b. For parallel systems, the system failure domain  $\Omega$  is expressed as:

$$\Omega = \bigcap_{k=1}^n \{g_k(\mathbf{X}) < 0\} \quad (\text{A.7})$$

Figure A.6c depicts an idealized series-parallel system with  $n$  sub-systems of 4 parallel components in series. In general, the failure domain of a series-parallel system may be expressed in terms of component failure events as

$$\Omega = \bigcup_{k=1}^n \bigcap_{j=1}^{c_n} \{g_{k,j}(\mathbf{X}) < 0\} \quad (\text{A.8})$$

where  $c_n$  is the number of components in the  $n$ th cut set.

An example of a system reliability model for a bridge with a reinforced concrete deck and steel girders is shown in Figure A.7. Figure A.7a presents the transverse cross section of the investigated bridge superstructure while Figure A.7b shows the idealized system reliability model. In this system reliability model, it is assumed that failure of the entire bridge superstructure (i.e., the system) is modeled as

a series-parallel system consisting of a failure of the deck or the failure of any two adjacent girders. Considering that  $F_j$  represents the failure of component  $j$ , the event set describing the failure of the entire bridge system is:

$$F_{system} = F_{deck} \cup (F_{girder1} \cap F_{girder2}) \cup (F_{girder2} \cap F_{girder3}) \cup (F_{girder3} \cap F_{girder4}) \cup (F_{girder4} \cap F_{girder5}) \quad (A.9)$$

#### ***A.4.11 Bridge sub-system reliability***

Similar to the definition of bridge system reliability, bridge sub-system reliability is calculated considering the sub-system's reliability block diagram. The sub-system's reliability model is representative of a sub-system's reliability in an event diagram format. As an example, the reliability associated with sub-systems A, B, and C within Figure A.3 are calculated considering the event sets  $F_1 \cup F_2$ ,  $F_3 \cap F_4$ , and  $F_5 \cup (F_6 \cap F_7 \cap F_8)$ , respectively.

#### ***A.4.12 Post-failure behavior***

The structural response of bridge components beyond the elastic limit can be characterized by brittle, ductile, or mixed (ductile-brittle) behavior. The parameter utilized to express the post-failure behavior is  $\delta$ , with  $\delta = 1$  and  $\delta = 0$  representing a ductile and brittle component, respectively.  $\delta$  is called the post-failure behavior factor.

For component  $j$ , the representative force-deformation relationships, considering the post-failure behavior of the component, is shown in Figure A.8.

#### ***A.4.13 Ductile component***

As defined by AASHTO, ductility refers to a “property of a component or connection that allows inelastic response.” Additionally, if, by means of confinement or other measures, a bridge component or connection can sustain inelastic deformations without significant loss of load-carrying capacity, this component can be considered ductile (AASHTO 2010).

#### ***A.4.14 Brittle component***

Brittle behavior, or “the sudden loss of load-carrying capacity immediately when the elastic limit is exceeded,” refers to the post-failure behavior of a bridge component. According to AASHTO, “brittle behavior is undesirable because it implies the sudden loss of load-carrying capacity immediately when the elastic limit is exceeded” (AASHTO 2010).

#### ***A.4.15 Semi-brittle component***

A component which exhibits post-failure behavior in between the brittle and ductile response extremes. A semi-brittle component is represented by  $0 < \delta < 1$ .

#### ***A.4.16 Correlation between two random variables***

Correlation indicates the amount of relative dependency among random variables. The most common measure of dependence between two quantities is the Pearson's correlation coefficient, commonly called "the correlation coefficient." It is obtained by dividing the covariance of the two investigated variables by the product of their standard deviations. The correlation coefficient  $\rho(X_1, X_2)$  between two random

variables  $X_1$  and  $X_2$  with expected values  $\mu_{X1}$  and  $\mu_{X2}$  and standard deviations  $\sigma_{X1}$  and  $\sigma_{X2}$  is defined as:

$$\rho(X_1, X_2) = \frac{E[(X_1 - \mu_{X1})(X_2 - \mu_{X2})]}{\sigma_{X1} \cdot \sigma_{X2}} \quad (\text{A.10})$$

Statistical independence between the two random variables  $X_1$  and  $X_2$  implies  $\rho(X_1, X_2) = 0$  (i.e., no correlation). In contrast, perfect correlation between the two random variables  $X_1$  and  $X_2$  implies  $\rho(X_1, X_2) = 1$ . Figure A.9 depicts different correlations between two random variables  $X_1$  and  $X_2$ .

#### ***A.4.17 Correlation among bridge loads***

Correlation among bridge loads occurs when the loads applied to a structural system are related. Typically, separate loads are independent when the occurrence of one load has no bearing on the occurrence of the other load. As an example, the dead load and live load on a bridge are independent; in other words, these two loads have no correlation.

Since statistical independence between two random variables  $X_1$  and  $X_2$  (i.e.,  $\rho(X_1, X_2) = 0$ ) implies that the two variables are not related, the value of one variable has no influence on the value of the other variable. An example of statistically independent variables with application to bridges is the loading applied to the structure. For example, traffic loading and dead loads are independent and traffic loads and seismic loads are also independent; the amount of traffic has no bearing on the occurrence and magnitude of dead or seismic loads.

#### ***A.4.18 Correlation among bridge component resistances***

Correlation among bridge resistances occurs when the structural resistances associated with multiple components (e.g.,  $R_1, R_2, \dots, R_N$ ) are related. In practice, the resistances of bridge components could be correlated, like in the case of multiple interior bridge girders. However, the resistances of an interior girder and the deck of a bridge (see Figure A-15a for an example) are typically not correlated (e.g., independent).

#### ***A.4.19 Correlation among bridge failure modes***

Correlation among bridge failure modes occurs when some or all of the components of limit state functions of the two failure modes are related (e.g., same load present in the two failure modes, same resistances present in the two failure modes). Typically, only the correlation among the random variables involved in the reliability assessment are known and/or quantified. However, the correlation among different performance functions (e.g.,  $g_1, g_2, \dots, g_N$ ) may also be calculated considering the relationships among all the investigated random variables.

Since perfect correlation between two random variables (i.e.,  $\rho = 1$ ) implies that the two variables are fully interrelated, the value of one variable has complete influence on the value of the other variable. An example with application to bridges is found when analyzing the bending and shear failure of a simply supported span of a two lane bridge with two independent truck loads (e.g., two trucks following each other in the same lane). The simply supported span with the two applied truck loads  $P_1$  and  $P_2$  is shown in Figure A.10. The free body diagram of the span is also shown in

Figure A.10 where vertical reaction forces at the left and right support are

denoted as  $Y_1$  and  $Y_2$ , respectively. Because the expressions for the vertical reactions at the supports of the span are functions of similar terms (i.e.,  $P_1$  and  $P_2$ ), there exists some inherent correlation between the reaction forces (i.e.,  $\rho(Y_1, Y_2) > 0$ ). For this particular span, the two modes of failure considered are bending and shear.

The bending moment at point A is denoted as  $M_A$  and is a function of both truck loads  $P_1$  and  $P_2$ . Similarly, the shear force at point C,  $V_C$  is also a function of both truck loads  $P_1$  and  $P_2$ . In general, the expressions for moment and shear in the span contain terms representing the magnitude of the two applied loads. Because both equations used to calculate  $M_A$  and  $V_C$  contain  $P_1$  and  $P_2$ , the bending moment at point A and shear force at point C are correlated. In this case, the magnitude of the applied loads are independent (i.e., no correlation) but their load effects are correlated. The bending moment at points A and B,  $M_A$  and  $M_B$ , respectively, will be correlated, as well.

Furthermore, the failure modes associated with bending and shear of the bridge may be analyzed. The performance function associated with bending is

$$g_M = R_M - Q_M \quad (\text{A.11})$$

where  $R_M$  is the bending resistance and  $Q_M$  is the bending load effect. Similarly, the performance function corresponding to shear failure is expressed as:

$$g_V = R_V - Q_V \quad (\text{A.12})$$

where  $R_V$  is the shear resistance and  $Q_V$  is the shear load effect. Since the two load effects  $Q_M$  and  $Q_V$  are correlated, it is evident that the performance functions (i.e., failure modes) presented in Eqs. (A.11) and (A.12) are also correlated. Therefore, even

if the resistances in bending and shear are independent, their respective failure modes will always be correlated.

## **A.5 SYSTEM RELIABILITY MODELING**

This section outlines the methodology for developing system reliability models corresponding to bridge systems. First, fundamental nomenclature and definitions are clarified. Additionally, several examples of modeling simple structures (e.g., beams and trusses) and bridges, in general, are presented.

### Element

For the purposes of this report, an element is defined as any physical piece of material that comprises a bridge system. Examples of bridge elements include structural members such as girders, decks, and piers. Each element has particular material, geometrical, and physical properties that contribute to its overall internal capacity. Hazards and loading events may affect elements in various ways (e.g., uniformly, selectively), depending upon the location and intensity of loadings.

### Component

A component is defined as a “place” where a limit state could occur. The reliability of each element of a bridge may be evaluated with respect to various limit states and at different locations. For instance, a bridge girder can fail in many ways (e.g., bending, shear) and in various locations (e.g., mid-span for bending, at the support for shear). Components characterizing the main failure modes of a system are arranged in specific configurations (i.e., series, parallel, series-parallel) to form an

idealized representation of the reliability performance of the system denoted as the system reliability model.

This next section of the commentary presents a collection of examples of system reliability modeling regarding various applications including beams, trusses, and simple bridges.

### **A.5.1 Beams**

Consider a simply supported beam structure, as shown in Figure A.11. The beam is subjected to a distributed load  $w$  and two points of interest are established: one at midspan where the bending moment is largest, point A, and one near the left support where the shear force is maximum, point B. It is assumed that the resistance in shear is weaker near the left support than that near the right support. The bending moment at point A is denoted as  $M_A$  and the shear force at point B as  $S_B$ . The performance function associated with bending at point A is

$$g_M = R_M - Q_M \quad (\text{A.13})$$

where  $R_M$  is the bending resistance and  $Q_M$  is the bending load effect. Similarly, the performance function corresponding to shear failure at point B is expressed as

$$g_S = R_S - Q_S \quad (\text{A.14})$$

where  $R_S$  is the shear resistance and  $Q_S$  is the shear load effect. The load effects  $Q_M$  and  $Q_S$  are correlated because they both are dependent on the same uniform load  $w$ ; thus, the performance functions (i.e., failure modes) presented in Eqs. (A.13) and (A.14) are also correlated. Considering shear and bending failure modes, the beam

system in Figure A.11 may be idealized as two components arranged in series, as shown in the reliability model in Figure A.12.

The event set describing the failure of the beam system is

$$F_{beam} = (g_M < 0) \cup (g_S < 0) \quad (\text{A.15})$$

where the union  $\cup$  represents the occurrence of event  $g_M < 0$ , event  $g_S < 0$ , or both events.

### ***A.5.2 Trusses***

Consider the ten-bar symmetric truss system shown in Figure A.13. The truss is subjected to two concentrated loads  $W$ .

In order to determine a system reliability model, several collapse mechanisms are considered. If bar 1 or bar 9 fails, then the entire truss fails. Additionally, if failure of two members, including only failure of member 3 or member 4 or member 5 is considered, failure of both bars 3 and 1, or 3 and 4, or 3 and 5, or 3 and 6, or 3 and 8, or 3 and 9, or 4 and 1, or 4 and 5, or 4 and 6, or 4 and 8, or 4 and 9, or 5 and 1, or 5 and 6, or 5 and 8, or 5 and 9, will cause the truss system to collapse. This system failure model considering failure of one member, or failure of two members including members 3 or 4 or 5, is depicted in the system reliability model shown in Figure A.14.

Considering that  $F_j$  represents the failure of bar  $j$ , the event set describing the failure of the entire truss structure under the assumption that one member fails or two member fail, including members 3, 4 or 5, is

$$\begin{aligned}
F_{truss} = & F_1 \cup F_9 \cup (F_3 \cap F_1) \cup (F_3 \cap F_4) \cup (F_3 \cap F_5) \cup (F_3 \cap F_6) \\
& \cup (F_3 \cap F_8) \cup (F_3 \cap F_9) \cup (F_4 \cap F_1) \cup (F_4 \cap F_5) \cup (F_4 \cap F_6) \\
& \cup (F_4 \cap F_8) \cup (F_4 \cap F_9) \cup (F_5 \cap F_1) \cup (F_5 \cap F_6) \cup (F_5 \cap F_8) \\
& \cup (F_5 \cap F_9)
\end{aligned} \tag{A.16}$$

where the intersection  $\cap$  represents the simultaneous occurrence of all events investigated.

### A.5.3 Bridge modeling – general

Bridges are designed/constructed using a wide array of methods/materials and, at the same time, subjected to a variety loads. These factors affect the resistance and load effects parameters which are embedded in component performance functions. This section contains an example that illustrates the process of developing a system reliability model considering a variety of different limit states, such as strength (e.g., bending, shear), serviceability (e.g., maximum deflection), and fatigue-and-fracture (e.g., fatigue cracking).

In general, three components, or performance functions may be considered to form a system reliability model of this bridge. Figure A.15 depicts, at the most basic level, the system reliability model of the bridge; three basic failure modes are defined for this bridge: (1) strength  $g_{st}$ , (2) serviceability  $g_{ser}$ , and (3) fatigue  $g_f$ . This reliability model may be further refined when more information about each of the failure modes is included; for example, the single reliability block representing strength limit states in Figure A.15 may be considered a sub-system consisting of three components, shear  $g_s$ , bending  $g_b$ , and torsion  $g_t$  failure modes arranged in series. Additionally, multiple serviceability limit states may be included within the model by breaking down the

component related to serviceability within Figure A.15 into two components representing deflection  $g_\delta$  and vibration comfort  $g_v$ . Similarly, the component corresponding to fatigue limit states in Figure A.15 may be further broken down into a series sub-system composed of multiple fatigue critical details (e.g., bolted  $g_{bc}$  and welded  $g_{wc}$  connections). The refined system reliability model for the investigated bridge is shown in Figure A.16.

A similar approach is applied by Estes and Frangopol (2001), where a hypothetical series system for a girder consisting of components relating to failure by shear, moment, and excessive deflection is developed (see Figure A.17). Using the general approach outlined herein, one can idealize any type of bridge systems including girder, cable-stayed, and suspension bridges.

## REFERENCES

AASHTO (2008). Manual for Bridge Evaluation. American Association of State Highway and Transportation Officials, Washington, DC.

AASHTO (2010). LRFD bridge design specifications, 5<sup>th</sup> Ed., Washington, DC.



Figure A.1 Component  $j$ .

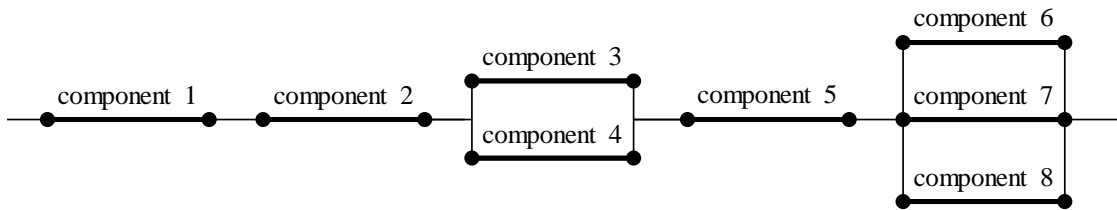


Figure A.2. Eight-component bridge system.

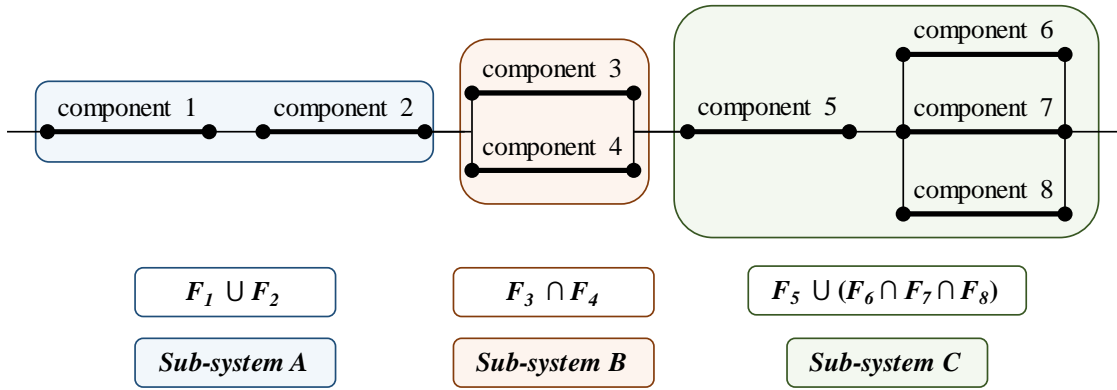


Figure A.3. Sub-systems of a bridge system.

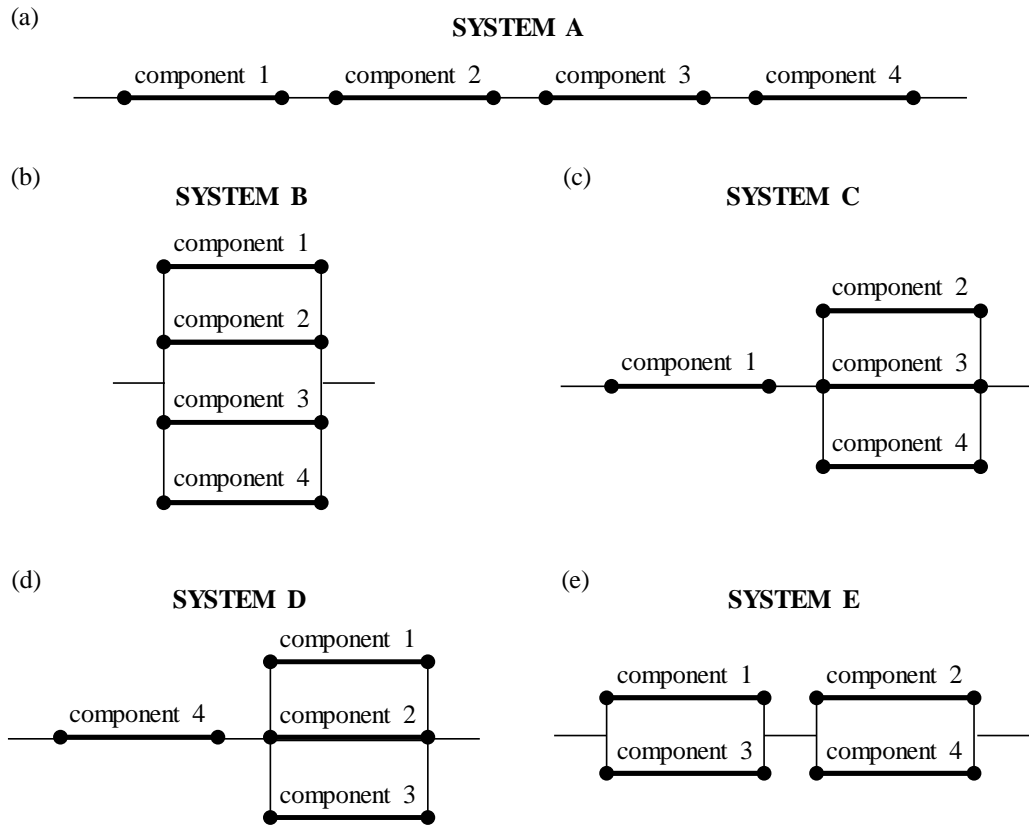


Figure A.4. Five configurations of a four-component system.

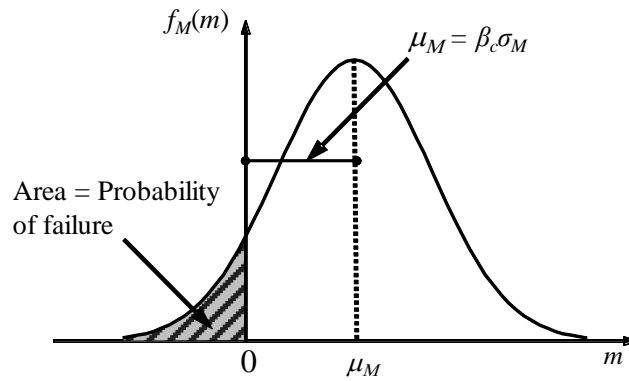


Figure A.5. PDF of the safety margin  $f_M(m)$ .

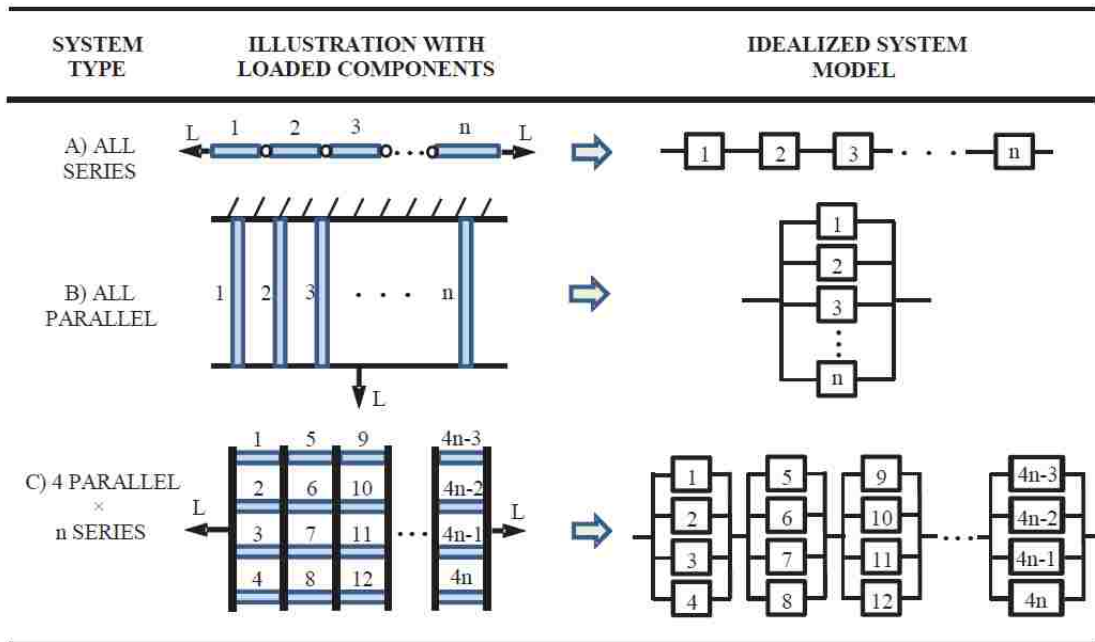


Figure A.6. Idealized series, parallel, and series-parallel systems.

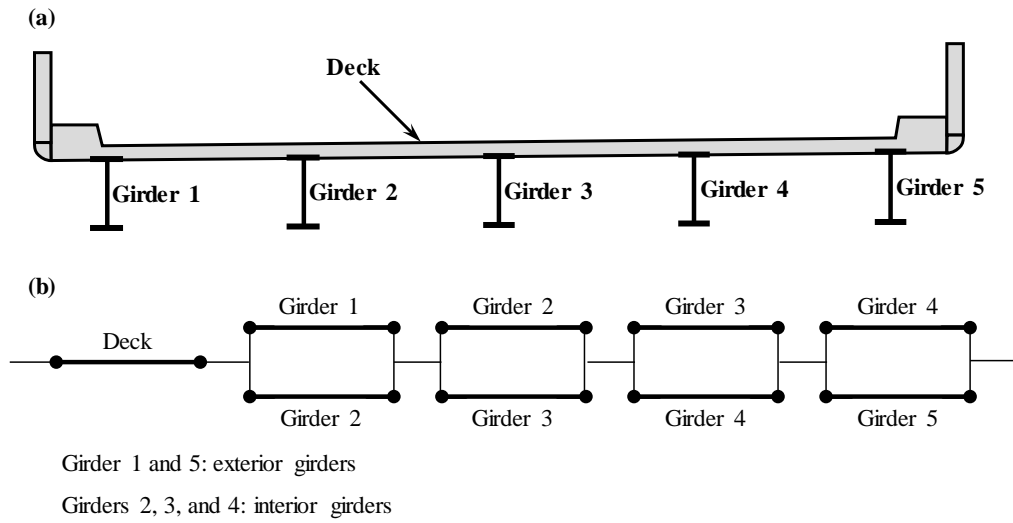


Figure A.7. Transverse cross-section and (b) system reliability model of the superstructure of a bridge.

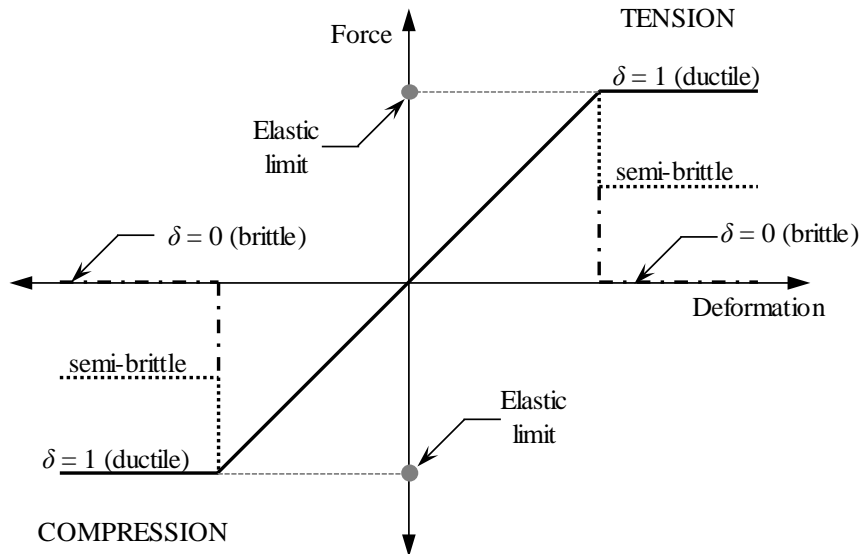


Figure A.8. Force-deformation relationship considering the effect of the post-failure behavior  $\delta$ .

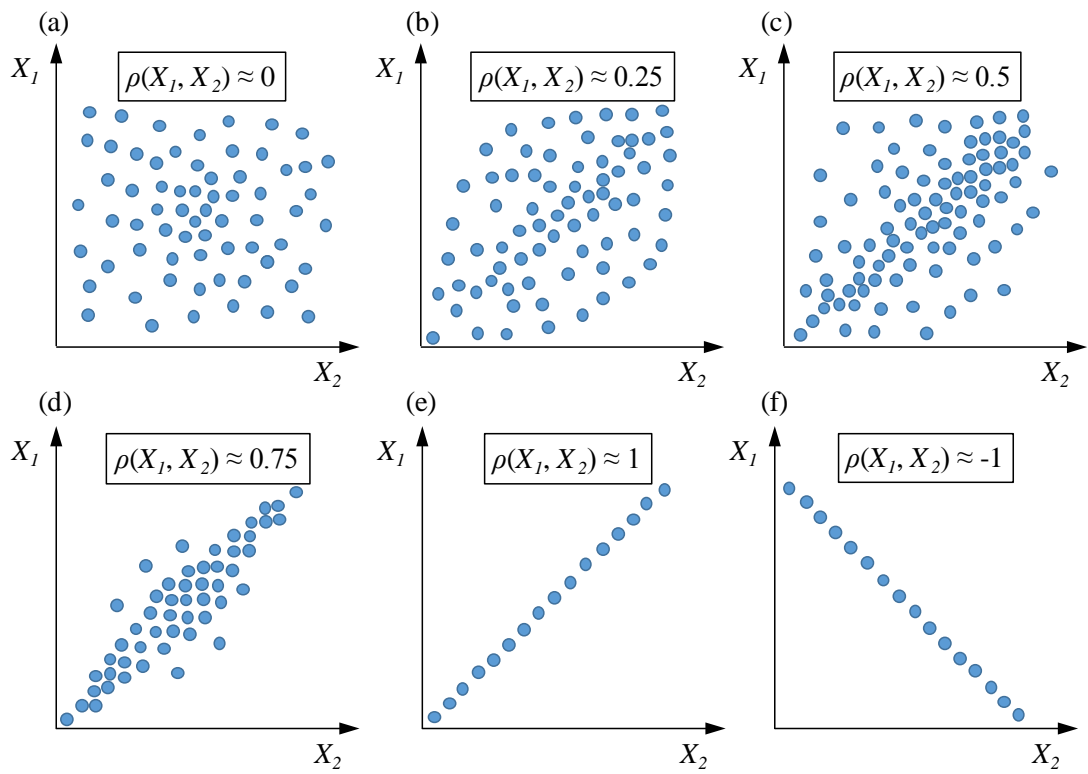


Figure A.9. Correlation coefficient  $\rho(X_1, X_2)$  between two random variables  $X_1$  and  $X_2$ .

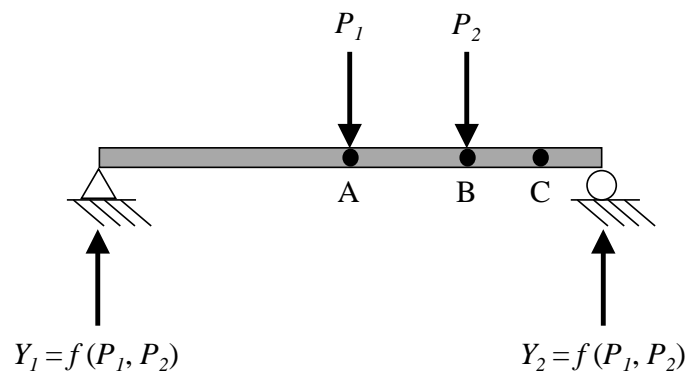


Figure A.10. Simply supported bridge span with two truck loads

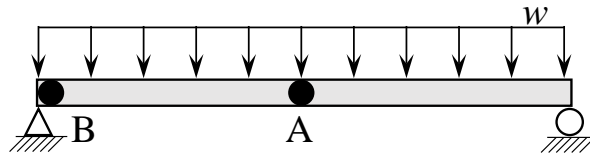


Figure A.11. Simply supported beam with uniform load.



Figure A.12. System reliability model of the beam in Figure A.11 considering bending and shear failure.

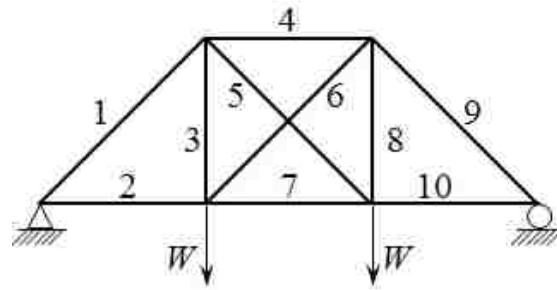


Figure A.13. 10 bar symmetric truss (adopted from Frangopol and Curley 1987)

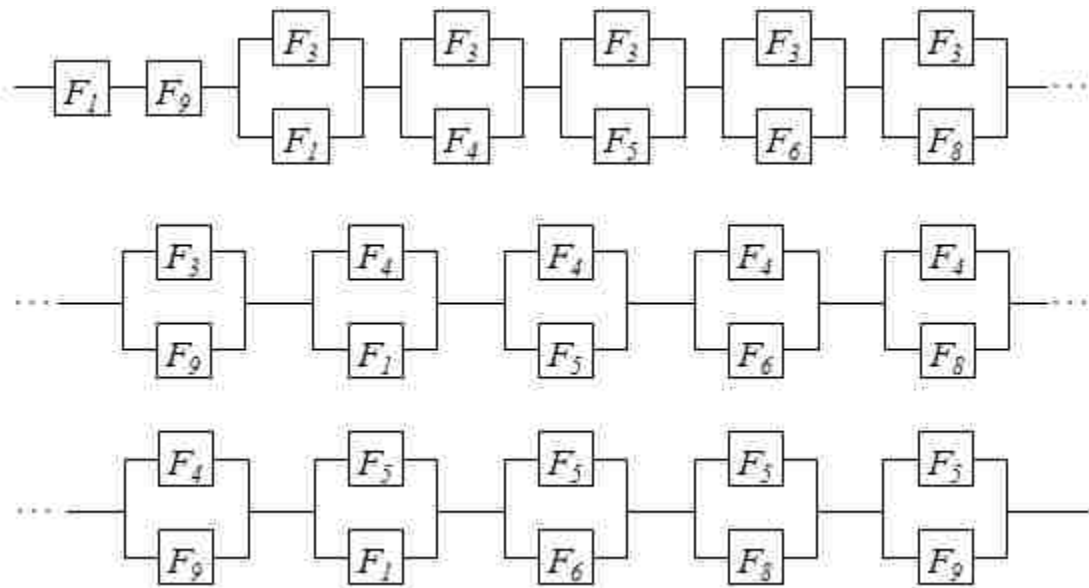


Figure A.14. System reliability model for the 10 bar truss in Figure A.13, considering failure of one member and failure of two members including failure of members 3, 4, or 5.

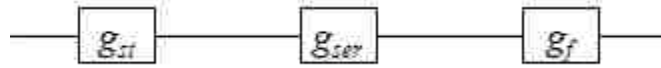


Figure A.15. System reliability model for investigated steel bridge.

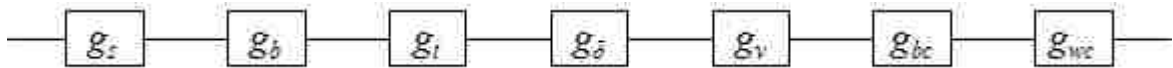


Figure A.16. Refined system reliability model for the investigated bridge.



Figure A.17. Hypothetical series system model of typical girder (Estes and Frangopol 2001).

## APPENDIX B LIST OF NOTATIONS

### B.1 NOTATION FOR CHAPTER 2

$A(t)$  = availability function

$C_F$  = expected failure cost

$C_{INS}$  = expected cost of inspections

$C_m$  = consequences of failure

$C_{PM}$  = expected cost of routine maintenance

$C_{REP}$  = expected cost of repair

$C_T$  = initial cost

$E_{CO}$  = value of the economic metric associated with sustainability

$E_{ENV}$  = value of the economic metric associated with sustainability

$F(t)$  = cumulative probability of failure

$f(t)$  = probability density function of time-to-failure

$f_R$  = PDF of resistance effect  $R$

$f_{R,S}$  = joint PDF of the random variables  $R$  and  $S$

$f_S$  = PDF of load effect  $S$

$f_{\mathbf{X}}(\mathbf{x})$  = the joint PDF describing the probabilistic behavior of the random variables

$$\mathbf{X} = \{ X_1, X_2, \dots, X_m \}.$$

$h(t)$  = hazard function

$k_{ECO}$  = weighting factor corresponding to economic sustainability metric

$k_{ENV}$  = weighting factor corresponding to environmental sustainability metric

$k_{SOC}$  = weighting factor corresponding to societal sustainability metric

$n$  = total number of hazards considered within the analysis

$P(H_i)$  = probability of occurrence of a hazard

$P_{F|H_i}(t)$  = conditional failure probability given the occurrence of a hazard

$P_F(t)$  = time-variant probability of failure

$R$  = resistance effect

$RISK(t)$  = time-variant risk

$S$  = load effect

$S(t)$  = survivor function

$Soc$  = value of the economic metric associated with sustainability

$u_{Eco}$  = utility function for economic attribute

$u_{Env}$  = utility function for environmental attribute

$u_s$  = multi-attribute utility associated with a structural system representative of sustainability

$u_{Soc}$  = utility function for societal attribute

$\Phi^{-1}(\cdot)$  = inverse of the standard normal CDF

$\beta$  = reliability index

$\kappa(\mathbf{x})$  = consequences associated with events resulting from certain hazards  $\mathbf{x}$

## B.2 NOTATION FOR CHAPTER 3

$A$  and  $B$  = parameters based on environmental aggressivity

$ADT(t)$  = average daily traffic during year  $t$

$AER_{DET,C}$  = annual expected amount of carbon dioxide emissions due to detour of a bridge

$AER_{DET,E}$  = risk associated with the annual amount of energy consumption due to detour

$AER_{REP,C}$  = annual expected amount of carbon dioxide produced from the repair of a bridge

$AER_{REP,E}$  = annual expected amount of energy consumption associated with the repair of a bridge

$A_s(t)$  = top transversal tensile steel reinforcement area ( $\text{mm}^2$ )

$A_{sr}(t)$  = area of transverse steel reinforcing in the slab at time  $t$  ( $\text{m}^2$ )

$C(t)$  = corrosion penetration depth ( $\mu\text{m}$ )

$C_I$  = rebuilding cost per square meter ( $\$/\text{m}^2$ )

$C_c$  = corrosion coefficient

$CD_{REB}$  = amount of carbon dioxide associated with rebuilding ( $\text{kg}/\text{m}^2$ )

$C_{EM,i}(t)$  = cost of a maintenance action  $i$  that is applied at year  $t$  (USD)

$C_{maint}$  = total cost of a lifetime maintenance strategy

$C_{maint}$  = total maintenance cost

$C_{max}$  = maximum maintenance cost

$CPD_C$  = carbon dioxide emissions per unit distance associated with cars ( $\text{kg}/\text{km}$ )

$CPD_T$  = carbon dioxide emissions per unit distance associated with trucks ( $\text{kg}/\text{km}$ )

$D_0$  = initial top reinforcement diameter (mm)

$D_d$  = duration of detour (days)

$D_f$  = the distribution factor

$EC_{REB}$  = total energy consumption associated with the rebuilding ( $\text{GJ/m}^2$ )

$EPD$  = energy consumption per unit distance associated with any vehicle ( $\text{MJ/km}$ )

$f'_{cs}$  = compressive strength of the concrete slab (MPa)

$f_y$  = yield strength of reinforcing steel in slab (MPa)

$F_y$  = yield strength of steel girder (MPa)

$g_{deck}$  = time-variant performance function associated with a reinforced concrete bridge deck in bending  $g_{deck}$

$g_{girder}$  = performance function describing the time-variant behavior of bending in the steel girders

$i_c$  = corrosion parameter ( $\text{mA/cm}^2$ )

$I_f$  = impact factor

$K_1, K_2, K_3, K_4,$  and  $K_5$  = Deterministic quantities that take on specific values depending on bridge type and geometric properties

$K_6, K_7, K_8, K_9, K_{10},$  and  $K_{11}$  = Deterministic constants

$k_{econ}$  = weighting factor corresponding to the economic metric of sustainability

$k_{env}$  = weighting factor corresponding to the environmental metric of sustainability

$k_{soc}$  = weighting factor corresponding to the societal metric of sustainability

$L$  = length of the bridge (m)

$L_d$  = detour length (km)

$M_{trk}(t)$  = moment due to truck load (kN-m)

$n$  = number of top transversal steel bars

$N_{EM}$  = total number of essential maintenance actions considered through the lifetime of a structure

$O_r$  = occupancy rate for non-truck vehicles

$p$  = probability of occurrence of an adverse event

$P_{f,sys}$  = probability of system failure

$RA$  = expected value of the risk-attribute value under investigation

$RA_{max}$  = maximum value of a risk-attribute

$RA_{min}$  = minimum value of a risk-attribute

$R_{EC}$  = risk-attribute value corresponding to carbon dioxide emissions

$R_{EE}$  = risk-attribute value corresponding to energy consumption

$R_{ETD}$  = risk attribute corresponding to the extra travel distance

$R_{ETT}$  = risk associated with the extra travel time for users that must use a detour

$R_{FT}$  = estimated annual expected number of fatalities

$r_m$  = discount rate of money

$r_m$  = discount rate of money

$R_{RB}$  = risk associated with the rebuilding cost

$S_d$  = average detour speed (km/hour)

$S_p(t)$  = plastic section modulus at time  $t$  ( $m^3$ )

$t$  = time (years).

$T_i$  = corrosion initiation time (years)

$TT_p$  = percentage of average daily traffic that is trucks (%)

$u_c$  = utility associated with a given maintenance cost

$u_{econ}$  = utility value associated with economic risk attribute

$u_{env}$  = utility value associated with environmental risk attribute

$u_{RA}$  = utility associated with a single attribute

$u_s$  = multi-attribute utility function associated with the sustainability performance metric

$u_{soc}$  = utility value associated with societal risk attribute

$W$  = width of the bridge (m)

$\gamma$  = risk attitude of the decision maker

$\gamma_{mfg}$  = modeling uncertainty for flexure in girder

$\gamma_{mfs}$  = modeling uncertainty for flexure in the slab

$\lambda_a$  = asphalt weight uncertainty factor

$\lambda_c$  = concrete weight uncertainty factor

$\lambda_{deff}$  = reinforcing depth uncertainty factor

$\lambda_s$  = structural steel weight uncertainty factor

$\lambda_{trk}(t)$  = effect of the load

$\chi$  = consequences of an adverse event

### B.3 NOTATION FOR CHAPTER 4

$a$  = expected value of the attribute value under investigation

$A(t)$  = availability function

$A_{i,m}(t)$  = availability function corresponding to a maintained component  $i$

$a_{max}$  = maximum value of the attribute

$a_{min}$  = minimum value of the attribute

$A_{sys}(t)$  = system availability function

$C_{direct}(t)$  = direct consequences associated with system failure

$C_{EM,j}$  = cost of maintenance action  $j$  applied at year  $t$  (USD)

$C_{indirect}(t)$  = indirect consequences

$C_{maint}$  = total cost of a lifetime essential maintenance strategy

$F(t)$  = cumulative-time failure probability

$f(t)$  = PDF of component time-to-failure

$h(t)$  = hazard function

$h_{i,m}(t)$  = hazard function corresponding to a maintained component  $i$

$h_{sys}(t)$  = system hazard function

$k$  = shape of the Weibull distribution

$N$  = total number of essential maintenance actions considered throughout the lifetime  
of a structure

$p$  = probability of occurrence of an adverse event

$P_{f,sys}(t)$  = probability of system failure during year  $t$

$RA_{direct}(t)$  = time-variant direct risk attribute

$RA_{indirect}(t)$  = time-variant indirect risk attribute

$r_m$  = annual discount rate of money

$S(t)$  = survivor function

$S_i(t)$  = survivor function associated with component  $i$  considering no maintenance.

$S_{i,m}(t)$  =  $i$ th component's resulting survivor function adjusted for maintenance

$S_{sys}(t)$  = system survivor function

$T_F$  = time-to-failure of the investigated component or system

$T_L$  = Lifetime under investigation

$u_A$  = utility associated with minimum lifetime system availability

$u_{a,dec}$  = utility function that is monotonically decreasing

$u_{a,inc}$  = utility function that is monotonically increasing

$u_{b,0}$  = performance utility without maintenance

$u_{b,m}$  = utility associated with the performance benefit considering maintenance

$u_{benefit}$  = total utility associated with the performance benefit

$u_h$  = utility associated with maximum lifetime system hazard

$u_{r,d}$  = utility associated with direct risk

$u_{r,i}$  = utility associated with indirect risk

$u_{r,tot}$  = utility associated with the total risk

$\gamma$  = risk attribute of the decision maker

$\lambda$  = shape of the Weibull distribution

$\chi$  = consequences of an adverse event

## B.4 NOTATION FOR CHAPTER 5

$C_m$  = cumulative monitoring cost

$E(\bar{A})$  = expected average availability of a monitoring plan

$ex$  = number of future exceedances

$n$  = total number of monitoring cycles investigated

$P_{ex}$  = probability of observing at least  $ex$  exceedances

$r_m$  = daily discount rate of money

$T_h$  = time horizon (days)

$u_a$  = utility associated with expected average availability

$u_c$  = utility associated with monitoring cost

$\alpha$  = parameter associated with the quadratic utility function

$\beta$  = parameter associated with the logarithmic utility function

$\gamma$  = most extreme risk attribute over attribute values (coefficient representative of the risk attitude of the decision maker)

$\rho$  = parameter associated with the exponential utility function

$\tau$  = time that the system is not monitored in uniform SHM plans (days)

$\tau_1, \tau_2, \dots, \tau_n$  = non-monitoring intervals in non-uniform SHM plans (days)

$\tau_{ini}$  = initial unmonitored time period in optimized SHM plans (days)

$\tau_m$  = monitoring period in uniform SHM plans (days)

$\tau_{m1}, \tau_{m2}, \dots, \tau_{mn}$  = monitoring periods in non-uniform SHM plans (days)

## **APPENDIX C LIST OF ACRONYMS**

ASCE: American Society of Civil Engineers

CDF: cumulative distribution function

FE: finite element

FHWA: Federal Highway Administration

GA: genetic algorithm

NBI: National Bridge Inventory

PDF: probability density function

SHM: structural health monitoring

## VITA

Samantha Sabatino was born on August 25, 1987 in Somerville, New Jersey, USA to Thomas and Randy Sabatino. Because of her childhood passion for rollercoasters, her interest in civil, and particularly, structural engineering was piqued at a very young age. After riding the tallest and fastest rollercoaster in the World in 2005 (i.e., Kingda Ka at Six Flags Great Adventure, Jackson, NJ), she was convinced to pursue a career in engineering. To this end, she earned two bachelor degrees in mathematics and civil engineering at Vanderbilt University in 2009, supporting her passions for both probabilistic mathematics and engineering. Following her undergraduate studies, Ms. Sabatino enrolled in a civil engineering Master's program at the University of Mississippi where she investigated the effectiveness of widely employed structural damage detection techniques. Upon completion of the M.S. degree in 2011, she began her Ph.D. studies at Lehigh University in structural engineering. At Lehigh, her current focus is the lifetime management of civil and marine infrastructure in a probabilistic, life-cycle context. One of her most notable research contributions was the development of a novel sustainability performance metric based on multi-attribute utility theory that effectively captures the consequences of structural failure to society, the environment, and the economy while also accounting for the decision maker's risk attitude. Overall, Ms. Sabatino is excited to begin her career as a young research professor and is eager for the opportunity to cultivate life-long learners in the field infrastructure engineering.